OAK RIDGE NATIONAL LABORATORY LIBRARY
3 4456 0022245 3

CENTRAL RESEARCH LIBRARY
DOCUMENT COLLECTION

3

DEC 4 1964

ORNL-3578
UC-37 – Instruments
TID-4500 (29th ed.)

INSTRUMENTATION AND CONTROLS DIVISION
ANNUAL PROGRESS REPORT
FOR PERIOD ENDING SEPTEMBER 1, 1963

OAK RIDGE NATIONAL LABORATORY
operated by
UNION CARBIDE CORPORATION
for the
U.S. ATOMIC ENERGY COMMISSION

CENTRAL RESEARCH LIBRARY
DOCUMENT COLLECTION
LIBRARY LOAN COPY
DO NOT TRANSFER TO ANOTHER PERSON
If you wish someone else to see this document, send in name with document and the library will arrange a loan.

Printed in USA. Price: $2.75 Available from the
Office of Technical Services
U. S. Department of Commerce
Washington 25, D. C.

LEGAL NOTICE

This report was prepared as an account of Government sponsored work. Neither the United States, nor the Commission, nor any person acting on behalf of the Commission:

A. Makes any warranty or representation, expressed or implied, with respect to the accuracy, completeness, or usefulness of the information contained in this report, or that the use of any information, apparatus, method, or process disclosed in this report may not infringe privately owned rights; or

B. Assumes any liabilities with respect to the use of, or for damages resulting from the use of any information, apparatus, method, or process disclosed in this report.

As used in the above, "person acting on behalf of the Commission" includes any employee or contractor of the Commission, or employee of such contractor, to the extent that such employee or contractor of the Commission, or employee of such contractor prepares, disseminates, or provides access to, any information pursuant to his employment or contract with the Commission, or his employment with such contractor.

ORNL-3578
UC-37 – Instruments

Contract No. W-7405-eng-26

INSTRUMENTATION AND CONTROLS DIVISION
ANNUAL PROGRESS REPORT
For Period Ending September 1, 1963

C. J. Borkowski, Director
C. S. Harrill, Associate Director

JUNE 1964

OAK RIDGE NATIONAL LABORATORY
Oak Ridge, Tennessee
operated by
UNION CARBIDE CORPORATION
for the
U. S. ATOMIC ENERGY COMMISSION

OAK RIDGE NATIONAL LABORATORY LIBRARY
3 4456 0022245 3

Contents and Summary

1. BASIC INSTRUMENTATION

1.1 *SEMICONDUCTOR RADIATION-DETECTOR RESEARCH*

J. L. Blankenship 1

Detectors having a 4-cc active volume were prepared, and their performance as gamma-ray spectrometers was evaluated. The detectors were superior to scintillation crystals in their response to gamma-ray energies below 200 kev. One technique which involves compensating steam-grown oxides for surface passivation of lithium-drifted detectors is described.

1.2 *MEASUREMENT OF DELAYED LIGHT FROM PLANTS AT 10^{-3} TO 10^{-5} sec AFTER ILLUMINATION*

J. B. Davidson and W. A. Arnold 4

Two schemes were devised for making measurements of the delayed light emitted by plants in the time region of 10^{-3} to 10^{-5} sec after illumination.

2. ELECTRONIC SYSTEMS AND COMPONENTS

2.1 *TUNNEL DIODE AND TRANSISTOR LOGIC CIRCUITS USED IN THE ORNL SPACE PROGRAM*

N. W. Hill *et al.* 6

Nanosecond electronic techniques have become an inseparable part of nuclear and particle physics. These techniques offer the experimenter the possibility of accumulating selected data in the presence of intense backgrounds of uninteresting and deleterious events. Modular circuits employing tunnel diodes for discrimination, coincidence, and anticoincidence functions are described. These circuits, along with transistor modules, have been used in experiments for high-energy recoil proton telescopes, time-of-flight instrumentation, and gamma-ray anticoincidence and pair spectrometers. Performance results of these circuits to variations in operating temperature and input-signal magnitude are given.

2.2 *INSTRUMENTATION OF A GAMMA-RAY PAIR SPECTROMETER TO REJECT NEUTRONS BY TIME-OF-FLIGHT TECHNIQUES*

R. J. Scroggs 19

Nanosecond circuitry was designed to exploit the difference in flight time of neutrons and gamma rays emitted from a target bombarded with a pulsed beam of monoenergetic protons. This circuitry allows a multicrystal gamma-ray spectrometer to be used concurrently as a pair spectrometer for energies from 1.5 to 10 Mev, and as a total absorption spectrometer for energies from 200 kev to 2.5 Mev.

2.3 *NANOSECOND PULSE PILE-UP DISCRIMINATOR FOR TIME-OF-FLIGHT MEASUREMENTS*

R. J. Scroggs 21

An instrument was designed to detect the passage of two or more protons through a plastic scintillator within a period of 0 to 25 nsec. If more than one proton traverses the scintillator during this period, an inhibit pulse is generated that is used in the logic network of the associated experiment.

2.4 *IMPROVEMENTS IN THE SNIP-SNAP SINGLE-CHANNEL ANALYZER*

R. W. Peelle and T. A. Love 21

The addition of a zero set and a hysteresis set to the Snip-Snap single-channel analyzer resulted in larger input dynamic range of operation.

2.5 *ISOLATED SIGNAL DETECTOR*

N. W. Hill, R. W. Peelle, and J. W. Madison 23

An instrument is described for time-of-flight applications which is capable of distinguishing primary events sufficiently isolated in time from other possible primary events. Different energy secondaries of different time origins giving rise to identical times of flight are thus avoided. This system responds to pulses within 10 nsec of each other and rejects any events in which two primary events are spaced by less than the preset isolation interval (115 nsec).

2.6 *TIME–TO–PULSE-HEIGHT CONVERTER*

F. M. Glass 25

A time–to–pulse-height converter was designed to measure time signals as short as 0 to 50 nsec in a neutron time-of-flight spectrometer.

2.7 *TIME–TO–PULSE-HEIGHT CONVERTER*

J. L. Lovvorn 26

A transistorized time–to–pulse-height converter was designed to cover the ranges of 4, 8, and 80 μsec. Pulses from avalanche transistors were provided from the input start and stop pulses to operate a digital time-interval meter for calibration checking.

2.8 *AMPLITUDE-CORRECTING CIRCUIT FOR TIME ANALYZER IN THE NANOSECOND RANGE*

W. H. duPreez and C. W. Williams 27

A circuit was designed that corrects for amplitude-dependent "walk" in the output of a time–to–pulse-height converter in the nanosecond range.

2.9 *FAST DOUBLE PULSER*

F. M. Glass 28

This pulser provides two simultaneous 8-v negative pulses, each 4 nsec wide with a rise time of 0.7 nsec and a fall time of 0.7 nsec into 50-ohm lines, and three simultaneous 8-v pulses (two negative and one positive) that are delayed with respect to the first pulses. The delay is continuously variable over a range of 100 nsec.

2.10 *DEVELOPMENT OF TIME-INTERVAL METER WITH 1-nsec RESOLUTION*

J. L. Lovvorn 29

Specifications for a digital-type time-interval meter having a resolution of 2 nsec were written, and development by contract with an instrument manufacturer was completed.

2.11 *INSTRUMENTATION FOR MULTIPARAMETER FISSION-FRAGMENT ENERGY-CORRELATION MEASUREMENTS*

C. W. Williams *et al.* 29

The system in present use is a three-parameter punch-tape storage system having a fast coincidence resolving time (40 nsec) and a circuit to reduce distortion from pileup.

2.12 *NEUTRON TIME-OF-FLIGHT SPECTROMETER FOR NEUTRON ENERGIES OF 100 kev OR MORE*

C. W. Williams, R. K. H. Wagner, and P. D. Miller 30

A spectrometer was designed to give a time resolution of about 2 nsec and an efficiency of approximately 20% for a neutron energy of 350 kev. The resolution was measured using an Na^{22} source. With a start-level range corresponding to 6 to 60 kev electron energy, the time resolution is approximately 1.6 nsec fwhm.

2.13 INDICATING AND LOGIC MODULES

J. H. Todd 31

A series of modules was developed to monitor the outputs of various instruments. These modules perform logic functions to determine the status of certain combinations of signals and to indicate, both locally and at a remote central point, the condition of any number of widely scattered instruments or combination of instruments. The modules are actuated by signals with two discrete states. All module dimensions are in accordance with CERN standards, which are being considered for adoption by ORNL.

2.14 LINEAR COUNT-RATE METER

J. H. Todd 35

A solid-state linear count-rate meter was designed with full-scale readings from 10 to 10^5 counts/sec in five ranges. The discriminator operates on signals from 0 to 10 v, and its paired-pulse resolution is 200 nsec.

2.15 REMOTE-CONTROL CONSOLE FOR THE 300-kv LINEAR PROTON ACCELERATOR

J. H. Todd 36

A parallel remote-control console containing duplicates of all control functions was fabricated to facilitate accelerator operation.

3. RADIATION MONITORING SYSTEMS

3.1 MODERNIZATION AND EXPANSION OF ORNL RADIATION MONITORING AND CONTROL SYSTEMS

D. J. Knowles *et al.* 37

The status of the installation of radiation monitoring and control systems at the Laboratory is discussed.

3.2 FALLOUT MONITORING SYSTEM

D. J. Knowles *et al.* 40

The system consists of 44 stations located at strategic points in the Laboratory area. Each station consists of both an alpha monitor and a beta-gamma monitor. Two pairs of telephone lines transmit analog signals, which indicate radiation level, and an ac tone, which indicates the condition of the alarm levels. All alarm indicators are displayed at a central point. Only 12 of the analog signals are monitored; these are randomly selected until an alarm signal indicates that a certain station or stations should be selected.

3.3 IODINE MONITOR FOR RADIOACTIVE EXHAUST GASES

R. L. Shipp, R. K. Abele, and D. J. Knowles 43

A detector was developed for use with stack or duct particulate monitors. The detector consists of a charcoal trap and shielded GM tubes. A detector installed at the 3039 stack has a good sensitivity for iodine and a fair sensitivity for xenon.

3.4 SMALL RADIATION-MONITORING SYSTEMS

D. J. Knowles, J. L. Kaufman, and T. A. Lewis 44

Three small projects are reported: a radiation detector which monitors trucks leaving the Burial Ground, a detector which monitors airborne contamination in the intake ventilation air for Building 3025, and a particulate sampler for off-gas lines.

3.5 LABORATORY CONTAINMENT PROJECTS

D. J. Knowles *et al.* 44

A status summary is given of the installation of a central display panel and instruments and controllers for containment of radiochemical processing buildings.

3.6 TONE TELEMETRY SYSTEM
J. H. Todd and A. L. Case 45

With this system, a tone of fixed frequency is inserted onto a line carrying other signals and is extracted at a receiving end where display is made by means of lights. A memory permits sampling of many units on the receiving end.

4. RADIATION-DETECTION INSTRUMENTS AND COMPONENTS

4.1 AIR ALPHA PROPORTIONAL COUNTER INSENSITIVE TO ATMOSPHERIC HUMIDITY
A. M. R. Ferrari and C. J. Borkowski 46

Abstract of published paper: *Rev. Sci. Instr.* 33(10), 1047 (1962).

4.2 VARIABLE-APERTURE ALPHA PROPORTIONAL COUNTER
W. T. Clay 46

A gas-flow proportional counter was designed to measure the uniformity and thickness of an alpha-emitting isotope being electroplated either upon a flat plate or inside small-diameter cylinders. Six different apertures were included in the detector collimator to extend the range of activities to be monitored.

4.3 ALPHA OR BETA-GAMMA RADIATION MONITOR
F. M. Glass and E. E. Waugh 47

This instrument provides a 1-ma telemetering signal, a 10-mv strip-chart recorder signal, and an alarm or audible indication of count rate. A charge-sensitive amplifier at the input eliminates the need for preamplifiers for remotely located detectors.

4.4 GAMMA-RAY MONITOR
R. J. Scroggs, J. H. Todd, and H. N. Wilson 49

An instrument was developed that measures both the integrated gamma-ray dose and the rate of dose accumulation. Separate alarms are provided for each measurement. The integrating dosimeter is automatically reset every 8 hr.

4.5 GAMMA-BACKGROUND INTEGRATOR
R. W. Ingle 49

A portable GM counter was designed to record background counts at outlying stations.

4.6 PERSONAL RADIATION MONITOR: STATUS REPORT
R. W. Ingle and C. J. Borkowski 50

A PRM was designed to operate for 1 yr before battery replacement becomes necessary.

4.7 PARALLEL-PLATE FISSION CHAMBER FOR DETERMINATION OF α FOR U^{235}
M. M. Chiles 51

A 5-in.-diam parallel-plate fission chamber was designed and fabricated for experiments designed to measure α (the ratio of capture cross section to fission cross section) for U^{235}.

4.8 X-RAY PROPORTIONAL COUNTER FOR THE 5- TO 35-kev ENERGY RANGE
R. E. Zedler 52

An x-ray proportional counter was designed and fabricated to analyze the 5- to 35-kev x-ray photon ranges. The detector has beryllium windows on both sides and at its ends, and is filled to 79 cm pressure with Xe–10% CH_4 gas. For low-energy measurements, the x-ray beam enters through the side window, while for high-energy measurements, the counter is rotated 90° so that the beam may enter the end window.

4.9 NEW GAMMA IONIZATION CHAMBER

H. R. Brashear and R. K. Abele 54

This new gamma ionization chamber may be used in radiation fields from 25 mr/hr to 10^5 r/hr at low saturation voltages. The chamber is filled with high-pressure xenon and is contained in a stainless steel housing less than 1 in. in diameter.

4.10 ION CHAMBER FOR DEPTH-DOSE MEASUREMENTS IN A WATER PHANTOM

M. M. Chiles 55

An ion chamber was designed to measure primary and secondary radiation inside a water-filled phantom. Dose measurements were made at different positions inside the spherical phantom while it was being irradiated by high-energy protons from an accelerator.

4.11 TARGET AND COUNTER HOLDER FOR RADIATION SHIELDING EXPERIMENT

T. F. Sliski and H. J. Stripling, Jr. 56

This device is used for experiments in neutron and proton spectroscopy. The experiments are being conducted to provide verification of theoretical calculations for the design of radiation shielding for space vehicles. Functionally, the device is used to locate a cyclotron beam and to position detectors in a polar coordinate system about a target. The device also positions the target with its axis coincident with the beam axis.

4.12 DOSIMETER FOR SPACE SHIELDING STUDIES

T. F. Sliski and H. J. Stripling, Jr. 57

A dosimeter was designed for the Space Shielding Program to determine whether calculated radiation doses are in agreement with those measured with the dosimeter.

4.13 LITHIUM-DRIFTED SILICON RADIATION DETECTORS

R. E. Zedler 59

The preparation and properties of lithium-drifted silicon radiation detectors prepared at ORNL are described.

5. DATA HANDLING AND COMPUTATION

5.1 DIGITAL ANALYZER SYSTEM FOR NEUTRON TIME-OF-FLIGHT STUDIES

J. W. Woody and J. L. Lovvorn 60

Commercial components were assembled into a digital system for neutron time-of-flight studies. Resolution of the time-interval meter is 10 nsec with a maximum time span of 4 μsec.

5.2 X-RAY SCANNER

J. W. Reynolds *et al.* 60

An experimental model of an automatic control system for scanning reactor fuel plates was fabricated and tested. A collimated x-ray beam scans a fuel plate, and a scintillation detector detects variations of transmitted x-ray intensity to indicate the fuel distribution as well as total fuel within a plate. The readout is a printed paper tape and a strip-chart record. Test results were satisfactory.

5.3 NONLINEAR LEAST-SQUARES FITTING APPLIED TO GAMMA-RAY SCINTILLATION DETECTOR RESPONSE FUNCTIONS

R. O. Chester, R. W. Peelle, and F. C. Maienschein 61

Abstract of published paper: *Proc. Symp. Appl. Nucl. and Radiochem.*, NAS-NS-3107.

5.4 *APPROXIMATE MODELS FOR DISTRIBUTED-PARAMETER HEAT TRANSFER SYSTEMS*
S. J. Ball 62

Abstract of published paper: *Preprints of Technical Papers, Fourth Joint Automatic Control Conference*, AIChE, pp. 131–39.

5.5 *APPLICATION OF DATA-LOGGING SYSTEMS*
R. K. Adams, C. D. Martin, and R. E. Whitt 62

Changes and additions to ORNL data-logging facilities are described.

5.6 *DEVELOPMENT OF DIGITAL COMPUTER CODES FOR SYSTEMS ANALYSIS*
S. J. Ball 64

Several codes are described which make use of frequency response techniques for a variety of control and analysis problems.

5.7 *INTERFACE PROGRAMMING*
R. K. Adams, E. G. Davisson, and C. D. Martin 64

Interface programming is defined and the special problems associated with computer input programs for data-logging systems are discussed.

5.8 *PROPOSED METHOD OF DATA REDUCTION FOR EGCR CONTROL-ROD-PROTOTYPE TESTS*
R. K. Adams and C. D. Martin 65

The EGCR control-rod-prototype test and the proposed methods of data reduction are presented.

5.9 *THERMOCOUPLE CALIBRATION COMPUTER PROGRAMS*
C. D. Martin and R. K. Adams 66

A computer program was developed to facilitate the calibration of thermocouples by the Instrumentation and Controls Division Standards Laboratory.

6. PROCESS INSTRUMENTATION AND CONTROL SYSTEMS ENGINEERING

6.1 *SYSTEMS DESIGN GROUP ACTIVITIES*
Bernard Lieberman 67

A tabulation of systems design group activities is presented.

6.2 *INSTRUMENTATION FOR ORNL EXPERIMENT 41-8 AT THE ENGINEERING TEST REACTOR*
A. H. Malone and B. C. Duggins 68

An instrument control console was designed, fabricated, and subjected to extensive analog simulation tests.

6.3 *OXYGEN SEPARATION PLANT*
L. H. Chase 70

A process instrumentation and control system was designed to provide a very high degree of reliability.

6.4 *POOLSIDE EXPERIMENTAL FACILITY IN THE ORR*
A. H. Malone 70

Equipment was provided to measure and control the temperature of specimens of structural materials during irradiation in the ORR.

6.5 NUCLEAR SAFETY PILOT PLANT INSTRUMENTATION
Corbett Brashear 72

The design of the instrumentation and control system for the Nuclear Safety Pilot Plant is 50% complete, procurement of instruments and equipment is 80% complete, and installation is 20% complete.

6.6 INSTRUMENTATION FOR THE HIGH-RADIATION-LEVEL EXAMINATION LABORATORY
C. S. Lisser *et al.* 72

Progress in instrumentation of the HRLEL is reported.

6.7 EMERGENCY PANEL FOR THE RADIOCHEMICAL PILOT PLANT
M. B. Herskovitz 73

An emergency panel was provided to monitor variables associated with the containment of processing facilities and to isolate the processing cells automatically in the event of an accident.

6.8 TESTS OF A FOAM DECONTAMINATION TECHNIQUE
Corbett Brashear and B. C. Thompson 74

An instrumentation and control system was designed, fabricated, and installed to implement the foam suppression tests.

6.9 SCHEDULING
C. S. Lisser 75

A Division-wide system of work scheduling, based on a modification of the critical path method, was adopted and is now fully operational.

7. PROCESS INSTRUMENTATION DEVELOPMENT

PROCESS INSTRUMENTATION

7.1 TELEMETERING OF LIQUID LEVELS IN WASTE STORAGE TANKS
T. M. Gayle 78

Tank-level telemetering from 24 intermediate level waste tanks to Building 3105 for the Operations Division was updated to provide greater accuracy with less maintenance and to utilize a minimum of leased telephone lines for the system.

7.2 CONTINUOUS MEASUREMENT OF HEXAVALENT CHROMIUM
T. M. Gayle 79

Instrumentation was developed for the Chemical Technology Division to permit continuous monitoring of the Cr^{6+} concentration in a Darex dissolver effluent stream. Both ultraviolet absorption and oxidation potential techniques were investigated; the oxidation potential method appeared more promising, and subsequent development work was concentrated on this technique.

7.3 DYNAMIC GAS THERMOMETRY
E. W. Hagen 80

Investigations were continued in dynamic gas thermometry, utilizing sonic flow nozzles as high-temperature measuring devices. Stability tests of nozzle flow coefficients produced new information and also confirmed and clarified some previously reported data. Nozzle-mounting techniques were studied.

7.4 VACUUM ION GAGE AND CONTROLLER

J. H. Todd, G. A. Holt, and E. E. Waugh 81

An ion gage and controller for vacuum systems was developed which has three ranges: 10^{-3} to 10^{-4}, 10^{-4} to 10^{-5}, and 10^{-5} to 10^{-6} torr. A set point for a control function (actuation of a relay) is adjustable from zero to full scale on all ranges. A high-voltage monitoring circuit actuates the control relay if the high voltage falls below a set value.

POWER CONTROL UNITS

7.5 PROPORTIONAL POWER-CONTROL UNIT EMPLOYING SILICON CONTROLLED RECTIFIERS

J. L. Horton 82

A proportional power-control unit with silicon controlled rectifiers was designed and built.

7.6 NOISE PROBLEMS ASSOCIATED WITH SILICON CONTROLLED RECTIFIERS USED IN POWER CONTROL

J. L. Horton 83

Transient and radio-frequency noise problems associated with silicon controlled rectifiers in power-control circuits were studied.

TEST AND CALIBRATION INSTRUMENTS

7.7 MAINTENANCE TESTING OF AUTOMATIC CONTROLLERS

W. R. Miller 84

Test equipment was developed to rapidly determine the operating condition of three types of electronic process controllers. Three testers were built and operating procedures were written for their operation. A substantial saving in time has been realized over previous methods of controller testing which consisted of mocking up the process conditions at the repair facility.

7.8 LOW-VELOCITY-AIR CALIBRATION FACILITY

T. M. Gayle and A. H. Malone 85

A low-velocity-air calibration facility was designed and built for the precise calibration of air velocity instruments and all types of hot-wire and rotating-cup anemometers.

7.9 NEW EQUIPMENT AND FACILITIES OF THE STANDARDS LABORATORY

M. H. Cooper and W. W. Johnston 87

A primary-reference voltage standard, a series of freezing-point temperature standards, and a universal ratio set for dc resistance measurements were placed in service in the Instrumentation and Controls Division Standards Laboratory.

7.10 FACILITY FOR INSPECTION AND CALIBRATION OF THERMOCOUPLES

W. W. Johnston and W. R. Miller 88

A thermocouple inspection calibration facility was established for the inspection of thermocouples and thermoelectric materials.

7.11 AC-INTERFERENCE TESTS OF FOXBORO M63 ALARM SWITCHES
C. D. Martin and J. R. Sutton 88

Foxboro M63 alarm switches were tested to determine the effects of various modes of ac interference, and a modification which solved a false-signal problem was recommended and installed.

7.12 HIGH-TEMPERATURE SAMPLING PROBE FOR HELIUM LEAK DETECTION
T. F. Sliski, H. J. Metz, and H. J. Stripling, Jr. 89

A probe for helium leak detection in hot systems was designed. The probe is essentially a differential-screw-operated needle valve and differs from commercially available probes in that it has been made relatively insensitive to temperature changes.

ANALYTICAL INSTRUMENTS

7.13 MODIFIED ANALYZER FOR AIRBORNE FLUORIDES
E. W. Hagen 90

A portable analyzer for airborne fluoride compounds was redesigned to simplify field servicing by reducing the amount of laboratory hardware involved and by improving the accessibility to the analytical components.

7.14 SENSITIVE PHOTOMETER FOR EMITTED-LIGHT MEASUREMENTS
T. M. Gayle 90

A sensitive photometer was developed for the Isotopes Division for evaluating commercially available watch and instrument dials containing tritium and other low-energy radioactive materials. The instrument measures the intensity of the emitted light from the dial to levels as low as 5×10^{-7} lumen.

7.15 MICRODOSIMETER READER MODIFICATIONS
T. M. Gayle 91

A Bausch & Lomb No. 33-66-02 microdosimeter reader was modified to provide better long-term stability with increased reading accuracy.

7.16 CHEMICAL DOSIMETER READER
T. M. Gayle 92

A method for reading chemical dosimeters by measurement of transmitted monochromatic light was demonstrated, and instrumentation for rapidly checking ORNL dosimeter ampoules was developed.

7.17 INSTRUMENT FOR MEASURING SMALL WEIGHT CHANGES
C. D. Martin 95

An instrument was developed to measure and record weight changes as small as 10 mg in chemical samples weighing up to 8 g.

7.18 ADJUSTABLE APPORTIONIZER
E. W. Hagen 95

An adjustable apportionizer was designed and developed to inoculate simultaneously up to ten sterile compartments in a containment tray, each with an individually selected and metered quantity of fluid.

7.19 EGCR ANALYTICAL INSTRUMENTATION CONSULTING
T. M. Gayle 95

Consultation on a number of analytical instruments for the EGCR was held with the Engineering Division, Oak Ridge Operations, AEC.

8. REACTOR INSTRUMENTATION AND CONTROLS SYSTEMS ENGINEERING

8.1 STATUS OF INSTRUMENTATION AND CONTROLS FOR THE HEALTH PHYSICS RESEARCH REACTOR

L. C. Oakes and C. F. Holloway 96

The Health Physics Research Reactor has been installed and operated in its permanent location at ORNL after having been checked at the ORNL Critical Facility and operated at the Nevada Test Site. Each of these phases of operation is briefly discussed.

8.2 STATUS OF INSTRUMENTATION FOR THE MOLTEN-SALT REACTOR EXPERIMENT

R. L. Moore *et al.* 97

Design of the MSRE instrumentation and control system was continued. Requirements for the nuclear and safety systems were determined. Procurement of process instrumentation is nearing completion and procurement of nuclear instrumentation is under way. Installation of equipment at the reactor site was begun.

8.3 PROCESS INSTRUMENTATION AND CONTROLS FOR ORR-GCR LOOP NO. 2

C. M. Burton *et al.* 99

The types and cost of instrumentation installed in this large in-pile experiment are discussed.

9. REACTOR INSTRUMENTATION AND CONTROLS DEVELOPMENT

NUCLEAR INSTRUMENTATION

9.1 MODULAR ELECTRONIC INSTRUMENTS FOR REACTOR CONTROL AND SAFETY

S. H. Hanauer *et al.* 100

A system of reactor-control modules has been devised; each member is a functional unit of one or more transistor electronic instruments for reactor use. To date, 18 different modules have been designed and prototypes built.

9.2 LOW-CURRENT TRANSISTOR AMPLIFIER

Ronald Nutt 103

A current-sensitive amplifier was developed to amplify the current from the ionization chamber in the range of 10^{-8} to 10^{-5} amp. The amplifier has medium sensitivity, good stability, and high reliability.

9.3 FAST-TRIP COMPARATOR CIRCUIT

J. F. Pierce and D. C. Shattuck 105

A study was begun to develop a fast-trip transistor comparator with an accuracy of ±25 mv over a range of 1 to 10 v and a temperature range of 10 to 55°C.

9.4 PROGRESS IN DEVELOPING A WIDE-RANGE COUNTING INSTRUMENT FOR REACTOR CONTROL

E. N. Fray and J. T. DeLorenzo 107

The wide-range counting system was tested in the ORR, using newly developed components which include the ¾-in. flexible fission chamber and preamplifier assembly, and prototypes of some of the modules described in the accompanying paper. Reactor power and period were measured over eight decades (cold startup), as well as during normal startup, operation, and shutdown.

9.5 *USE OF REACTOR GAMMA RADIATION AS A REACTOR CONTROL AND SAFETY PARAMETER*
D. P. Roux and S. H. Hanauer 108

Abstract of published paper: *Trans. Am. Nucl. Soc.* **6**, 74 (1963).

9.6 *A NEW CONFIGURATION FOR AN ELECTRICALLY ADJUSTABLE GAMMA-COMPENSATED IONIZATION CHAMBER*
D. P. Roux *et al.* 109

By making the signal plates smaller than the positive and negative high-voltage plates in a parallel-circular-plate compensated chamber, the effective volumes of the two portions can be varied by changing the ratio of positive to negative polarizing voltages. Both neutron and gamma sections are well saturated at voltages normally used, giving an electrically adjustable compensation independent of chamber current.

9.7 *A METHOD FOR MEASUREMENT OF NEGATIVE REACTIVITY BY ANALYSIS OF NEUTRON FLUCTUATION SPECTRAL DENSITY*
C. W. Ricker, A. L. Colomb, and E. R. Mann 111

Abstract of published paper: *Trans. Am. Nucl. Soc.* **6**, 75–76 (1963).

9.8 *LOW-NOISE SOLID-STATE DIFFERENTIAL AMPLIFIER*
F. M. Glass 113

This amplifier was developed for reactor noise studies and was designed to achieve long-term gain stability, a gain of 10,000, and a flat response within 1 db from 0.1 to 1000 cps.

9.9 *DESIGN OF MSRE AUTOMATIC ROD CONTROLLER*
E. N. Fray, S. J. Ditto, and D. N. Fry 113

An automatic rod controller was designed for controlling the reactor outlet temperature over a range of 1100 to 1300°F. The ORNL Analog Computer Facility was used to establish design criteria. Analog studies indicate that the outlet temperature can be controlled within acceptable limits for all operating conditions between 1 and 10 Mw.

9.10 *MECHANICAL DRIVE FOR POSITIONING A FISSION CHAMBER IN THE MSRE*
G. W. Allin and H. J. Stripling, Jr. 114

A mechanical fission chamber positioner has been designed for use in the Molten-Salt Reactor Experiment. This positioner will be servo operated to maintain constant reactor power operation in the low- and medium-power regions. A design stroke of 90 in. and a design speed of 72 in./min will permit multidecade power-level control.

PROCESS INSTRUMENTATION

9.11 *MSRE PROCESS INSTRUMENT DEVELOPMENT*
R. L. Moore *et al.* 116

Development and tests of a ball float and single-point molten-salt level indicators and of a temperature scanner were continued and are discussed. The feasibility of using closed-circuit television viewing systems during remote maintenance operations at the MSRE was investigated.

9.12 *PBRE BALL COUNTER*
H. D. Wills 118

A method was developed which counts the number of graphite balls flowing through a stainless steel pipe.

9.13 WATER FLOWMETER
J. H. Todd and E. E. Waugh 118

A meter was designed to measure the water flow rate through the seat switches and clutch assemblies in the TSR-II reactor. The meter consists of a transducer, a preamplifier, a frequency meter, and a control meter. Output relays are utilized in the reactor safety circuits.

COMPONENTS AND MATERIALS

9.14 TESTS OF STRAIN-GAGE PRESSURE TRANSDUCERS ON IN-PILE EXPERIMENTS
T. L. McLean 119

Operating experiences with strain-gage pressure transducers used on in-pile experiments are discussed.

9.15 DEVELOPMENT AND TESTING OF THERMOCOUPLE MATERIALS
N. H. Briggs *et al.* 120

Results of the continuing program in development and testing of thermocouple materials are summarized.

9.16 POTTED HERMETIC SEAL FOR SHEATHED THERMOCOUPLES
T. L. McLean 121

A potted hermetic thermocouple seal was developed to seal the ends of sheathed thermocouples and connect them to 24-gage extension wires.

10. SUPPORT FOR THE HIGH-VOLTAGE ACCELERATOR PROGRAM

10.1 SECOND-STAGE PULSE COUNTDOWN SYSTEM FOR THE ORNL 3-Mv VAN DE GRAAFF
R. F. King 122

By superimposing a 31.25-kc signal on the same deflector system with the lowest countdown frequency previously used (125 kc) a 32-μsec repetition rate may be obtained from the 3-Mv ORNL Van de Graaff. This now gives a choice of 1 μsec (1 Mc) basic rate to 2 μsec (500 kc), 4 μsec (125 kc), or 32 μsec (31.25 kc) for the pulse repetition rate.

10.2 IMPROVED KLYSTRON BUNCHER FOR THE ORNL 3-Mv VAN DE GRAAFF
J. P. Judish and R. F. King 123

A new klystron buncher capable of delivering higher voltage to the buncher electrode has replaced the previously reported 3-Mv ORNL Van de Graaff buncher. Measurements of buncher effect on pulse duration at beam energies up to 2.1 Mv and on beam energy spread at 1.747 Mv have been made.

10.3 TANDEM VAN DE GRAAFF MODIFICATIONS
G. F. Wells and C. D. Moak 124

A new inclined-field accelerator tube, two product-90 analyzing magnets, and an improved tank gas mixture have improved operations on the Tandem machine by reducing terminal radiation levels, extending the useful energy range of analyzed beams, and increasing the allowable terminal voltage.

10.4 NEGATIVE-ION SOURCE DEVELOPMENT
W. H. duPreez, J. W. Johnson, and R. F. King 124

Two methods of producing a negative hydrogen-ion beam were investigated: charge exchange of a positive ion beam in a gas target and direct extraction from the plasma in a duoplasmatron ion source. The best results were obtained with direct extraction; a negative-ion beam of 30 μa and of good ion optical quality was extracted through a source aperture of 0.0085 in.

10.5 THERMAL LEAK VALVE DEVELOPMENT
J. W. Johnson and C. D. Moak 125

A hot-wire thermal leak valve, based on a Harwell design, was developed for accelerator ion-source gas feed. By using the same heater as is used for the ORNL palladium leak valve, the control system does not have to be changed when the thermal valve is used in place of a palladium leak valve for feeding gases other than hydrogen, that is, helium, oxygen, bromine, and iodine.

11. MISCELLANEOUS

11.1 COSTS AND MANPOWER SUPPORT OF LABORATORY PROGRAMS
Joseph Guarneri 127

Approximately $3 million was expended in fiscal year 1963 for 304 man-years of Division labor in support of Laboratory programs. The cost of capitalized instrumentation and components and the distribution of manpower to Laboratory Divisions are discussed.

PUBLICATIONS 129

PAPERS PRESENTED AT PROFESSIONAL MEETINGS 131

ORGANIZATION CHART 133

1. Basic Instrumentation

1.1 SEMICONDUCTOR RADIATION-DETECTOR RESEARCH

J. L. Blankenship

Until recently, it was difficult to make x- and gamma-ray spectroscopic measurements at energies below 200 kev, because the responses of the available detectors were inadequate to resolve energies in this range. Now, however, silicon diodes made with a lithium-ion drift can resolve these energies and make low-energy measurements practical. In Fig. 1.1.1, the response of a large-volume, lithium-drifted silicon-diode detector is compared with the response of an NaI(Tl) scintillation spectrometer for Co^{57} gamma rays. (The energies for Co^{57} gamma rays are 122 and 136 kev.) This silicon diode has an active volume 2.3 cm in diameter and 1.2 cm thick and was operated at a 300-v bias at 77°K. With this diode, the Co^{57} gamma-ray spectrum is 6.8 kev fwhm, but with an NaI(Tl) spectrometer, the same Co^{57} gamma-ray spectrum is 16 kev fwhm. The net improvement in resolution is a factor greater than 2.

The resolution of a lithium-drifted diode with a volume 2.3 cm in diameter and only 5 mm thick was 5 kev fwhm for the 59.6-kev Am^{241} gamma ray. This smaller-volume detector required only a 30-v bias and was operated at temperatures up to 200°K. The spectrometer noise was contributed primarily by the electronics, virtually none by the detector.

Earlier diffusion techniques for producing a lithium-drifted diode gave poor results, mainly because they yielded thick dead layers ($\sim 100\ \mu$) on both the lithium-doped N and the undoped, or undrifted, P faces of the detector. Still, such a diode could detect charged particles incident on its sides.

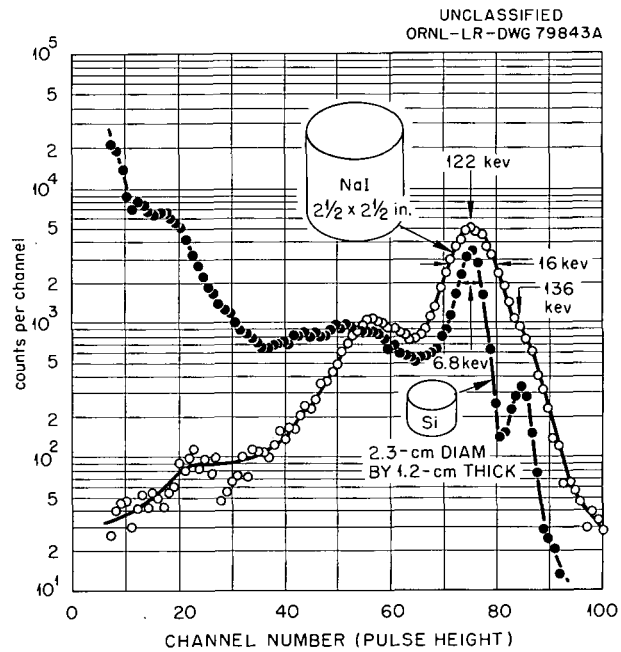

Fig. 1.1.1. Cobalt-57 Gamma-Ray Spectrum Determined with Two Detectors. The 2.3- by 1.2-cm detector was operated at a 300-v bias and at 77°K.

Presently, dead layers as thin as 1.3 μ can be produced on the lithium-doped face.[1,2] A surface-barrier contact may be applied to the intrinsic side of the drifted diode, which is reached after the undrifted P material is removed by lapping.

[1] J. L. Blankenship and C. J. Borkowski, *IRE Trans. Nucl. Sci.* 9(3), 181–89 (1962).

[2] J. L. Blankenship and C. J. Borkowski, *Rev. Sci. Instr.* 33(7), 778–80 (1962).

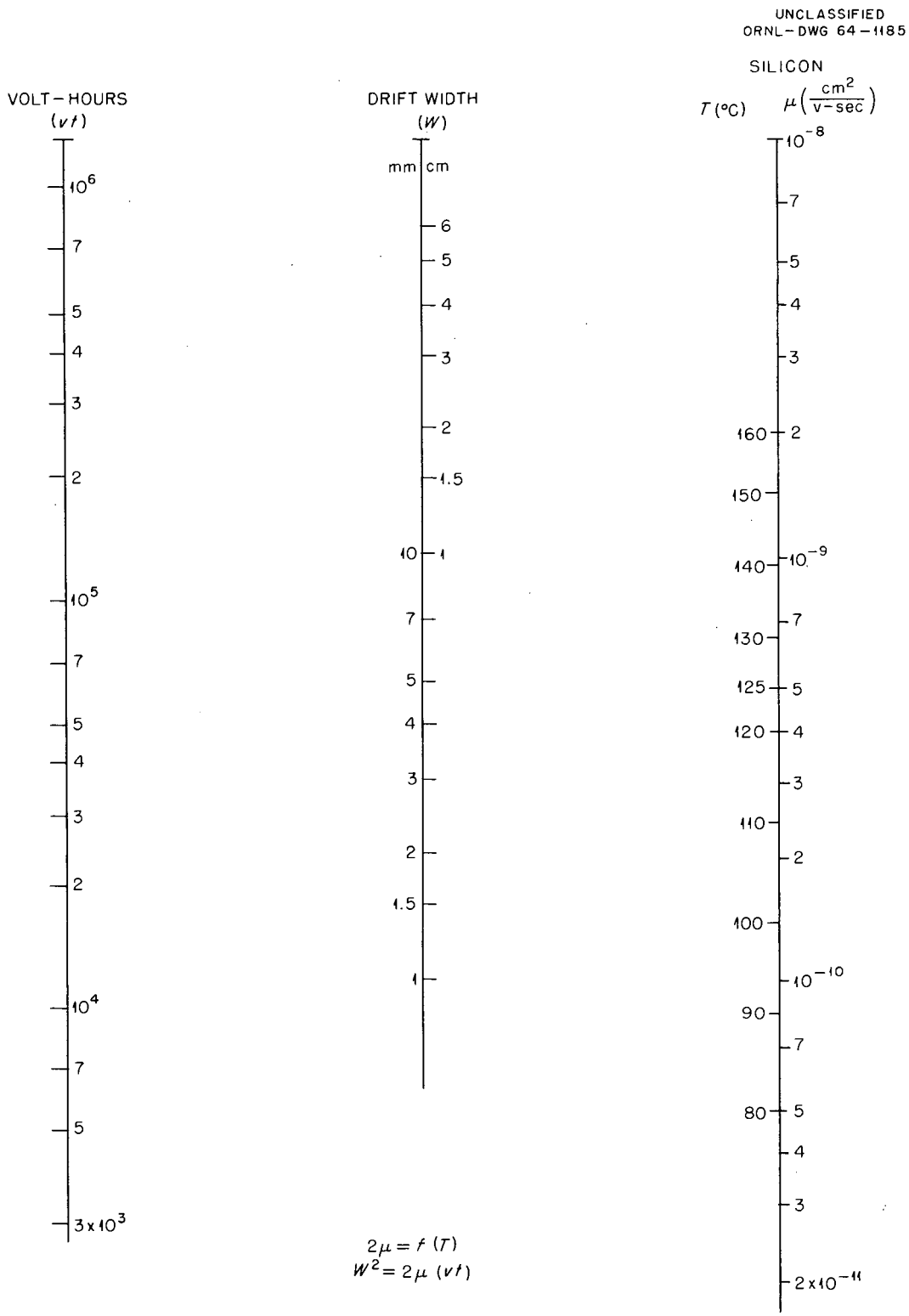

Fig. 1.1.2. Nomograph of Volt-Hours to Drift Width for Various Temperatures.

Diode detectors so produced exhibit dead layers whose depth is determined primarily by the thickness of the gold layers evaporated onto them,[3,4] namely, $\sim 50\ \mu g/cm^2$.

A number of programs for drifting lithium into silicon-diode detectors are available. The properties which these programs produce in detectors are summarized in the following discussion.

The constant-temperature-voltage program[1] reproduces drift depths within $\sim 5\%$. This program is most useful for shallow drifts (~ 3 mm). The drift-depth parameters can be determined from a nomograph and a family of curves;[1] however, a nomograph has been devised which eliminates the need for the family of curves (Fig. 1.1.2).

The constant-power drifting program[1,3] produces deep drifts in short times, but suffers from poor reproducibility, when compared with the constant-temperature-voltage program. The constant-power program utilizes a servo[1] and appears to be more efficient in time than the fluorocarbon evaporative-cooling bath and constant-power program[3] in producing drifts up to 1.2 cm. The latter program is useful for whole-ingot-diameter diodes after the drift depth exceeds ~ 5 mm, although complete drifts can be made.

To redistribute the lithium uniformly throughout a detector after it has been subjected to a high-power drift (50 w at 176°C), the detector is maintained at a lower temperature (100°C) with a high bias voltage across it for about 10 hr.

The saturation reverse current per unit volume for the best detectors of each size of lithium-drifted diodes is the same, 5×10^{-9} amp/mm^3 $\pm$ 20% at 23°C; hence, with this value of saturation current and a given noise figure requirement, a small-volume detector will operate at room temperature. However, it is still necessary to cool the detector to achieve the combination of lowest noise performance and largest active region.

The surface states of lithium-drifted silicon-diode detectors are sensitive to changes in their environment; consequently, means to passivate the detector surfaces were investigated. One technique is to grow an oxide layer on the detector surface. Diodes protected by an oxide layer, atmospheric steam-grown and 3000 A thick, showed virtually no measurable response (< 1% over a long time) to changes in ambient; that is, from vacuum to dry oxygen and from room air (50% relative humidity) to ammonia vapor. However, the steam-grown oxide induces a strong *N*-type surface conductance on the diode; consequently the reverse current is 100 to 1000 times higher than for an unprotected lithium-drifted diode.

A technique was developed for producing a highly compensated surface at the silicon-oxide interface. Hansen[5] compensated the oxide layer on conventional diffused-junction diodes by diffusing gallium, a *P*-type dopant, into the silicon surface before performing the steam oxidation. This process requires rigid control over the gallium diffusion. At ORNL, a gallium diffusion hot enough to overcompensate the effects of the oxide is performed (the actual sheet resistance is not critical). Lithium is then drifted into a diode made of this material. During the drift process the lithium, an *N*-type dopant, very nearly compensates all the excess gallium (*P*-type) dopant.

The *N*-type surface of an ordinary oxide-protected diode cannot be compensated by the lithium, because lithium itself is an *N*-type material. Such diodes have much smaller reverse currents than diodes protected only by the steam-grown oxides, but not as small as for unprotected ordinary lithium-drifted diodes.

---

[3] G. L. Miller, D. B. Pate, and S. Wagner, *IRE Trans. Nucl. Sci.* **10**(1), 220–29 (1963).

[4] C. Chasman and J. Allen, *Nucl. Instr. Methods* **24**, 253–55 (1963).

[5] W. L. Hansen, F. S. Goulding, and R. P. Lothrop, *J. Appl. Phys.* **34**(5), 1570–71 (1963).

1.2 MEASUREMENT OF DELAYED LIGHT FROM PLANTS AT 10^{-3} to 10^{-5} sec AFTER ILLUMINATION

J. B. Davidson W. A. Arnold[1]

For several minutes after illumination, green plants emit a dim, red light from the first excited state of chlorophyll.[2] It has been shown that this delayed light (measured at times longer than 0.1 sec after illumination) comes from chlorophyll, the agent which is active in photosynthesis, and that this light is also closely associated with the mechanism of quantum energy conversion.[3]

The present work is an extension of the measurement of this delayed light to shorter times, in which a direct display of the light decay is obtained along with a measure of the relative intensities of delayed light and of plant fluorescence. Plant fluorescence is more intense and has the same emission spectrum as the delayed light, but decays within a few nanoseconds after the excitation is removed.

Two schemes were devised for making measurements in the time region of 10^{-3} to 10^{-5} sec. In the first scheme (Fig. 1.2.1) a disk with two illuminating holes and a two-bladed sector are mounted on the shaft of a variable-speed motor having a maximum speed of 8000 rpm. The sample consists of a suspension of the one-celled organism *Chlorella* in a nutrient solution contained in a 2-ml plastic tube. (The tube was carefully selected for its lack of an afterglow when struck by light.) While the sample cells are illuminated through one of the holes in the front disk, the propeller-shaped sector blocks the exciting light from the photomultiplier tube which is used to measure the delayed light. At the same time, the sector turns and exposes the cells to the photomultiplier tube for approximately 130° of rotation. During this time the output of the photomultiplier tube is amplified and displayed on an oscilloscope. Two decay curves are displayed for each revolution of the shaft.

The pinhole in one blade of the sector allows a small, experimentally determined, fraction of the much stronger fluorescence emitted only during illumination to strike the photomultiplier. The fluorescence is seen as a spike on the oscilloscope just before the start of the decaying delayed-light signal. From the amplitude of the spike, the ratio of the intensities of fluorescent to delayed light is obtained. At maximum disk speed, it is possible to measure the delayed light at 0.5 msec after the illumination is blocked.

Because the intensity of the delayed light continued to rise sharply at 0.5 msec, and because this time represented the limit of the speed of the rotating-disk instrument, a new shutter was required to obtain data at shorter than the 0.5-msec limit.

With the device shown in Fig. 1.2.2, measurements were made at 50 μsec. The device consists of a metal block with a 45° face, through which two intersecting holes are drilled at right angles to each other. A third hole, into which the sample tube is placed, intersects one of these holes. A piece of 0.25-mil-thick, aluminum-coated Mylar film is arranged so that it can be blown over the illuminating aperture with a blast of compressed CO_2. The film, serving as a shutter, cuts off the exciting light. It remains over the aperture for several milliseconds; during this time, it reflects the delayed light from the plants onto the

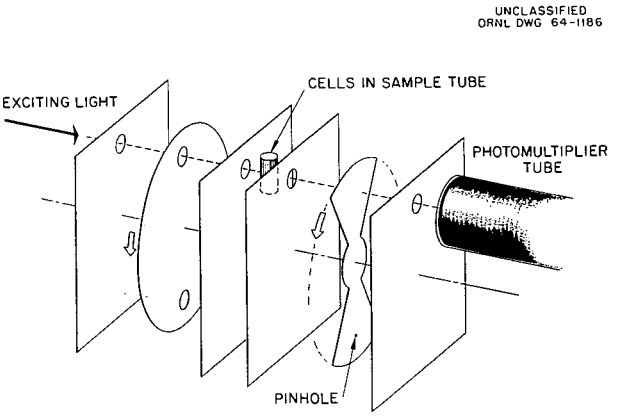

Fig. 1.2.1. Apparatus for Delayed-Light Measurements in the Millisecond Range.

[1]ORNL Biology Division.

[2]B. Strehler and W. A. Arnold, *J. Gen. Physiol.* 34, 809 (1951).

[3]W. F. Bertsch, *Proc. Natl. Acad. Sci. U.S.* 48, 2000–2004 (1962).

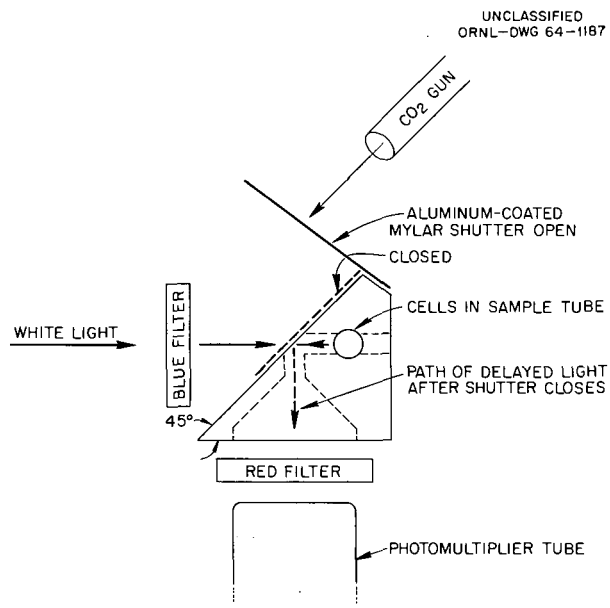

Fig. 1.2.2. Fast Shutter for Measuring Delayed Light at 50 μsec.

photomultiplier. The resulting photomultiplier signal is amplified and photographed on the oscilloscope. By replacing the Mylar shutter with a partially silvered mirror, the cells can be excited and a known fraction of their fluorescence will be reflected onto the photomultiplier. Again, the ratio of the delayed–to–fluorescent-light intensity can be determined in the same manner as with the disk shutter.

Figure 1.2.3 shows a decay curve for delayed light from *Chlorella* at 25°C. The delayed-light signals are plotted as fractions of the steady-state fluorescence signal, which is normalized to 1.0. The points at 0.6 msec and longer times were taken with the rotating-disk shutter. The points for the shorter times were taken with the Mylar film shutter. The solid curve is a decaying exponential function with a time constant of 1.7×10^{-9} sec. This value is the lifetime for the fluorescence of *Chlorella* as given by Tomita and Rabinowitch.[4]

The shortest measurement time achieved with the Mylar film shutter was 50 μsec; this appears to be its limit. To clarify the relation between fluorescence and delayed light even further, faster measurements are required. To this end, electronic shutters are being investigated.

[4]G. Tomita and E. Rabinowitch, *Biophys. J.* **2**, 483 (1962).

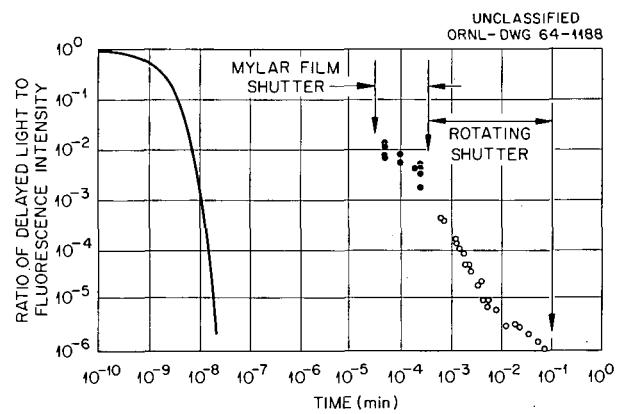

Fig. 1.2.3. Decay of Delayed Light from *Chlorella* at 25°C.

2. Electronic Systems and Components

2.1 TUNNEL DIODE AND TRANSISTOR LOGIC CIRCUITS USED IN THE ORNL SPACE PROGRAM

N. W. Hill[1]

J. T. DeLorenzo F. M. Glass R. J. Scroggs

Modular circuits employing tunnel diodes are used extensively in the complex of electronics associated with the various high-energy particle experiments for the Neutron Physics Division space shielding studies. These tunnel diodes are inherently high speed, can be operated over a wide range of temperatures, and are resistant to radiation damage. Because their current-vs-voltage response (Fig. 2.1.1) is unique, they are useful in nanosecond logic circuitry as current-sensing and active memory-switching elements. Various applications of tunnel diodes to high-speed circuitry have been described in the literature (see Bibliography, this section).

In the present work[2] a detailed study was made of the response of several circuit modules, all employing tunnel diode elements, to variations in operating temperature and input-signal magnitude. These modular circuits, which include circuits designed for discrimination, coincidence, and anticoincidence functions, were used in gamma-ray spectrometers, high-energy recoil proton telescopes, time-of-flight experiments, and scaler-driver applications.

The slow-discriminator module (Fig. 2.1.2), based on a design by Whetstone [described in Ref. (*4*) of Bibliography], operates on pulses from a photomultiplier and performs as a lower-level discriminator, pulse shaper, or as a "fan-out" for counting purposes. Performance data for the discriminator are summarized in Table 2.1.1.

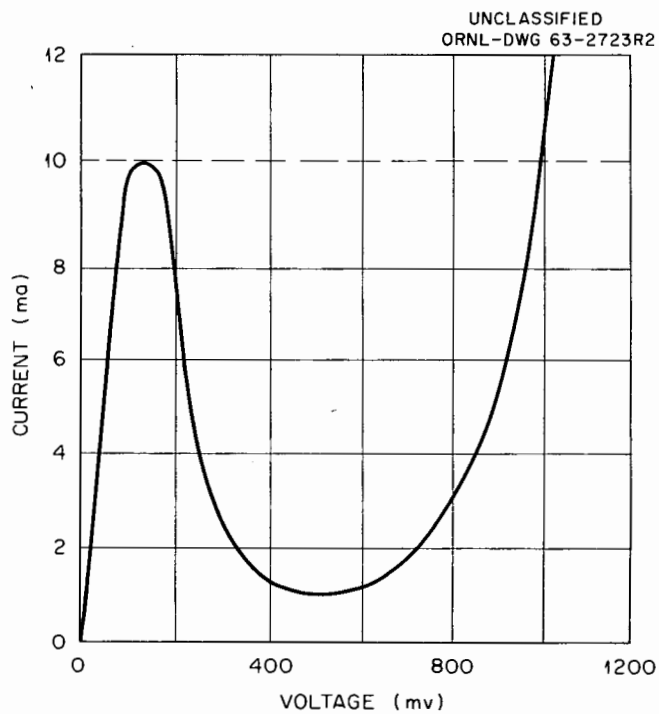

Fig. 2.1.1. Typical Current vs Voltage Plot for a Tunnel Diode.

For experiments in which the pulse-pair resolution of the slow discriminator was inadequate, the discriminator was modified with the "nonlinear biasing" technique.[3–5] The usual resistive load

[1]The authors acknowledge the contribution of D. D. Walker, W. H. Williams, W. H. Houston, and A. E. Ball to various phases of this work.

[2]The results are described in detail in *Neutron Physics Div. Ann. Progr. Rept. Aug. 1, 1963*, ORNL-3499, vol. II.

[3]J. Amodei and W. F. Kosonocky, *RCA Rev.* **22**, 669 (1961).

[4]R. H. Bergman, M. Cooperman, and H. Ur, *RCA Rev.* **23**, 152 (1962).

[5]V. Radeka, *Nucl. Instr. Methods* **22**, 153 (1962).

(13 ohms, Fig. 2.1.2) in the tunnel diode univibrator was replaced by a nonlinear load (such as the 2N976 transistor diode clamp shown in Fig. 2.1.3). A comparison of the two biasing techniques for a 10-ma GaAs tunnel diode is displayed in Fig. 2.1.4. Also shown is the comparatively high resistance of the transistor clamp when the tunnel diode switches over the peak and its higher conductance after switching than is afforded with the linear load. Thus, the transistor clamp does not act as a shunt during switching, and therefore requires less current for the slower rise-time inputs. Since the voltage across the inductance, V_L (Fig. 2.1.3), is much larger than it is with the linear load, the time required for recovery to the original bias point is much less with nonlinear loads; and because transistors are more nearly ideal switching devices, the recovery time is more easily defined. When the univibrator is in its high-voltage state, where V_L is much smaller for the nonlinear load, the output pulse width is longer for a given value of L; thus, the nonlinear load provides faster recovery for a wide pulse.

Comparison of the performance data of the two discriminators in Table 2.1.1 shows that for fast input pulses, the fast discriminator requires 2.4

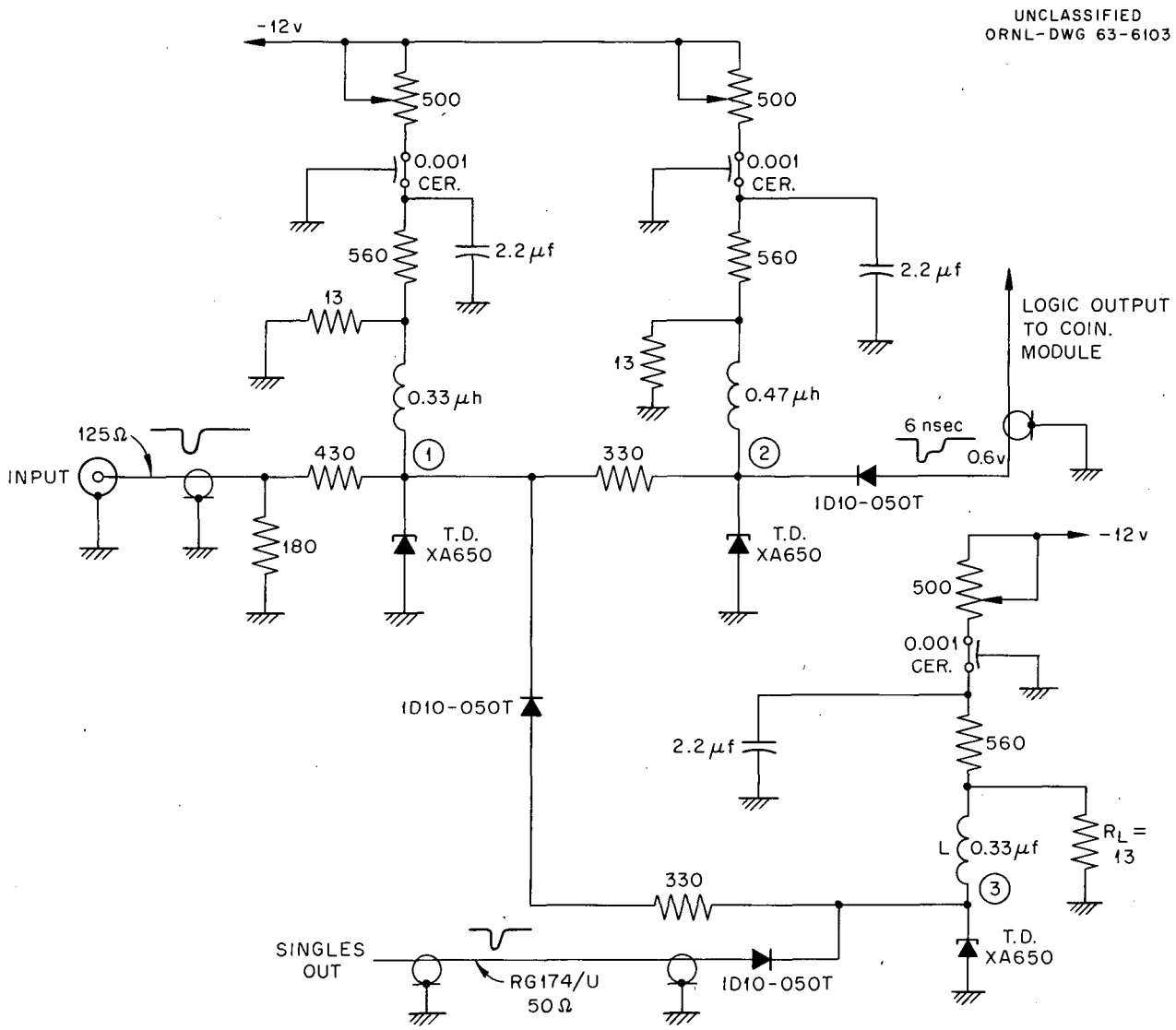

Fig. 2.1.2. Circuit for a Slow-Discriminator Module.

Table 2.1.1. Performance Data for Fast and Slow Discriminators

	Slow Discriminator[a]	Fast Discriminator[b]
Threshold output (fwhm)	50 mv, 4.2 nsec for $L = 0.33$ μh, ~13 nsec/μh	120 mv, 3.8 nsec for $L = 0.27$ μh, 4.6 nsec for $L = 0.33$ μh, ~14 nsec/μh
Pulse-pair resolution for input 10% above threshold	55 nsec or ~14 times fwhm of output pulse	15 nsec or ~14 times fwhm of output pulse
Pulse-pair resolution for input 2 times threshold	41 nsec	12 nsec
Pulse-pair resolution for input 3 times threshold	39 nsec	10 nsec
Delay change of output with input amplitude change	4.5 nsec from threshold to 120 times threshold	2.9 nsec from 1.25 times threshold to 15 times threshold
	~2.5 nsec for 2 times threshold to 120 times threshold	~1.0 nsec for 2 times threshold to 15 times threshold
Width change of output with input amplitude change	2.6 nsec increase from threshold to 120 times threshold	0.5 nsec increase from 1.25 times threshold to 20 times threshold
Amplitude change of discriminator output with input amplitude change	20% increase from threshold to 120 times threshold	27% increase from 1.25 times threshold to 15 times threshold
Threshold stability with temperature	−0.5 mv/°F	−0.83 mv/°F
Change of output (fwhm) vs temperature	+5% from 0 to 120°F	−1.5% from 0 to 120°F
Amplitude change of output vs temperature	+6% from 0 to 120°F	−11% from 0 to 120°F

[a]Shown in Fig. 2.1.2.
[b]Shown in Fig. 2.1.3.

times more input amplitude than the slow discriminator. (This disparity in input amplitude requirement has been reported[6] to disappear when the value of L is raised above 0.5 μh.)

Since the nonlinear load results in recovery times shorter than 10 nsec, care must be exercised to ensure that broad input pulses, especially from overloads, do not induce multiple pulsing. In the circuit shown in Fig. 2.1.3, the termination of the 125-ohm input by the 2:4 ratio transformer reduces such multiple pulsing at some sacrifice in sensitivity. The low-frequency response of the transformer is insufficient to couple the slower components of the input pulses.

[6]A. L. Whetstone, *Rev. Sci. Instr.* **34**(4), 412 (1963).

Circuit diagrams for slow- and fast-coincidence modules employing tunnel diode univibrators are shown in Figs. 2.1.5 and 2.1.6 respectively. Standardized pulses from suitable discriminators are added linearly at the input univibrator. The input univibrator can be biased to trigger on a single pulse, on any two of three pulses, or on all three input pulses in coincidence. Since the input pulses from the discriminators are essentially triangular in shape, the coincidence resolution can be varied over several nanoseconds without single-pulse feedthrough. Typical delayed-coincidence edges for pulses from a pulse generator are $\leq$0.1 nsec wide.

The behavior of a slow-coincidence circuit and dual discriminator combination as a function of temperature is summarized in Table 2.1.2. For

UNCLASSIFIED
ORNL-DWG 63-6089R

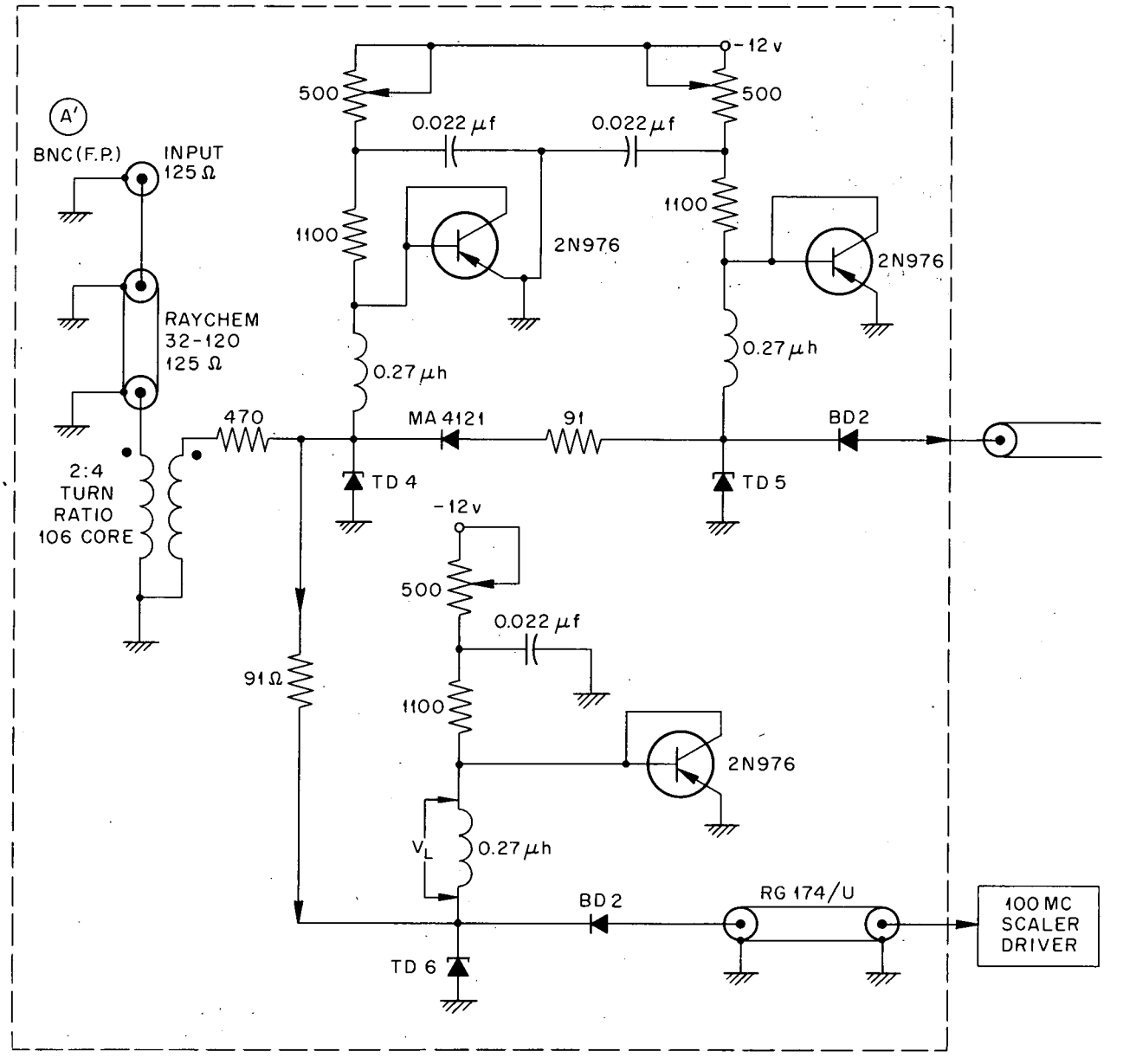

Fig. 2.1.3. Circuit for a Fast-Discriminator Module.

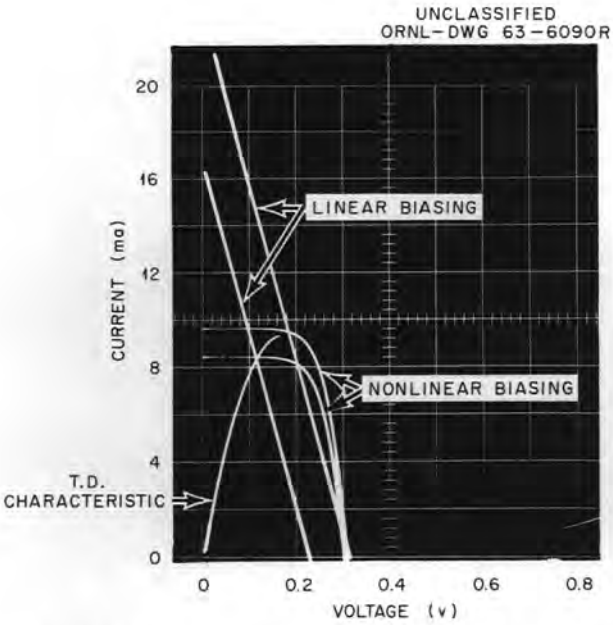

Fig. 2.1.4. Current vs Voltage Curves for Linear and Nonlinear Discriminator Biasing.

Table 2.1.2. Response of Coincidence Module at Various Temperatures

Temperature (°F)	Half-Fire Point (nsec)		Resolution (nsec)
	Lower Pulse Edge	Upper Pulse Edge	
20	12.35	19.12	6.77
40	12.57	19.30	6.73
60	12.69	19.45	6.76
80	12.81	19.70	6.89
100	12.93	19.95	7.02
120	13.07	20.15	7.08

a change in temperature from 20°F to 120°F, the variation in resolution is about 4%, while the change in edge timing is about 1 nsec.

A circuit diagram of a slow-anticoincidence module is shown in Fig. 2.1.7. The anticoincidence function is performed by a discriminator that feeds a modified scaler-driver module. The width of this scaler-driver pulse is accurately controlled by a delay line; that is, two 10-nsec, 4-v pulses with 4-nsec edges can be produced within a period of 30 nsec. This resolution is more than adequate to meet the resolution requirements ($\gtrsim$40 nsec) of the experiments in which it was employed.

At each logic step in the modules described above, a tunnel-diode fan-out is provided for counting purposes. The nominal 1-v pulse of the GaAs tunnel diodes, when used with an isolating coupling diode, was insufficient to operate commercially available scalers reliably. For this reason, as well as to meet the $\gtrsim$40-nsec resolution requirement, several scaler-driver modules were designed to operate scalers from either positive or negative tunnel-diode pulses. The positive-output scaler driver (Fig. 2.1.8) delivers a 4-v pulse with 4-nsec edges into 125 ohms, whereas the negative-output scaler driver (Fig. 2.1.9) delivers a 4-v pulse with 7-nsec edges into the same load. Both scaler drivers can be operated with delay-line width control to produce accurate and stable output pulse widths for use in such logic functions as shown in Fig. 2.1.7. Output-pulse widths, controlled by delay lines, have ranged from 10 to 90 nsec. More generally, however, the output-pulse widths have been controlled by the collector time constant in the trigger pair (Figs. 2.1.8 and 2.1.9). The behavior of both positive- and negative-output scaler drivers as a function of temperature is dependent on the output-pulse width. Performance data for these scaler drivers are shown in Table 2.1.3. Since precise widths and amplitudes of the output pulses from the normal scaler drivers were not necessary, no attempts were made to provide additional temperature compensation. For the negative-output scaler driver, the lack of temperature compensation produces a very slight negative slope on the peak of the wave form at temperatures above 100°F.

When the discriminator driving both the positive- and the negative-output scaler drivers, with and without delay lines, was subjected to 120 times overdrive, the delay change ($\sim$4.5 nsec) in the output of the scaler drivers was observed to be dependent on delay changes or "walk" in the discriminator alone. However, the delay change of the scaler-driver output as a function of a temperature change of 120°F was approximately 2 nsec for both polarity scaler drivers, as compared to a 0.3-nsec "walk" in the discriminator alone.

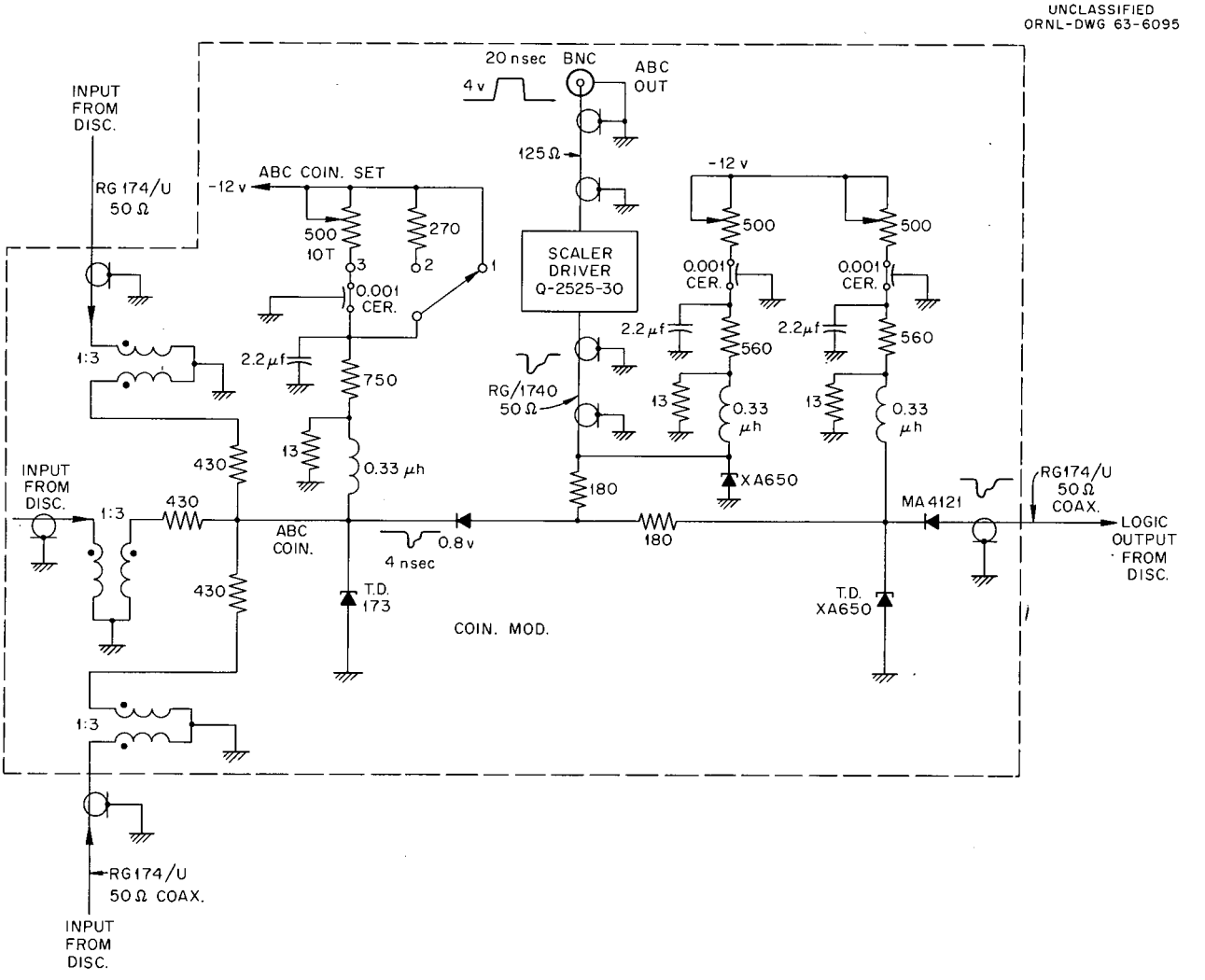

Fig. 2.1.5. Circuit for a Slow-Coincidence Module.

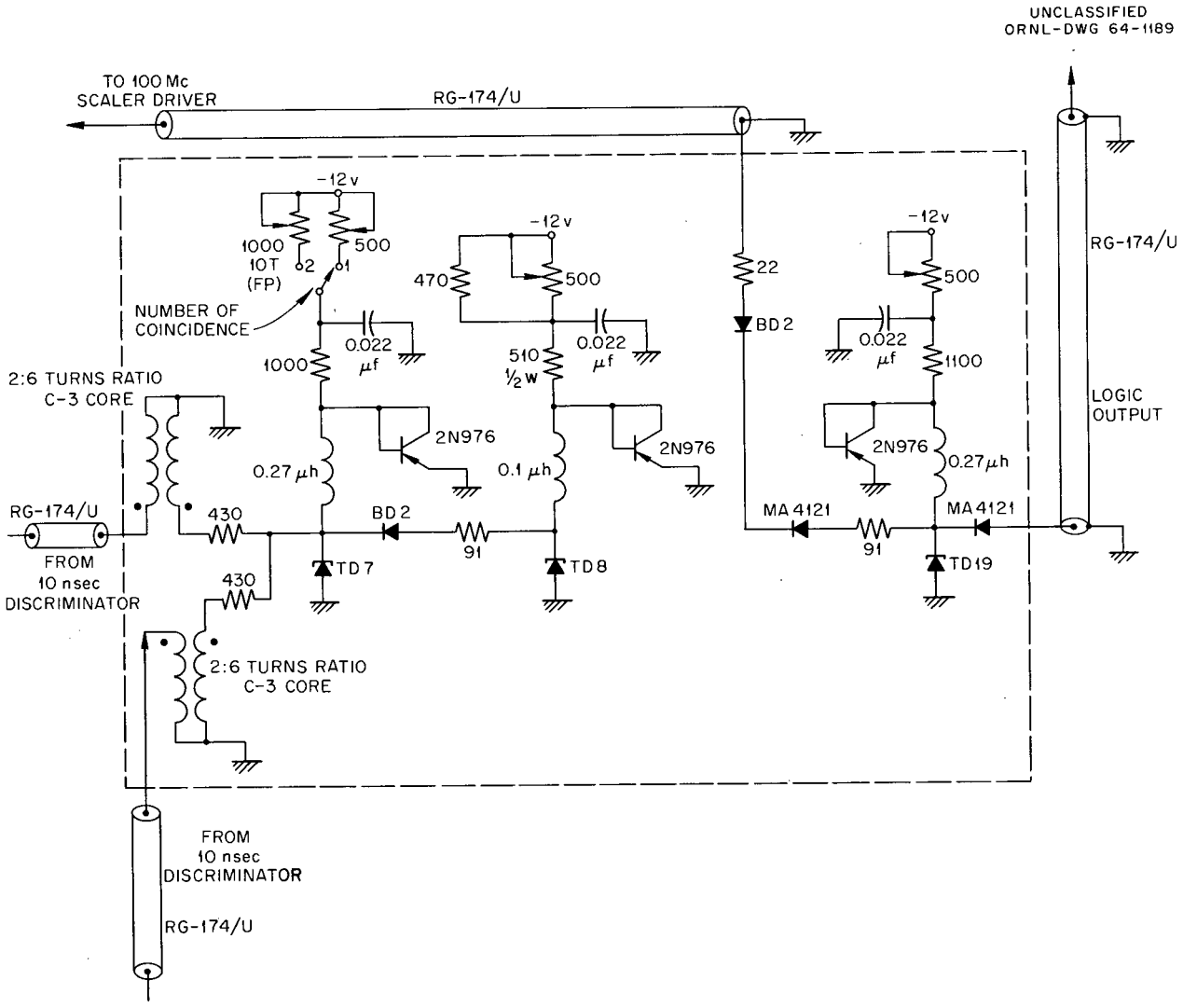

Fig. 2.1.6. Circuit for a Fast-Coincidence Module.

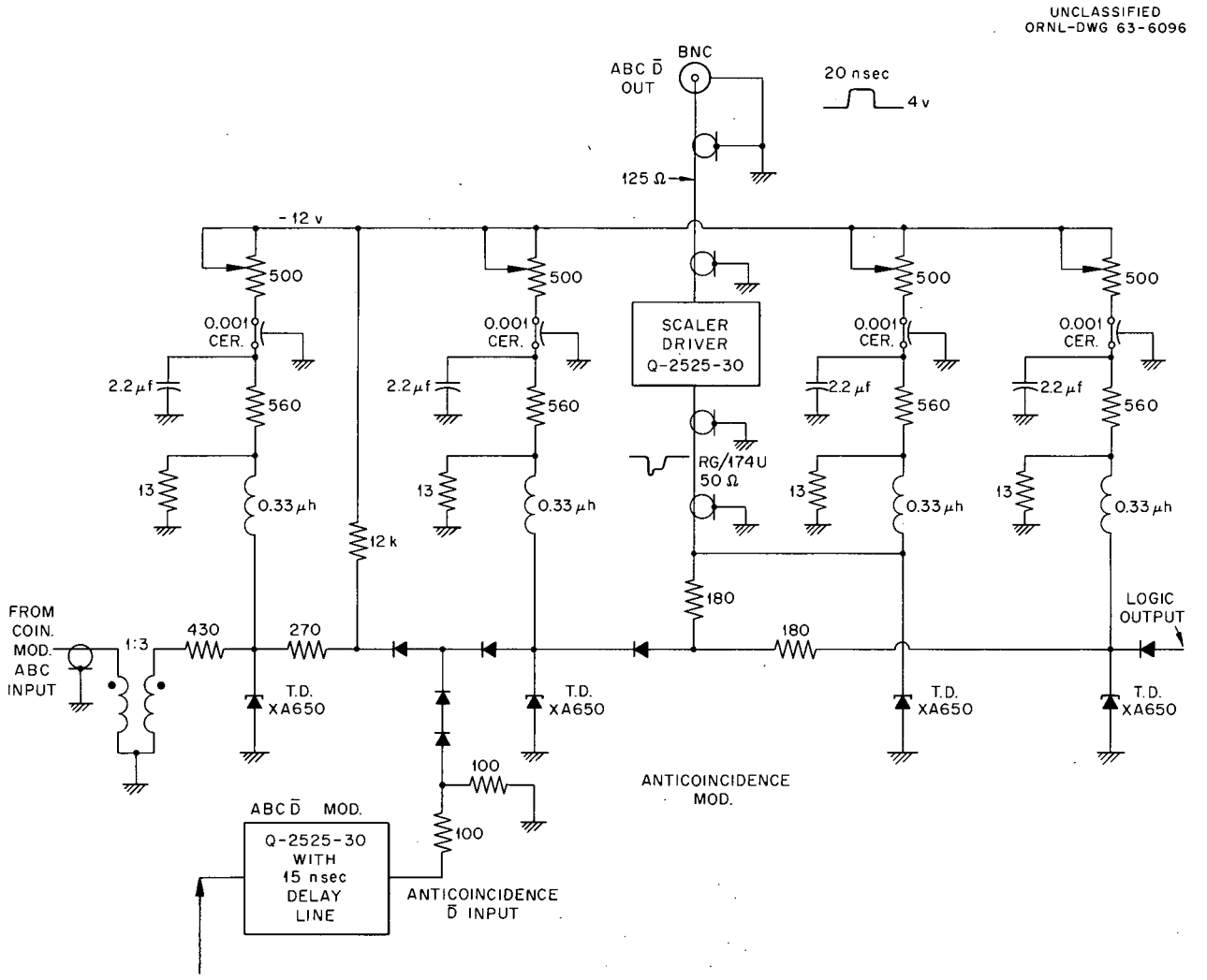

Fig. 2.1.7. Circuit for an Anticoincidence Module.

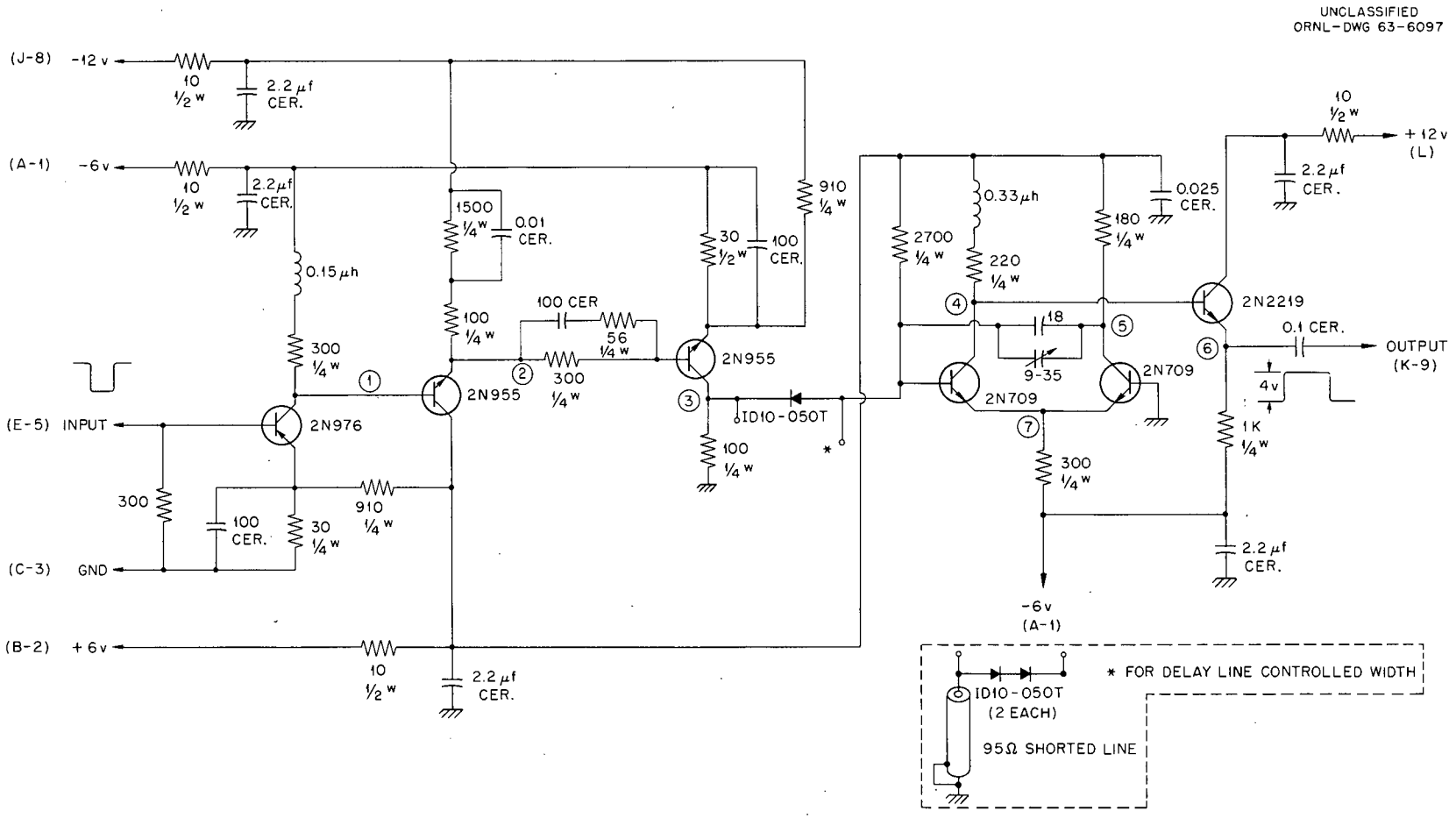

Fig. 2.1.8. Circuit for a Positive-Output Scaler Driver.

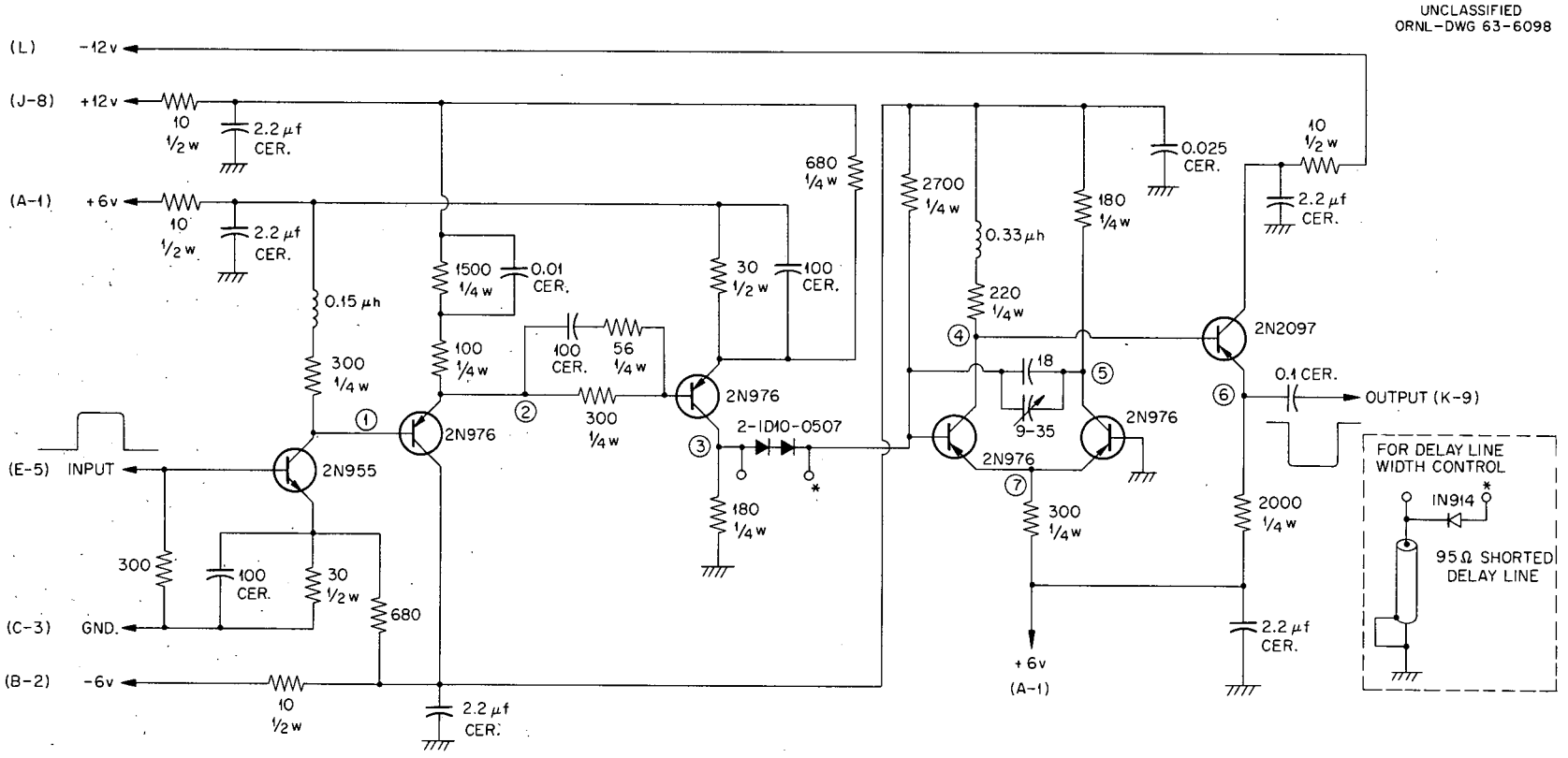

Fig. 2.1.9. Circuit for a Negative-Output Scaler Driver.

Table 2.1.3. Performance Data of a Positive-Output and a Negative-Output Scaler Driver With and Without Delay Lines

	Positive Output	Negative Output
	Without Delay Lines	
Output amplitude	+4 v	−4 v
Rise and fall time of output	4 nsec	7 nsec
Width change for 120°F change	19 nsec, or 0.16 nsec/°F, for 60-nsec width at 75°F	13 nsec, or 0.11 nsec/°F, for 50-nsec width at 75°F
	53 nsec, or 0.44 nsec/°F, for 490-nsec width at 75°F	92 nsec, or 0.77 nsec/°F, for 460-nsec width at 75°F
Amplitude stability for 120°F change	2% for 60-nsec width at 75°F	~7% for 50-nsec width at 75°F
	3.3% for 490-nsec width at 75°F	~7% for 460-nsec width at 75°F
Delay change in output for 120°F change	2.3 nsec (0.3 nsec due to discriminator "walk")	2.6 nsec (0.3 nsec due to discriminator "walk")
	With Delay Lines	
Width change for 120°F change	0.75 nsec for 122°F change for a 17-nsec width	1.0 nsec for 18-nsec width
Amplitude stability for 120°F change	5% for 122°F change for a 17-nsec width	2.4% for 18-nsec width

In order to satisfy the ≧40-nsec resolution requirement for the counting equipment, it was necessary to modify the input gate, limiter, and pulse shaper of the scalers (Computer Measurements Corp.) used in these experiments. The circuit designed to serve this modification is shown in Fig. 2.1.10. When this circuit is used with input *A*, the scalers have a pulse-pair resolution of less than 40 nsec for input pulses with widths ranging from 6 to 20 nsec and rise times ranging from 2 to 8 nsec. The input-pulse amplitude required for a 15-nsec-wide pulse of either polarity is 1.5 v. With input *A*, a continuous counting rate in excess of 12 Mc is possible, and pulse amplitudes in excess of 20 v can be tolerated and gated out. However, this circuit does not respond to pulses with rise times slower than 1.5 μsec; therefore, input *B* was developed. With this modification, the circuitry is capable of a pulse-pair resolution of less than 35 nsec for input pulses with widths ranging from 6 to 20 nsec and rise times ranging from 2 to 8 nsec. The amplitude required for a pulse of either polarity and 20 nsec wide is 1.0 v. Modification *B* also permits operation in excess of 12 Mc, and permits scaling sine-wave inputs well below 60 cps. (Amplitude requirements to scale sine waves down to 17 cps are less than 2.5 v peak.)

For those experiments requiring resolving times of 10 nsec, the circuit shown in Fig. 2.1.11 was designed. This scaler-driver module, in conjunction with the nonlinearly loaded univibrators described earlier, was capable of pulse quintuplicate (pulse train with five pulses separated ~10 nsec) resolution at a rate of 50 kc and delivers an ~4-nsec pulse of 3.5 v into a 50-ohm load. Figure 2.1.12 shows the behavior of one such unit as a function of ambient temperature.

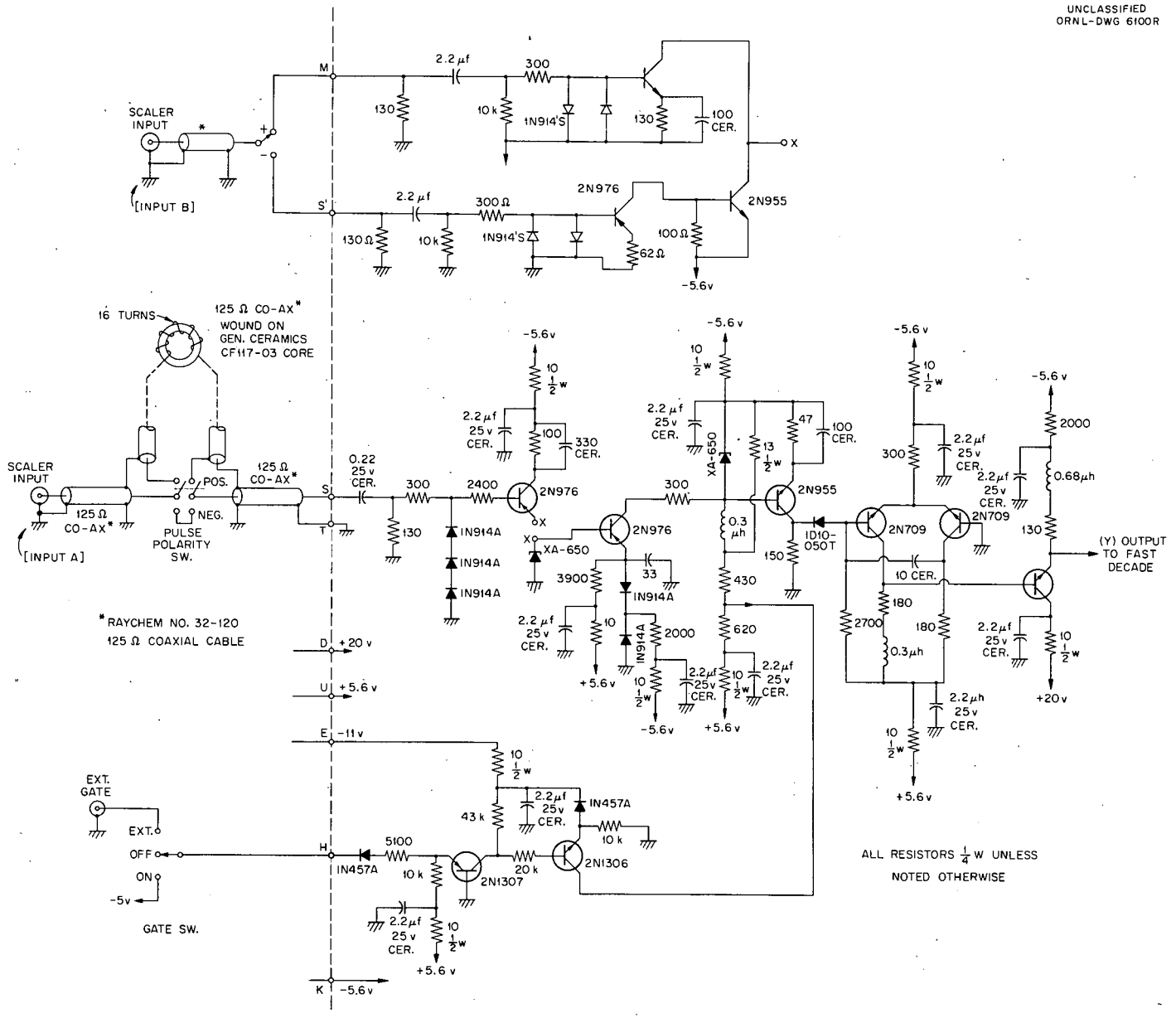

Fig. 2.1.10. Input Gate, Pulse Shaper, and Limiter for Computer Measurements Corporation Scaler.

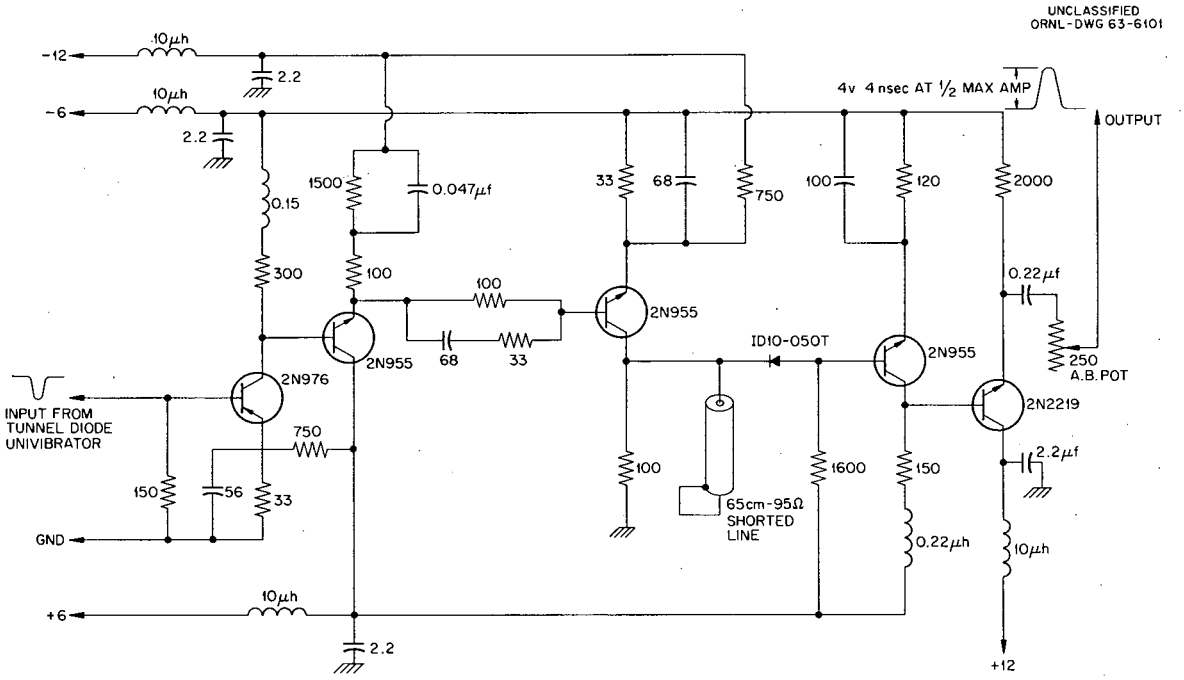

Fig. 2.1.11. Circuit for 100-Mc Scaler-Driver Module.

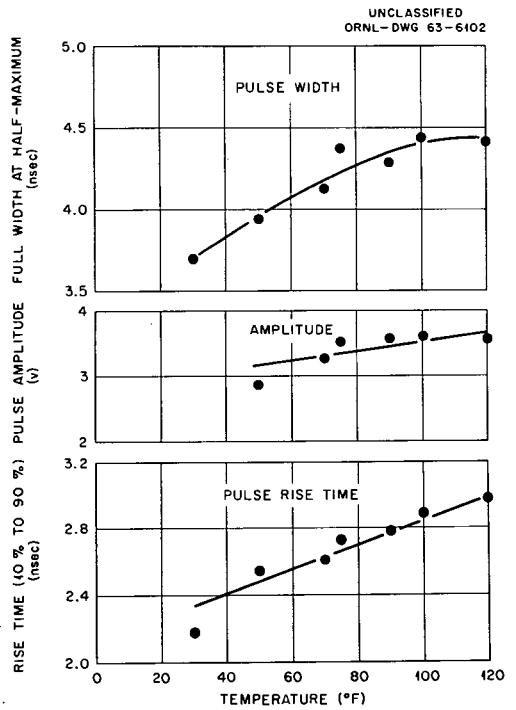

Fig. 2.1.12. Variation of Pulse Rise Time, Pulse Amplitude, and Pulse Width of 100-Mc Scaler Driver with Temperature.

Bibliography

(1) H. Ur, "Tunnel Diode High-Speed Circuits," p. 45 in *Proc. Intern. Conf. Instr. High Energy Phys., Berkeley, Calif., Sept. 12–14, 1960,* Interscience, New York, 1961.

(2) R. H. Bergman, "Tunnel Diode Logic Circuits," *IRE Trans. Electron. Computers* **9**(4), 430 (1960).

(3) G. Infante and F. Pandarese, "The Tunnel Diode as a Threshold Device: Theory and Application," p. 29 in *Nucl. Electronics,* Collective Vol. III, IAEA, Vienna, 1962.

(4) A. Whetstone and S. Kounosu, "Nanosecond Coincidence Circuit Using Tunnel Diodes," *Rev. Sci. Instr.* **33**(4), 423 (1962).

(5) A. L. Whetstone, "Survey of Nanosecond Techniques," *IRE Trans. Nucl. Sci.* **9**(3), 280 (1962).

(6) M. J. Morgan, "Comparison of Tunnel Diode Monostable Multivibrators," *Semicond. Prod.* **5**(7), 9 (1962).

(7) M. Cooperman and R. H. Bergman, "Tunnel Resistor – New Device to Speed Up Tunnel Diodes," *Electronics* **36**(28), 42 (1963).

2.2 INSTRUMENTATION OF A GAMMA-RAY PAIR SPECTROMETER TO REJECT NEUTRONS BY TIME-OF-FLIGHT TECHNIQUES

R. J. Scroggs

To measure only the gamma-ray energy spectra resulting from the bombardment of elemental targets with pulsed monoenergetic 150-Mev protons, a multicrystal gamma-ray spectrometer utilizing nanosecond circuitry was designed as part of the Experimental Space Shielding Program of the Neutron Physics Division.[1] Previous spectrometers were characterized by a large detrimental neutron background, attributable to the neutrons produced during proton bombardment. In these earlier spectrometers, bulk shielding was used to reduce the background generated by scattered neutrons. The present spectrometer also utilizes bulk shielding to reduce the background due to scattered neutrons, but in addition employs electronic time-of-flight techniques to discriminate against neutrons generated during the fixed-duration proton burst; thus, the high-energy neutron background is reduced – ideally by the time ratio of proton burst duration to repetition rate.

The nanosecond circuitry (ORNL model Q-2525-23A) is designed to open a gate when the proton beam strikes a target and holds the gate open for the duration of the beam, nominally 7 nsec. This gate action permits an energy analysis to be performed on the gamma rays arriving at the spectrometer as a result of the primary protons striking the target, but the associated slower-moving secondary neutrons and protons arrive at the spectrometer after the gate closes and are rejected from analysis.

To detect the primary proton beam, a 2-mm plastic scintillator coupled to a 56AVP photomultiplier tube is inserted into the beam, normal to the beam flight path and about 12 in. before the target (Fig. 2.2.1). The current pulse generated by the photomultiplier tube is transmitted through 200 ft of transmission line into one input of the coincidence detector where it is fed directly into a tunnel-diode limiter-discriminator-shaper circuit. The output of the shaper feeds one input of the tunnel-diode twofold coincidence circuit. The other input of the coincidence detector is fed from the anode of a second 56AVP photomultiplier tube which is coupled to an NaI(Tl) crystal. To prevent multiple pulsing from the slow decay of the NaI(Tl) crystal, the current pulse is clipped by a 13-nsec delay line. The clipped signal is fed through a limiter-discriminator-shaper circuit, identical to the one previously mentioned, and into the second input of the tunnel-diode twofold coincidence circuit. The resolution time of the coincidence circuit can easily be made as small as 5 nsec; by simple adjustment of bias current, the resolution time can be trimmed ±50% from any given value.

In these proton bombardment experiments, the neutron rejection rates varied from (59 ± 1)% for carbon to (77 ± 1)% for water. For an assumed constant-energy neutron spectrum, the maximum rejection ratio is limited by the machine to 83%.

[1]W. Zobel, F. C. Maienschein, and R. J. Scroggs, *Spectra of Gamma Rays Produced by the Interaction of ~160-Mev Protons with Be, C, O, Al, Co, and Bi*, ORNL-3506 (to be published).

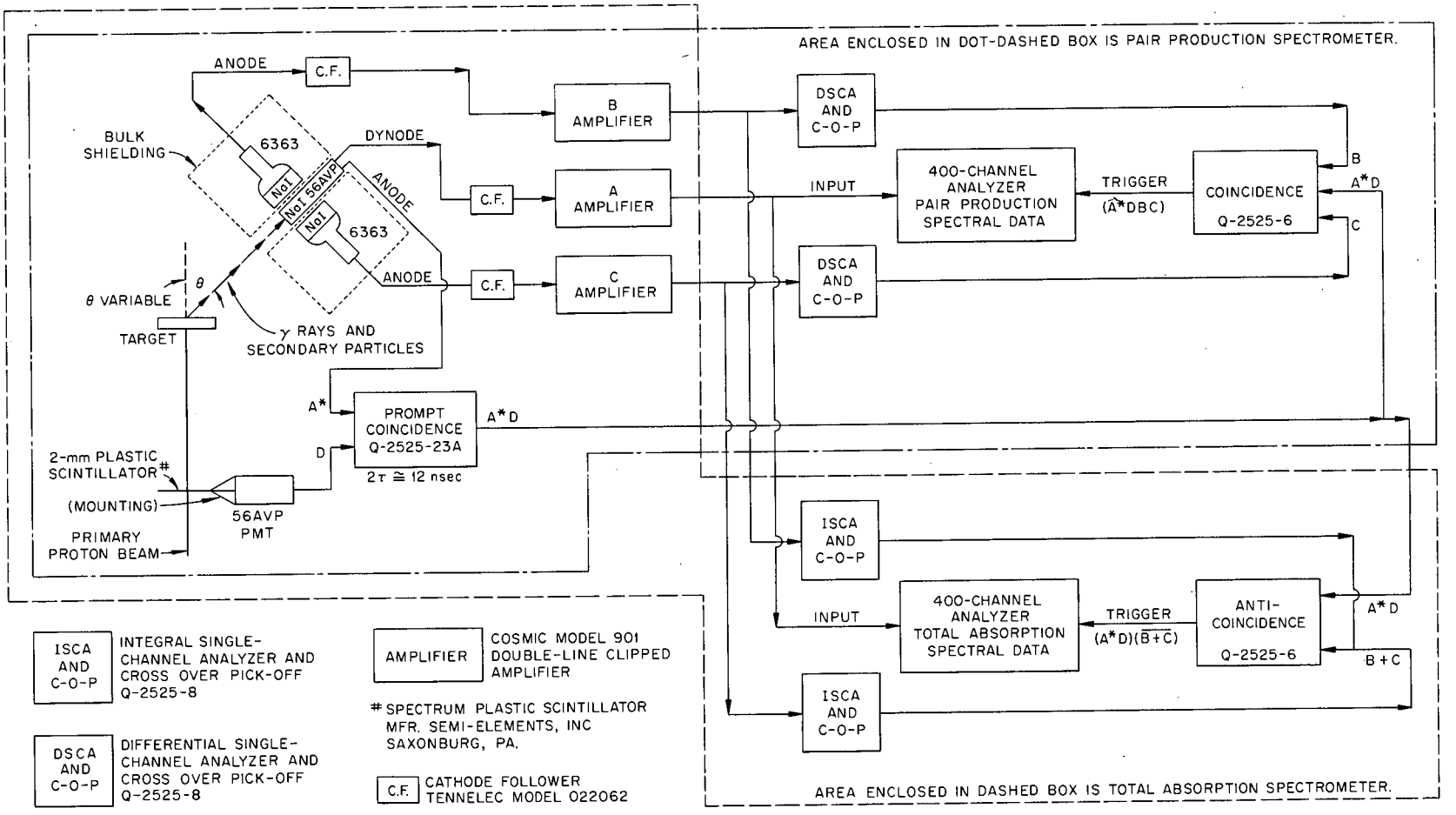

Fig. 2.2.1. Diagram of Gamma-Ray Spectrometers.

2.3 NANOSECOND PULSE PILE-UP DISCRIMINATOR FOR TIME-OF-FLIGHT MEASUREMENTS

R. J. Scroggs

This discriminator (ORNL model Q-2525-32) is one component of a time-of-flight system for studying the energy of secondary neutrons and protons emitted from an elemental target when it is bombarded with a pulsed monoenergetic 150-Mev proton beam. The time-of-flight measurement in this system is based on the assumption that one, and only one, primary proton strikes the target during an analysis period.[1] The pile-up discriminator was designed to add support to the realization of the experimental conditions predicated by this assumption.

This support is realized by interrogating the primary proton beam with a Spectrum Plastic Scintillator (Semi-Elements, Inc.) optically coupled to a photomultiplier tube whose output is a voltage pulse. This voltage pulse is suitably amplified and shaped and then fed into one input of a dc tunnel-diode amplitude discriminator. Because one primary proton may be accompanied by additional scattered particles whose combined actions in the scintillator can produce voltage pulses great enough to trigger the discriminator, a second interrogator system is employed. Its output is fed in coincidence with the output of the first system, with the result that two constraints are placed on the primary proton beam: one is time coincidence; the other, amplitude discrimination. If both constraints are violated, the instrument produces an output signal indicating pulse pile-up.

This instrument was used successfully in the time-of-flight experiment at the Harvard University Synchrocyclotron.[2] Details of the circuitry and performance characteristics are published elsewhere.[3]

[1] R. W. Peele *et al.*, *Flight Time Spectroscopy for Neutron and Proton Yields from Nuclei Bombarded by Protons*, ORNL-3360 (Sept. 1, 1962), p. 286.

[2] R. W. Peele *et al.*, *Neutron Physics Div. Ann. Progr. Rept. Aug. 1, 1963*, ORNL-3499, vol. II, p. 73.

[3] N. W. Hill and R. J. Scroggs, *Tunnel Diode Logical Circuitry and Associated Instrumentation for the Apollo Shielding Program of the Neutron Physics Division*, ORNL-TM-615 (to be published).

2.4 IMPROVEMENTS IN THE SNIP-SNAP SINGLE-CHANNEL ANALYZER

R. W. Peelle[1] T. A. Love[1]

Pulse-shape discrimination in accelerator experiments by pulse crossover timing requires a double-delay-line amplifier and a zero-crossing detector capable of processing the large range of energies encountered. In preparation for a neutron time-of-flight experiment to be conducted at the Harvard proton accelerator, zero-crossover pulse-shape discrimination was used to separate gamma rays (~150 kev to ~8 Mev) from neutrons (~1 to ~14 Mev) in experiments at the ORNL Neutron Physics and Shielding Laboratory (Building 3010). These radiations were detected in an NE-213 liquid scintillator, which is designed to produce the optimum difference in shape between pulses generated by neutrons (recoil protons) and gamma rays (electrons). This shape difference is inherent in the decay characteristics of the scintillations produced by light and heavy charged particles. Since the ratio of slow to fast optical decay components changes with incident radiation energy, the range of gamma-ray (electron) energies detectable through shape difference is approximately 30 to 1. (The slow-decay-light–to–total-light ratio for the higher-energy heavy particles approaches

[1] ORNL Neutron Physics Division.

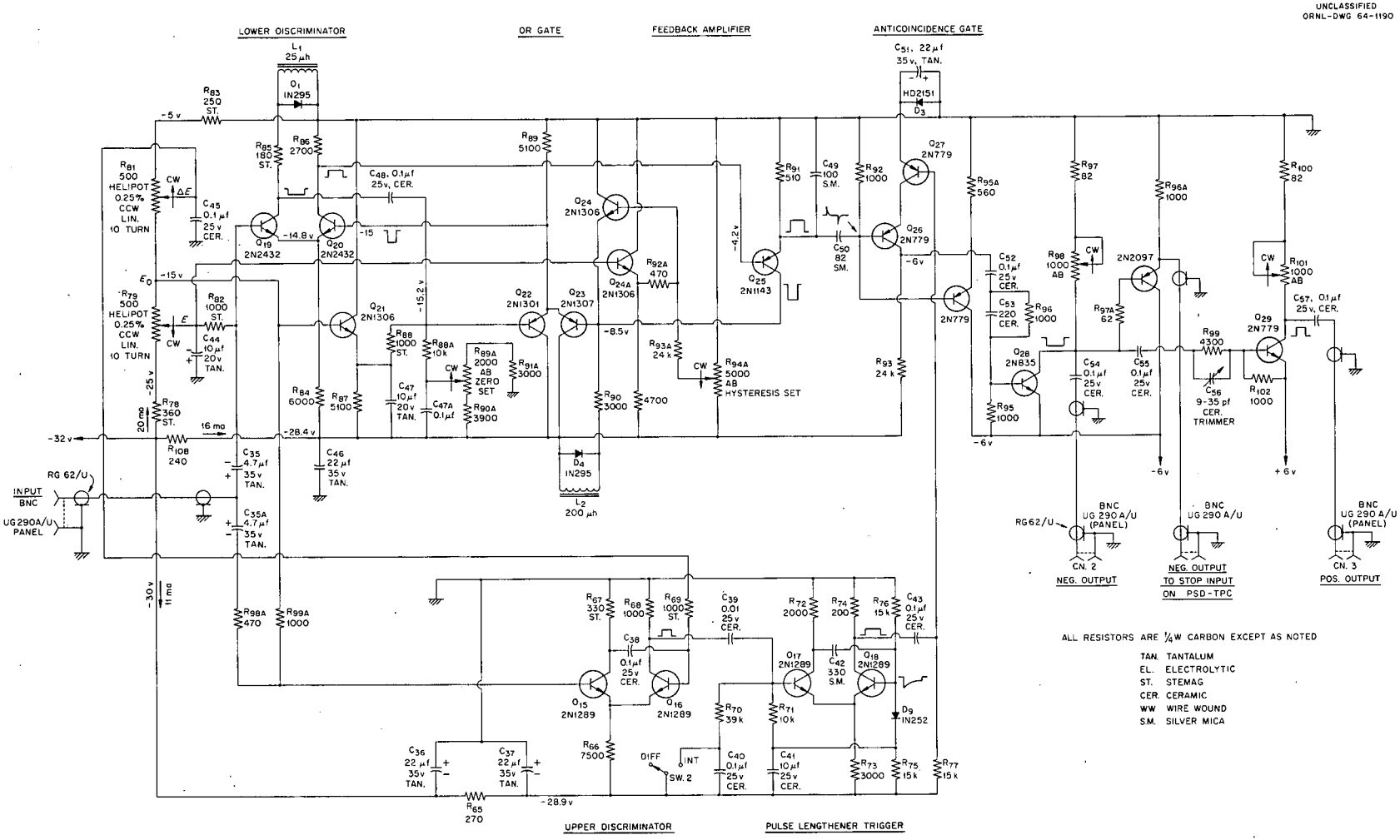

Fig. 2.4.1. Improved Snip-Snap Single-Channel Analyzer.

the ratio produced by electron excitation. The lower limit of 150 kev for the gamma-ray energy was chosen arbitrarily, and the dynamic range may, in fact, be greater than 30 to 1.)

The original design of the "snip-snap" single-channel analyzer[2] proved to have reliable zero-crossing detection over a narrow range of amplitudes; for example, when used with a double-delay-line amplifier,[3] this circuitry exhibited 6-nsec "walks" over amplitudes from 0.5 to 10 v when tested with a mercury pulser (ORNL model No. Q-1212). This range of 20 to 1 in voltage amplitude was obtained only after careful selection of 2N1289 transistors (no longer manufactured) for Q19 and Q20 in Fig. 2.4.1; however, small variations in the transistor parameters produced zero-level variations, for which there was no adequate adjustment, in the lower-level discriminator. In addition, comparable transistor-parameter variations produced hysteresis levels that caused severe zero-crossing-time differences from unit to unit. Thus, the 2N1289 transistors were selected to offset the slight variations in the other transistors in the lower-level discriminator.

These problems were eliminated by the addition of the potentiometer R89A (Fig. 2.4.1) to furnish a "zero-set," by the addition of transistor Q24A and potentiometer R94A, and by the reduction of the collector load of Q19 to 180 ohms to permit adjustment of the hysteresis. Moreover, these modifications permit the use of unselected 2N2432 and GA568305 (Texas Instruments) to replace the 2N1289 transistors. (The lower value of the reverse base–to–emitter-voltage rating of these two transistor types does not permit operating at bias levels above 5 v for the lower discriminator.) With a modification to the standard amplifier to permit 12-v output amplitudes, this combination of amplifier and snip-snap single-channel analyzer exhibits "walks" of less than 6 nsec for pulser amplitudes of 0.15 to 12 v. The time of zero crossing is independent of pulse-generator amplitude over a range of approximately 80 to 1.

[2]T. L. Emmer, *Instrumentation and Controls Div. Ann. Progr. Rept. July 1, 1961*, ORNL-3191, p. 8.

[3]R. L. Chase, *IRE Trans. Nucl. Sci.* **8**(3), 45 (1961).

2.5 ISOLATED SIGNAL DETECTOR

N. W. Hill R. W. Peelle[1] J. W. Madison

In the application of time-of-flight techniques to the study of the energy spectrum of secondary radiation produced in targets by accelerated particles, it is of interest to analyze only those secondaries whose time of origin is uniquely known. Secondaries of different energies created by primaries of different time origins could give rise to the same measured "time of flight"; consequently, an instrument capable of distinguishing a primary event sufficiently isolated in time from other possible primary events is highly desirable.

The proton beam from a synchrocyclotron occurs in bursts. Since the beam is extracted only when the frequency of the accelerating voltage is within narrow limits of the operating frequency, a burst structure, called macrobursts, occurs at the modulation frequency of the cyclotron. Macrobursts at the Harvard cyclotron, for instance, occur at 288 bursts/sec with a duty cycle from 2 to 6%. A study of the fine detail of these macrobursts shows that a time distribution of protons occurs within the macrobursts. This substructure, called microbursts, occurs at the rf accelerating frequency. The period between bursts is about 42 nsec. Delayed coincidence of the burst widths with resolving times of 3.5 to 6.2 nsec gave delayed coincidence curves of 4.5 to 6.3 nsec. Visual observations and photographs of microstructure detail for many rf cycles show no protons outside this time domain.

[1]ORNL Neutron Physics Division.

Instrumental selection of a suitably isolated proton is accomplished in the following manner. Fast current pulses from the 1-mm-thick plastic scintillators, A and A', in Fig. 2.5.1 are fed to tunnel diode discriminators shown in Sect. 2.1, Fig. 2.1.3. The output of these two discriminators is then applied to a fast (2-nsec resolving time) coincidence circuit shown in Sect. 2.1, Fig. 2.1.6. This coincidence system collimates the beam to be analyzed by determining if the detected proton passed through both counters. Delayed coincidence curves made at Harvard indicate that this circuit operated with a coincidence efficiency in excess of 99%. The dead time (pulse-pair resolution) of the tunnel diode univibrators used in this "isolated signal detector" is 10 nsec, which means that two protons in the same rf microstructure burst cannot be resolved, whereas those in adjacent rf cycles always generate coincidence pulses. The isolated signal system shown in Fig. 2.5.2 was fabricated with tunnel diode and transistor circuit elements. Outputs at each logic level in the instrument are provided for counting purposes. Before the data on any detected secondary particle can be stored, pulses from the fast (AA') coincidence must survive inspection by the isolated signal system, which also includes a pulse pile-up anticoincidence network.

For operation at Harvard, the isolated signal detector was adjusted to eliminate any grouping of protons within a train of pulses falling within 115 nsec of each other. (Synchronizing delays D_1, D_2, and D_3 of Fig. 2.5.2 account for circuit dead times and delays, but are not essential to the basic understanding of the operation of the circuitry.) The pulse storage delays, I and II, were set at the desired isolation interval (115 nsec, in this case). An isolated-coincidence input pulse fired both binaries and reset them at the end of the isolation time, giving an output via the "trailing edge coincidence" shown in Fig. 2.5.2. When two input pulses were too closely spaced, the first input pulse set binary I and then reset it after passage through pulse storage delay I. The second input pulse was therefore eliminated by binary I, which was already set by the first input pulse. The first input pulse itself was then eliminated by the action of the second input pulse which had already reset binary II. Practical circuit delays were important because binary dead times were about 5 nsec, while the reset and output coincidence circuits had ~3-nsec resolving times. When tested with a pulse-train generator that produced three and four pulses whose time separations were adjustable, the finite pulse widths, the resolving times of the included coincidence circuits, and the inherent circuit delays limited the proper operation of the system about a narrow time region, ~2 nsec wide. This limitation occurred for pulse trains whose individual pulses were centered on or about the selected isolation period (115 nsec). In actual operation, such a pulse train represents an unlikely event, based on statistics and the observed microstructure periods (41.2 to 44 nsec).

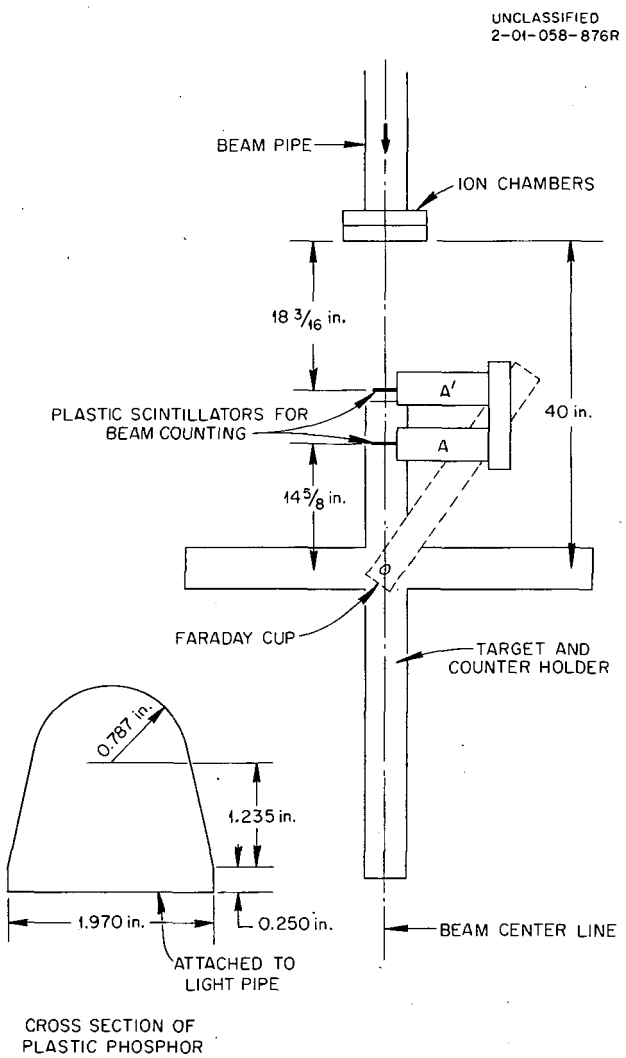

Fig. 2.5.1. Experimental Geometry for Flight-Time Experiments, Including Cross Section of the 1-mm-thick A and A' Beam Scintillators.

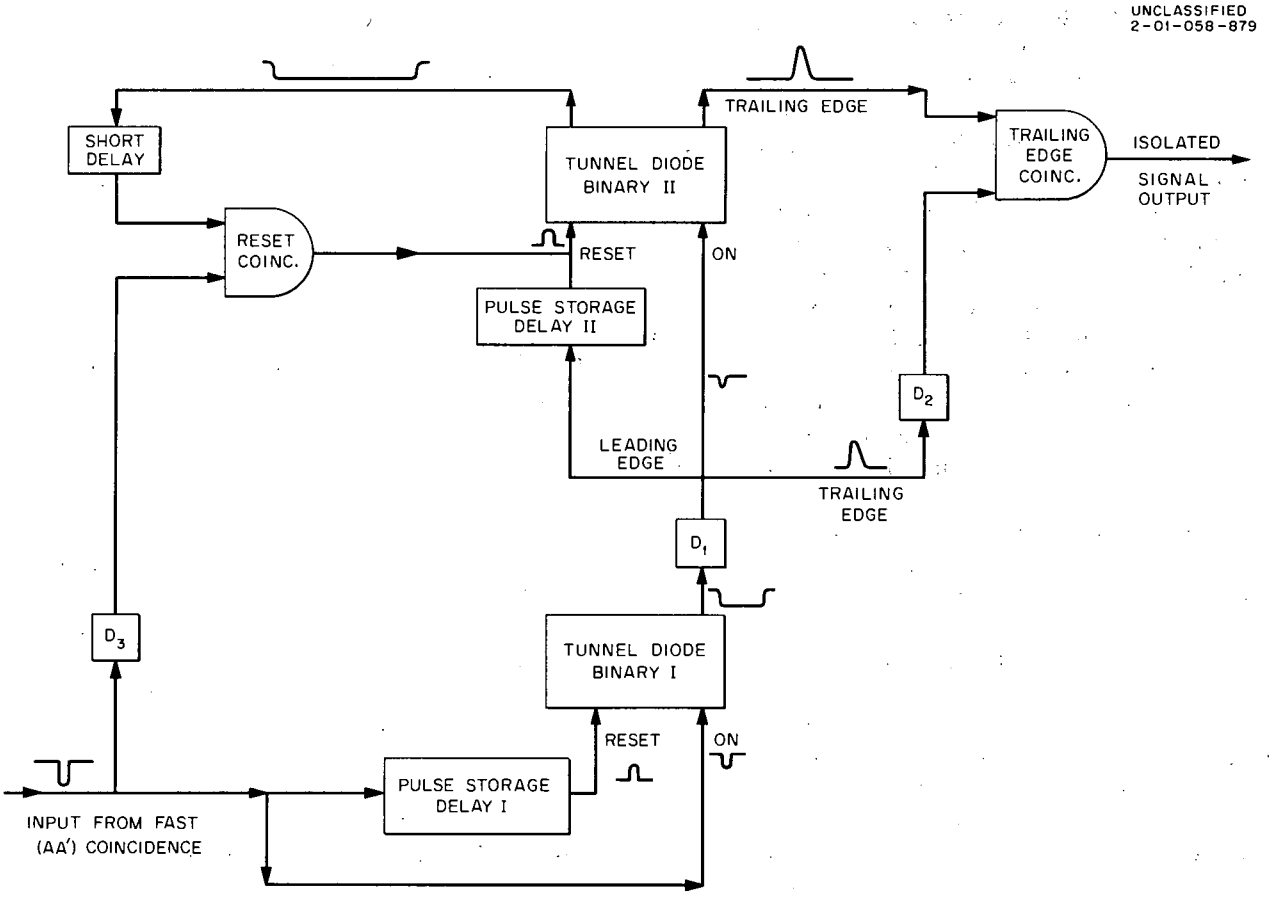

Fig. 2.5.2. Diagram of Isolated Signal Detector.

2.6 TIME–TO–PULSE-HEIGHT CONVERTER

F. M. Glass[1]

To measure time intervals shorter than 1 μsec electronically, it is currently necessary to rely on a transformation of the timing information from the nanosecond to the microsecond time domain, where electronic time processing can take place using a voltage-pulse lengthener, ramp generator, comparator, and oscillator countdown technique.[2] The transformation involves the conversion of two fiducial signals which mark the edges of a given timing interval into a voltage amplitude directly proportional to the duration of the timing interval. The device which performs the conversion is a time–to–pulse-height converter.

As part of the Neutron Physics Division effort in obtaining data about the behavior of neutrons, a time–to–pulse-height converter was designed

[1]The author acknowledges the assistance of W. H. Williams in laying out and constructing the instrument.

[2]F. J. Walter *et al.*, *Physics Div. Ann. Progr. Rept. Jan. 31, 1962*, ORNL-3268, p. 55.

and fabricated to measure time intervals as short as 0 to 50 nsec in a neutron time-of-flight spectrometer. Severe electronic design restrictions must be met in measuring such short time intervals. All the details of fast-circuit requirements must be considered. To this end, tunnel diodes are employed in the start and stop discriminators and in the fast-gate circuit. Fast transistors are employed in all other circuits, and the outout signal is appropriately shaped for analysis in an RIDL model 34-12 (or 34-128) 400-channel analyzer.

The converter incorporates a variable delay line through which the output signal can be delayed from 0.2 to 2.2 μsec; during this time, the circuit logic can reach decisions about the status of associated experimental constraints. Additionally, the converter provides a fast-rise gating signal as well as a signal that indicates the total open time of the fast gate.

Double-sided printed-circuit techniques were employed in fabricating the converter. A fiberglass base board, $\frac{1}{8}$ in. thick, has 0.0028-in.-thick copper foil epoxyed to it. One side of the board serves as the front panel and the copper foil associated with it serves as the HQ (high quality) ground and power distribution ground only (Fig. 2.6.1). Printed strip lines provide clean power distribution with minimal decoupling and bypassing, because every effort was made to assure balanced currents along all feed lines; for example, the power ground return is connected to the HQ ground at only one point. Similarly, power lines on the opposite side of the board are fed as nearly alike as possible. All input and output connectors are mounted directly on the HQ ground.

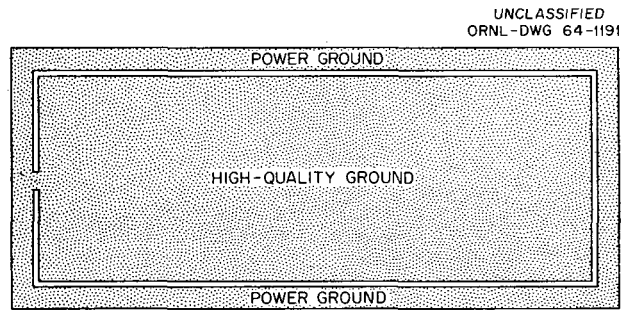

Fig. 2.6.1. Typical Ground Side of Double-Sided Board.

The converter spans three timing ranges: 0 to 50 nsec, 0 to 100 nsec, and 0 to 150 nsec. Its sensitivity is 1 ma or 50 mv for both discriminators. The integral linearity is 0.5%, while the walk is 0.7 nsec for 50 times overdrive. The input impedance of the start and stop discriminators is 50 ohms; the input impedance of the inhibit gate is 125 ohms. All output impedances are 10 ohms.

2.7 TIME-TO-PULSE-HEIGHT CONVERTER

J. L. Lovvorn

An improved time–to–pulse-height converter was developed for the Neutron Physics Division to help obtain more reliable data from neutron time-of-flight measurements. The timing circuitry utilizes transistors of high stability and fast switching response. A toggle circuit ultimately controls the start and stop of a constant current, which charges a capacitor for the time–to–ramp-voltage conversion. A univibrator circuit in the start line has an 80-μsec dead time which inhibits succeeding pulses from retriggering the start circuit until the maximum time period of the converter has elapsed. Either a stop signal or the automatic dump circuit acts to dump the charge on the capacitor to reset the converter for the next event. A Darlington pair (double emitter-follower circuit) on the output provides a low-impedance output to feed a modified Nuclear Data

multichannel analyzer. Pulses suitable for driving the start and stop inputs of a time-interval meter are provided coincident with the start and stop pulses of the time–to–pulse-height converter. The entire timing system covers three distinct ranges of 0 to 4 μsec, 0 to 8 μsec, and 0 to 80 μsec, and has a stability of 5 channels in 250. This stability factor is not all attributable to the time–to–pulse-height converter itself, but represents the stability factor of the entire timing system, including a modified multichannel analyzer.

A similar unit is being constructed for use in a mass spectrometer in which the arrival times of electrons and ions formed during the bombardment of a gas with x rays will form the start and stop signals. In this sense, the time–to–pulse-height converter will act as a coincidence unit.

2.8 AMPLITUDE-CORRECTING CIRCUIT FOR TIME ANALYZER IN THE NANOSECOND RANGE

W. H. duPreez[1] C. W. Williams

Time shifts caused by the variation of signal amplitude in the start and stop channel of a time–to–pulse-height converter can seriously deteriorate the time resolution of a neutron time-of-flight spectrometer.[2] A circuit (Fig. 2.8.1) was designed which corrects the output of a time–to–pulse-height converter by adding to the output a signal dependent on the amplitude of the start pulse. In the present application, the signal used to stop the converter is a constant-amplitude signal derived from the pulsed beam of a Van de Graaff accelerator, so that this "amplitude effect," or "walk," occurs only in the start channel.

The start-pulse amplitude information is brought to the antiwalk circuit through a slow side channel of the spectrometer. This linear signal is compared with a standard reference signal, and the difference is added to the output of the time–to–pulse-height converter. A suitable signal from the side channel is used to trigger the reference generating circuit. Means are provided to change the position in the pulse-height spectrum below which the corresponding time signals are linearly corrected. The amplitude of the correction signal can also be adjusted before it is added to the time signal from the converter.

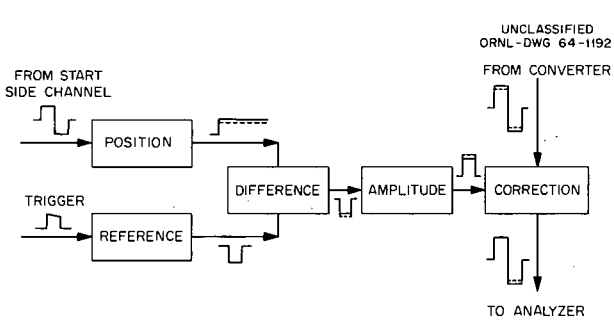

Fig. 2.8.1. Diagram of Amplitude-Correcting Circuit.

The circuit was tested by measuring the width of an Na^{22} prompt γ-γ coincidence line. A narrow side channel (from approximately 135 to 225 kev electron energy) was used in the stop side to limit its contribution to the time spread. A time spectrum obtained with a wide window (for approximately 45 to 340 kev electron energy) in the start side channel and with the antiwalk circuit switched off was compared with the same time spectrum with the antiwalk circuit switched on and with the same windows and accumulation time (Fig. 2.8.2). It is concluded that this circuit makes it possible to obtain excellent time resolution while using almost the total Compton spectrum to start the converter.

[1]Visitor from the South Africa Atomic Energy Board, Pretoria, South Africa.

[2]P. Huber *et al.*, *Nucl. Instr. Methods* **14**, 131 (1961).

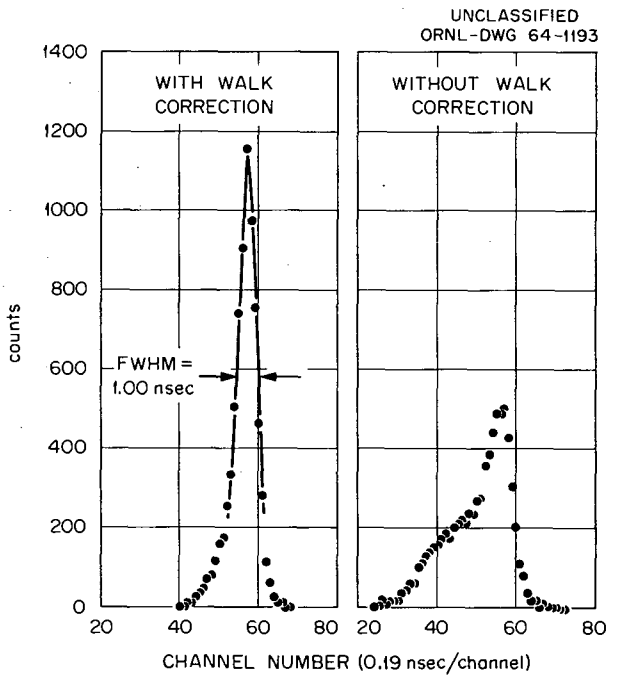

Fig. 2.8.2. Time Spectra of Na^{22} Prompt γ-γ Coincidence Line.

2.9 FAST DOUBLE PULSER

F. M. Glass

In evaluating time–to–pulse-height converters and fast-coincidence circuits, a need for a multiparameter double pulser arises. To satisfy this need, a fast double pulser (ORNL model Q-2525-4) was developed.

The outputs from the pulser are: two simultaneous negative pulses, two delayed negative pulses, and one delayed positive pulse. The delay is 0 to 100 nsec. Pulse rise time is 0.9 nsec, and fall time is 2 nsec. The pulse width at 10% value is 4 nsec. The amplitude is 15 v, and the overshoot is 1%.

A 2N491 silicon unijunction transistor in a variable-frequency relaxation oscillator supplies trigger pulses over a frequency range from 1 to 10 kc. These pulses trigger an avalanche transistor (SM1569 or 2N2219) which delivers fast negative pulses through parallel networks to a pair of connectors. Additionally, this same transistor provides a trigger for a second comparable avalanche transistor; however, this trigger signal is delayed from 0 to 100 nsec by a continuously variable delay line. The second avalanche transistor delivers two negative pulses and a positive pulse through parallel networks. All outputs have 50-ohm terminations; no reflection or ringing in any output occurs from cable mismatch at the other outputs.

2.10 DEVELOPMENT OF TIME-INTERVAL METER WITH 1-nsec RESOLUTION

J. L. Lovvorn

The basic limitation to the measurement of nanosecond time intervals has been the response times of standard circuits and vacuum tubes. To circumvent this limitation, timing information in the nanosecond time domain is presently transformed to the microsecond time domain, where conventional techniques are relatively simple, via a time–to–pulse-height converter. However, recent electronic advances have suggested the possibility of a nanosecond clock, whereby short time intervals could be measured directly; consequently, specifications for a 2-nsec-resolution, digital-type time interval meter were formulated. Development of the meter was undertaken under contract by Eldorado Electronics, Berkeley, California, and the development has been completed. Performance of the meter meets or exceeds the contract specifications.

The time interval of the meter is 1 nsec to 0.1 sec with an accuracy of 1 nsec and resolution of ±0.5 nsec. The deviation of the least significant digit (where the indicated digit fluctuates between two numbers) is only 30 psec. The clock stability is 5 parts in 10^6 parts, short term. Input is 1 v minimum to 10 v maximum, either polarity, with 4-nsec pulse width minimum into 50 ohms. The slope of the input is 0.2 v/nsec, or more. Succeeding start pulses are prevented from triggering the instrument by a lockout feature which holds until the instrument is reset. Reset is either automatic, manual, or remote. The output is displayed by Nixie tubes and is binary-coded decimal (BCD) for recording.

2.11 INSTRUMENTATION FOR MULTIPARAMETER FISSION-FRAGMENT ENERGY-CORRELATION MEASUREMENTS

C. W. Williams

H. W. Schmitt[1] F. J. Walter[1] J. H. Neiler[2]

Experiments for correlation of fission-fragment energies have been conducted at ORNL for some time.[3,4] Although the electronic system for these experiments is conceptually simple, it is quite complex in operation. The system (Fig. 2.11.1) is presently limited to three parameters with 128 by 128 by 16 channels of memory in an event-by-event punched-paper-tape acquisition system. A new analyzer being procured will have a 256 by 256 by 256 channel memory with provisions for adding a fourth parameter.

Conventional charge-sensitive preamplifiers having high feedback factors are used with large-area solid-state detectors. Each output of the double delay-line clipped amplifiers is fed in parallel to a single-channel analyzer and crossover pick-off[5] and through a delay to one of the analyzer analog-to-digital converter (ADC) inputs. The outputs of the crossover pick-off units are fed to a fast coincidence unit, whose resolving time is adjusted

[1]Physics Division.

[2]Formerly with the Physics Division; now with Oak Ridge Technical Enterprises Corp., Oak Ridge, Tenn.

[3]H. W. Schmitt *et al.*, *Phys. Rev. Letters* **9**, 427 (1962).

[4]F. J. Walter *et al.*, *Fragment Mass Distribution for Thermal- and Resonance-Neutron-Induced Fission of* Pu^{239}, ORNL-3425, p. 79.

[5]T. L. Emmer, *IRE Trans. Nucl. Sci.* **9**(3), 305–13 (1962).

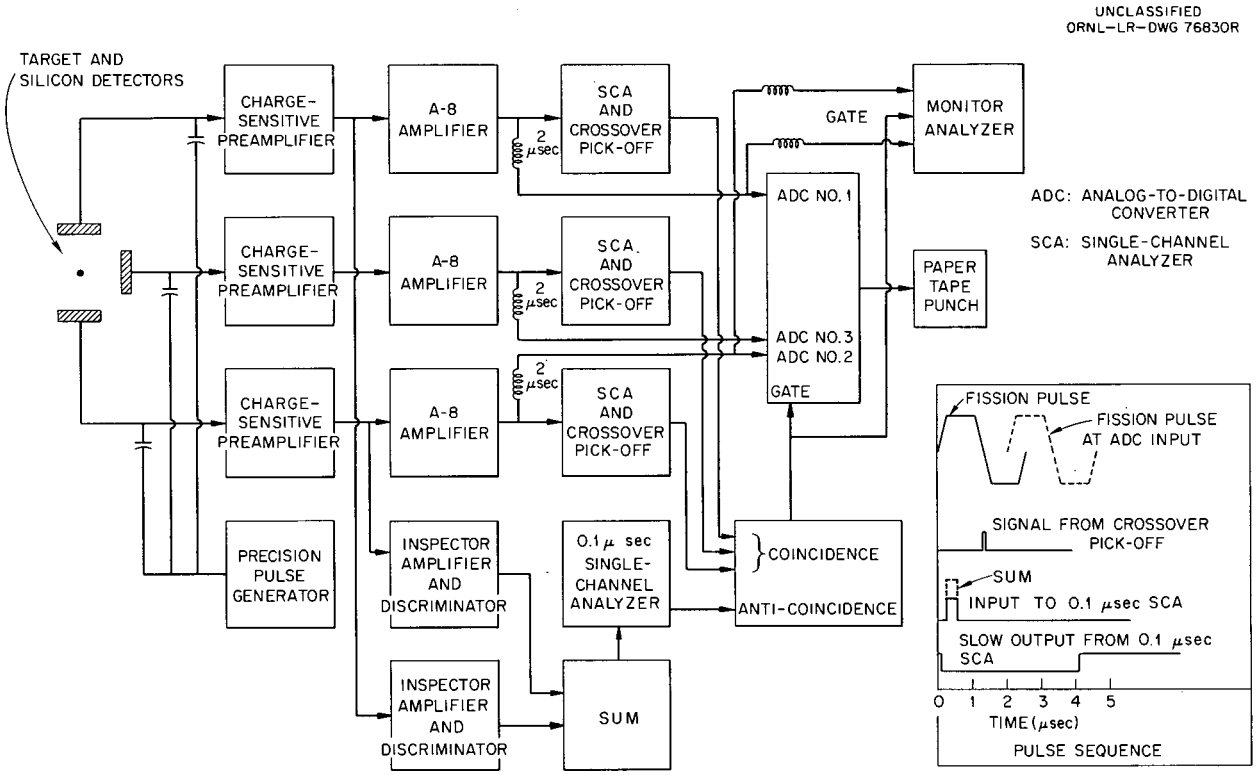

Fig. 2.11.1. Instrumentation for Fission-Energy Correlation Measurements.

to be 40 nsec; this is about three times the minimum time necessary for operation of the circuit.

Reduction of the coincidence resolving time reduces the effective gate-open time but cannot reduce the effect of pile-up (multiple pulses arriving within the amplifier resolving time). This system contains an inspector circuit which reduces the pile-up time by approximately a factor of 4. The fission spectra from two of the preamplifiers are inspected, and all noncoincident events within the inspector resolving time are removed by preventing the coincidence-enabling signal from reaching the analyzer.

2.12 NEUTRON TIME-OF-FLIGHT SPECTROMETER FOR NEUTRON ENERGIES OF 100 kev OR MORE

C. W. Williams R. K. H. Wagner[1] P. D. Miller[1]

To investigate the spin-spin interaction term in the optical-model potential, an experiment has been scheduled in which polarized neutrons obtained from the $Li^7(p,n)Be^7$ reaction are to be scattered from a polarized Ho^{165} sample.[2] At 51° and 350 kev neutron energy, the polarization is 55%.[3] A spectrometer (Fig. 2.12.1) was designed for this experiment to give a time resolution of approximately 2 nsec and an efficiency of approximately 20% for 350-kev neutrons.

[1]Physics Division.

[2]R. K. H. Wagner *et al.*, "Scattering of Polarized Neutrons from Polarized Ho^{165}," submitted to *The Physical Review*.

[3]A. J. Elwyn and R. O. Lane, *Nucl. Phys.* **31**, 78 (1962).

UNCLASSIFIED
ORNL-DWG 63-2174R

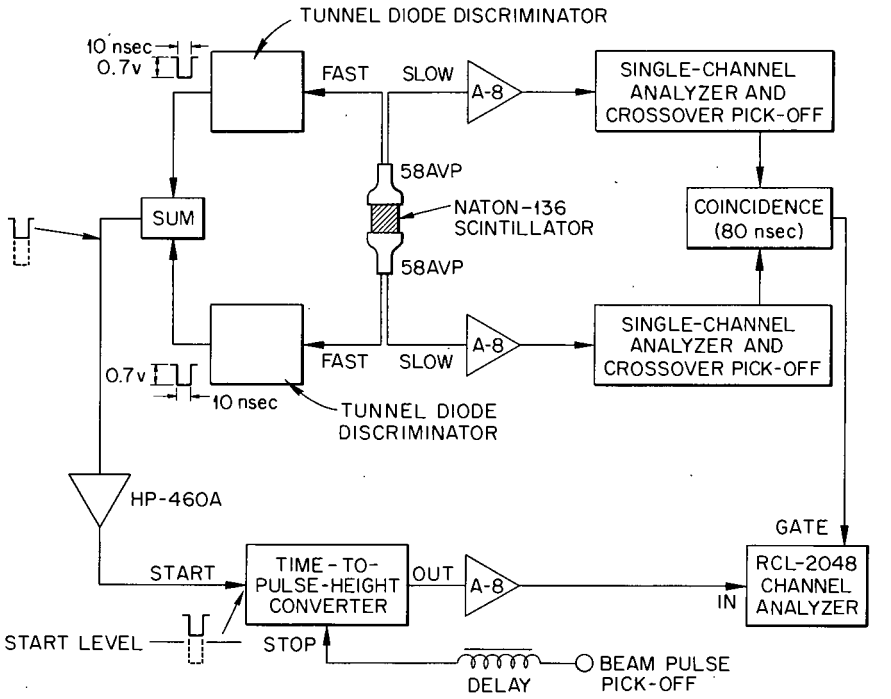

Fig. 2.12.1. Diagram of Time-of-Flight Spectrometer for 350-kev Neutrons.

To reduce the effect of photocathode noise and to maintain good detection efficiency, two phototubes view the same scintillator and require a fast coincidence between their outputs. The system, incorporating antiwalk correction (Sect. 2.8), was tested with an Na^{22} source and a third tube, which provided the time reference. With a start-level range of 6 to 60 kev electron energy, the time resolution was measured to be 1.6 nsec fwhm. The neutron energy corresponding to this lower level is approximately 75 kev. Experiments with unpolarized neutrons are now in progress.

2.13 INDICATING AND LOGIC MODULES

J. H. Todd

A series of modules (ORNL model No. Q-2563) was developed to monitor the outputs of various instruments. These modules perform logic functions to indicate certain combinations of signals, as well as to indicate, both locally and at a remote central point, the condition of any number of widely scattered instruments or combination of instruments. The modules are actuated by signals with two discrete states. Although the modules were designed specifically to recognize the opening of a closed contact, an analog signal can be used just as easily.

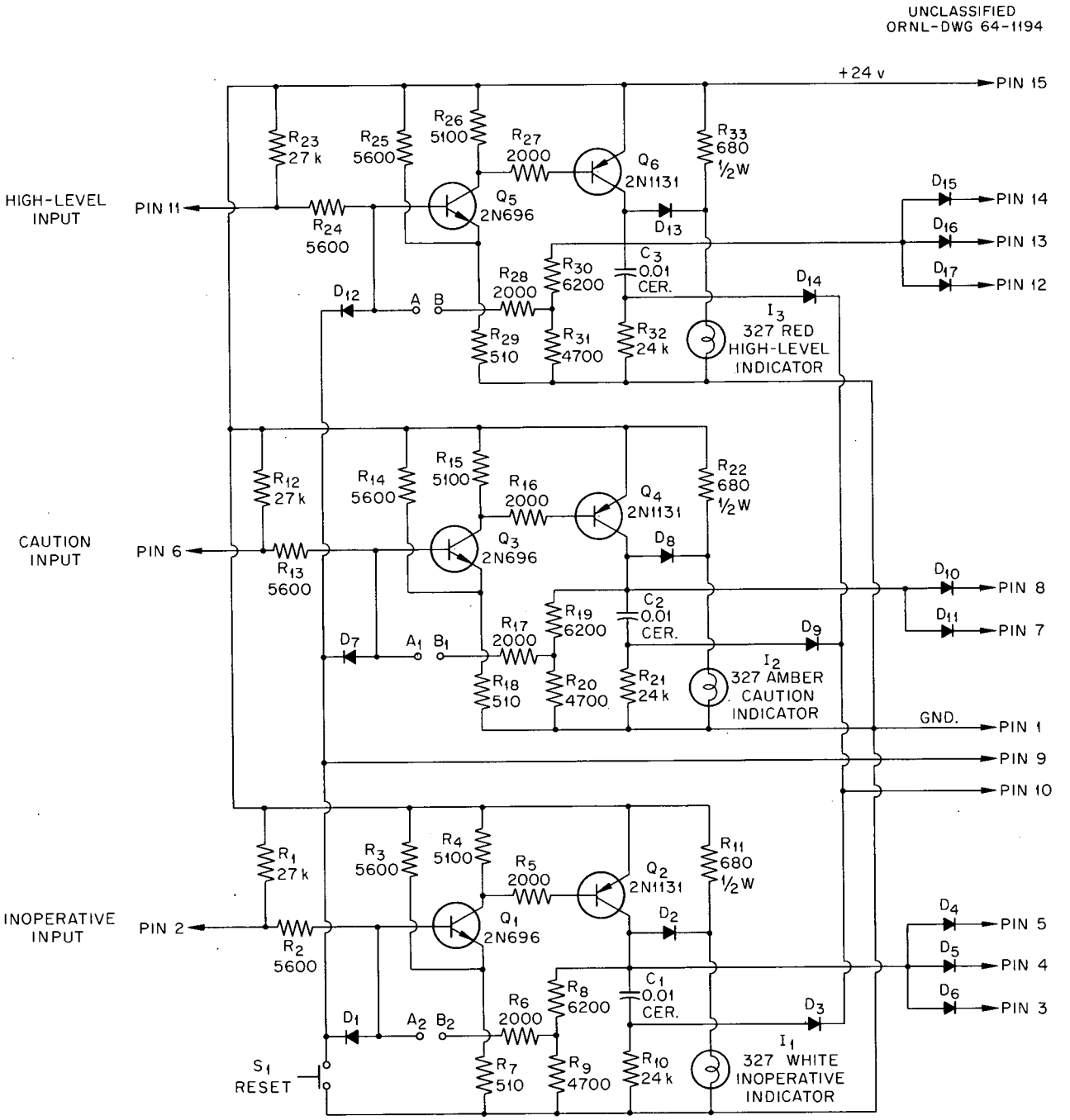

INSTALLATION OF A JUMPER BETWEEN POINTS A TO B, A_1 TO B_1 AND A_2 TO B_2 WILL PROVIDE LATCHING ACTION.

Fig. 2.13.1. Three-Channel Indicating Module with Outputs.

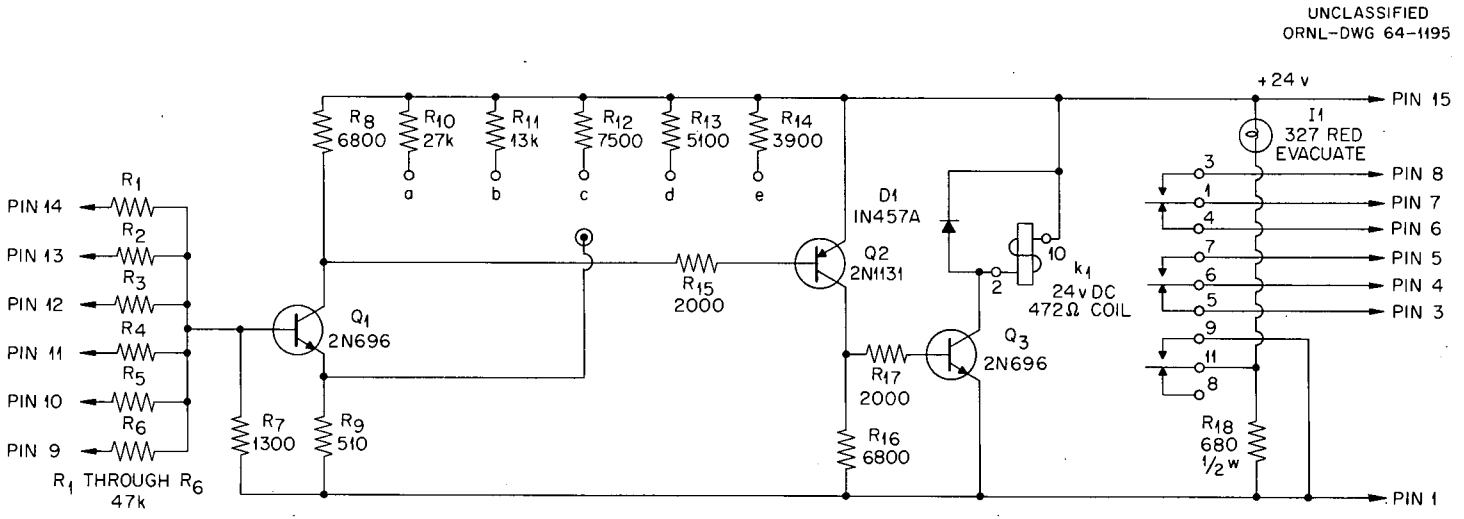

ONE JUMPER AT POINTS, a THROUGH e WILL DETERMINE NUMBER OF INPUTS REQUIRED TO ACTUATE THE MODULE

INPUTS REQUIRED TO ACTIVATE

JUMPERS	INPUTS
a	2
b	3
c	4
d	5
e	6

Fig. 2.13.2. Six-Input *And* Matrix Module with Relay Outputs.

The modules were developed because no commercial modular annunciators could be accommodated in the space available in the reactor control rooms. In addition, available units did not provide the flexibility needed for installation of successive systems that were similar, but with requirements for different logic functions.

All modules are 35.8 mm by 120 mm on the front panel and 115 mm deep. These dimensions are derived from a CERN publication.[1] This modular system is being considered for adoption as a standard at ORNL.

Four modules were constructed and tested: (1) a three-channel indicating module with outputs (dc level and pulse), (2) a six-input "and" matrix module with relay outputs, (3) a three-channel remote indicator, and (4) an audible annunciating module with a twelve-input "or" matrix.

Module 1 contains three identical channels. The only common feature is a common ground. The two possible states of each channel are indicated visually on the front of the module by an incandescent lamp operating at either a low level or at full brilliance. A 0-v or +24-v dc signal, corresponding respectively to the low level or full-brilliance level of the lamp, is available at the connector terminals of the module (Fig. 2.13.1). In addition, a positive 24-v pulse is generated when the module changes state from the low level to the high-brilliance level. This pulse is used to energize module 4. The dc signals are used to perform logic functions with module 2. Provision for adding a memory to each channel has been provided in the module.

Module 2 (Fig. 2.13.2) provides the "logic" in the system. A six-input "and" matrix accepts from one to six signals from module 1 (the +24-v dc signal). An internal connection made before installation of the module determines the number of these signals required to energize the module and the internally contained relay. The contacts of the relay are available at the module connector terminals.

Module 3 (Fig. 2.13.3) is a remote indicator of module 1 for installations where a second, or a central, observation station is required. The three channels are controlled by the three channels in module 1. The 0-v or +24-v dc output signal of each channel in module 1 controls the corresponding channel in module 3. A remote reset that will reset the controlling module 1 is included in the module.

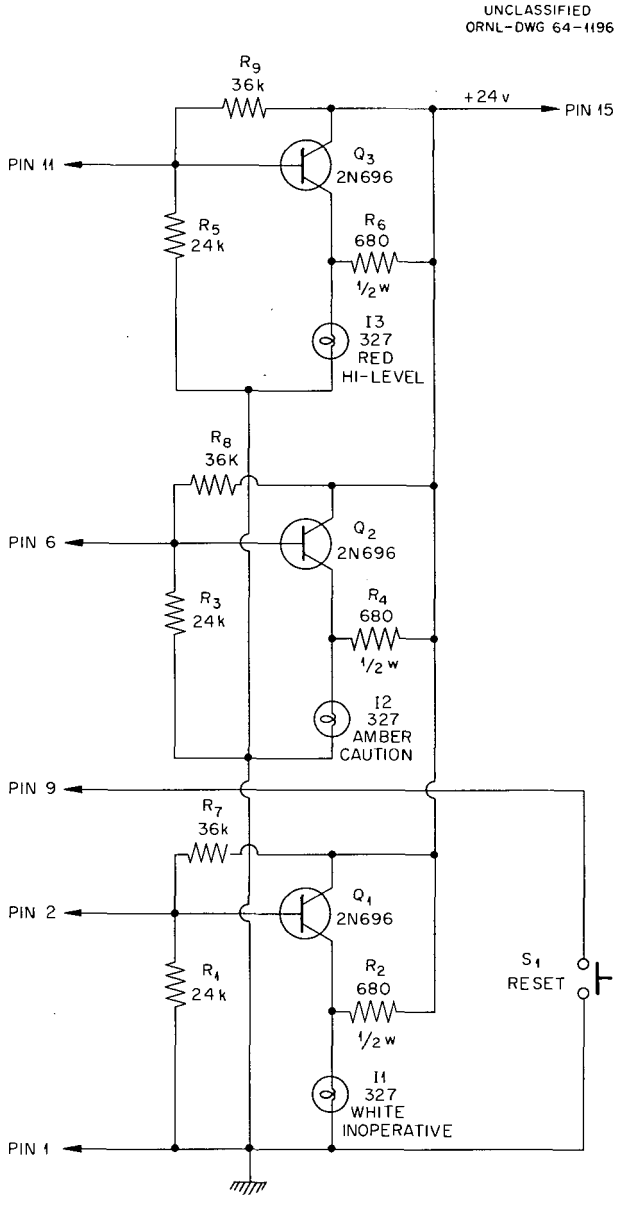

Fig. 2.13.3. Three-Channel Remote Indicator Module.

[1] *CERN 19-Inch Chassis System*, CERN Report No. 62-9.

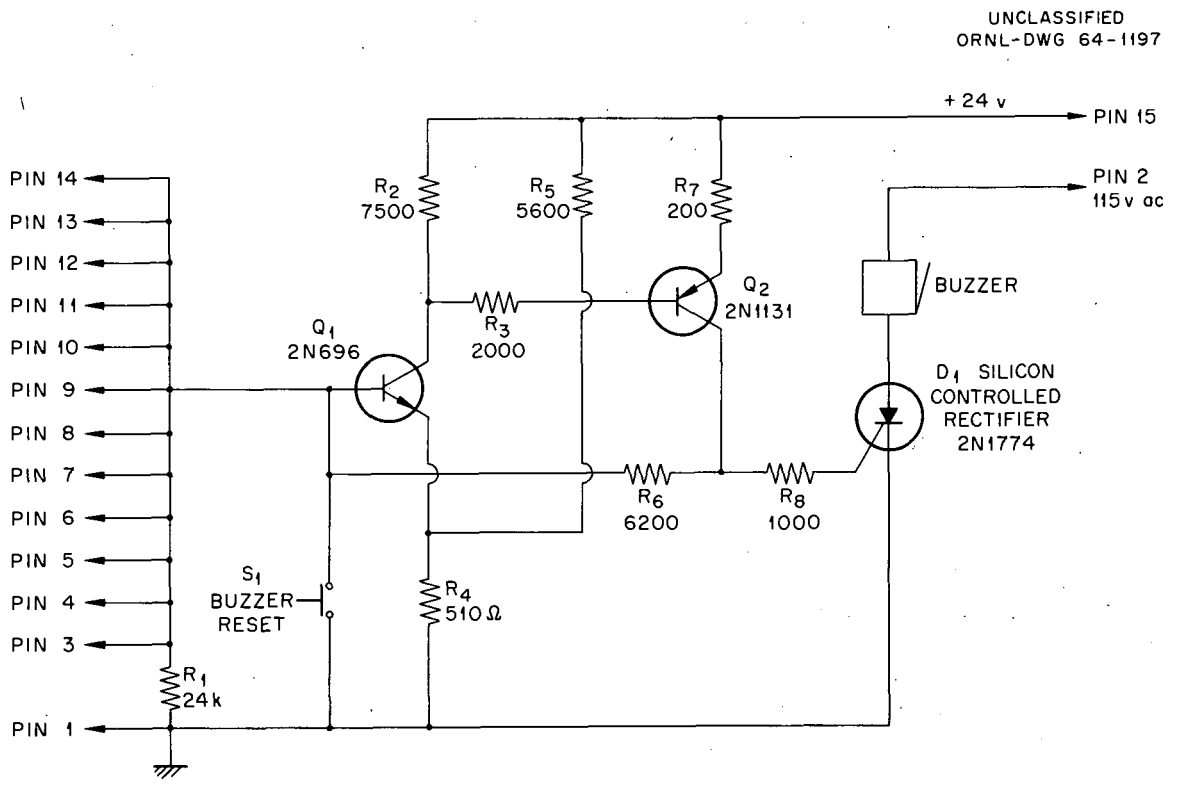

Fig. 2.13.4. Twelve-Input *Or* Matrix Annunciating Module.

Module 4 (Fig. 2.13.4) is energized by the +24-v pulse produced by module 1. Through additional matrices, any number of inputs can be used. Any positive pulse on the input will cause the module to be energized and locked in until the module is manually reset. The purpose of the module is to supply an audible signal which indicates a change in one channel of a connected module 1.

Operation of the lamps in the *on* condition, but at different levels of intensity, eliminates the possibility of missing a visual signal caused by the failure of a bulb.

2.14 LINEAR COUNT-RATE METER

J. H. Todd

A linear count-rate meter (ORNL model No. Q-2515-14) was designed to count random pulses and to display a time-averaged signal. This unit gives a paired-pulse resolution of 200 nsec, which is superior to the resolution of 1 μsec or more obtained with presently available units.

The range of the unit can be set at 0–10, 0–100, 0–1000, 0–10^4, or 0–10^5 counts/sec, and each range can be multiplied by a factor of 0.25, 0.5, or 1. An integrating time constant of 0.5, 1, or 10 sec can be selected.

Either positive or negative pulses from 1 to 10 v may be discriminated by connecting separate inputs to separate, independent discriminators, or both inputs may be used simultaneously to totalize the count rate from two sources.

A boot-strapped diode pump in conjunction with a field-effect transistor is used as the digital-to-analog converter.

The count rate is displayed by a front-panel meter. A remote meter and a 10-mv recorder can be connected to the count-rate meter.

Nonlinearity does not exceed 3%, except on the lowest scale. Zero drift was not detectable over a period of one week. The instrument is contained in a standard 19-in. chassis, $3\frac{1}{2}$ in. high.

2.15 REMOTE-CONTROL CONSOLE FOR THE 300-kv LINEAR PROTON ACCELERATOR

J. H. Todd

Previously, when aligning and adjusting the accelerator beam, personnel performed the operations by means of controls on a portable console inside the beam and target room. As long as the beam was interrupted by a quartz viewer, the radiation level at the console was negligible; however, when the viewer was removed and the beam was allowed to strike the target, the personnel were exposed to radiation. To eliminate this source of radiation exposure, a remote-control console (ORNL model No. Q-1820) was designed and installed outside the beam and target room. The console also permits personnel to monitor and optimize the beam during a long run with the machine without entering the target room.

The new console, connected in parallel with the portable console, duplicates all control functions of the portable console. Seven synchro transmitters, paralleled with seven synchro transmitters on the portable console, control two Einzel lenses, a beam focusing magnet, a beam probe control, and a deuterium control. Two additional synchro transmitters were installed on both consoles to control potentiometers for coarse and fine adjustment of high voltage. *On* and *off* switches for high voltage were installed.

Repeaters of all indicating meters located on the existing console were installed on the new control panel. These repeaters indicate target current, high-voltage output, current output, and vacuum. All meters, except the high-voltage output meter, were connected in series with the meters of the existing console. The high-voltage-output-metering circuit was located in the feedback circuit of the high-voltage regulator. Pickup or unwanted signals and noise on the long leads required for the repeater of the high-voltage meter caused the system to be unstable. Consequently, these leads were isolated by a source-follower configuration incorporating a field-effect transistor.

3. Radiation Monitoring Systems

3.1 MODERNIZATION AND EXPANSION OF ORNL RADIATION MONITORING AND CONTROL SYSTEMS

D. J. Knowles
J. H. Holladay
J. L. Kaufman
R. L. Shipp
J. E. Inman
J. A. Russell
J. H. Todd

The programs for the expansion and modernization of ORNL radiation and control systems were discussed in previous reports.[1,2] Although the overall scope of the work is essentially as reported previously,[2] several changes in detail were made.

Work completed includes the new radio communications systems, expansion of the local air monitoring system, and the central alarm display of the process waste water system (Fig. 3.1.1).

Work in progress, which is scheduled for completion by December 31, 1963, includes the Fallout Measurement System, the gross-gamma monitor at the top of the 3039 stack, and the Radiation Warning and Control System in six buildings.

Operations Division Systems

The status of systems supervised by the Operations Division at the Waste Monitoring Control Center (Building 3105) is as follows:

Process Waste Water System. – This system has been expanded. A monitor is being installed on the waste effluent from Building 3525 (HRLEL), and when construction of Building 2531 and the High Radiation Level Analytical Laboratory is completed, water monitors will also be installed.

Stream Monitors. – At the present time there are seven stream monitors in operation. New are the flume station on White Oak Creek southeast of the settling basin and a station still farther upstream, which monitors both the White Oak Creek branch and the Fifth Street storm drain. These stations telemeter radiation levels and/or flow information to Building 3105 and also take samples of the water. A portable stream monitor equipped to measure and telemeter radiation level and to allow the collection of grab samples is also operational.

Stack Monitoring Systems (Building 3039). – A new I^{131} monitor (Sect. 3.3) has been operating on the stack for about four months and will eventually replace the present device. A device to allow the positioning of a gross-gamma detector near the top of the stack is complete and a developmental detector is being designed.

Auxiliary System. – The liquid-level transmitters on 15 intermediate level waste tanks were replaced with new transmitters. The remaining tanks will be sealed, and a different type of liquid-level transmitter will be installed. The liquid levels at waste disposal trenches 5, 7a, and 7b are now being telemetered to Building 3105.

Health Physics Division Systems

The status of systems supervised by the Health Physics Division at Building 4500S is as follows:

Local Air Monitor System. – Twelve additional stations were installed and are operational.

[1] D. J. Knowles *et al.*, *Instrumentation and Controls Div. Ann. Progr. Rept. July 1, 1961*, ORNL-3191, pp. 34–35.

[2] D. J. Knowles *et al.*, *Instrumentation and Controls Div. Ann. Progr. Rept. Sept. 1, 1962*, ORNL-3378, pp. 22–26.

UNCLASSIFIED
ORNL-LR-DWG 75048R

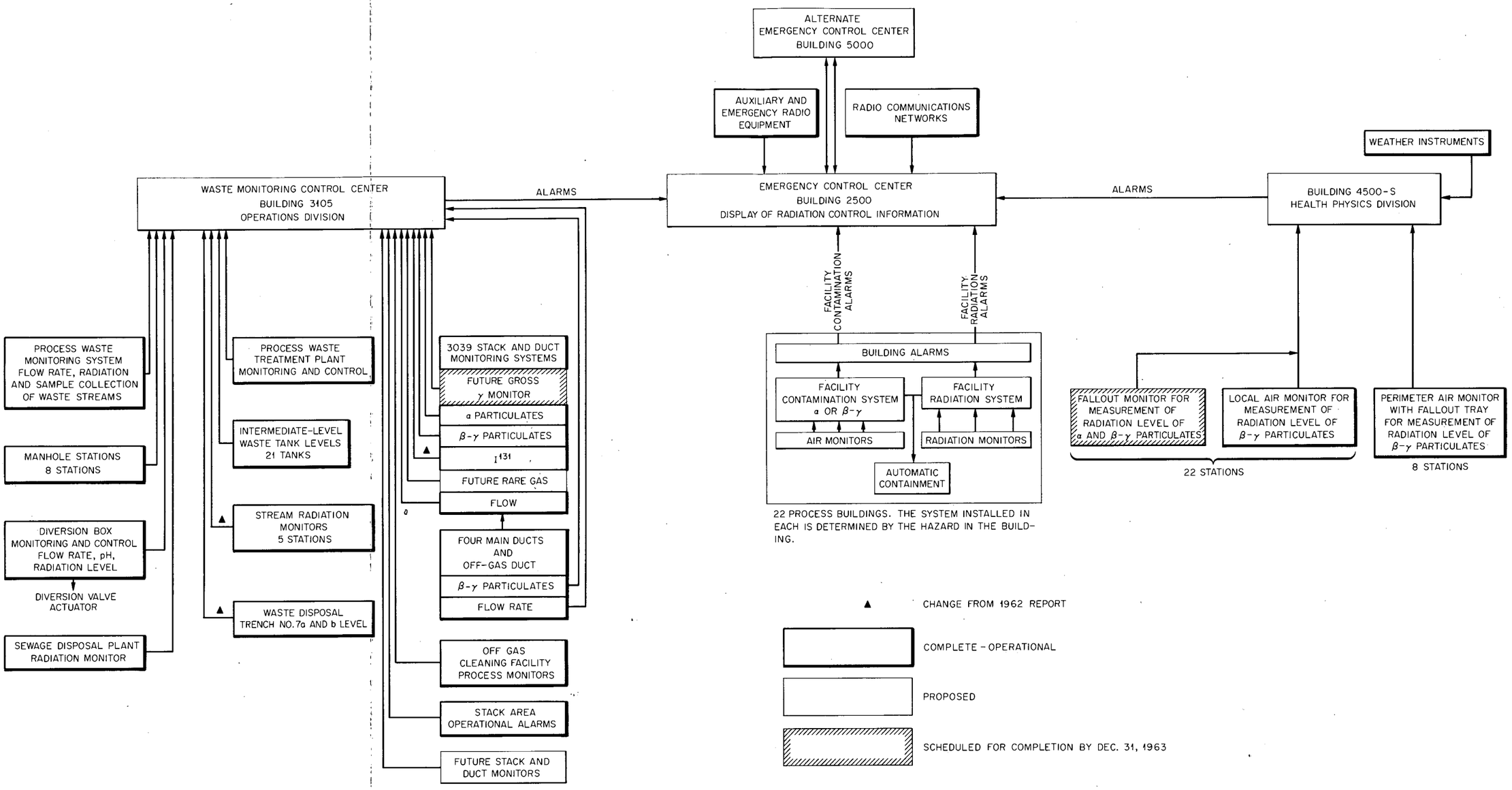

Fig. 3.1.1. Existing and Proposed Laboratory Radiation Monitoring and Control Systems.

Fallout Monitoring Net. – The system is 40% complete and is scheduled for completion on Jan. 31, 1964 (Sect. 3.2).

Laboratory Radiation Warning and Control Systems

The status of these programs is as follows:

Radio Communications. – The new high-frequency narrow-band FM radio equipment has been installed and is operational. One channel is for exclusive use by the Laboratory Protection Division, with the option of direct communications on the common AEC frequency. A repeater channel for routine communications can be operated as part of the Laboratory Protection System during emergencies.

Central Display Panel. – An illuminated map of the Process Waste Water System showing the condition of all monitoring stations has been installed at the Emergency Control Center (Building 2500).

Table 3.1.1. Status of Installation of Facility Radiation and Contamination Systems

Facility	Building No.	Control Systems Being Installed		Percent of Completion
		Radiation	Contamination	
	Phase I[a]			
Oak Ridge Research Reactor	3042	Yes	Yes	80
Low Intensity Test Reactor	3005	Yes	Yes[b]	50
High Radiation Level Examination Laboratory[c]	3525	Yes	Yes	90
	Phase II[a]			
Neutron Physics and Shielding Laboratory	3010	Yes	Yes	10
Graphite Reactor[d]	3001	Yes	Yes	10
Chemical Processing Pilot Plant[c]	3019	Yes	Yes	10
	Phase III[e]			
Rolling Mill[f]	3012	Yes	No	0
Source and Special Materials[f]	3027	Yes	No	0
Special Materials Machine Shop[f]	3044	Yes	No	0
Solid State Laboratory	3025	No	Yes	0
Transuranic Laboratory[c]	3508	Yes	Yes	0
Fission Products Pilot Plant[g]	3517	Yes	Yes	0
Source Garden	3597	Yes	No	0
High Radiation Level Chemical Development[c,f]	4507	Yes	Yes	0
Metals and Ceramics Laboratory[c]	4508	Yes	Yes	0

[a]Scheduled for completion Dec. 31, 1963.
[b]Operates containment controls on alarm.
[c]Neutron detection (criticality) capability included.
[d]Design only was completed. Facility now on standby.
[e]Proposals being prepared.
[f]Neutron detection (criticality) capability only.
[g]Containment system exists.

This display utilizes a new alarm telemeter system (Sect. 3.6). Spare panel space in the same cabinet will be used to display alarm information originating in the Facility Radiation and Contamination Systems and for alarm information now at other locations in the Building 2500 control console.

Area Mapping System. – This system has been deferred indefinitely as a low-urgency project.

Facility Radiation and Facility Contamination Systems. – A brief description of the systems being installed in each building and the status of installation are summarized in Table 3.1.1.

3.2 FALLOUT MONITORING SYSTEM

D. J. Knowles R. L. Shipp J. H. Todd
R. K. Abele G. A. Holt
T. F. Sliski H. J. Stripling

The Fallout Monitoring System at ORNL was designed to measure deposition of radioactive particles which could originate at the Laboratory from a nuclear incident or from failure of air-cleaning components, such as filters in a gaseous waste disposal system, and to give warning when a preset tolerance level has been reached. For years, fallout had been collected on gummed paper held in trays at various locations at the Laboratory site. The paper was replaced periodically and the samples were taken to a counting room for scanning and analysis. The obvious problems of handling such large amounts of sticky paper and the time delay in obtaining useful information outmoded this method. A new system was designed and is being installed. The design of this system was guided by the following criteria:

1. Collect fallout continuously and measure the alpha and beta-gamma radioactivities emitted by the particles.
2. Transmit the count data to a central receiving station and give warning when a tolerance level has been reached.
3. Record count data when the tolerance level has been reached.
4. Give sufficient information for determining the source of the fallout, if it is a local source.

These criteria were to be met with a system that would be simple and which could be installed and maintained at a reasonable cost.

A network of 22 collector-detector assemblies with signal transmission and receiving equipment is being installed throughout the Laboratory and its environs. An assembly will be placed on top of each local air monitoring station, since these stations are already located in strategic positions on the basis of meteorological studies of airflow and dispersion patterns of stack effluent in the surrounding valley. At each station, alpha and beta particles and gamma rays emitted by collected particles are counted, and the information is transmitted over telephone lines to a central receiving station (Building 4500S, Health Physics Division, Fig. 3.1.1).

Collector-Detector Assembly

In the collector-detector assembly (Fig. 3.2.1), a disk covered with aluminum foil rotates at 1 rpm, with 50% of the disk area always exposed to collect fallout.

Ordinary, heavy-duty 18-in.-wide household-type aluminum foil is used to cover the disk. This is a convenient and inexpensive covering for the disk. The foil cover is easily removed from the disk and serves as a convenient container for carrying the fallout particles to a laboratory for further analysis.

As the disk rotates, it carries the particles under a shielded GM tube, which counts the beta-gamma

UNCLASSIFIED
ORNL-DWG 64-1198

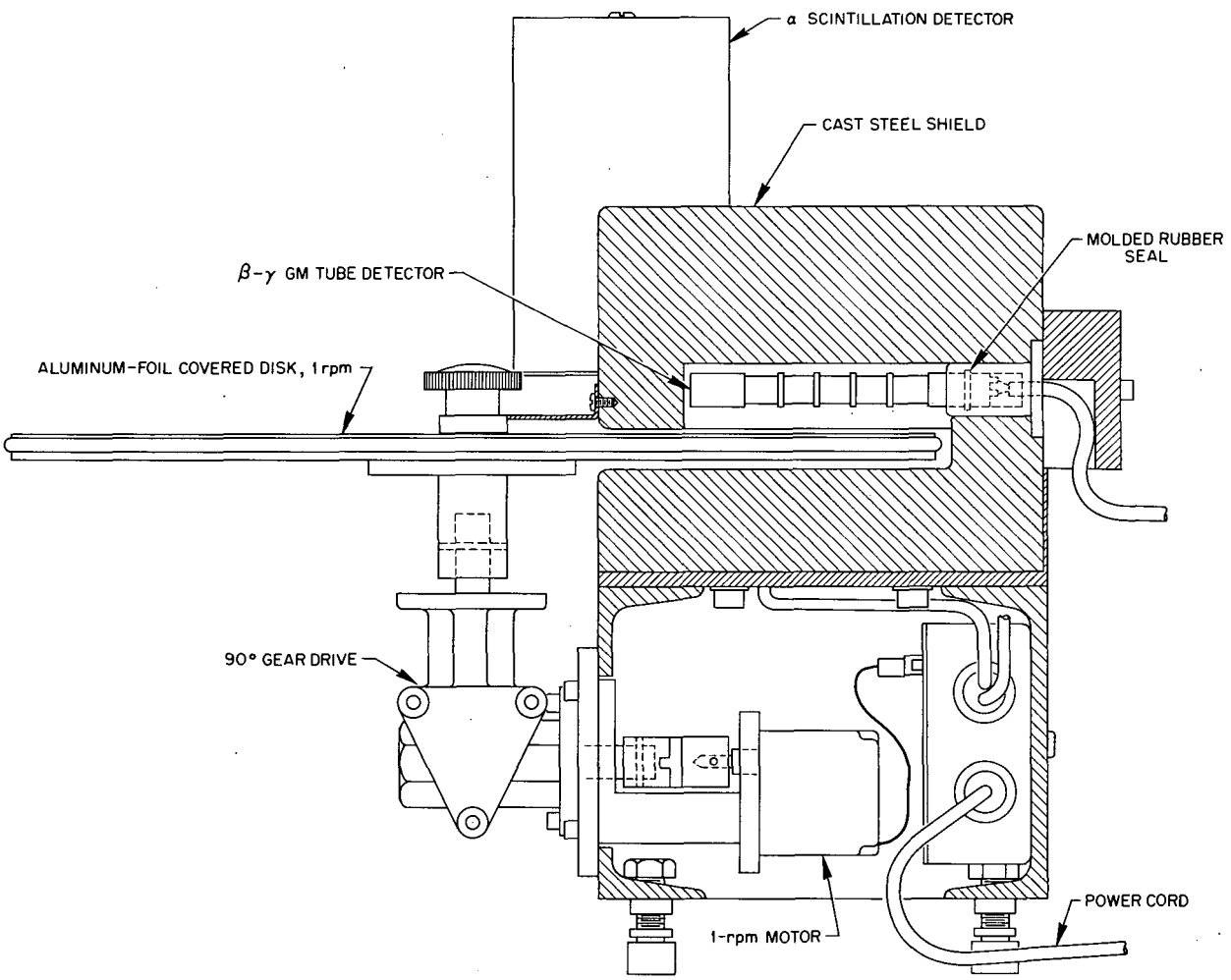

Fig. 3.2.1. Collector-Detector Assembly for Fallout Monitor.

radioactivity, and under a scintillation-type probe,[1] which counts the alpha radioactivity.

The assembly was designed to achieve low production costs, all-weather protection of the components, and simple, low-cost servicing in the field. The shield for the GM tube is cast steel. A molded rubber seal was developed to hold the GM-tube socket and to seal the tube and cable connector from moisture. Routine replacement of the aluminum foil keeps the background count rate of the disk at a low level.

[1]M. M. Chiles and R. K. Abele, *Instrumentation and Controls Div. Ann. Progr. Rept. July 1, 1960*, ORNL-3001, p. 55.

Signal Transmission

Two analog signals, corresponding to the alpha and beta-gamma radioactivities collected on the disk, are generated by the count-rate meters (Fig. 3.2.2). The signals are transmitted via telephone lines to a central location. Continuous information, indicating whether the activities are below or above a preselected alarm level, is also generated and transmitted over these same telephone lines. All alarm signals are continually monitored and a choice of 12 dc "activity" level signals can be monitored through a patch panel.

Each station contains two ORNL model Q-2191A count-rate meters. Recorders, one integrally

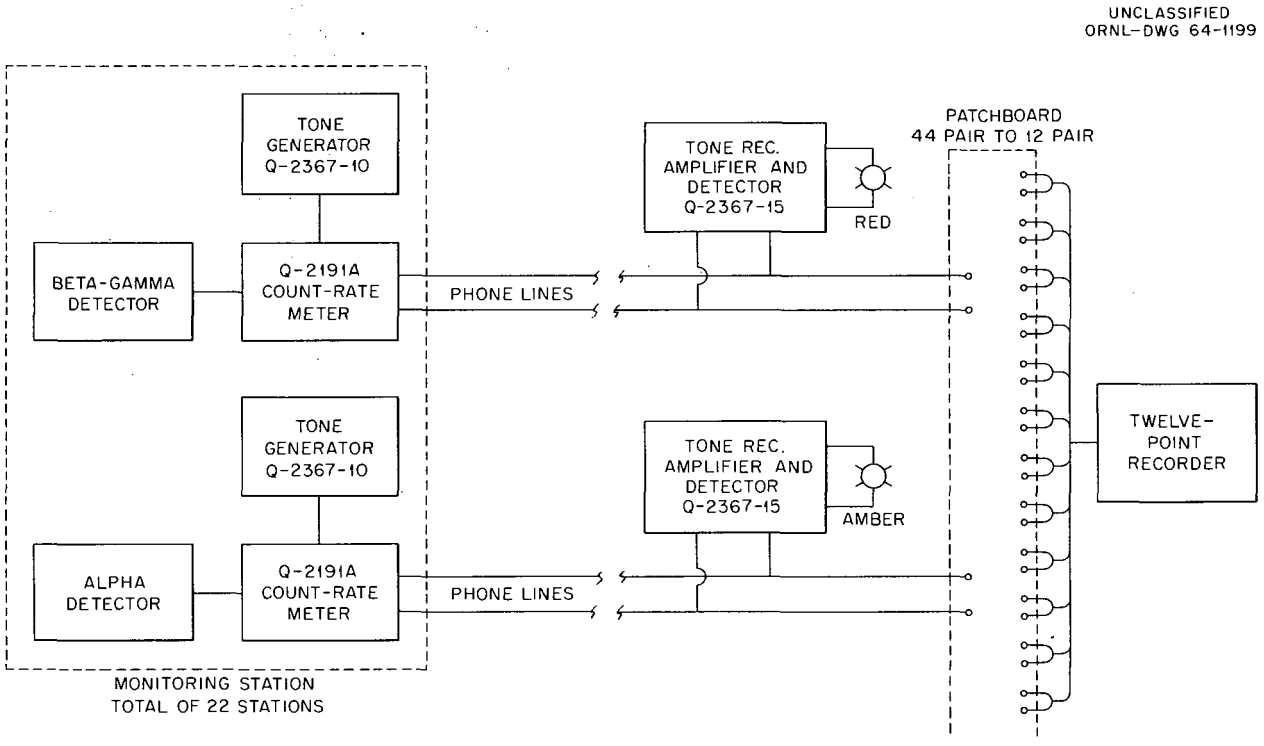

Fig. 3.2.2. Fallout Monitoring System.

mounted on each count-rate meter, were removed and replaced by tone generators, ORNL model Q-2367-10. After this modification the telemetry output of the count-rate meter is a 0- to 1-ma analog signal and a 2.5-kc tone – together these two signals establish a "nonalarm" condition. At the receiving station, the absence of the 2.5-kc tone indicates either that an alarm level of activity has been reached, that a phone line has opened, or that power has failed at the monitoring station.

Specifically, the 2.5-kc tone modulates the light intensity of an incandescent bulb. The presence of tone causes the lamp to glow at a lower-than-normal intensity. With the absence of the tone, the lamp glows at full intensity.

Two lamps are located at the receiving end of each station – one lamp indicates the condition of the beta-gamma monitor alarm and the other indicates the condition of the alpha monitor alarm.

Any 12 of the 44 analog signals can be connected to a 12-point Brown recorder by means of a patch panel.

The combination of two lamps will give warning if tolerance is reached by either alpha or beta-gamma activity or both. In such an event, the recorder can be connected to record beta-gamma count signals from 12 stations, or alpha count signals from 12 stations, or both beta-gamma and alpha signals from 6 stations.

3.3 IODINE MONITOR FOR RADIOACTIVE EXHAUST GASES

R. L. Shipp R. K. Abele D. J. Knowles

Iodine is the only radioactive gas likely to pass in hazardous quantities through the bank of absolute filters in the exhaust duct from the High Radiation Level Examination Laboratory (HRLEL), even should a maximum credible accident occur.[1] A new monitor (Fig. 3.3.1) was designed for continuous surveillance of this off-gas stream. The design overcomes two disadvantages of a previously described[2] ORNL monitor: the new monitor is more sensitive, and replacement of the charcoal trap is easier. One detector was installed at the HRLEL and one was installed and tested at the Radioisotope Stack Area (3039 Stack).

At the HRLEL, a side stream of off-gas is withdrawn from the exhaust duct downstream from the absolute filters. The gas sample passes through a paper-tape filter in a particulate monitor and then through an activated-charcoal trap in the iodine monitor, where iodine and other gases are adsorbed on the charcoal. The gas sample from the iodine monitor is returned to the off-gas duct. The detectors in both monitors are GM tubes; in the iodine monitor, a ring of GM tubes surrounds the trap, and the trap and tubes are enclosed in lead to shield the tubes from background radiation. The GM tubes in both monitors feed a common circuit to a count-rate meter, an alarm, and a recorder.

Since frequent trap replacement is essential to maintain a low background and high sensitivity in the iodine monitor, an important feature of the new monitor is the simplicity with which the trap is replaced. The charcoal is contained in a disposable plastic jar which may be removed after the detector assembly is lifted off the jar. The trap is replaced when the gamma count rate of the charcoal reaches an operationally determined limit peculiar to each exhaust system.

At the 3039 Stack, a correlation between the response of the iodine monitor and iodine processing[3] was observed. (The particulate monitor and the iodine monitor feed separate alarms and recorders.) At the start of processing, radioactive xenon was released and temporarily held in the trap. This produced a noticeable sharp peak on the recorder chart. Later in the process, as radioactive iodine escaped to the stack, the iodine was retained in the trap. On the recorder chart, the count rate increased to a maximum and then decreased at a rate consistent with the radioactive decay of the mixed radioactive-iodine isotopes. Spectral analysis of the gamma activity of a trap showed that radioactive cesium, in addition to iodine, was retained.

UNCLASSIFIED
ORNL-DWG 64-1200

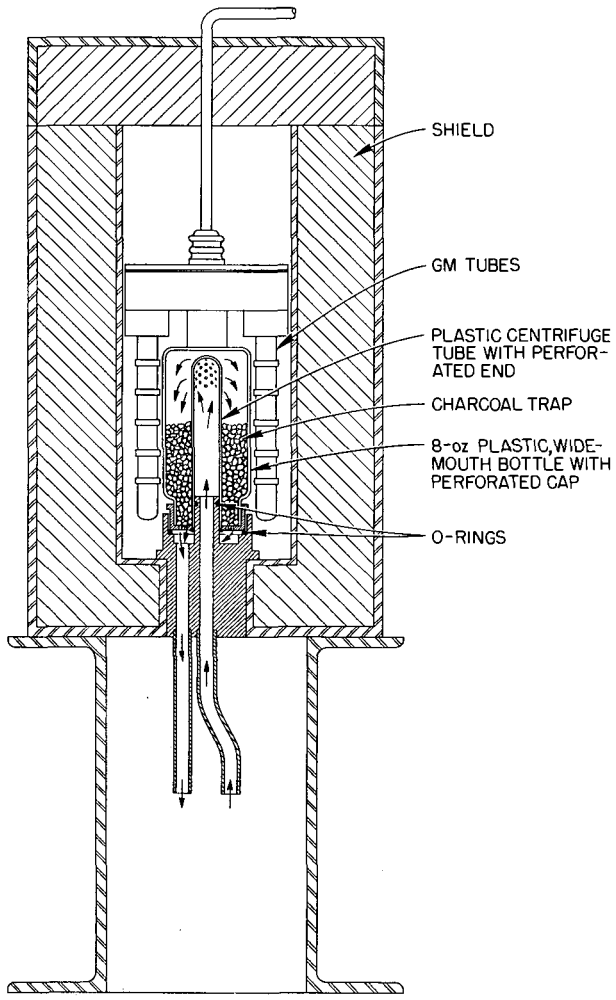

Fig. 3.3.1 Iodine Monitor Detector.

[1]Personal communication from G. W. Parker, ORNL Chemistry Division.

[2]F. J. Manneschmidt, *Equipment and Procedures for Stack Gas Monitoring at ORNL*, paper presented at the Seventh Air Cleaning Conference, Oct. 10–12, 1961, Brookhaven National Laboratory.

[3]By the ORNL Isotopes Division.

3.4 SMALL RADIATION-MONITORING SYSTEMS

D. J. Knowles

J. L. Kaufman T. A. Lewis

A vehicle monitor was designed for service at ORNL Burial Ground No. 5. Detectors, mounted on posts, monitor outgoing trucks as they pass through the exit gate, and an alarm is sounded if the truck is contaminated. The detectors are sensitive to a contamination level of 5 mr/hr at contact.

A system to detect airborne radioactivity in the ventilation air in the office portion of Building 3025 was designed and is being installed. This system protects the office portion of the building against the spread of airborne contamination by the air-conditioning equipment. Based on modules of the ORNL model Q-2240 air monitor, the system is sensitive to the maximum permissible concentration (MPC) level of beta-gamma particulates and will shut off the intake blowers when the alarm point is reached. Identical units will be installed at the ORIC to monitor the exhaust air from the experimental areas.

A particulate sampler utilizing a filter was designed for use on off-gas lines which normally operate at approximately 20 in. H_2O vacuum. The device allows the insertion and removal of 2-in.-diam filter papers in the usually contaminated off-gas ducts without opening the duct to the atmosphere.

3.5 LABORATORY CONTAINMENT PROJECTS

D. J. Knowles

J. H. Holladay J. E. Inman R. L. Shipp

Prior to the implementation of the Laboratory radiation warning and control projects, ORNL had under way several containment programs.[1,2] A status report of these projects is presented in Table 3.5.1. The basic concept of these systems requires, first, a central display panel indicating the alarm condition of most of the health physics monitors in a given facility. Second, the concept requires a control output from the system when a given combination of air monitors reaches the alarm condition in coincidence. In practice, the control output will change the air-handling equipment to an emergency condition. This design concept is compatible with the design concepts of the newer radiation safety and control systems (Sect. 3.1), and the containment systems are being incorporated into the radiation safety and control systems as necessary.

[1]D. J. Knowles *et al.*, *Instrumentation and Controls Div. Ann. Progr. Rept. July 1, 1961*, ORNL-3191, p. 33.

[2]D. J. Knowles *et al.*, *Instrumentation and Controls Div. Ann. Progr. Rept. Sept. 1, 1962*, ORNL-3378, p. 25.

Table 3.5.1. Status of Installation of Containment Instrumentation

Location	Building No.	Description	Percent of Completion
Radioisotope Production Laboratory (A)	3028	Building being revised to accommodate a new program. Existing containment system being expanded	75
Radioisotope Production Laboratory (B)	3029	Air monitor alarm actuates containment	100
Radioisotope Development Laboratory	3047	Air monitor alarm actuates containment. Expansion contemplated	100
Fission Products Development Laboratory	3517	Air monitor alarms actuate containment	100
High Radiation Level Examination Laboratory	3525[a]	Air monitor alarms and radiation monitor alarms actuate containment	100
High Level Radiochemical Laboratory	4501	Supervision only; no automatic containment	100
High Radiation Level Chemical Development Laboratory	4507[b]	Air monitor alarms actuate containment	100

[a]Included in Phase I of Laboratory Radiation and Contamination System.
[b]To be included in Phase III of Laboratory Radiation and Contamination System.

3.6 TONE TELEMETRY SYSTEM

J. H. Todd A. L. Case

To maximize the utility of an installed telephone system, a tone telemetry system was designed that permits the transmission of a two-state signal over a pair of telephone lines without disruption to or interference with an analog signal already present on the same lines. This system has been installed and is presently in use with the Process Waste Monitoring System at ORNL. A slightly modified system is being installed in the ORNL Fallout Monitoring System (Sect. 3.2).

The telemetry system is composed of three units: (1) a tone transmitter with a self-contained 115-v ac power supply; (2) a receiver system, with an amplifier and detector, which provides a discrete two-level dc output signal; and (3) a memory circuit and lamp driver.

The transmitter produces a 2500-cps sine-wave output, which is adjustable from 0 to 6 v in amplitude into a 600-ohm load. The receiver is frequency selective and has a bandwidth of 150 cps centered at the 2500-cps frequency. The presence or absence of the 2500-cps tone on the input of the receiver produces, respectively, a 0- or a −12.5-v dc signal. The lamp driver lights either of two lamps. When a 0-v signal is received, one lamp is lit and remains so (because of the memory circuit) even though the 0-v signal no longer is present. When a −12.5-v signal is received, the first lamp goes out and a second lamp is lit and remains so until a 0-v signal is received.

4. Radiation-Detection Instruments and Components

4.1 AIR ALPHA PROPORTIONAL COUNTER INSENSITIVE TO ATMOSPHERIC HUMIDITY[1]

A. M. R. Ferrari[2] C. J. Borkowski

A conventional alpha proportional counter which uses air as the counter gas is sensitive to high relative humidity of this air and generates spurious pulses that cannot be distinguished from actual alpha pulses. It has been found possible to operate such a counter satisfactorily with air at high relative humidity by passing a small current (~15 ma) through the center wire. In this manner, the center wire is heated and the relative humidity of the surrounding sheath of air is reduced sufficiently so that operation of the counter with air at high relative humidity is comparable to operation with dry air. Two different mechanisms are proposed for the formation of spurious pulses in such a counter filled with air at high relative humidity.

[1]Abstract of paper published in *Rev. Sci. Instr.* 33(10), 1047–50 (1962).

[2]Formerly on loan from Instituto de Fisica de San Carlos de Bariloche, Argentina.

4.2 VARIABLE-APERTURE ALPHA PROPORTIONAL COUNTER

W. T. Clay

A gas-flow proportional counter (ORNL model Q-2541) was designed to measure the uniformity and thickness of an alpha-emitting isotope being electroplated either onto a flat plate or inside a small-diameter cylinder. Periodic measurements on the extent and uniformity of the deposition can be made during short interruptions in the electroplating process; therefore, one can readily converge upon the desired deposition. Counter resolution was not a major design criterion. No detector that met all the requirements of this application was commercially available.

The detector is coaxial with an indexed cylindrical collimator, which can be rotated to provide any one of six different apertures (Fig. 4.2.1). Since the measurements were to be made inside a contaminated cell, the collimator was fabricated of stainless steel to simplify decontamination. The sealed window into the sensitive volume of the detector is 0.00025-in.-thick, doubly aluminized Mylar film. The cost of fabrication and checking the detector is approximately $400.

The proportional region of operation was chosen for the detector, because there was a need to

UNCLASSIFIED
ORNL-DWG 64-1201

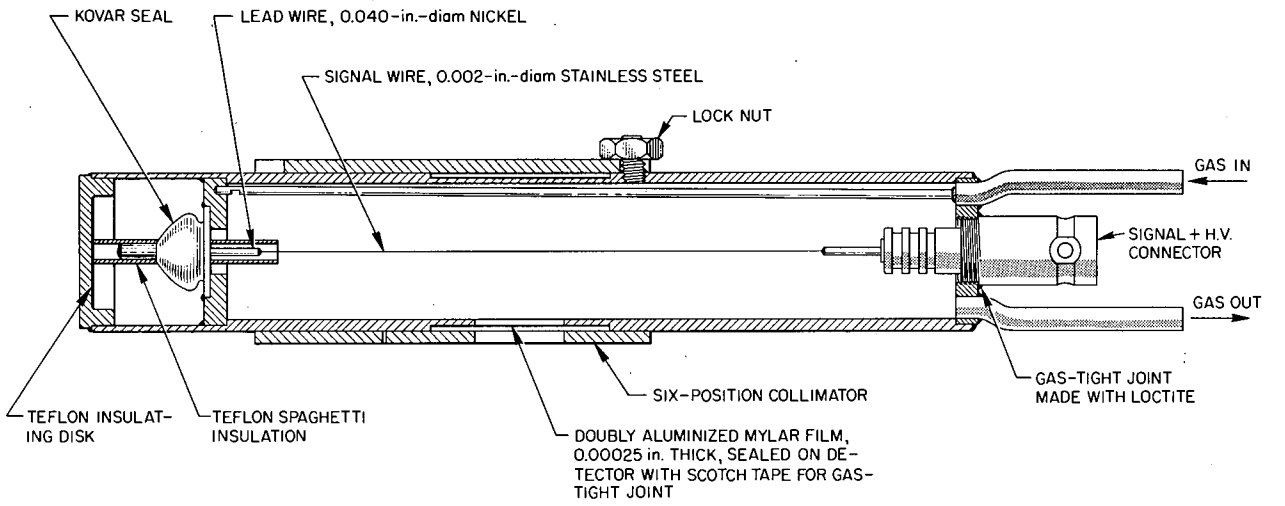

Fig. 4.2.1. Variable-Aperture Alpha Proportional Counter.

discriminate against beta and gamma backgrounds, and a large range of activities could be handled. The detector operating voltage is 1000 v when a gas mixture of 90% Ar and 10% CH_4 is used at a low flow rate. The plateau region is 300 to 400 v wide with a typical slope of 0.8% per 100 v. The detector output was $\sim 2 \times 10^3$ counts/sec when exposed to a 4×10^8 dis sec^{-1} cm^{-2} plate source through the smallest aperture ($^1/_{64}$-in.-diam hole). Reproducible count rates (±10%) have been obtained with a test source.

The electronics for the detector system includes an A1D linear amplifier, a positive high-voltage supply, and a decade scaler (ORNL models Q-1326A, Q-2057, and Q-1743B respectively).

4.3 ALPHA OR BETA-GAMMA RADIATION MONITOR

F. M. Glass E. E. Waugh

The ORNL model Q-2277 alpha or beta-gamma radiation monitor is a transistorized version of a previous vacuum tube instrument (ORNL model Q-2091). Like its predecessor, the model Q-2277 instrument (Fig. 4.3.1) provides a 1-ma telemetering signal, a 10-mv strip-chart-recorder signal, an alarm-control signal, and an audible indication of counting rate. A charge-sensitive amplifier at the input eliminates the need for preamplifiers for remotely located detectors. The monitor performs equally well with either Geiger-Mueller counters or alpha scintillation probes over a wide range of temperatures.

Six ranges of the monitor provide full-scale calibrations of 500, 1000, 2500, 5000, 10,000, and 25,000 counts/min. The accuracy of the panel meter is ±2.5% of full scale at 25°C. Circuit accuracy is ±0.5%, excluding the meter. There is no measurable drift in the zero setting. The calibration drift as a function of the line voltage is less than 0.1% per 20-v change and as a

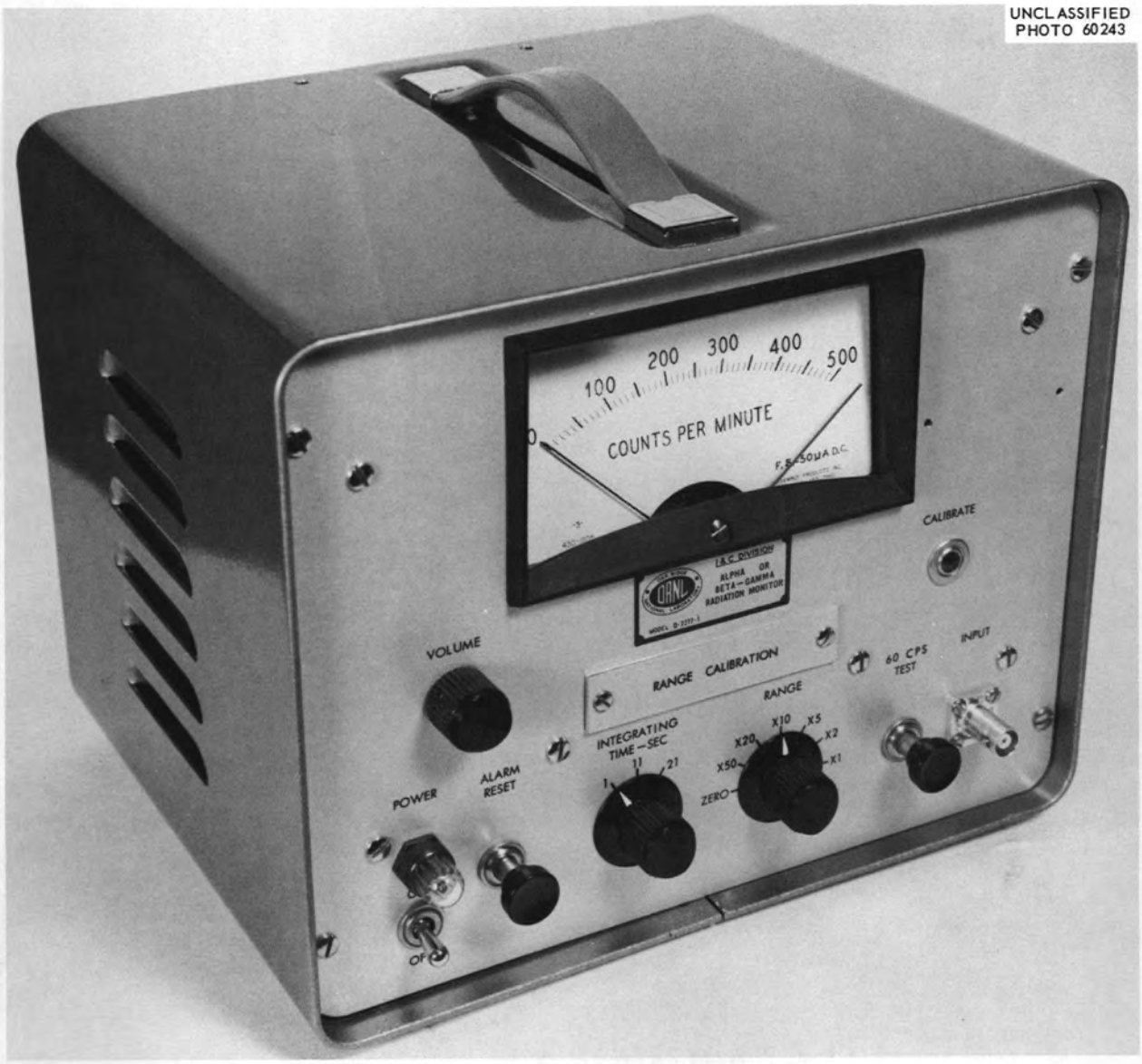

Fig. 4.3.1. Alpha or Beta-Gamma Radiation Monitor.

function of temperature is less than 0.1%/°C. The charge sensitivity is 5×10^{-12} coulomb/μsec.

Because of special compensation, the full-scale counting loss is nil for randomly spaced pulses on all ranges except the 20,000-count/min range. This range has a counting loss of 2.25% at full scale. Circuit linearity is 0.2% for randomly spaced pulses on all ranges except the 20,000-count/min range, which has a 2.25% departure from true linearity. For evenly spaced pulses, the departure from true linearity is 1.5% (overcompensated) on all scales.

4.4 GAMMA-RAY MONITOR

R. J. Scroggs
J. H. Todd H. N. Wilson

As a supplement to the ORNL Area Safety Program, an instrument was developed that measures both the dose rate and integrated dose in a gamma radiation field. The instrument has two separate sections: a dose-rate monitor with an alarm which can be set at any dose rate from 1 to 12 r/hr, and an integrating dosimeter with fixed alarm points at 20 and 100 mr.

The dose-rate monitor (ORNL model Q-2274-1) is a gamma-sensitive, ionization-chamber–electrometer bridge circuit. The monitor is powered by nickel-cadmium batteries, which are kept continuously on trickle charge by line power. The batteries provide power for continued short-term operation of the monitor whenever line power is disrupted and also render the instrument portable for operation in areas without line power. The dose rate at which the monitor will actuate an alarm is selected by setting a pointer on a meter relay mounted on the front panel. Low-level contacts in the meter relay actuate an alarm to warn of "instrument failure" if the internal circuit of the instrument should fail.

The integrating dosimeter (ORNL model Q-2274-2) is a combined integrating ionization chamber and a counting circuit. The chamber produces one pulse per 0.2 mr of dose. These pulses are counted by scaler glow tubes, and at preselected values of counts, the 20- and 100-mr alarms are actuated. The alarm points can be set at several values by changing the connectors to other calibrated terminals on a terminal strip on the chassis. The time period during which the dose is integrated can continue indefinitely, or it can be set to integrate the dose for a desired period of time, after which it will be reset automatically. Normally, the dose is integrated for successive 8-hr periods.

4.5 GAMMA-BACKGROUND INTEGRATOR

R. W. Ingle

A gamma-background integrator, ORNL model Q-2595, was developed for monitoring areas of relatively low radioactivity. A prototype was fabricated and is now being evaluated for use in the Laboratory perimeter air-monitoring system.

The instrument is a modification of the portable alpha counter, model Q-1975A.[1] The detector is an Anton 114/6993 halogen-quenched Geiger-Mueller tube, which may be mounted within the chassis or mounted remotely and connected to the chassis by a coaxial cable. Each pulse from the detector records one count on a six-digit Sodeco mechanical register, and the counts are continuously totaled by the register. Because the paired-pulse resolution is approximately 30 msec, counting losses will be ~1% for a normal (0.4 count/sec) background rate, but will be large (approaching 50% for 30 counts/sec) if the counting rate exceeds 10 counts/sec.

The electronic circuit is completely transistorized. The housing is similar to, but a little larger than, the housing for the portable alpha monitor. Nickel-cadmium batteries, continuously recharged by line power, supply electrical power for the instrument and provide continued short-term operation of the instrument during electrical outages. The batteries also provide for portable operation of the instrument.

[1] F. M. Glass, *Instrumentation and Controls Div. Ann. Progr. Rept. July 1, 1960*, ORNL-3001, p. 8.

4.6 PERSONAL RADIATION MONITOR: STATUS REPORT[1]

R. W. Ingle C. J. Borkowski

Because of the relatively short battery life (2 to 4 weeks) of the Personal Radiation Monitor (PRM), ORNL model Q-2041, a new model (Fig. 4.6.1) was developed to achieve a longer battery life and to improve other characteristics of the monitor. Several units were constructed and are being evaluated.

The monitor currently in use at ORNL requires an idling current of 1.5 to 2.5 ma. This current drain required frequent battery replacement. Recently, the availability of low-cost silicon transistors makes possible the design of an instrument with an idling current of 130 μa over a temperature range of 0 to 130°F. As a result, the battery life is extended to nearly 1 yr.

The physical size and appearance of the PRM were not changed from the original model, and the principle of operation is the same. The changes which were made are described in the following discussion.

In the blocking-oscillator power supply, a silicon transistor is used for *Q*1 instead of a germanium transistor. With this replacement, a reduction of the no-signal oscillator frequency from 100 to 15 cps is possible. Since the average current (dc) required by a blocking oscillator is a function of its operating frequency and load conditions, and since the load requirement in the absence of radiation is nearly zero, the frequency may be profitably reduced to 15 cps without a decrease in instrument sensitivity. Another advantage gained by the use of the silicon transistor is the improvement in the temperature stability of the oscillator; temperature stability is inherent in a silicon transistor. The high leakage current of a germanium transistor makes it necessary to use temperature-sensitive components for stability over temperature extremes.

In the original PRM, transistors *Q*1, *Q*2, *Q*3, and *Q*4 of Fig. 4.6.1 were PNP germanium transistors, but in the new model, *Q*1 and *Q*4 are silicon transistors (*Q*2 and *Q*3 are still germanium). Furthermore, in the new model, only *Q*3 is a PNP type, while *Q*1, *Q*2, and *Q*4 are NPN types. The lower cost of NPN transistors makes their use more economical, even though their use requires reversal of the high voltage from a negative to a positive 520 v as well as reversal of the GM tube connections.

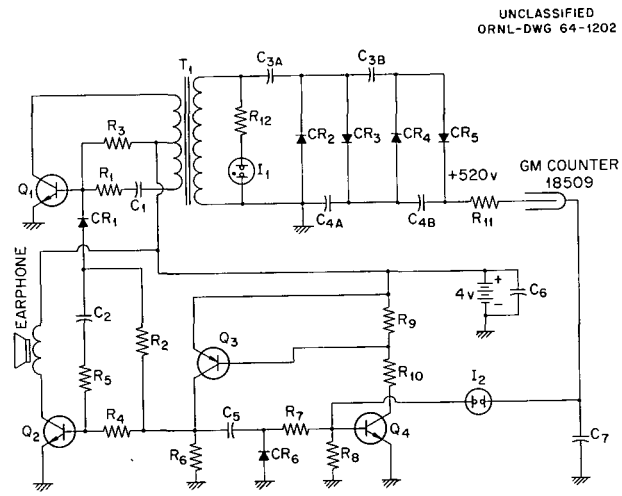

Fig. 4.6.1. Low-Current Personal Radiation Monitor.

Two emitter followers, used in the original PRM as a triggering device, were replaced by a monostable multivibrator *Q*3 and *Q*4, which requires no current until triggered. With this multivibrator, several advantages are realized:

1. The new instrument is more sensitive, because it can produce an output signal for each GM tube pulse. In the previous model, 20 GM tube pulses were required for each output signal.
2. Because the output voltage from the multivibrator is the same for a single input signal as for a saturating signal (approximately 10 r/hr), the audible alarm frequency does not change with radiation intensity. Only the alarm rate changes.
3. Since the audible alarm frequency does not change with radiation intensity, tuning is easier and is accomplished by adjusting *R*2 for an audible alarm frequency of approximately 2800 cps. In the original PRM, both *R*1 and *R*2 were adjusted and tuning was more difficult because the audible frequency changed when the radiation intensity increased.

[1]R. H. Dilworth and C. J. Borkowski, *Instrumentation and Controls Div. Ann. Progr. Rept. July 1, 1960*, ORNL-3001, p. 22; R. H. Dilworth and C. J. Borkowski, *Instrumentation and Controls Div. Ann. Progr. Rept. July 1, 1961*, ORNL-3191, p. 25.

4.7 PARALLEL-PLATE FISSION CHAMBER FOR DETERMINATION OF α FOR U^{235}

M. M. Chiles

The value of α (the ratio of the neutron-capture cross section to the neutron-fission cross section) for U^{235} and other fissionable materials is important to progress in nuclear reactor technology. Several experiments are planned at ORNL[1] to determine this ratio for U^{235}, U^{233}, and Pu^{239} at neutron energies ranging from 1 ev to 20 kev. A 5-in.-OD parallel-plate fission chamber was designed and fabricated for the experiments with U^{235}.

The fission chamber was placed inside a large liquid-scintillation gamma-ray detector, and the values of α were determined at several neutron energies within the range previously mentioned. With this device, α can, in principle, be determined by analyzing the gamma-ray pulses from the scintillation detector that are anticoincident with fission pulses from the fission detector, and the gamma-ray pulses that are coincident with the fission pulses.[2] The values for α determined with this chamber are in close agreement with the values determined by independent investigators employing comparable techniques.[3] We believe that the accuracy of the measurement can be improved with a shorter chamber (to be made with closer spacing between electrodes), which will reduce the neutron transit time through the chamber. For future experiments, such a chamber is being designed. Also, other chambers are being designed to determine α for U^{233} and Pu^{239}.

The fission chamber was irradiated by a 4-in.-diam beam of neutrons centered on the axis of the chamber. To reduce the error caused by neutron capture in nonfissionable material within this 4-in. diameter, the plates and end windows were made thin; that is, the plates were fabricated from special 0.005-in. 1145-alloy, H-19 aluminum foil, whereas the end windows were made 0.020 in. thick from 1100-alloy aluminum. Design and fabrication were complicated in that the electrical connector, the gas filling tube, O-ring seals, screws, and other such components had to be located within the annulus between the 4-in. and the 5-in. diameters of the chamber, because the materials in these components are characterized by relatively high neutron-capture cross sections. During the gas-filling process, both sides of each thin end window were evacuated and then filled along with the chamber volume to prevent a pressure differential from developing across the windows. The chamber was filled with a 97% Ar–3% CO_2 gas mixture to a pressure of 72 cm Hg abs.

In the chamber, 30 plates are electrically connected in parallel (Fig. 4.7.1), 28 are coated on both sides with highly enriched (99.888%) U^{235}, and the two end plates are coated only on the inside. To prevent oxidation of the aluminum while immersed in the electroplating bath, a very thin zinc coating was deposited on the plates before the U^{235} was electroplated. The U^{235} layer was approximately 1 mg/cm^2. A total of 4.534 g of U^{235} was used in the chamber.

Because the range of alpha particles from U^{235} is greater than the electrode spacing, the electronic pulses from alpha particles are not proportional to the total alpha energy; hence, this design feature aids in discriminating against the alpha particles. However, if alpha particles emitted from the outer edge of a plated surface escape beyond the edge of an adjacent plate, they will have a longer ionization path and give rise to an electronic pulse equivalent to a pulse from a fission particle. (This is referred to as edge effect.) To minimize edge effect, the 4-in.-diam layer of U^{235} was centered on the $4\frac{9}{16}$-in.-diam plates, leaving a $\frac{9}{32}$-in.-wide uncoated edge on each plate.

Even though the alpha pulses are attenuated as a result of the electrode spacing, the natural alpha emission rate is high enough to cause a

[1] By the ORNL Neutron Physics Division.

[2] G. de Saussure *et al.*, *Neutron Physics Div. Ann. Progr. Rept. Sept. 1, 1961*, ORNL-3193, p. 177.

[3] G. de Saussure *et al.*, *Neutron Physics Div. Ann. Progr. Rept. Aug. 1, 1963*, ORNL-3499, vol. 1, p. 3.

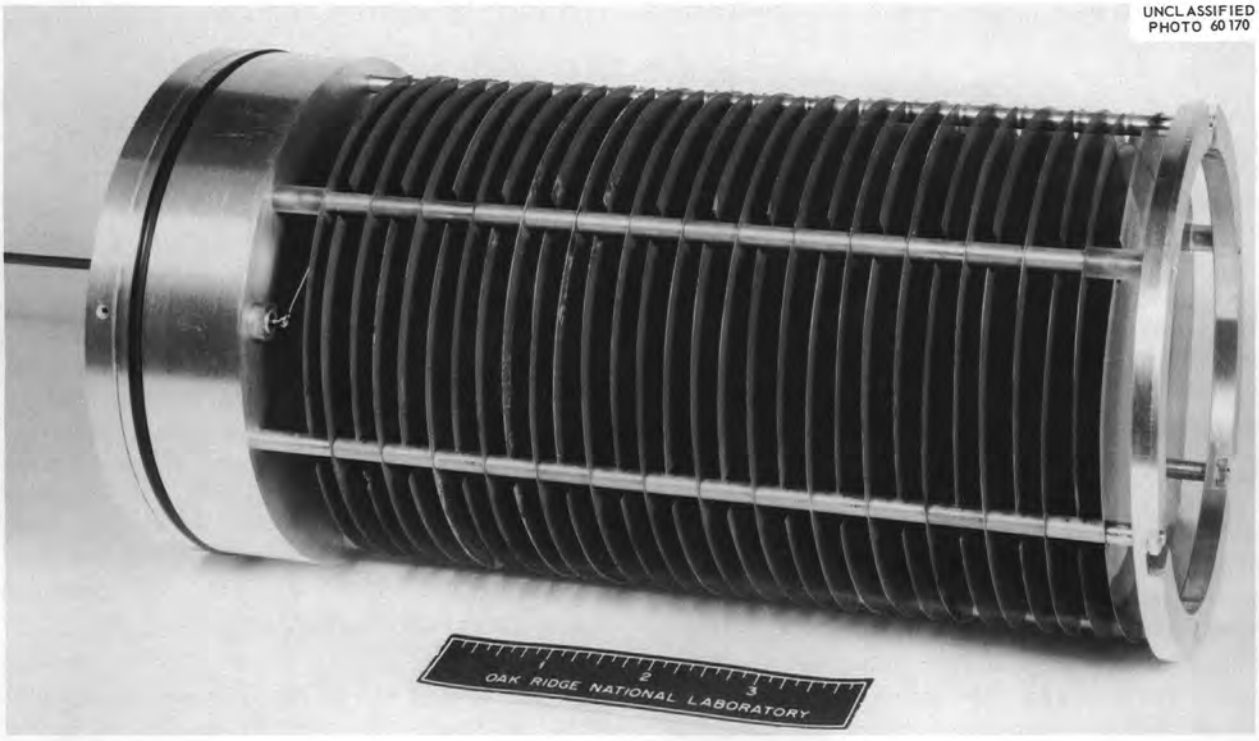

Fig. 4.7.1. Fission-Chamber Electrode Assembly.

serious pulse pile-up problem. It was concluded from a previous investigation of this problem with a similar fission chamber[4] that the electrode spacing should be 0.250 in. in combination with a gas pressure of 1 atm abs. This combination of electrode spacing and gas pressure yielded the best fission-fragment detection with the optimum discrimination against alpha pulse pile-up. These values were used in the design of this new chamber.

[4]Fission chamber built by F. E. Gillespie, ORNL Instrumentation and Controls Division, and described by G. de Saussure *et al.*, *Neutron Physics Div. Ann. Progr. Rept. Sept. 1, 1961*, ORNL-3193, p. 182.

4.8 X-RAY PROPORTIONAL COUNTER FOR THE 5- TO 35-kev ENERGY RANGE

R. E. Zedler

An x-ray proportional counter to analyze the 5- to 35-kev photon range was needed for an ORNL x-ray absorption spectrograph, because no single counter was available to cover this range with adequate resolution and efficiency. Such a counter was designed and fabricated.

The counter dimensions are limited by the equipment surrounding the space in which the counter is mounted. The inside length of the brass-cathode counter is 8 in., and the inside diameter is $2\frac{1}{8}$ in. The maximum outside length, including the connector caps, is $10\frac{1}{2}$ in., and the cathode outside diameter is $2\frac{1}{2}$ in. The anode is a 4-mil tungsten wire. The counter is filled to a pressure of 73 cm of xenon and 6 cm of methane.

Four beryllium windows, $\frac{1}{4}$ by $\frac{1}{2}$ in. and 0.010 in. thick, are vacuum sealed to the counter with epoxy cement. Two of these windows are mounted

diametrically opposite each other and in the center of the side of the cathode. The other two windows are mounted axially opposite each other and in the end plates of the counter (Fig. 4.8.1).

To obtain maximum resolution for the 5- to 14-kev range, the counter is oriented so that the beam enters a side window. To obtain the higher absorption efficiency (Fig. 4.8.2) needed for the 14- to 35-kev range, the counter is rotated 90° so that the beam enters an end window. The second window of each pair serves as an exit for unabsorbed x-ray photons. These photons pass through the window and do not produce any background of fluorescent radiation.[1]

The length of field tubes in proportional counters is usually made equal to the inside diameter of the counter. When the proper voltage is applied to the field tubes relative to that of the anode wire, the gas amplification factor for electrons produced by the ionizing events is uniform over the exposed anode wire. However, no electrons are collected from the volumes defined by the length of the field tubes. The field tubes in this counter are made very short ($^3/_{16}$ in. long) to eliminate this dead space, which would result in a large loss in detection efficiency when the x-ray beam travels axially through the counter. Because the field tubes are short relative to the inside diameter of the counter, the gas amplification factor is not uniform over the entire length of the anode wire. Nevertheless, the practice is to adjust the field-tube potential until maximum resolution is achieved with the x-ray beam passing axially through the counter. The exact field-tube potential does not affect the resolution of the detector when the beam passes through the side window, because the ionization is confined to a small region over which the gas amplification is uniform and is independent of the field-tube effect.

The counter has a resolution of about 13.5% for the 5- to 35-kev energy range when used as described above, and may be operated at counting rates of up to 50,000 counts/sec.

[1]A. R. Lang, *J. Sci. Instr.* 33(3), 96 (1956).

UNCLASSIFIED
ORNL-DWG 64-1203

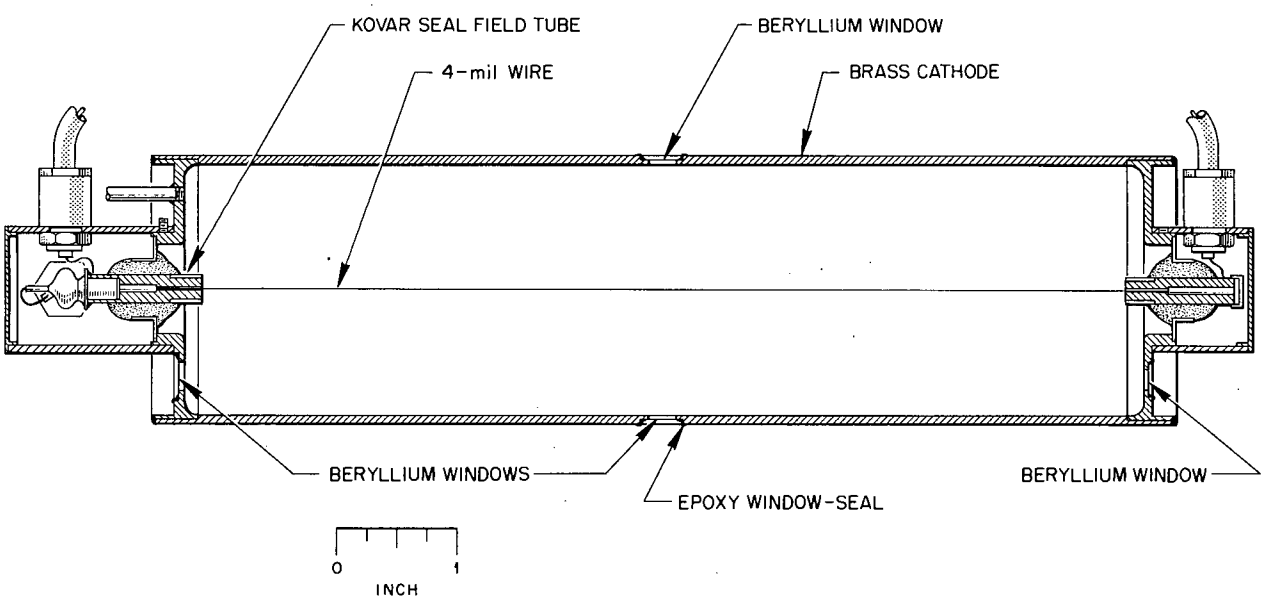

Fig. 4.8.1. X-Ray Proportional Counter.

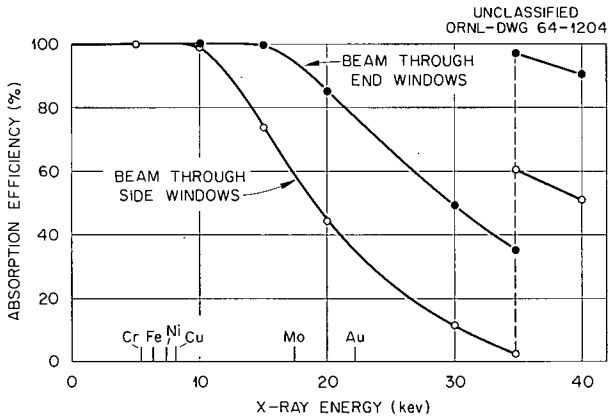

Fig. 4.8.2. Absorption Efficiency of X-Ray Proportional Counter.

4.9 NEW GAMMA IONIZATION CHAMBER

H. R. Brashear R. K. Abele

A new gamma ionization chamber was designed and fabricated commercially according to ORNL specifications for use at ORNL. This chamber, available in ORNL Stores, complements the ORNL standard 2-in.-diam chamber (ORNL model No. Q-2045), but has better saturation characteristics (5 to 1000 v applied chamber voltage) (Fig. 4.9.1) and has a useful range of 25 mr/hr to 10^5 r/hr.

The chamber is filled with 4.37 atm of xenon over a 5-in. active length, which yields a sensitivity of 4×10^{-11} amp/r/hr. Physical dimensions are 0.937 ± 0.005 in. OD and $7\frac{7}{8}$ in. in length, including the cable connector. The chamber housing is made of stainless steel, with all-welded construction. An O-ring seals the single two-pin connector against moisture. The cost of the chamber is less than $300.

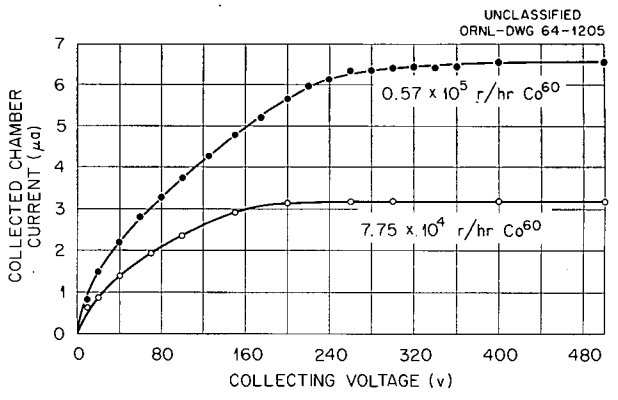

Fig. 4.9.1. Saturation Characteristics of Gamma Ionization Chamber.

4.10 ION CHAMBER FOR DEPTH-DOSE MEASUREMENTS IN A WATER PHANTOM

M. M. Chiles

In connection with the ORNL Space Program, experiments were performed by the Neutron Physics Division[1] to investigate the radiation exposure that would be experienced in a manned spacecraft from high-energy proton radiation. A 42-cm-diam shell made of methyl methacrylate (Lucite) was filled with water and exposed to the primary (160-Mev) proton beam from the Harvard University synchrocyclotron and to the secondary radiation from targets of different shielding materials (water, aluminum, carbon, copper, and bismuth) which were placed in the proton beam. The ion chamber described in this article was located at various positions inside the spherical water-filled phantom (Sect. 4.12) to measure the radiation dose from both the primary and the secondary radiations.

All electrodes and components in the vicinity of the radiation detector cavity were constructed of materials similar to water in atomic structure, for example, methyl methacrylate or polyethylene. The electrodes were coated with a carbon-particle suspension ('dag') for electrical conductivity. Connectors and other metal parts were located approximately 5 in. behind the center of the detector to minimize contributions to the dose measurements from nonhydrogenous materials.

The internal volume of the ion chamber is 21.6 cc and is spherically shaped for isotropic effect (Fig. 4.10.1).

Four ion chambers were constructed; two were filled with ethylene gas and two with a 97% Ar–3% CO_2 gas mixture. The gas pressure was 75 cm Hg abs in all four chambers.

Gas diffusion occurred through the 0.125-in. Lucite wall and was accompanied by a continuous decrease in sensitivity of the detectors. To correct for the decrease in sensitivity, the chambers were calibrated against a known standard source before each experimental run.

[1] F. C. Maienschein and T. V. Blosser, *The Depth-Dose Distribution Produced in a Spherical Water-Filled Phantom by the Interactions of a 160-Mev Proton Beam*, ORNL-3457 (June 7, 1963).

UNCLASSIFIED
ORNL-DWG 64-1206

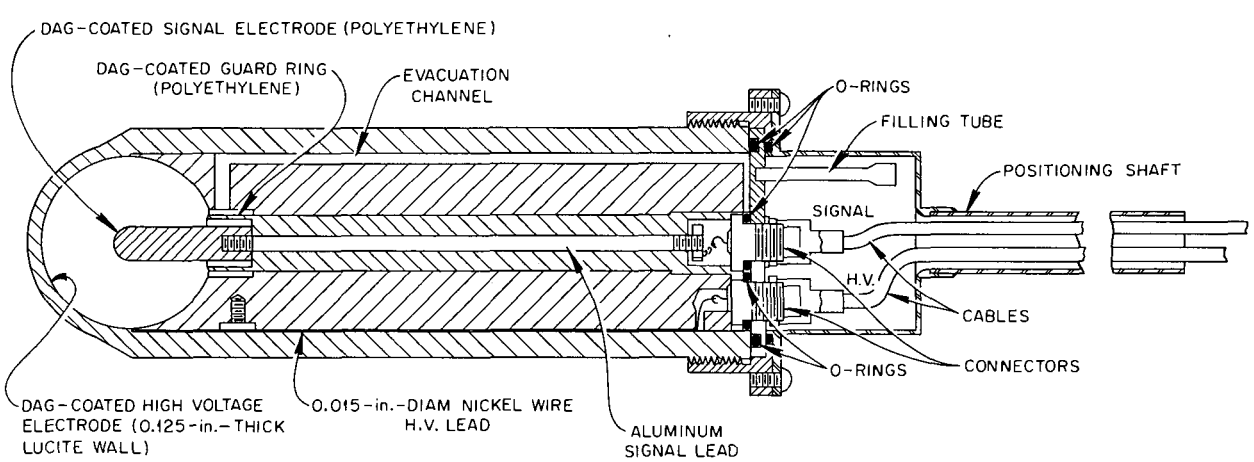

Fig. 4.10.1. Cross Section of Ion Chamber.

4.11 TARGET AND COUNTER HOLDER FOR RADIATION SHIELDING EXPERIMENT

T. F. Sliski H. J. Stripling, Jr.

The Neutron Physics Division is conducting, as part of the Space Shielding Program, experiments in neutron and proton spectroscopy. These experiments are aimed at providing experimental data for validating theoretical calculations on the design of radiation shielding for space vehicles. In the experiments with protons, a cyclotron is used as the proton source. Three design criteria were required of the apparatus to execute these experiments: (1) a means for locating the proton beam from the cyclotron, (2) a means for holding various targets in and concentric with the proton beam, and (3) a means for positioning different detectors in a polar coordinate system about the target. A target and counter holder was designed and fabricated to satisfy these three requirements.

The device (Fig. 4.11.1) consists of a cross-shaped frame which is positioned flat on the floor and is fitted with level-adjusting screws at the four extremities of the cross. A socket is attached to the frame at the intersection of the cross members. The socket accepts the center post and allows it to pivot about a horizontal and a vertical axis. It also allows for vertical adjustment of the center post over a range of 4 in. The outside diameter of the center post is stepped to provide for vertical location of three detector arms which may be positioned at any horizontal

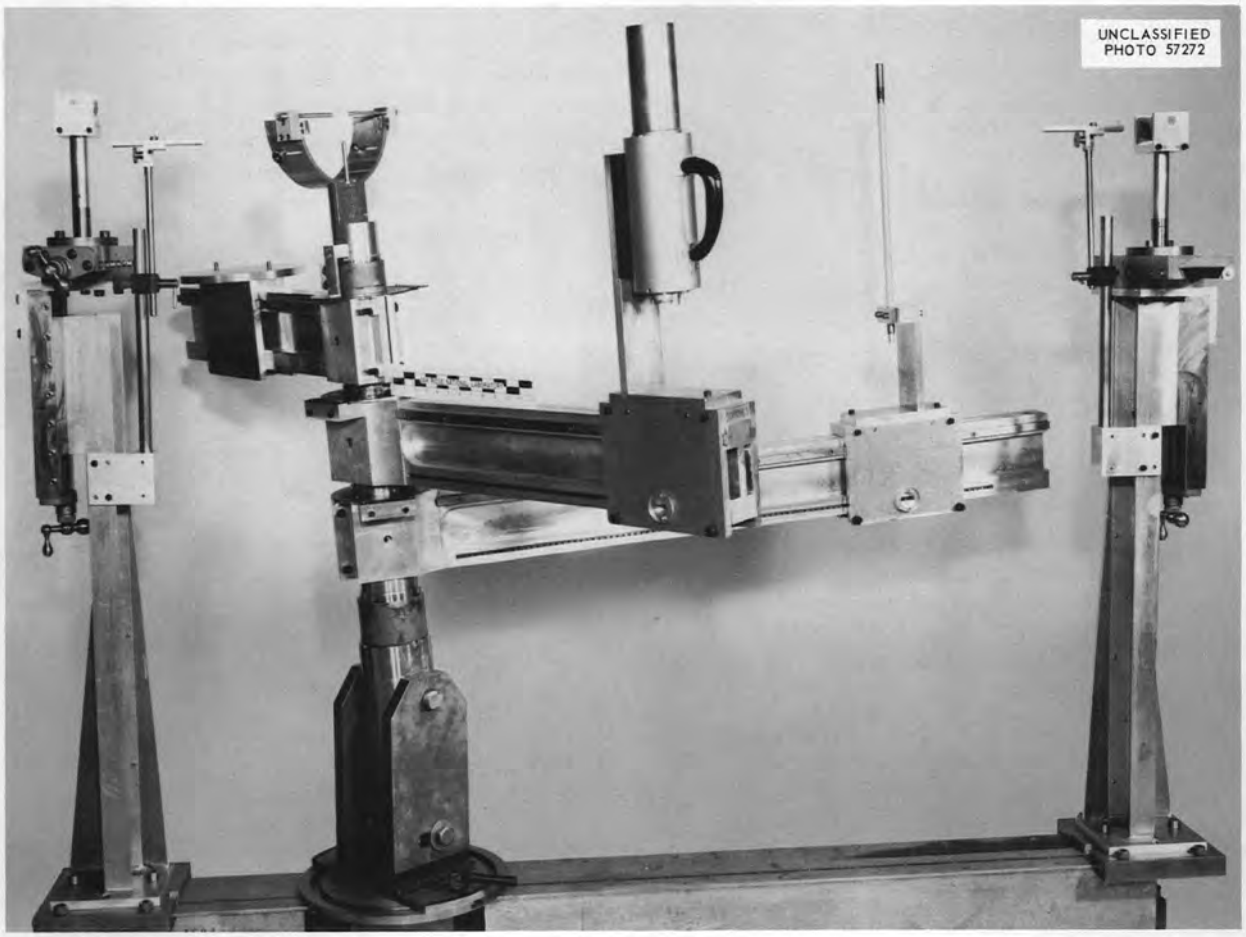

Fig. 4.11.1. Target and Counter Holder for Radiation Shielding Experiment.

angular position about the center post. Each arm is fitted with a slide for mounting detectors and for adjusting the radial distances of the detectors relative to the target.

The target is placed in a target holder, which fits a socket atop the center post. At either end of the longer frame member, an end post is attached to the frame by a slide with which the position of the end post can be adjusted along the frame member. Two slides mounted at the top of each end post provide 4 in. of vertical and 4 in. of horizontal (crosswise the longer frame member) adjustment for different fixtures attached to the top slide. These fixtures include photographic film holders, a profile telescope, and pivoted cradles which can be used with an alignment bar when aligning the center post.

This device was used in numerous experiments at the Harvard University synchrocyclotron. It has since been fitted with shorter center and end posts for use at the Oak Ridge Isochronous Cyclotron. The modifications were required because the proton beam at Oak Ridge is located about 6 in. lower than the one at Harvard.

4.12 DOSIMETER FOR SPACE SHIELDING STUDIES

T. F. Sliski H. J. Stripling, Jr.

In the Space Shielding Program, proton-induced reactions in shields are a major concern (Sect. 4.11). One aspect of the problem involves measurements of the ionization produced in a tissue-like material by secondary particles resulting from proton reactions with various targets. A dosimeter was designed and fabricated for making these measurements.

The dosimeter consists of four principal components. The first component is a water-filled methyl methacrylate spherical phantom, 42 cm in diameter (Fig. 4.12.1). This phantom simulates a man in terms of density, total weight, and the way primary radiations are attenuated and secondary radiations are produced. The second principal component is an ion chamber (Sect. 4.10). Third is a remote-control positioner for locating the ion chamber along a diameter of the sphere. Fourth is a positioner for locating the sphere relative to a target held in alignment with a proton beam from a cyclotron. This positioner is attached to the center post of the target and counter holder (Sect. 4.11) which holds the target in alignment with the proton beam.

The sphere positioner provides five degrees of freedom, two translational and three angular: the sphere may be moved vertically on a line parallel to the vertical axis of the target, it may be moved horizontally in a radial direction relative to the target, it may be moved in a horizontal orbit about the target, and it may be rotated about its own horizontal and vertical axes.

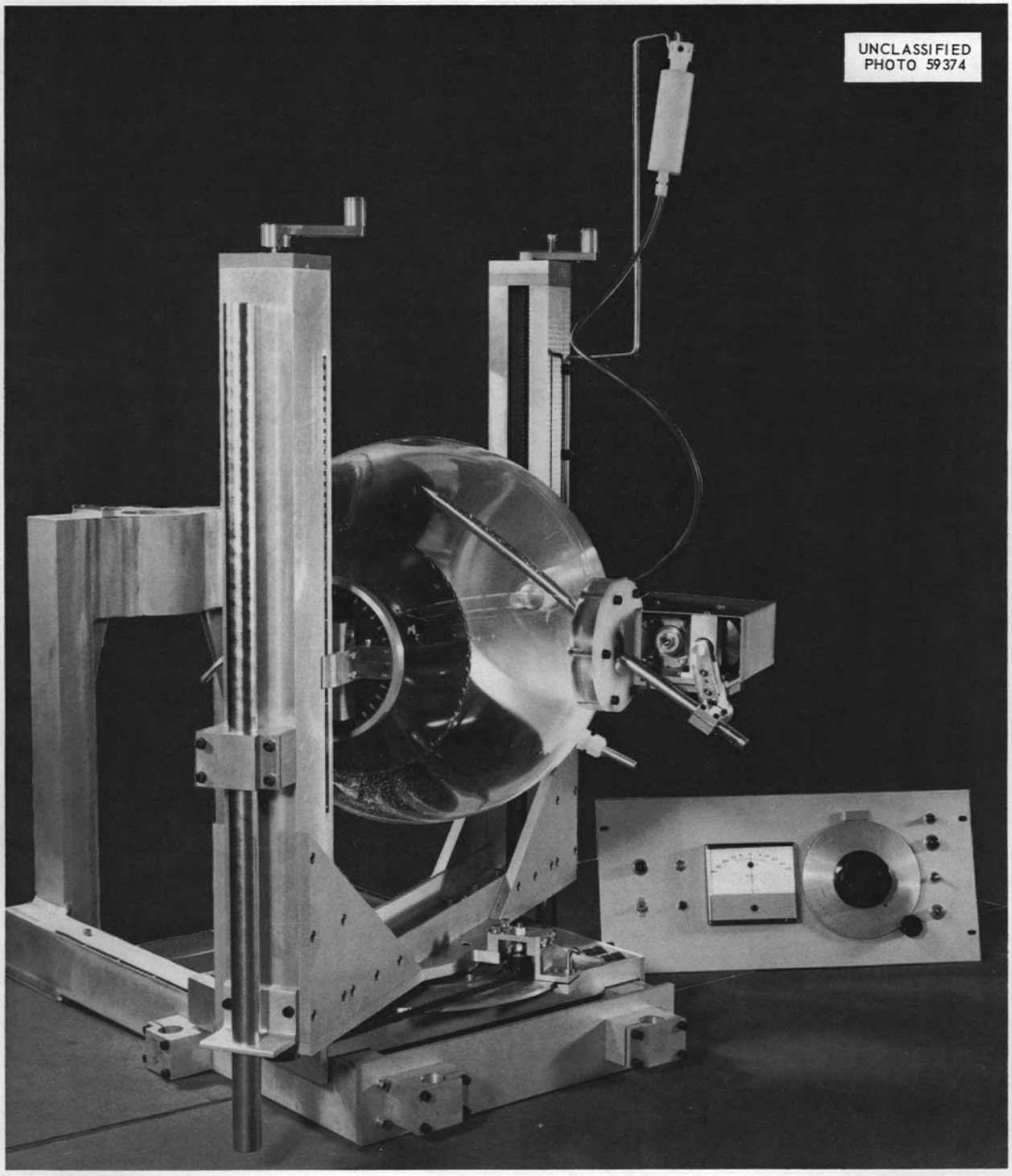

Fig. 4.12.1. Dosimeter for Space Shielding Studies with Dummy Rod Inserted in Place of Ion Chamber.

4.13 LITHIUM-DRIFTED SILICON RADIATION DETECTORS

R. E. Zedler

Because they possess properties which can be profitably exploited in beta particle and high-energy heavy particle (e.g., proton) spectrometry, lithium-drifted silicon radiation detectors are being produced for use at the Laboratory.

The fabrication process and equipment are similar to those described by Blankenship and Borkowski.[1,2] Silicon wafers 2.1 cm in diameter (ingot diameter) and 4 mm thick are lapped on both surfaces. A heavy layer of lithium is evaporated on one face. The lithium is alloyed into the silicon at 450°C for 15 min in an argon-atmosphere furnace. The resulting sheet resistivity is 0.6 ohm/cm^2. The lithium is then drifted completely through the wafer at a temperature of 115°C and at 400 to 500 v applied across the wafer. Approximately 0.015 in. is then lapped off the back face. The remaining slice is heated to 300°C for 15 min to restore the junction and is then heated at 85°C and with 500 v reverse bias for 1 hr to redistribute the lithium.

Detectors prepared as described are characterized by resolutions of 19 kev for the 0.972- and 1.045-Mev conversion electrons of Bi^{207} at liquid-nitrogen temperature and 130 v reverse bias. The 1.68- and 1.75-Mev conversion electrons of Bi^{207} are measured with a resolution of 27 kev.

Figure 4.13.1 shows a typical spectrum for Bi^{207}.

[1] J. L. Blankenship and C. J. Borkowski, *Instrumentation and Controls Div. Ann. Progr. Rept. Sept. 1, 1962*, ORNL-3378, p. 21.

[2] Section 1.1 of this report.

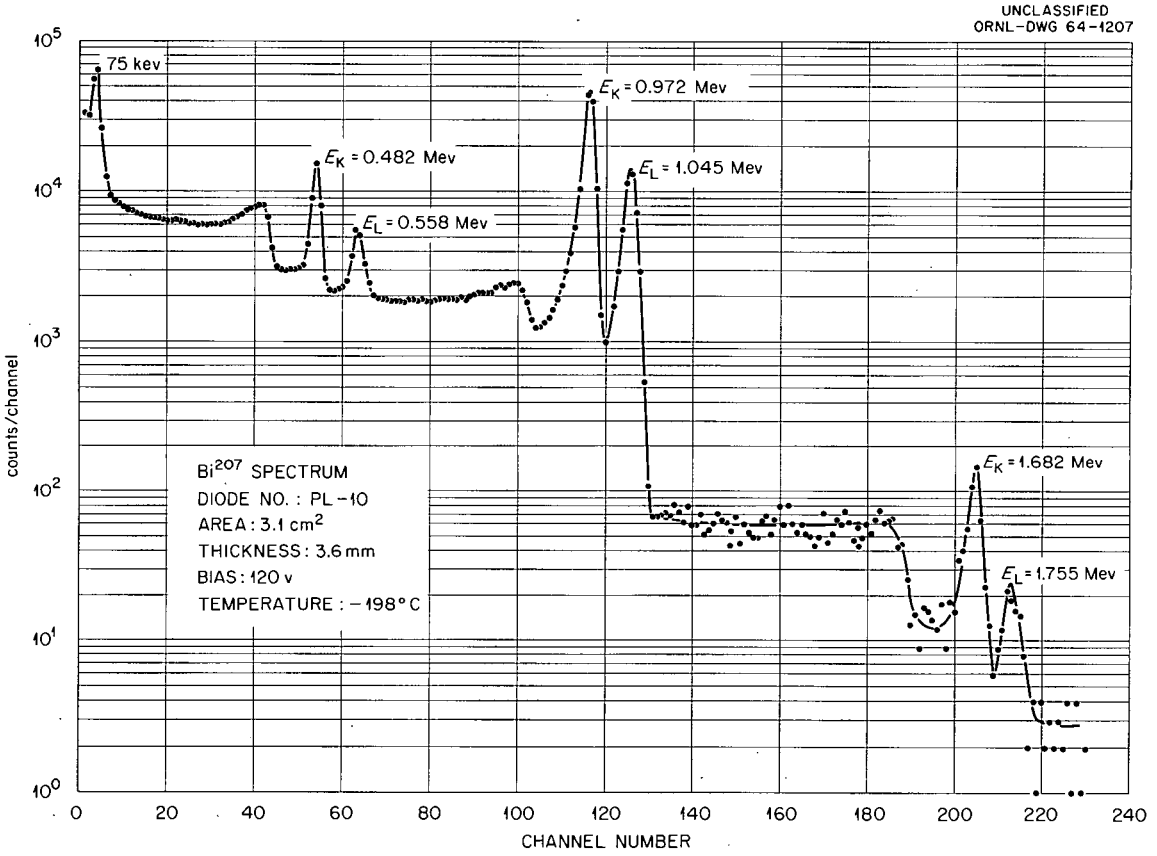

Fig. 4.13.1. Bismuth-207 Spectrum Determined with Lithium-Drifted Diode.

5. Data Handling and Computation

5.1 DIGITAL ANALYZER SYSTEM FOR NEUTRON TIME-OF-FLIGHT STUDIES

J. W. Woody J. L. Lovvorn

Oak Ridge National Laboratory participation in the SNAP[1] program includes neutron time-of-flight studies. One component of the data-acquisition complex is an analyzer system whose time span is readily adjusted with a knob setting. A digital system was selected to accommodate this feature because it is more compatible to the use of commercially available components.

The time-of-flight measurement is ultimately based on a 10-nsec-resolution time-interval meter, which is gated on and off by an appropriate nuclear event. The output of the time-interval meter is fed into a small BCD (binary coded decimal) arithmetic unit. It is this BCD arithmetic unit which lends the analyzer system to time-span expansion or contraction. The output of the time-interval meter is simply divided by an appropriate factor before it is fed to the BCD arithmetic unit. A Technical Measurements Corporation 400-channel analyzer memory is used as the system memory; hence, the basic time span is 4 μsec, since the timer resolution is 10 nsec. Because the number of channels is fixed, expanding the time span by a given multiple reduces the effective system resolution by the same factor.

The present analyzer system can be made to operate with a 10,000-channel memory without any major alterations to the data-acquisition complex. The corresponding channel widths would be narrowed accordingly.

Recently, a time-interval meter with a 1-nsec resolution was obtained. It will replace the present 10-nsec-resolution timer and will yield a tenfold increase in resolution.

[1]Space Nuclear Auxiliary Power.

5.2 X-RAY SCANNER

J. W. Reynolds

B. E. Foster[1] R. W. McClung[1] T. F. Sliski
S. D. Snyder[1] K. E. Toomey[2]

Because heat transfer values and neutron flux levels are very high in the HFIR, close limits must be placed on the fuel distribution within each fuel plate; consequently, the fuel distribution in each fuel plate must be measured after the plate has been fabricated. Conceptually, the measurement is accomplished by scanning the plate with collimated x rays and detecting those which are transmitted through the plate. Fuel density variations are manifested as variations

[1]Metals and Ceramics Division.

[2]Plant and Equipment Division.

in the absorption of the transmitted x-ray beam. Results to date indicate that the prototype system will perform with an accuracy of ~1%.

A pilot model is under construction and will incorporate an ion-chamber and electrometer detection system. It will be used to examine fuel plates for the HFIR criticality experiments and to provide the ultimate manufacturer of the fuel elements with a production prototype.

5.3 NONLINEAR LEAST-SQUARES FITTING APPLIED TO GAMMA-RAY SCINTILLATION DETECTOR RESPONSE FUNCTIONS[1]

R. O. Chester R. W. Peelle[2] F. C. Maienschein[2]

Pulse-height spectral response functions for three gamma-ray scintillation spectrometers have been fitted to empirical interpolation functions, using a nonlinear least-squares method. An IBM 7090 was used to determine the solutions to the normal equations which arise in the iterative procedures required to obtain the fitting parameters. This work was undertaken in an effort to obtain objective fits to experimental response functions, including plausible error estimates on output parameters.

The pulse-height spectra were obtained as part of an experiment to determine the prompt gamma-ray spectrum associated with the thermal fission of U^{235}. A single-crystal (1 in. by $1\frac{3}{4}$ in. diam) spectrometer was used for the energy range below 400 kev. The energy ranges above 400 kev were covered by pair and Compton scintillation spectrometers.

Calibration pulse-height spectra for the spectrometers were taken with sources of known disintegration rates placed in the region occupied by the U^{235} fission chamber during the experiment. Source strengths were determined with a 4π ionization chamber standardized by coincidence measurements.

Each response function approximates in a single complex formula the counts per pulse-height interval as a nonlinear function of the pulse height, the input gamma-ray energy, and a set of empirically determined parameters. The form of the response function was selected to minimize the number of parameters needed for a fit to the data. Consideration was given to physically reasonable extrapolation of the response function to input gamma-ray energies outside the range of available data.

A modified Gauss-Seidel method of analysis was employed to determine the fitting parameters. That is, the response function was approximated by the value of the response function at a previously estimated set of parameters plus the first-order terms in a Taylor series expansion in parameter differences. Setting the derivatives of the weighted residual sum of squares to zero gave a correction to the estimated set of parameter values. This process was iterated until there was no noticeable improvement to the residual sum of squares.

Included in the response function are the parameters which describe the spectrometer peak efficiency as a function of gamma-ray energy; thus, spectral shape and efficiency problems are solved in one operation.

---

[1]Abstract of paper presented at the Symposium on Applications of Computers to Nuclear and Radiochemistry, Gatlinburg, Tenn., October 1962; *Proc. Symp. Appl. Computers Nucl. and Radiochem.*, NAS-NS-3107, pp. 201–12.

[2]Neutron Physics Division.

5.4 APPROXIMATE MODELS FOR DISTRIBUTED-PARAMETER HEAT TRANSFER SYSTEMS[1]

S. J. Ball

The use of dimensionless-parameter frequency response diagrams to determine accuracies of lumped-parameter approximations is demonstrated by two examples: calculation of the heat flux at the surface of a semi-infinite solid due to temperature fluctuations of an adjacent fluid; and the response of a counterflow heat exchanger to inlet fluid temperature perturbations. Dimensionless system parameters make it possible to use a function of the frequency of perturbation. Such plots are directly applicable to control-system stability problems, where the highest frequency of interest is usually apparent.

[1]Abstract of paper presented at 1963 Joint Automatic Control Conference, University of Minnesota, June 19–21, 1962; *Preprints of Technical Papers, Fourth Joint Automatic Control Conference*, AIChE, pp. 131–9.

5.5 APPLICATION OF DATA-LOGGING SYSTEMS

R. K. Adams C. D. Martin R. E. Whitt

Two data-logging systems were installed and several others were modified, as follows:

1. A single-channel (punched paper tape) data logger was installed to record quantitative spectral-analysis data from the Analytical Chemistry Division Quantometer.
2. A 30-channel punched-paper-tape logger was installed to investigate data acquisition and reduction techniques at the GCR-ORR Poolside Capsule Facility (Sect. 6.4).
3. A 60-channel punched-paper-tape logger was modified for the Chemical Technology Division (Fig. 5.5.1).
4. A spectrophotometer logging system was expanded to record data from two spectrophotometers.
5. A single-channel (punched paper tape) data logger is being constructed for application to optical-spectrum data reduction.
6. A 100-channel, medium-speed data system (CSC MILLISADIC) is being renovated for application to test engineering experiments which require data acquisition rates up to 400 channels/sec.

All the above equipment is operational; however, the ultimate successful use of such systems depends on the development of input programs which will allow the logged data to be fed directly into digital-computer data-analysis programs without intermediate manual treatment. Input programs for each of the six systems above have been or are being written (Sect. 5.7).

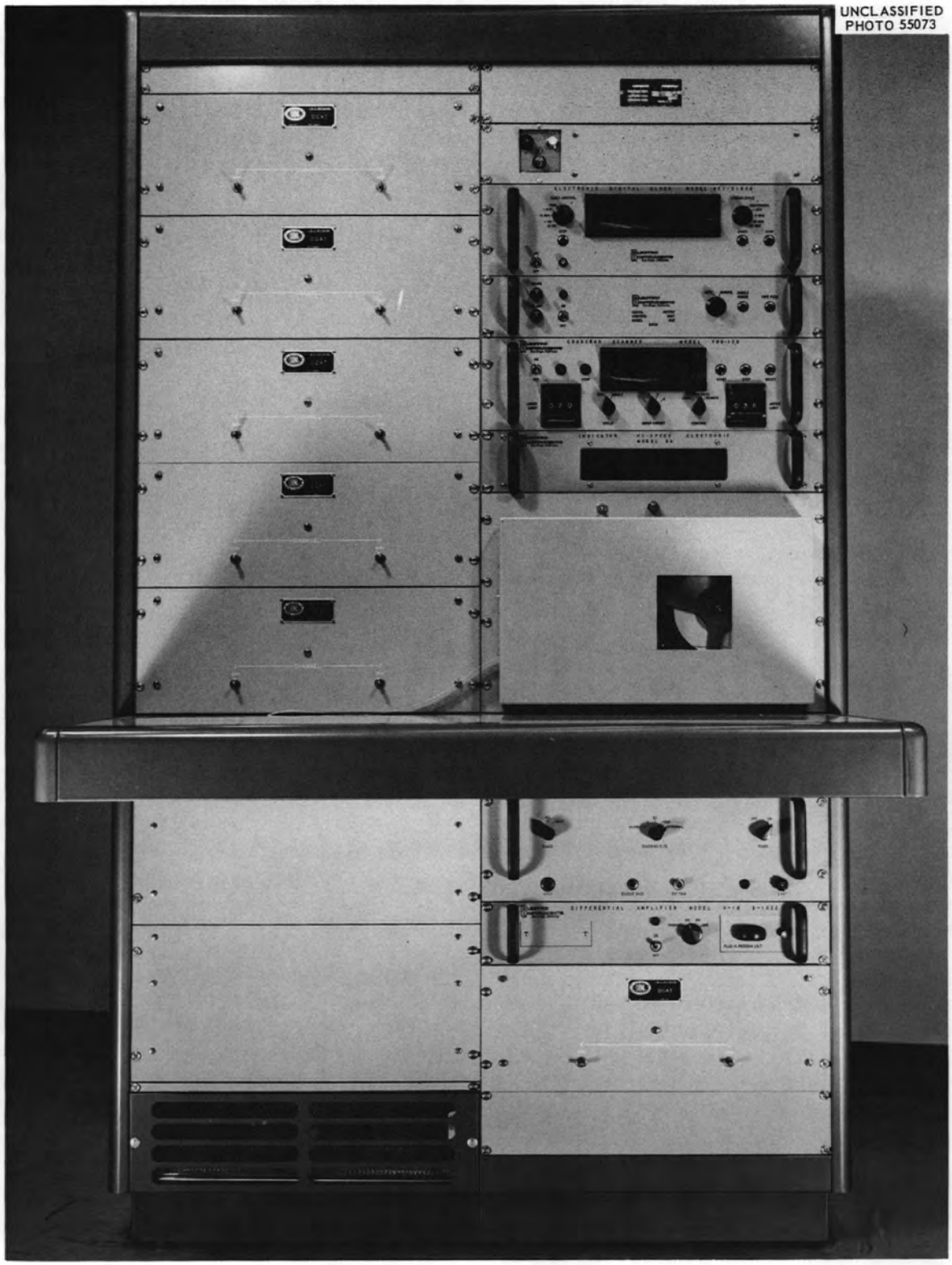

Fig. 5.5.1. Modified 60-Channel Punched-Paper-Tape Data Logger.

5.6 DEVELOPMENT OF DIGITAL COMPUTER CODES FOR SYSTEMS ANALYSIS

S. J. Ball

Analytical frequency-response methods are often not attempted in complex problems of systems control and analysis because of the prohibitive amount of hand calculating which must be done; consequently, several computer codes have been written to exploit these analytical methods.

"Samulon's method," an accurate means of computing frequency-response plots from step-response data, is useful for experimentally determining instrument and component characteristics as well as the characteristics of a complete system. A FORTRAN code was written which can accommodate up to 200 points of step-response data and calculates magnitude, ratio, and phase as a function of frequency.

It is known that frequency-response plots are useful in estimating the frequency-dependent accuracy of lumped-parameter approximations of distributed-parameter systems by comparing analytical solutions of the Laplace-transformed, distributed system equations with typical lumped-parameter transfer functions. The approximate models for particular components or systems – with their limitations exposed – can then be used in the simulation of the entire system on an analog or digital computer. Such codes have been written for slab-geometry diffusion problems and for counterflow heat exchangers. Codes for other typical systems are planned.

To aid in a frequency-response analysis of an entire system, a code was written which computes the closed-loop frequency response of arbitrarily complex multiloop systems, given the frequency responses of the components and the form of the closed-loop equation.

A simple code has been written which computes the frequency response of the linearized neutron kinetic equations with six delayed neutron groups.

5.7 INTERFACE PROGRAMMING

R. K. Adams E. G. Davisson C. D. Martin

Existing automatic data-acquisition systems exhibit a high degree of reliability; however, errors of two basic types occasionally occur. The "format error" is a machine-generated error in the data-acquisition system output (number of characters per word, word separator symbols, number of words per block, block separator symbol, etc.). Such errors are particularly troublesome and can result in the premature termination of a digital-computer data-analysis program, usually before any results are obtained, so that even one error in many thousands of data words is intolerable. In addition to format errors, the data system may record "wrong numbers" because of system malfunction or process noise. Wrong-number errors do not lead to premature termination of the data analysis program, but the accuracy of the analysis is adversely affected if such errors are not detected and eliminated.

Computer programming techniques are needed which recognize the primary sensor limitations, physical experiment design factors, and data system restrictions (speed, accuracy, etc.), and which attempt to do error correcting and data editing. This type of programming may be called "data acquisition system interface programming," because it provides the interface between the experiment (and data system) and the digital computer. Interface programming provides for recognition of format errors and corrects the format, or eliminates the particular data item which is affected by the error; wrong-number errors are accommodated by provisions in the program which analyze data trends and discard wild points.

The portion of interface programming which involves data editing is widely recognized as a difficult problem. Nevertheless, several successful programs have been written which recognize the specific characteristics and error tendencies of a particular data-logging system and accommodate format errors via an editing procedure. Two of these in present use are the CDC-160A read-in program for the 60-channel, Chemical Technology Division, Unit Operations data logger and the program for the Volatility Pilot Plant data logger. To date no successful generalized data editing, correcting, and checking programs have been devised; nevertheless work on generalized methods is being continued.

5.8 PROPOSED METHOD OF DATA REDUCTION FOR EGCR CONTROL-ROD-PROTOTYPE TESTS

R. K. Adams C. D. Martin

A computer program was required to process data acquired by a digital magnetic-tape system for the evaluation of velocity and acceleration characteristics of reactor control rods.[1] In an initial phase of this study, a curve-fitting procedure was developed for smoothing the digital data and putting it in a form that could be easily manipulated to obtain the control-rod velocity and acceleration characteristics. This procedure was applied to the scram retarder system originally proposed for the EGCR by Allis-Chalmers.[2] The position-vs-time characteristic derived from a mathematical model of this system is shown in Fig. 5.8.1. However, the retarder system was modified in the course of development to such an extent that this computer program could not be used. A graphic plot of position vs time for the modified system (Fig. 5.8.1) shows that the rod is retarded momentarily at a position about 38 in. from the crash stop during a scram from 175 in. This retardation occurs in drops from any height down to a few inches, and is the main factor in the modified system that voids the original program.

A general purpose program was written which is designed to accommodate all data obtained by the digital magnetic-tape system, regardless of the retardation scheme used. Curve smoothing and derivative extraction are accomplished by a numerical convolution method which fits a third-order polynomial to the data by the least-squares criterion.

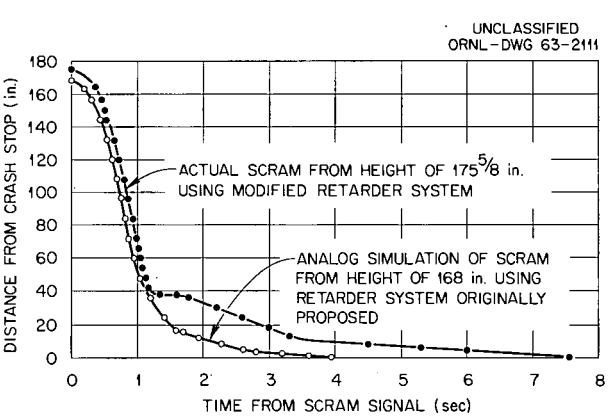

Fig. 5.8.1. Scram Tests of EGCR Control-Rod Drive.

[1] J. W. Reynolds, *Instrumentation and Controls Div. Ann. Progr. Rept. Sept. 1, 1962*, ORNL-3378, p. 38–9.

[2] Allis-Chalmers Manufacturing Company, "Study II – 401 Control Rod Drive System, Description and Design Criteria, Experimental Gas Cooled Reactor, June 9, 1961."

5.9 THERMOCOUPLE CALIBRATION COMPUTER PROGRAMS

C. D. Martin R. K. Adams

A computer program was developed for calibrating thermocouples in the Standards Laboratory (Sect. 7.10) of this Division. The program requires inputs of standard-thermocouple emf, standard-thermocouple temperature correction, and test-thermocouple emf. The computer converts these emf values to temperature, using the appropriate tables from NBS Circular 561; corrects the standard temperature; and computes the test-thermocouple error. The standard temperature, test-thermocouple emf and temperature, and test-thermocouple error are then printed out by the computer. The cost of the program is about 7¢ per calibration point, including keypunching the data on IBM cards. The program is currently operational on both the IBM 7090 and CDC-1604A computers.

From this work the following guide on the use of NBS thermocouple tables was developed:

1. The NBS thermocouple tables represent a compromise average of the emf-temperature relation of thermoelectric materials; therefore, for work where accuracy greater than ±0.75% is required, special calibration of the thermocouple is needed.

2. The precision of the NBS tables in Circular No. 561 is not consistent from table to table. For instance, the values expressed in Tables 1, 3, 5, 7, and 9 are rounded interpolated values obtained from the corresponding Celsius (centigrade) Tables 2, 4, 6, 8, and 10 respectively. The Fahrenheit tables are calculated from the Celsius tables. Therefore, the Celsius even-numbered tables in Part I of NBS Circular 561 are preferred.

Another computer program has been developed which accepts inputs of platinum resistance thermometer constants, and computes and prints a table of resistance vs temperature for 1° increments from −249°C to +499°C. This program will be incorporated in the thermocouple calibration program to accommodate platinum resistance thermometers as standard temperature sensors.

6. Process Instrumentation and Control Systems Engineering

6.1 SYSTEMS DESIGN GROUP ACTIVITIES

Bernard Lieberman

During this report period, the Systems Design Group was active on 22 projects (Table 6.1). The cost of instrumentation ranged from $2000 to $360,000; the total cost of the 22 projects was $1.4 million. Manpower for design and engineering of these projects totaled 150 man-months.

Separate reports on a few of these projects are given in the following sections.

Table 6.1. Summary of Systems Design Group Activities

Project	Total Cost (dollars)	Cost of Instrumentation (dollars)	Engineering and Drafting (man-months)	Percent Completion on July 1	
				1962	1963
Nuclear Safety Pilot Plant	450,000	100,000	11.25	0	50
TRU production facility	8,700,000	360,000	50	10	30
ORR scrubber improvement[a]	b	12,000	2.25	100	100
LITR process instrument system updating	b	40,000	8	0	100
ORR drawings and specifications updating	b	3,500	3	0	80
Desalinization reactor, fuel fabrication study			0.75		100
Radiochemical processing and Kilorod Pilot Plant modifications	b	30,000	8.5	0	100
Source fabrication facility	340,000	10,000	2.7	0	85
Rover Program, Bldg. 3503	100,000	25,000	2.25	0	100
In-pile loop instrumentation	b	15,000	8	0	80
Th-U fuel cycle development	7,000,000	~350,000	2.5	0	10
Metals and Ceramics, move to new building	1,000,000 (approx.)	60,000	5	65	100
Pot calcination, Cell 1	180,000	15,000	3	0	75
Vacuum pit instrumentation and alarm system revisions, Bldg. 4047	b	2,000	0.75	0	100
Low-Level Waste Treatment Pilot Plant	60,000	20,000	5	0	100
Waste treatment improvements	1,700,000	80,000	8	0	60
Transuranium development facility	750,000	46,000	6	0	95
Harvard foam tests	62,000	13,000	2	0	100
Containment control instrumentation for Bldg. 3019	b	17,000	7.5	0	80
Poolside facility in ORR	80,000	50,000	1.75	0	95
In-pile experiment at the ETR[a]	60,000	26,000	4	90	100
Volatility Pilot Plant modifications	b	65,000	8	c	c

[a]Not previously reported.
[b]Instrumentation was installed in an existing facility.
[c]This is a continuing, open order.

6.2 INSTRUMENTATION FOR ORNL EXPERIMENT 41-8 AT THE ENGINEERING TEST REACTOR

A. H. Malone B. C. Duggins

An instrument system was designed and fabricated for the Reactor Chemistry Division experiment 41-8, conducted in the Engineering Test Reactor (ETR) at Idaho Falls. The console instrumentation (Fig. 6.2.1) was subjected to extensive tests and evaluation using analog simulation of the experimental system before being shipped to the ETR.

Experiment 41-8 consisted of a number of beryllium oxide samples encapsulated and placed in the radiation field of the ETR. The experiment was divided into four channels, each channel containing four sample capsules. The instrumentation for each channel is identical, although the operating conditions for individual channels vary with the type of sample.

The system was designed to measure and control the temperature of these capsules with changes in reactor power level. The temperature of the capsules is controlled by varying the ratio of helium to argon in a gas mixture surrounding the test samples. The resulting change in the thermal conductivity of this mixture is used to regulate the rate of heat transfer from the sample to the reactor cooling water. The instrument system consists of gas-flow recording instruments, temperature recording and controlling instruments, pressure recording instruments, and high- or low-

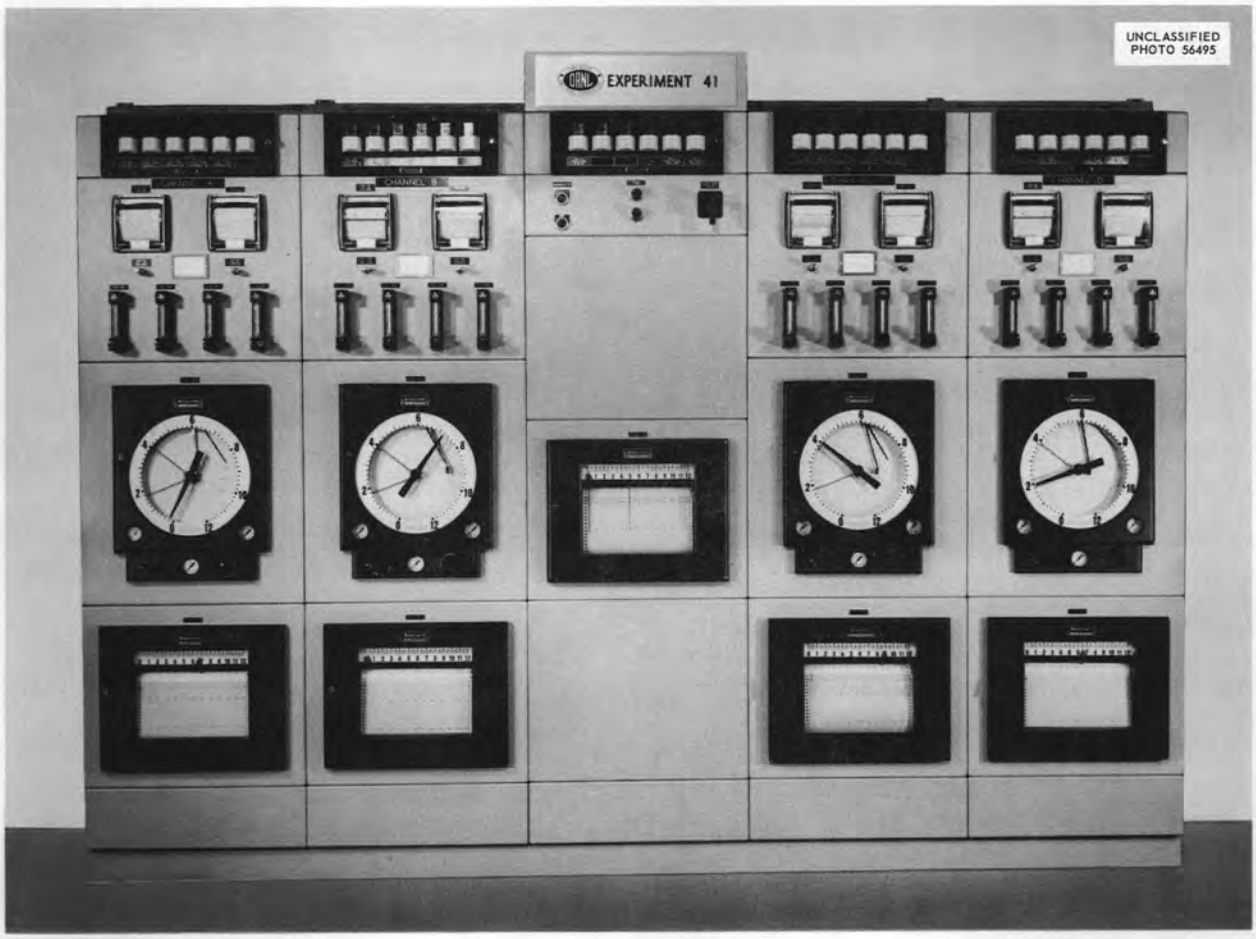

Fig. 6.2.1. Panel Board for Experiment 41–8.

limit alarms. All alarms are annunciated at the panel and may, as required, be incorporated in the reactor alarm and safety circuit. Provision was made to monitor all temperatures on the central data-logging system of the ETR.

A physical analog–part electrical analog computer simulation of experiment 41-8 was connected to the instrument panel board for the experiment to evaluate the performance of the temperature control instrumentation and to allow a preinstallation check-out and adjustment of the instruments (Fig. 6.2.2). For this simulation, a tubing network which approximated the restriction to gas flow in a channel housing the experiment was connected to the helium-argon piping at the panel board, and a desk-top analog computer to simulate the thermal response of a single specimen was connected to the panel board temperature control instruments through appropriate transducers. Since each experiment channel was to be entirely independent of all others, it was possible to check out and adjust all the instruments on the panel board by utilizing the above scheme and working with one channel at a time.

After the system was installed at the ETR by Phillips Petroleum personnel, startup assistance was provided by the Instrumentation and Controls Division. The instrument settings developed during the analog simulation permitted a very smooth startup and essentially eliminated the problems usually associated with the startup and adjustment of an in-pile experiment. The system has been operating successfully for about a year.

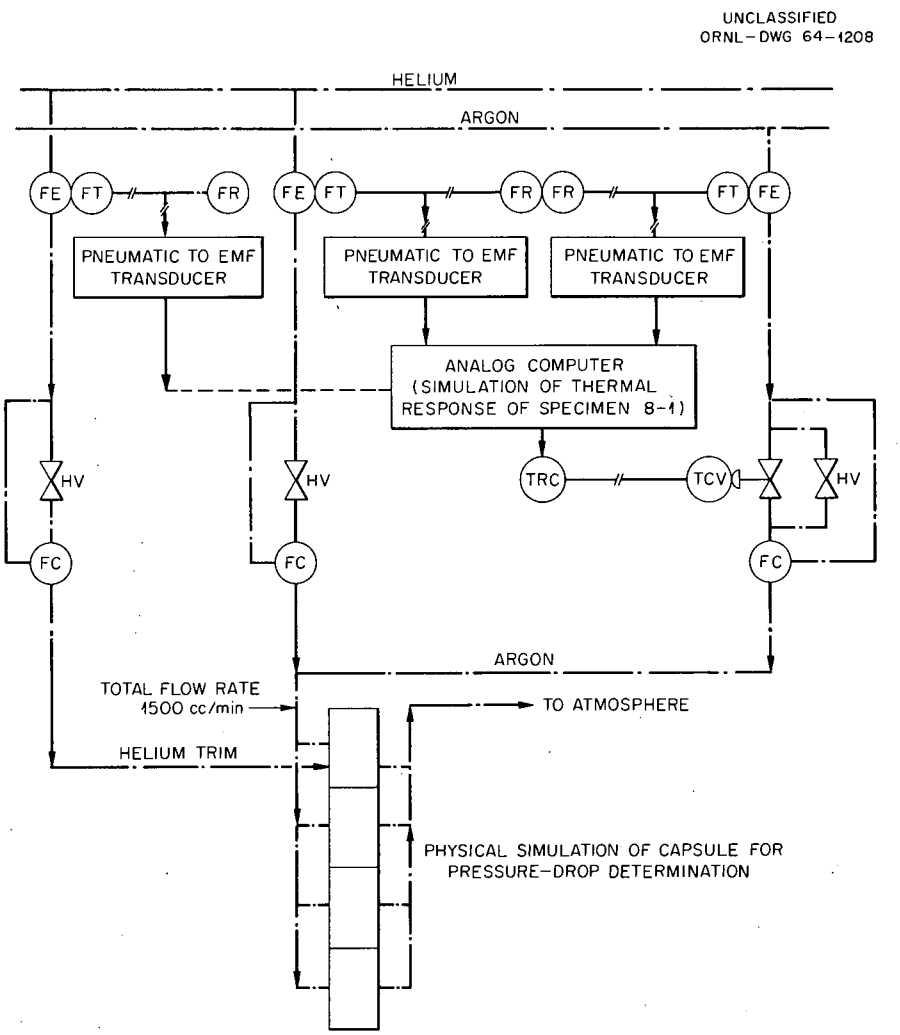

Fig. 6.2.2. Diagram of Simulated Experiment 41–8.

6.3 OXYGEN SEPARATION PLANT

L. H. Chase

The instrumentation and control system for the Oxygen Separation Plant was designed and installed in 1961–62; the plant is now in routine operation and has reached approximately 50% of isotopic equilibrium. During the past year, four extremely low-range (0 to 20 and 0 to 300 ml/day) flowmeters were installed, and an instrument system was added to record the power to the steam generators.

The plant separates O^{17} from natural oxygen by the isotopic distillation of water in a six-column distillation cascade, followed by a 13-column gas-phase thermal-diffusion cascade. Since 1 to 2 yr is required for the plant to reach isotopic equilibrium, the basic instrumentation problem was the need for 100% reliability.

Reliability considerations led to the use of manual control in all applications where automatic control was not essential. For example, manual control valves and flow indicators were used for regulating the flow of feed and reflux streams and for controlling the two product streams, each flowing at a rate of 20 ml/day of isotopically enhanced oxygen gas.

The most serious component failure that can occur is failure of the heaters in the steam generators, with the attendant loss of the isotopic distribution existing in the distillation columns at the time of failure. To reduce the probability of such a failure, the heaters are energized continuously at reduced voltage by a control system which acts to maintain constant steam pressure in the boilers.

6.4 POOLSIDE EXPERIMENTAL FACILITY IN THE ORR

A. H. Malone

An instrumentation system was provided to measure and control the temperatures of specimens of structural materials while being irradiated in the ORR.

The facility, proposed by the Solid State Division, will allow the irradiation of six capsules containing material samples. Resistance heaters adjacent to each sample supplement the radiation heating and allow control of the sample temperature. Because of the low power (less than 500 w) and high speed of response of these heating elements, a temperature controller that could be adjusted through a wide range of operating conditions was required; temperature must be maintained to less than 1% of the full operating range.

Special packaging was required to install 36 control units that could be easily replaced and maintained because the available space was too small to accommodate standard ORNL panel boards. A panel of modular construction (Fig. 6.4.1), requiring access only from the front, was designed to accommodate 36 Leeds and Northrup Speedomax-H recorders with current-adjusted temperature controllers and silicon controlled rectifier (SCR) power units driven by magnetic amplifiers. Space was inadequate in the control room to use other types of proportional controls, such as magnetic amplifier and saturable reactor. This was the first large-scale attempt at ORNL to apply SCR power controllers.

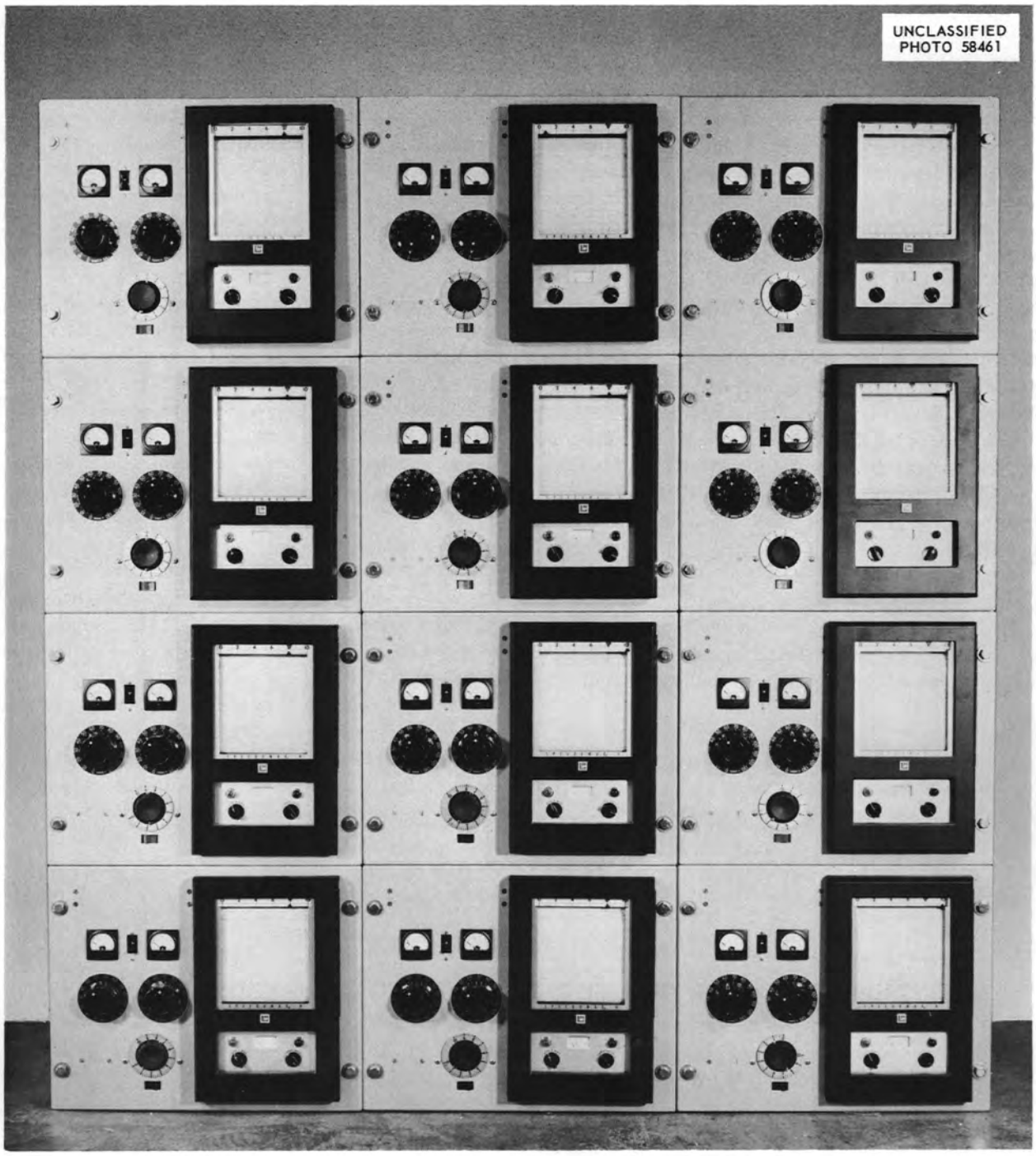

Fig. 6.4.1. Panel Board for ORR Poolside Experimental Facility.

6.5 NUCLEAR SAFETY PILOT PLANT INSTRUMENTATION

Corbett Brashear

The Nuclear Safety Pilot Plant is a facility for performing experiments to determine the characteristics of the release, dispersion, and deposition of fission products obtained by fusing irradiated reactor fuels.[1] Such an accident is simulated by directing the jet of a plasma torch on fuel specimens in a flowing gas stream of either helium, nitrogen, argon, oxygen, or air. After the fuel specimens have melted and the fission products are dispersed in a containment-vessel model, various experiments are performed to determine where specific types of activity are deposited and to evaluate the problems associated with decontamination of the containment vessel.

The design of the instrumentation and control system for the Nuclear Safety Pilot Plant is 50% complete, procurement of instruments and equipment is 80% complete, and installation is 20% complete.

Among the unusual problems encountered because of the special nature of the plant were:

1. To measure by remote means the temperature of melting UO_2 while being heated by a plasma torch at about 2800°C. An automatic optical-brightness recording pyrometer was investigated and appears to be promising.
2. To maintain, by remote means, equipment located inside the sealed cell and to seal all lines penetrating the cell walls.
3. To measure gas flow rates through an extreme range from 0.03 to 1000 scfm and to measure the specific gravity through a range from 0.138 to 1.38.
4. To control the release of gas from the containment-vessel model after completion of an experiment, at a rate determined from the concentration of radioactivities in the stack gas.
5. To sample automatically the atmosphere of the model containment vessel. Both the sampling period and the time between samples will be adjustable from the operating panel board. Fallout inside the containment vessel will be sampled automatically.
6. To design the system in such a manner that any component (even in the sealed cell) may be replaced with minimum effort. All components in the sampling train will be separated by valves and flanges.

The cost of the instrumentation and control system will be about $100,000, or 22% of the overall project cost. About $30,000 was saved by installing renovated surplus instruments.

[1] L. F. Parsly, Jr., *Nuclear Safety Pilot Plant Hazards Summary Report*, ORNL-TM-683 (Oct. 4, 1963).

6.6 INSTRUMENTATION FOR THE HIGH-RADIATION-LEVEL EXAMINATION LABORATORY

C. S. Lisser

G. W. Allin J. E. Inman V. A. McKay

The High-Radiation-Level Examination Laboratory (HRLEL), a 13-unit hot-cell facility, was previously described.[1] Since that report, 17 devices for remote handling and examination of highly radioactive specimens were completed. Also designed and installed were such general building facilities as a radiation monitoring system, an intercommunication system, cabling for more than 430 leads connecting out-of-cell control panels to in-cell equipment, and two remotely

[1] C. S. Lisser *et al.*, *Instrumentation and Controls Div. Ann. Progr. Rept. July 1, 1961*, ORNL-3191, pp. 46–50.

controlled closed-circuit television systems. A total of 170 instrumentation drawings were made. Installation and check-out of some of the in-cell equipment was started and will be continued until the facility is operational, probably in late 1963.

One of the instruments installed since the last report is the gamma-ray spectrometer,[2] which was designed for the determination of gamma-ray spectra at very high source intensities. Although the detector limit is 10^4 counts/sec, the high source intensities are accommodated by a variable-aperture collimator having a high attenuation factor. Preliminary measurements with a 100-mc Co^{60} source show that the primary and secondary collimators[1] can be aligned to allow uncollided photons to reach the detector; however, experimental confirmation of the calculated attenuation factors cannot be obtained until a high-intensity source is installed in the HRLEL spectrometer cell. A 512-channel analyzer is being provided for the spectrometer readout to replace the original 256-channel display.

[2]Designed by V. A. McKay and G. W. Allin, Instrumentation and Controls Division.

Another instrument to be installed is a remotely operated analytical balance. A Voland Speedigram balance of 200 g capacity and $\pm 5 \times 10^{-5}$ g sensitivity was equipped for remote operation and readout. To operate the balance, 10-step/revolution stepping motors and 36°/step rotary switches are aligned and coupled to each of the three original mass control rods of the balance, and a stepping motor and a contact-making digital counter are linked to the fine-adjustment chain drive. Rear-projection units display the mass readout numbers at the panel. The circuitry of the modified balance will accommodate the addition of a tape printer to the readout.

The cabling installation incorporates a recent development in large-size, heat-shrinkable molded boots to obtain a pressure-tight transition from conduits to connectors and cables. The boots prevent the exchange of atmospheres between the cells and operation areas.

For radiation monitoring, 22 monitors were installed at various locations throughout the building. Failure, off-limit conditions, and normal operation are indicated for each monitor on a central panel.

6.7 EMERGENCY PANEL FOR THE RADIOCHEMICAL PILOT PLANT

M. B. Herskovitz

A graphic instrument control panel (Fig. 6.7.1) was designed and fabricated and is being installed at the Radiochemical Pilot Plant, Building 3019. The installed panel, which will cost approximately $17,000, is 90% complete.

The building ventilation functions, radiation levels, and certain process variables will be indicated or recorded on the panel. Cell-ventilation inlet louvers will be controlled from the panel to isolate and contain contamination from any process mishap.

The annunciator portion of the panel is unique, in that a large number of monitored variables are displayed in a small area (600 available points in 12 ft^2), and the annunciators can easily be rearranged to meet changing requirements. The annunciator display consists of a grid system on which geographical portions of the building are indicated along the horizontal axis and various physical functions are displayed at specific levels along the vertical axis.

A relay-rack portion of the annunciator system will be remotely located to conserve graphic display space on the panel board.

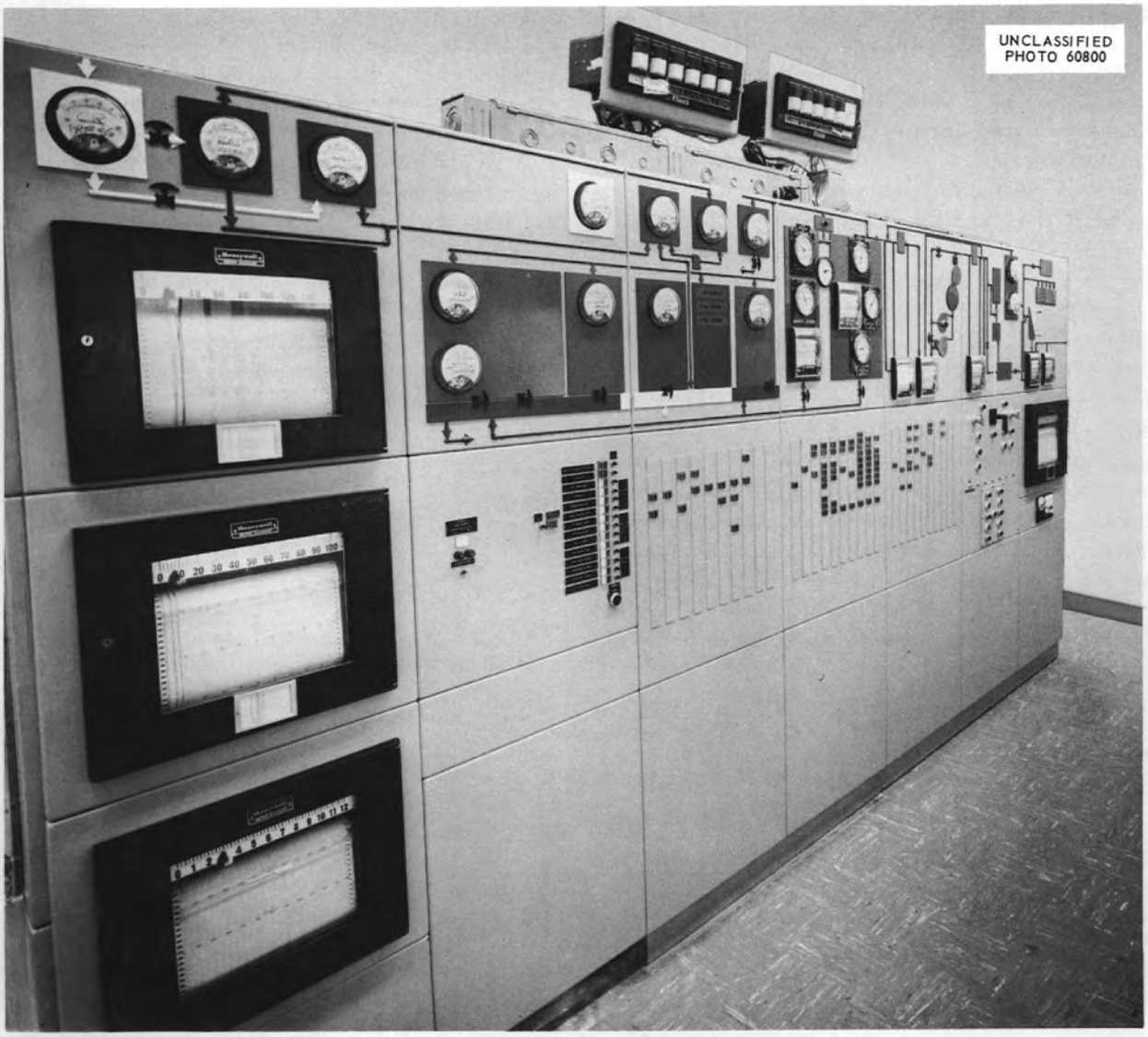

Fig. 6.7.1. Panel Board for Emergency Instrumentation.

6.8 TESTS OF A FOAM DECONTAMINATION TECHNIQUE

Corbett Brashear B. C. Thompson

Experiments were performed to evaluate the effectiveness of a foam technique, developed by a research group at Harvard, for decontaminating areas contaminated by high levels of airborne radioactivity, for example, the interior of a reactor containment structure after an accident. The decontamination technique is to fill the contaminated structure with an aqueous foam, allow

the foam to decay to a liquid residue, and remove the residue which carries away the entrained radioactivity.

An instrumentation and control system was designed, fabricated, and installed to provide the following:

1. controls for safely performing the experiments, in which radioactive iodine and fission products were released in the cell;
2. instrumentation for monitoring and controlling the degree of containment during the tests;
3. controls for removing the liquid residue and gases after the tests.

Some of the instrumentation removed from the Homogeneous Reactor Test Facility (HRT) was renovated for use in these experiments. Additional funds were saved by using instruments purchased for other projects, but which were not needed until after completion of these experiments. The total cost of additional instrumentation was $13,000. The total cost of the project was $60,000.

6.9 SCHEDULING

C. S. Lisser

The considerable increase in the amount of work done annually by the Instrumentation and Controls Division led to a more formalized handling of scheduling.

Beginning in August 1962, the Process Control and Instrumentation Section of the Division established a system of work scheduling based on a modified version of the critical-path method. Type-of-work and time coordinates are included (Fig. 6.9.1). The information in Fig. 6.9.1 shows pictorially the progress of a single job. The estimates for all jobs shown on many modified critical paths are consolidated to show the scheduled work load and manpower distribution for each divisional facility, such as a shop, and a sheet is prepared, as shown in Fig. 6.9.2, for each facility. The tabulation in Fig. 6.9.2 shows all jobs and the manpower scheduled for each job during a 22-week period for a fabrication shop. In the graphic representation in Fig. 6.9.2, the nonscheduled, routine work load and vacations are combined with the scheduled work.

This system was subsequently adopted for the whole division, and a full-time scheduler was added to the staff. Approximately 45 projects have been scheduled, and the scheduling system is considered fully operational. Additional groups of engineers, draftsmen, and craftsmen, not located at Building 3500, are now being included in the scheduling program. Monthly issues of all scheduling information are transmitted to interested parties. Steps are being taken: (1) to accumulate feedback information to permit determination of scheduling and estimating accuracy from the history of finished projects; and (2) to provide a computer-processed scheduling system to generate work order listings and engineering load graphs.

UNCLASSIFIED
ORNL-DWG 63-3142

MANPOWER AND TIME ESTIMATE SHEET
(MOD. CRIT. PATH)

NUCLEAR SAFETY PILOT PLANT
A-43008-84, 85, 86 CB 4-17-63

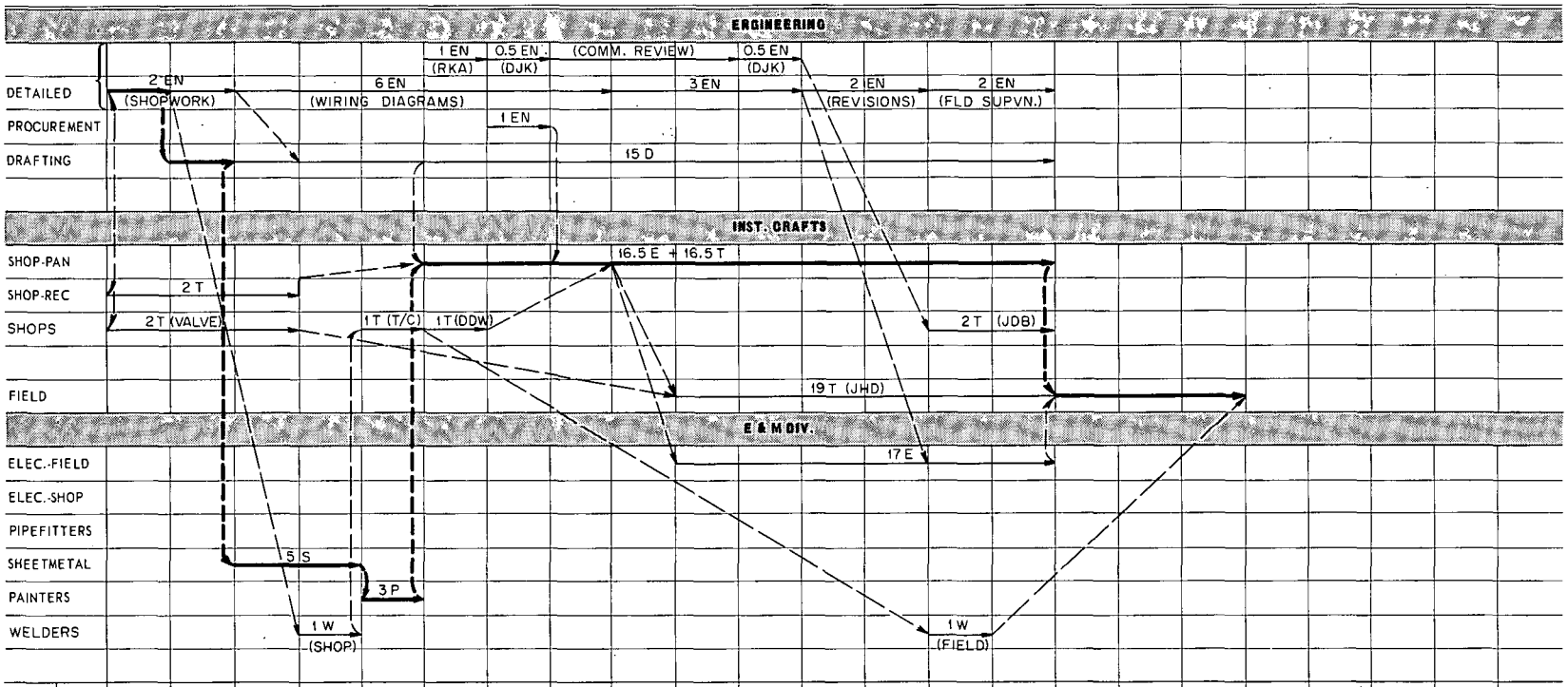

UCN-4667
(3 5-63)

CP563

Fig. 6.9.1. A Typical Manpower and Time Estimate Sheet.

UNCLASSIFIED
ORNL-DWG 63-3141

DDW (7 MEN, EXCEPT 6 ONLY, WEEKS 25 THROUGH 32)

JOB NO.	JOB	ENGR.	TOT. M/W	18	19	20	21	22	23	24	25	26	27	28	29	30	31	32	33	34	35	36	37	38	39
			WEEK NO.	WEEK BEGINNING DATE																					
				4/29	5/6	5/13	5/20	5/27	6/3	6/10	6/17	6/24	7/1	7/8	7/15	7/22	7/29	8/5	8/12	8/19	8/26	9/2	9/9	9/16	9/23
	NSPP A-43008-85	CB	1								1														
	RWCS A-93719-33	JAR	4										0.5	0.5	0.5	0.5	1					1			
	RWCS A-93719-34 (SBD)	JAR	9	0.5	1	1	1	3.5	2																
	RWCS A-94083-33	JAR	4								1	1	1	1					1	1					
	ORIC RAD. MON. A-94108-30	TAL	5	1		1					1	1	1												
	HFIR SCAN. A-94153 to 6-30	JWR	1.5			0.5	1																		
	RWCS A-94083-32	JAR	2																	1	1				
	HFIR PART 4 A-93125-16	JLA	6																				2	2	2
	HFIR PART 1 A-93125-16	DJK	3						0.5	1		0.5					0.5	0.5							
	HFIR PART 2 A-93125-16	DJK	4.5		0.5	0.5	1	0.5	0.5					0.5	0.5	0.5									
	HFIR PART 3 A-93125-16	JLA	26								2	2	2	2	2	2	2	1	1	2	2	2	2	1	1
	DATA LOG. SYS. A-94230-30	RKA	4											0.5	1	1	0.5	0.5	0.5						
	RWCS A-93719-32	JAR	2	1	1																				
	MSRE DRAWS. A-70708-83	ENF	8																		2	2	1	1.5	1.5
	MSRE MODULES A-70708-82	ENF	7									0.5	0.5	0.5	0.5	0.5	0.5	1			1	1		0.5	0.5
	SNIP-SNAP A-20843-11	JWJ	4						2	2															
	APOLLO A-20817-11	NWH	3.5										0.5	0.5	1	1	0.5								
	SPECTRAL DENS. ANAL.	CWR	1														1								
	BIOL. EXP. ORIC A-31397-41	WTC	5.5										0.5	0.5	0.5	0.5		1	1.5	1					

ORNL - I AND C DIVISION

FAB. SHOP SCHEDULE

SHEET 1 OF 2

DATE 6/20/63

VACATIONS

WS463

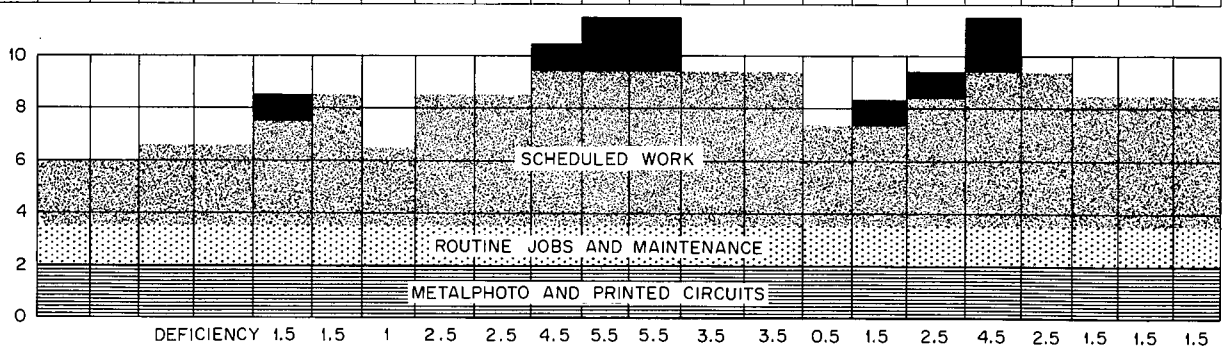

Fig. 6.9.2. A Typical Manpower and Time Estimate Sheet for a Shop.

7. Process Instrumentation Development

PROCESS INSTRUMENTATION

7.1 TELEMETERING OF LIQUID LEVELS IN WASTE STORAGE TANKS

T. M. Gayle

The system for telemetering the liquid levels in 24 imtermediate-level waste storage tanks to the Central Operating Facility (Building 3105) was redesigned, and installation is partially complete. The system gave dependable service for 12 yr; however, due to increased and extensive maintenance work required to keep it in operation, the present system is being replaced by a two-wire telemetering system and an improved null-balance electronic system of higher accuracy.

In the new system (Fig. 7.1.1), a common power supply feeds each of 24 transmitters through one conductor of a telephone line and a common ground. A cascaded Zener-diode regulating system, with the final diode temperature compensated, regulates the voltage to the transmitting slide-wire at 1.0 v ± 0.2%. The slide-wire is a ten-turn potentiometer, which is driven mechanically by the tank float movement. The 0- to 1.0-v signal is transmitted to Building 3105 through the other conductor of the telephone line and the same common ground. Two 12-point, 1.0-v recorders scan and print out these voltages, which are directly proportional to tank level.

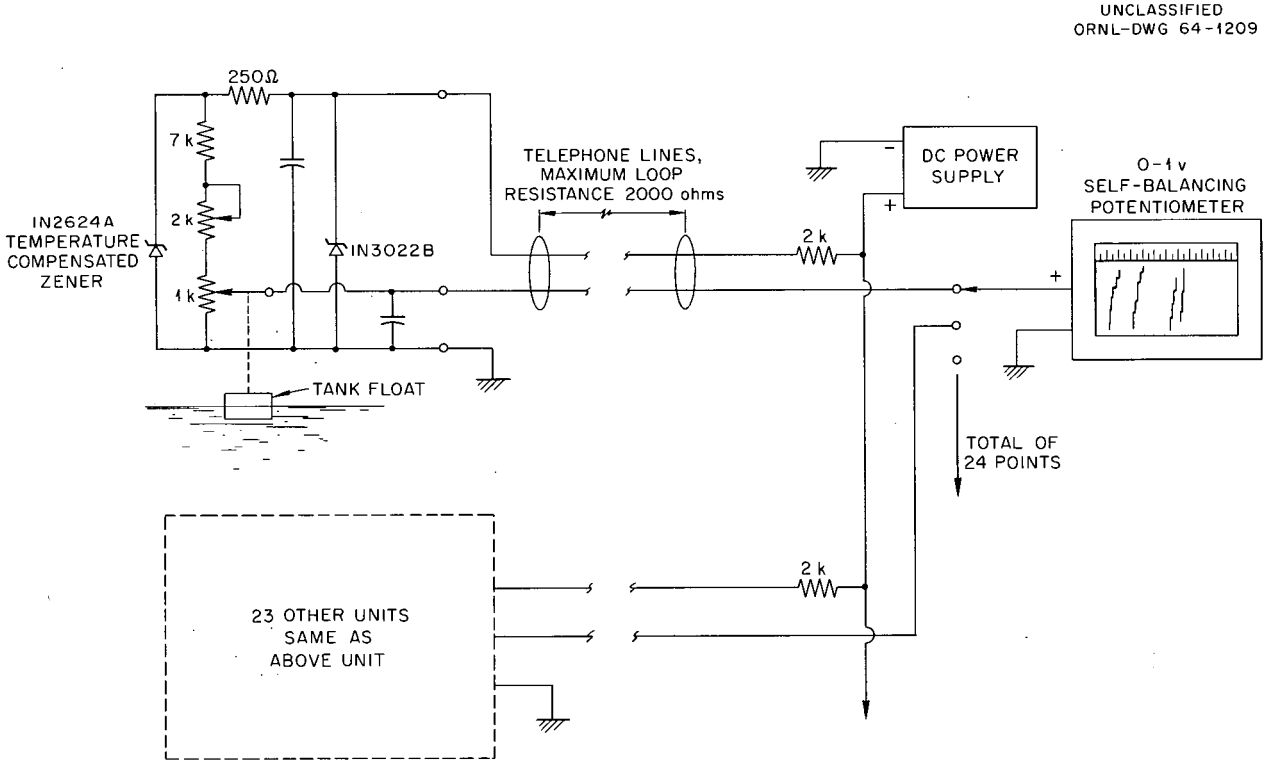

Fig. 7.1.1. Instrumentation for Telemetering Waste-Tank Liquid Levels.

7.2 CONTINUOUS MEASUREMENT OF HEXAVALENT CHROMIUM

T. M. Gayle

A method for continuously monitoring the concentration of hexavalent chromium in the effluent stream from a Darex process dissolver was developed for the Chemical Technology Division.

The work of Gens[1] on the continuous dissolution of zirconium reactor fuels in titanium equipment showed that excess Cr^{6+}, while not necessary for the dissolution reaction, was required for protection of the titanium system against corrosion by the excess fluoride which must be present to achieve a satisfactory dissolution rate. Gens also noted that the level of excess Cr^{6+} in the effluent was indicative of the reaction rate and could be used as a control variable for the addition of solvent.

Two methods of analysis were investigated: ultraviolet absorption in the region of 260 mμ, and oxidation potential measurements with a gold–potassium chloride electrode system. Flow-type instruments for both methods were fabricated and tested. The oxidation potential measurements proved the more successful, and subsequent laboratory demonstrations were made using this type of measurement.

Initially, a platinum-calomel electrode system was tried in the laboratory; however, poisoning of the platinum by components in the dissolver effluent was too rapid for dependable operation. Gold was tried in place of platinum, with excellent results. Basically, the electrode reaction system is represented by:

$$\mathrm{Pt} \,\Big|\, \mathrm{Hg} \,\Big|\, \mathrm{Hg_2Cl_2} \,\Big|\, \mathrm{KCl} \;\vdots\; \begin{matrix}\text{Liquid}\\ \text{junction}\end{matrix} \;\vdots\; \mathrm{Cr_2O_7} \,\Big|\, \mathrm{Cr^{3+}} \,\Big|\, \mathrm{Au}\,.$$

The standard half-cell potential of a saturated calomel electrode is 0.2450 v, including the liquid junction.[2] The Cr^{3+}, Cr^{6+} half-cell potential is assumed to be:

$$Cr_2O_7 + 6e^- + 14H_3O \longrightarrow 2Cr^{3+} + 21H_2O\,;$$

$$E_0 = -1.36 \text{ v}\,.$$

The total potential is 0.2450 v minus 1.36 v, or approximately −1.118 v, which agrees well with the experimental values. The shift in oxidation potential with pH was not considered, although it undoubtedly occurs. After successful demonstration runs, it was assumed that as long as reagent feed composition ratios were maintained, the effect of pH on oxidation potential would be entirely reproducible.

Figure 7.2.1 shows a diagram of a system that could be used in a pilot plant for continuous control.

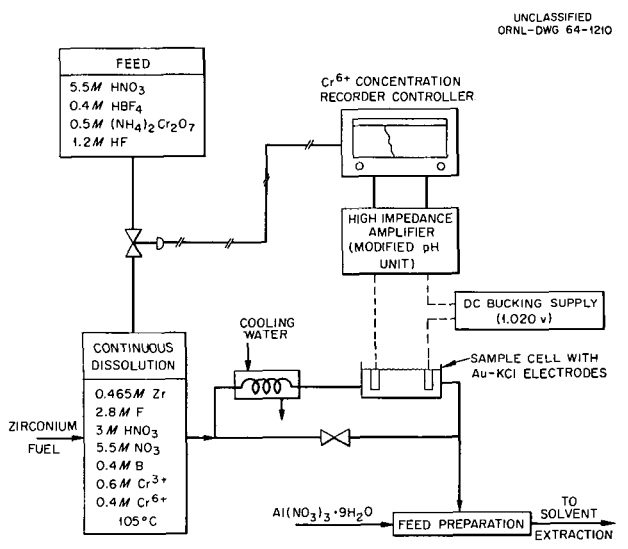

Fig. 7.2.1. Automatic Control of a Darex Dissolver Based on Oxidation-Potential Measurements.

[1]T. A. Gens, *Continuous Dissolution of Zirconium Reactor Fuels in Titanium Equipment: Laboratory Demonstration*, ORNL-TM-395 (Jan. 23, 1963).

[2]G. J. Janz and D. J. G. Ives, *Reference Electrodes*, p. 160, Academic Press, New York, 1961.

7.3 DYNAMIC GAS THERMOMETRY

E. W. Hagen

The investigation of dynamic gas thermometry as a method for making in-reactor high-temperature measurements was continued.[1,2] The system under development employs the predictable temperature-pressure relation of a gas flowing through two nozzles in series, at sonic velocity, to determine temperature.[1] The investigation is directed toward developing a general-purpose temperature measuring system which will be unaffected by prolonged exposure to temperatures in excess of 1000°F, or to radioactivity. The study was initiated when application of a pneumatic temperature-measuring (PTM) system was proposed for the EGCR. Informative data and consulting services were supplied to the local PTM-EGCR program.

A slight change in the physical characteristics of a small nozzle will appreciably alter the flow calibration and the accuracy of a dynamic gas thermometer.[2] Therefore, three nozzles, in addition to those previously reported,[1,2] were tested for flow-coefficient stability by thermally cycling them from 200 to 1200°F (rise time of 10 min, holding time at 1200°F of 50 min, cooling time of 20 min) and by exposing them to sonic flow velocities in a helium atmosphere at temperatures from 1000 to 1600°F for extended periods of time.

Two of the nozzles were made from type 304 stainless steel, since nozzles made of this material will be used in the EGCR-PTM system. As expected, the smallest nozzle showed the largest percentage change in flow coefficient, and the largest nozzle showed the smallest change (Table 7.3.1). Only the total change in value of flow coefficient is shown, because neither the elapsed time for each test nor the time between calibration checks was the same for these tests. In future tests, nozzles fabricated from carbides, tungsten alloys, and from oxides and ceramics of aluminum and beryllium will be investigated.

Unlike earlier reported tests on nozzle material stability, the shape of the flow-coefficient curve did not change during the test runs. However, changes were effected by the welding and brazing of the nozzles into sections of test loop tubing (Fig. 7.3.1).

Welding and brazing techniques are being investigated to find a satisfactory way to fasten nozzles

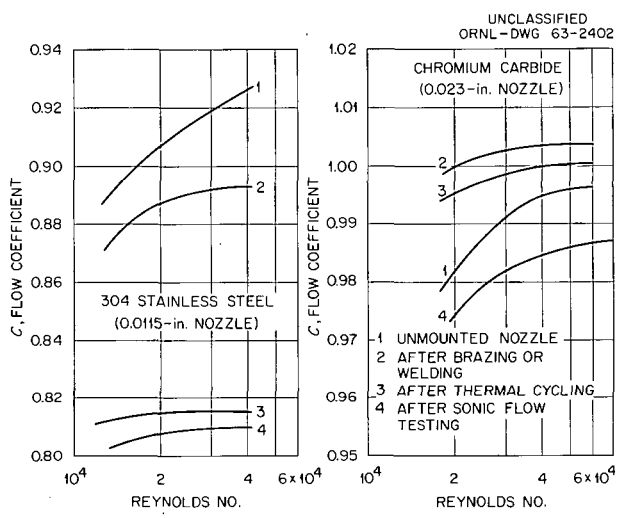

Fig. 7.3.1. Stability of Flow Coefficients for Stainless Steel and Chromium Carbide Nozzles.

Table 7.3.1. Change in Flow Coefficients of Nozzles After Thermal Cycling and Sonic Flow

Nozzle No.	Material	Throat Diameter (in.)	Number of Thermal Cycles	Hours in Sonic Flow	Change in Coefficient (%)
102	304 stainless steel	0.005	20	50	−25
109	304 stainless steel	0.0115	195	62	−8.1
150	Chromium carbide	0.023	82	393	−2.0

[1]H. M. Hochreiter, *Instrumentation and Controls Div. Ann. Progr. Rept. July 1, 1961*, ORNL-3191, pp. 57–60.

[2]E. W. Hagen, *Instrumentation and Controls Div. Ann. Progr. Rept. Sept. 1, 1962*, ORNL-3378, pp. 47–48.

of sapphire, tantalum, tungsten alloys, etc., into stainless steel tubing. Mounting the nozzle first into a collar of a metal having an intermediate coefficient of thermal expansion has produced promising results. A chromium carbide nozzle was pressed-fitted into a copper ring, and the unit was pressed into a type 304 stainless steel holder having the same wall thickness as that of the copper ring. This assembly was then copper brazed. Repeated cycling in an argon atmosphere from 200 to 1200°F produced no evidence of leakage, nozzle cracking, or deformation of the nozzle holder – all of which plagued earlier work with cemented carbide nozzles.

A temperature measuring system utilizing miniature nozzles, 0.0025 in. and 0.005 in. in throat diameter and made from type 304 stainless steel welded into $\frac{1}{8}$-in. stainless steel tubing, has successfully measured furnace temperatures up to 1600°F. Although the repeatability of the system was within 0.1%, the ratio of the computed temperature obtained from the system to the actual furnace temperature was not constant. It varied linearly with the high temperature. This discrepancy was traced to a change in the effective throat area of the hot nozzle (see nozzle No. 102 in Table 7.3.1) caused by material instability and partial plugging by foreign particles. A new probe assembly using a 0.005-in. tantalum-tungsten hot nozzle is being calibrated for this system demonstrator.

In cooperation with the EGCR-PTM program, a life test on a one-third-scale nozzle was conducted in an environment simulating reactor operating conditions of pressure, temperature, and gas composition. The nozzle flow coefficient was checked and monitored throughout 1300 hr of continuous testing, which is the equivalent of 17.8 yr of service in the proposed PTM system. At this constant temperature of 1050°F, the flow coefficient stabilized within 150 hr and the final value differed from the initial value by 0.75%; variations after the first 150 hr were not discernible. The change of 0.75% amounts to an error of +25°F.

The requirements for studying the stability of a full-size PTM nozzle were determined, and testing facilities both at ORNL and at the nozzle manufacturer's plant were investigated. A performance demonstration of the PTM system was observed at the manufacturer's plant, where the complete PTM system operated satisfactorily. A typical new nozzle of the type recommended by the General Electric Company was obtained and was subjected to metallographic examination at ORNL. The nozzle flow surface, a nitrided type 304 stainless steel, showed both longitudinal and transverse cracks.

7.4 VACUUM ION GAGE AND CONTROLLER

J. H. Todd G. A. Holt E. E. Waugh

A cold-cathode ion gage to be used as a vacuum indicator and controller (ORNL model No. Q-2572) was designed for general use on vacuum systems at the Laboratory. This instrument was designed to provide a simple, reliable, and accurate vacuum gage with a control function incorporated. Tests have shown this instrument to be at least as accurate as existing vacuum ion gages, even with its simplified circuitry. Also stability with line voltage variation is superior to existing vacuum ion gages. Reliability is enhanced by the simplicity of the circuitry.

The instrument is calibrated in three ranges, covering 1×10^{-3} torr to 1×10^{-6} torr. An indication can be obtained from 2.5×10^{-3} to 1×10^{-7} torr. A control signal in the form of a relay actuation can be obtained from 0 to 100% of full scale on any range. The contacts of this relay, rated at 5 amp, can be used to control equipment that could be damaged by either a loss or decrease in vacuum.

A circuit monitors the high voltage and actuates the alarm relay if the high voltage falls below a set value.

The system consists of a regulating transformer, a half-wave rectifier, alarm circuits, and a meter-controller module.

POWER CONTROL UNITS

7.5 PROPORTIONAL POWER CONTROL UNIT EMPLOYING SILICON CONTROLLED RECTIFIERS

J. L. Horton

A proportional power control unit employing silicon controlled rectifiers (ORNL model Q-1699-G) was designed and built. This unit is similar to the relay-type power control units (ORNL models Q-1699-A and -B) now in use.

Automatic temperature control systems for small furnaces and experiments are used in great numbers at ORNL. Commercially available recorder-controllers and indicator-controllers require auxiliary equipment to make a complete control system. Combining this auxiliary equipment into modular units designed for flexibility, as well as safety, reliability, and controllability, has provided a great saving in engineering and maintenance manpower in the past decade. The advent of the silicon controlled rectifier (SCR) has allowed a reduction in size and weight of such units, as well as improved control in some applications.

Units incorporating the firing circuits and fuses for use with the SCR are available from many commercial sources. However, the cost of these units, plus the cost of adding components to provide the flexibility and safety required, justifies the design of a unit which incorporates these features integrally. Improved packaging is also obtained in such modular units.

Commercial manufacturers are being encouraged to produce an identical or comparable unit. It is expected that such a commercial unit will be available in the near future.

The unit designed and built at ORNL in small quantities is for service on 120-208-230 v, 60-cycle ac systems, for loads up to 20 amp. Features which are incorporated include plug-in connections to other system components, circuit breakers for both the load and the controlling instrument, and backup safety relays, all of which were found necessary or desirable in earlier units. The required control signal is 0 to 5 ma at 0 to 15 v dc. Minor modification of the input allows control from almost any commercial proportional controller with a dc output. A running-time meter is optional. Figure 7.5.1 shows the front view of the rack mounting unit. Total enclosure, in a sheet metal chassis (Fig. 7.5.2) with perforated sheet metal covers, reduces radiated radio-frequency interference, and provides mechanical protection for the unit and personnel protection from electrical shock. (See Sect. 7.6 for more details regarding electrical noise problems associated with these devices.)

Fig. 7.5.1. Rack-Mounting Unit.

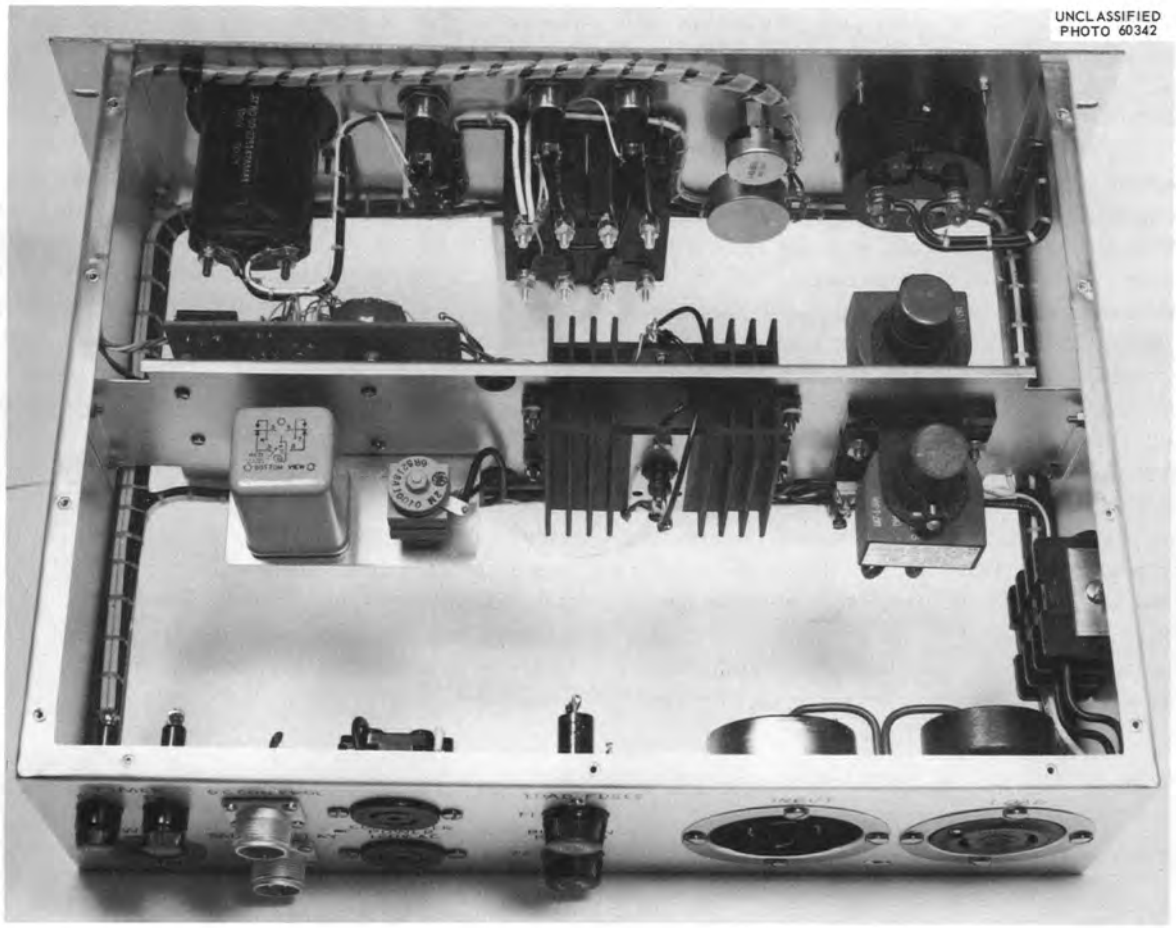

Fig. 7.5.2. Chassis of Power Control Unit.

7.6 NOISE PROBLEMS ASSOCIATED WITH SILICON CONTROLLED RECTIFIERS USED IN POWER CONTROL

J. L. Horton

A study of the transient and radio-frequency noise problems associated with silicon controlled rectifiers (SCR) in power control circuits is continuing. The sizes of commercially available SCR units for handling medium and high power are very attractive for power control. Their increased use in commercially built equipment, as well as in some ORNL-built equipment, requires that all associated problems be understood and accommodated.

The SRC is basically a high-speed switch with a turn-on time of 0.5 μsec or less. For 60-cycle ac power control, the usual configuration employed is two SCR units connected parallel-inverse (back to back) in one side of the line between the supply and the load. One SCR fires on each half cycle,

switching on rapidly at some point within the half cycle and conducting until the end of the half cycle. The other SCR repeats the action on the other half cycle. The transient due to the rapid redistribution of energy in the system during and immediately following the switching of the SCR is a source of rf interference. The magnitude and characteristics of the transient are primarily a function of the system parameters, that is, voltages, resistances, inductances, and capacitances, and their distribution. The switching transients from an SCR are essentially the same as those of power contactors operating under similar conditions, except that the repetition rate is much greater (120 per second) and the switching may always occur at the peak of the voltage, thus giving maximum transient amplitude. Interference is propagated by two means: transmission along the supply and load line, and electromagnetic radiation.

The seriousness of the interference problem is a function of many factors, for example, the sensitivity of the instrumentation and equipment connected to and located near the SCR control equipment, and the mode of interconnection through power and other circuits. Pulse-counting instrumentation (such as radiation counters and digital data systems) and wide bandwidth, high-input-impedance instrumentation are generally quite sensitive to the type of interference considered here and must be protected. Because of the wide variety of equipment in use at ORNL and the diversity of locations, each installation will be considered separately.

From results of the study to date, it appears that no universally applicable cure-all will be available. Therefore, it is recommended that each proposed SCR power-control installation be thoroughly reviewed during the planning and design stage. With proper precautions, and the application of filters and shielding where needed, these SCR control systems can afford unexcelled power control with a minimum of interference to other instrumentation or equipment.

TEST AND CALIBRATION INSTRUMENTS

7.7 MAINTENANCE TESTING OF AUTOMATIC CONTROLLERS

W. R. Miller

Three testers that allow maintenance personnel to rapidly ascertain whether electronic process controllers of specific manufacture meet operating specifications were designed and built. Testers to perform this function are not commercially available. In the past, a bench mockup of the process was required to obtain this information.

The first tester (No. 1 in Fig. 7.7.1) evaluates the condition of Leeds and Northrup three-action duration-adjusting-type (DAT) controllers. The impulse rate of the controller is artificially increased during the test to make it possible to rectify, filter, and integrate the output pulses; this permits the controller output to be read directly on a panel meter. Reset and rate action are tested by measuring the response of the controller during a timed period following a step set-point deviation.

The second tester (No. 2 in Fig. 7.7.1) evaluates Leeds and Northrup two-action DAT controllers. The tester employs an RC network to simulate the response of a furnace; this feature permits instant return to the "cold furnace" condition by shorting the RC network with a push-button switch. A recorder serves as the readout device for the controller under test. Chart records produced at specific controller settings are compared to records made under ideal conditions.

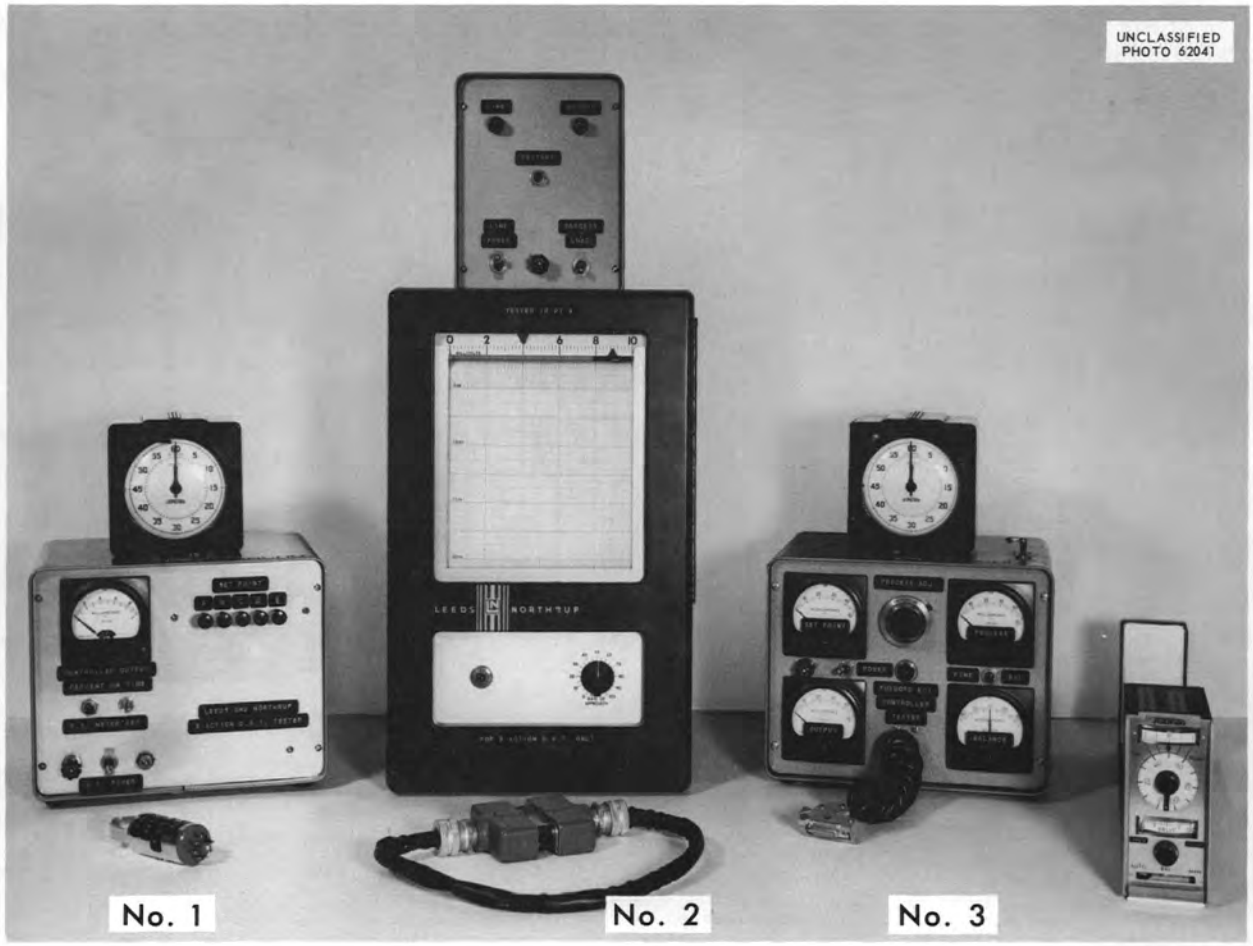

Fig. 7.7.1. Instruments for Testing Automatic Controllers.

The third tester (No. 3 in Fig. 7.7.1) evaluates Foxboro model M-62 electronic-control-instrumentation (ECI) controllers. Set-point, process, and output signals of 10 to 50 ma dc are displayed on panel meters. Fine balance is detected on a 50-0-50 microammeter. A simulated adjustable process signal permits all controller functions to be tested. Reset and rate actions are tested by the same techniques as described previously for the first tester.

7.8 LOW-VELOCITY-AIR CALIBRATION FACILITY[1]

T. M. Gayle A. H. Malone

A permanent facility (Fig. 7.8.1) was constructed for the precise calibration of air-velocity meters, anemometers, and other such devices, in the range of 30 to 1000 fpm. With this facility, portable air-velocity meters, used at ORNL for checking air velocities in hoods and ducts where radioactive materials are handled, can be calibrated frequently

[1]Planned in cooperation with the ORNL Plant and Equipment Division and the Health Physics Division.

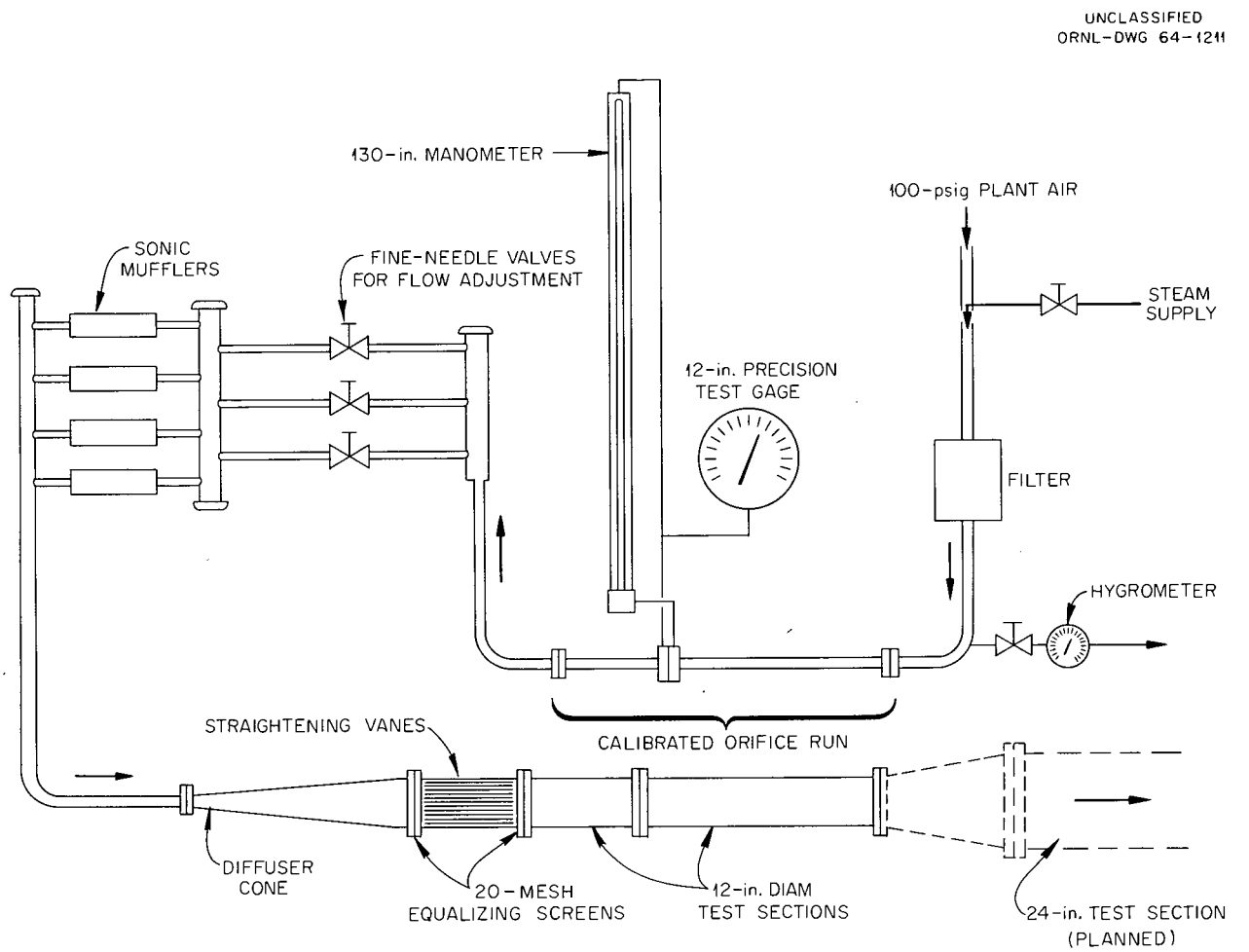

Fig. 7.8.1. Low-Velocity-Air Calibration Apparatus.

to ensure that the meters are operating properly. The characteristics of many portable air-velocity meters are unpredictable and erratic, and frequent calibration is required.

High-pressure air from the plant system is metered to better than 1% (flow rate) and expanded into a 12-in.-diam duct section made of acrylic plastic. The section is designed with a long diverging cone, straightening vanes, and equalizing screens to provide an extremely uniform velocity distribution in the test section. Test sections up to 2 ft in diameter were provided for in the basic design.

The very dry plant air to this facility can be humidified by injecting steam into the inlet air stream. The orifice and the orifice run (15 pipe diameters upstream and 5 pipe diameters downstream) to be used for long-term work will be sent to the National Bureau of Standards for final calibration to better than $\frac{3}{4}$% accuracy in the operating range. Consultations with industrial instrument companies and with the Hydraulics Section, National Bureau of Standards, have confirmed the validity of this design and calibration technique.

7.9 NEW EQUIPMENT AND FACILITIES OF THE STANDARDS LABORATORY

M. H. Cooper W. W. Johnston

The Standards Laboratory obtained and put into service new freezing-point temperature standards, primary voltage standards, and a universal ratio set. These items may, to some degree, improve the absolute accuracy of ORNL standards, but they are primarily intended to reduce direct dependence on the National Bureau of Standards.

The freezing-point temperature standards consist of five special furnaces, each containing an NBS certified sample of lead (327.4°C), zinc (419.5°C), aluminum (660.0°C), silver (960.8°C), or copper (1083°C). This facility provides direct reference to the international practical temperature scale, which is defined in terms of known freezing points. Previously, ORNL used NBS certified resistance thermometers in the temperature range of −150 to 500°C, and special NBS certified platinum vs platinum−10% rhodium thermocouples in the temperature range of 200 to 1200°C. A check of the previous standards with the new melting-point standards has shown agreement within the NBS certifying accuracy (0.3°C).

The voltage standard (at the right side of the table in Fig. 7.9.1) consists of a bank of six NBS-certified saturated standard cells in a temperature-controlled air bath. Saturated standard cells, while considered the ultimate in accuracy, are inconvenient and expensive to have certified by NBS, since they must be hand carried to and from NBS, preferably in their constant-temperature bath. The voltage standard previously used at ORNL consisted of a bank of six specially selected, temperature-controlled unsaturated standard cells. The accuracy of this type of standard has been controversial, but it was found that the unsaturated cells agreed with the new saturated cells to within 1.8 μv, which is within the NBS certifying accuracy for saturated cells.

A universal ratio set (at the left side of the table in Fig. 7.9.1) was obtained to facilitate the calibration of ultraprecision and submicrovolt potentiometers. Potentiometers of this type cannot be calibrated by comparison with other potentiometers, and the calibration must be made by checking each resistor of all voltage-divider networks.

Fig. 7.9.1. Voltage Standard (on Right) and Universal Ratio Set (on Left) in Instrument Standards Laboratory.

7.10 FACILITY FOR INSPECTION AND CALIBRATION OF THERMOCOUPLES

W. W. Johnston W. R. Miller

A thermocouple inspection and calibration facility was established for the inspection of thermocouples and thermoelectric materials to be used at ORNL. A calibration service for large quantities of thermocouples is now available at this facility. These inspection and calibration services are required because of the extensive use of sheathed, ceramic-insulated thermocouples at ORNL, and because of a large increase in the number of suppliers of thermoelectric material.

All thermocouple materials procured by this Division and ORNL Stores are inspected (when applicable) for conformance to specifications on calibration, homogeneity, insulator quality (impurities, moisture, etc.), drift, physical dimensions, and insulator spacing and twist.

In the inspection facility, calibration furnaces permit the calibration of a relatively large quantity of thermocouples in a short time.

7.11 AC-INTERFERENCE TESTS OF FOXBORO M63 ALARM SWITCHES

C. D. Martin J. R. Sutton

Considerable difficulty was experienced at the Oak Ridge Research Reactor (ORR) with Foxboro M63 alarm switches because they produced random false-alarm and shutdown signals. Because a sensitivity to external ac interference was suspected, tests were made to determine what type, amplitude, and frequency of interference would produce a false signal.

Several tests were performed to determine the following:

1. the effect of line voltage variations on set point;
2. the effect of 60-cycle interference (signal line to ground) of various phase angles with respect to line voltage;
3. the effect of high-frequency interference introduced on
   (*a*) 10- to 50-ma signal line and ground,
   (*b*) 60-cycle power line,
   (c) relay contact wiring and ground;
4. the effect of 60-cycle pickup from adjacent current-carrying lines on the signal line.

The results indicate that the style B switch manufactured prior to February 1963 was extremely sensitive to ac interference. From an analysis of the test results and from consultation with the Foxboro Company, the following conclusions were reached:

1. A 2.2-mf, 25-v capacitor should be connected from the base to the emitter of the first amplifier stage on all style B alarm units now in service.
2. A 1-mf capacitor should be connected across the signal-input terminals of all style A units.
3. All emf-to-current converters should be operated from a regulated, harmonic-neutralized power source (Sola-type, CVH voltage regulator).
4. Each signal transmission loop should be grounded at one point, preferably at the emf-to-current converter. If dc grounding is impractical, a 0.1-mf capacitor should be installed from the signal line to ground. Care must be exercised to prevent grounding the signal circuit at more than one point.
5. Because of the low impedance (600 ohms) of the signal-transmission line, ac pickup from adjacent wiring is minimized to the point that shielded cable is not required for the signal line.

No false signal actuations have been reported since the incorporation of these recommendations on systems currently in service.

7.12 HIGH-TEMPERATURE SAMPLING PROBE FOR HELIUM LEAK DETECTION

T. F. Sliski H. J. Metz H. J. Stripling, Jr.

A sampling probe (Fig. 7.12.1) was designed and fabricated for helium leak detection in high-temperature systems.

The probe is primarily a differential screw-operated needle valve of the same general design as commercially available sampling probes. However, this new probe is relatively insensitive to temperature changes because of two design features. First, the material in the screw assembly and housing is Invar. This material precludes differential expansion in the case of uniform heating, and minimizes differential expansion in the case of nonuniform heating of the screw assembly and housing. Second, the screw assembly is mounted close to the intake end of the probe, which further minimizes the effects of differential expansion due to nonuniform heating of the housing and screw assembly. Heating this probe from ambient to 300°F (by inserting approximately 3 in. of the tip into a furnace and increasing the temperature over a period of about 30 min) changed the reading of the leak-detector pressure gage only 30%, that is, from 0.1 to 0.7 μ.

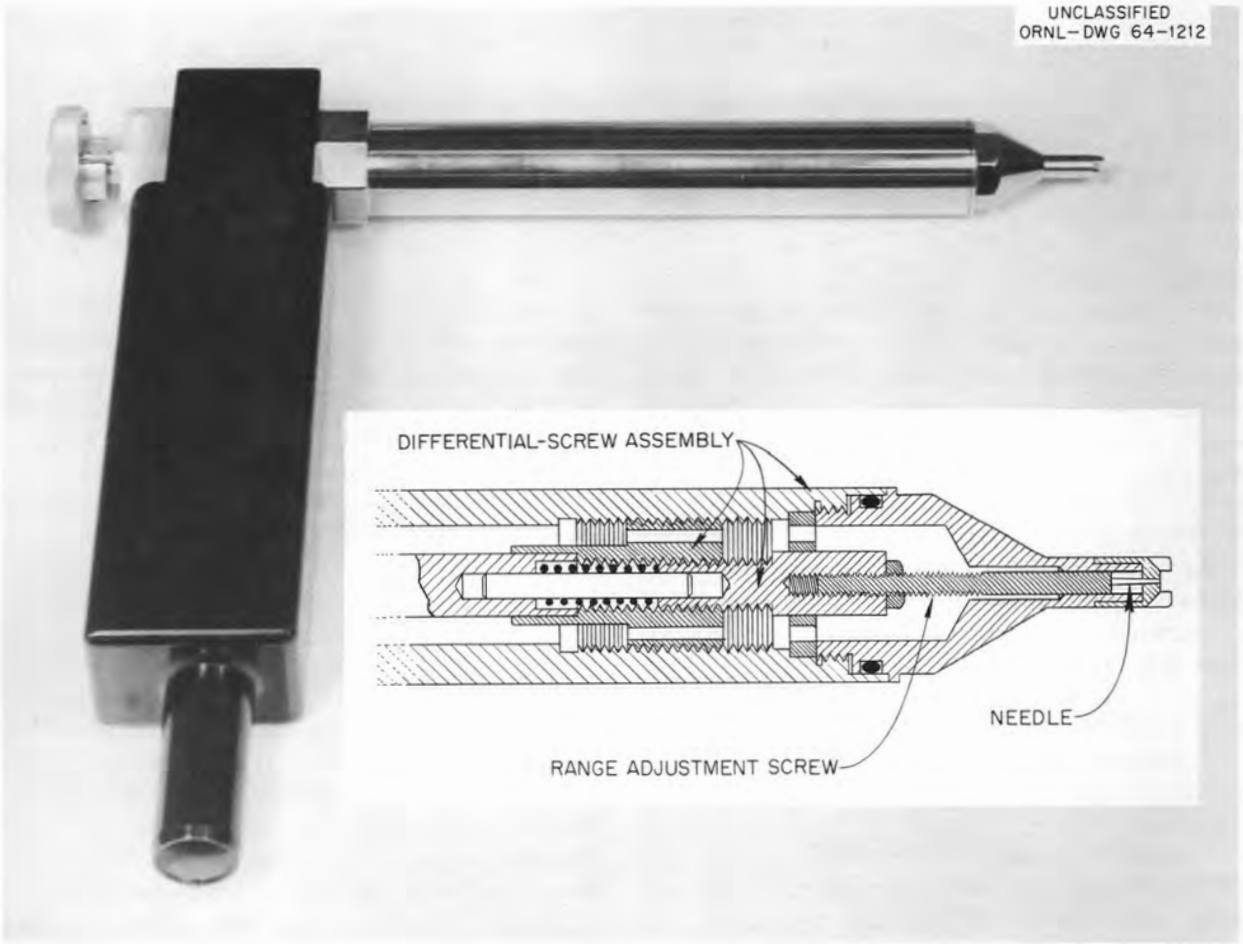

Fig. 7.12.1. High-Temperature Sampling Probe for Helium Leak Detection.

ANALYTICAL INSTRUMENTS

7.13 MODIFIED ANALYZER FOR AIRBORNE FLUORIDES

E. W. Hagen

A portable analyzer for airborne fluorides was originally developed at the Oak Ridge Gaseous Diffusion Plant to measure fluoride concentrations in environmental atmospheres in the range of 0.1 to 10 ppm. The airborne fluorides drawn into the analyzer are scrubbed with an aqueous solution to form hydrogen fluoride, which provides the electrolyte in a galvanic cell. Although the instrument performed as proposed, field maintenance was difficult; therefore, it was redesigned to reduce the quantity of glassware used in its construction, to eliminate all rubber tubing, and to improve service accessibility. Materials susceptible to corrosion were not used in construction of the instrument, and the readability of the flowmeters was improved. The analytical portion of the instrument is removable from the case.

7.14 SENSITIVE PHOTOMETER FOR EMITTED-LIGHT MEASUREMENTS

T. M. Gayle

The tritium used on many instrument and watch dials emits such a soft beta particle (18 kv) that scintillation counting is extremely difficult. Commercially available photometers lack both the necessary sensitivity and the desired optical geometry for making usable quantitative measurements. A technique which measures the intensity of the light emitted by the luminous dial and relates this value to the amount of tritium present was desirable. It was further desired that accurate light measurements be made at intensities as low as possible, at least to a value of approximately 5×10^{-7} lumen. Therefore a sensitive photometer was developed for the Isotopes Division for use in their program of evaluating commercially available instrument and watch dials containing radioactive materials.

The instrument is now being used by the Isotopes Division. Measurements are made both on new dials and on units that have been exposed to various environmental conditions of temperature, humidity, weathering, fire, or others. It was anticipated that dial sizes from $\frac{1}{2}$ to 5 in. in diameter with varying luminescence properties would be encountered. Preliminary plans are being made to develop a long-term light standard for use by the Isotopes Division to standardize the entire photometer periodically.

A 3-in. type 6363 photomultiplier tube with peak response at 4400 A (S-11 response) is used as the photometer detector and is mounted inside a 6-in.-diam cylindrical housing (Fig. 7.14.1), with the photocathode facing down. Samples to be measured are inserted in the lower opening of the tube and are supported by one of three removable plugs with which the samples can be positioned at various distances from the face of the photomultiplier. The plugs are held in the cylinder by spring-loaded connectors and can be inserted and removed in a matter of seconds. The plugs incorporate a lower flange section and a sliding O-ring seal inside the tube to make the inner chamber lighttight. The cylindrical chamber is mounted in a rectangular box assembly for mechanical protection and for shielding from

Fig. 7.14.1. Photometer for Emitted-Light Measurements.

room light. The entire assembly is fabricated of aluminum, and all surfaces are anodized black. The photomultiplier tube is fitted with a Mumetal shield contained inside the measuring cylinder.

The high-voltage power supply for the photomultiplier is a commercially available PRL Electronics, Inc., model DP-1447-HV supply, and the readout instrument is an E-H Research Laboratories model 202 electrometer amplifier. A Grya type CS-51 current calibrator has been used to buck out the photomultiplier dark current where extremely sensitive measurements were desired.

7.15 MICRODOSIMETER READER MODIFICATIONS

T. M. Gayle

A Bausch and Lomb No. 33-66-02 microdosimeter reader was modified for the Ecology Group of the Health Physics Division to provide increased long-term stability and approximately 10 to 15 times the galvanometer readout sensitivity originally provided. This modification was accomplished by a revision in the differential vacuum-tube voltmeter circuitry used to drive the galvanometer from the photomultiplier outputs. Over-range protection for the galvanometer was increased by using back-biased diodes from plate to plate in the voltmeter circuit. Other modifications included replacement of the No. 6328 reference photomultiplier tube with a more dependable 1P21 type, and the use of a ten-turn potentiometer for fine zero adjustment. Figure 7.15.1 shows the circuitry as modified.

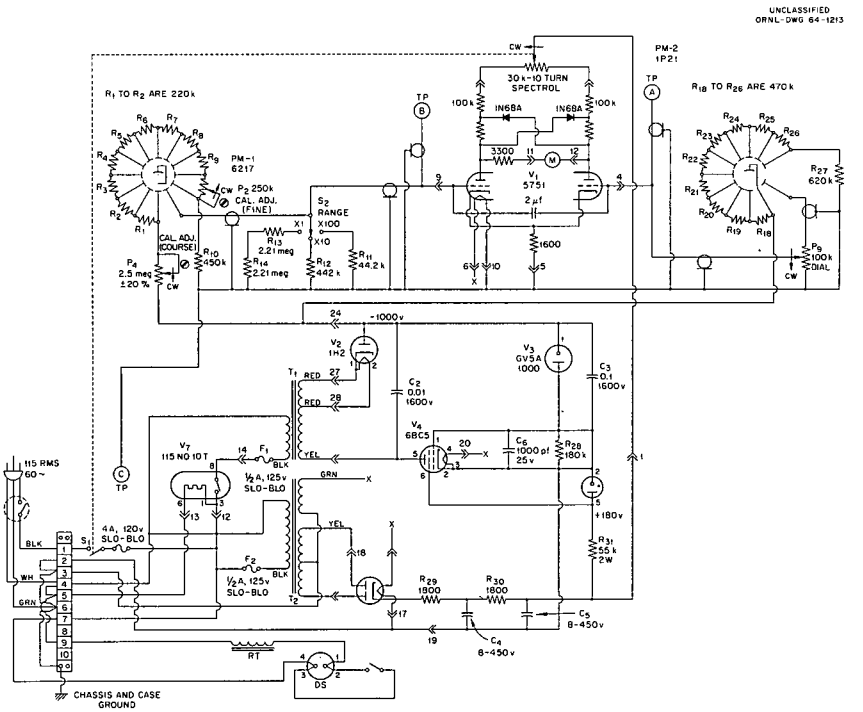

Fig. 7.15.1. Circuit for Microdosimeter Reader.

7.16 CHEMICAL DOSIMETER READER

T. M. Gayle

A method of reading chemical dosimeters by use of monochromatic light was investigated, and instrumentation for rapidly checking the dosimeter ampoules was developed for the ORNL Health Physics Division.

The instrument is being used to preselect ampoules and to grade approximately 5000 units each calendar quarter after exposure in film badges during that quarter.

The chemical dosimeter used in the ORNL film badges is a single-phase trichloroethylene–phenol-red type. The pH change produced by the interaction of radiation with trichloroethylene is indicated by a reduction of the phenol-red intensity. A spectrum analysis, made with a Bausch and Lomb Spectronic-20 spectrophotometer on a number of ampoules which were subjected to various radiation exposure doses up to 100 r, showed that the transmittance at 550 mμ was approximately proportional to dose (Fig. 7.16.1). No other single point in the spectrum was definitive with respect to radiation exposure.

After a valid correlation between exposure and transmitted monochromatic light (550 mμ) was demonstrated, fabrication of a suitable device for rapidly checking ampoules began; the logical approach was to modify the Bausch and Lomb Spectronic-20 machine for this service. The electronic circuit was modified by making minor refinements in the existing amplifier circuit and by providing a large external meter (Fig. 7.16.2) with adjustable zero suppression and with increased

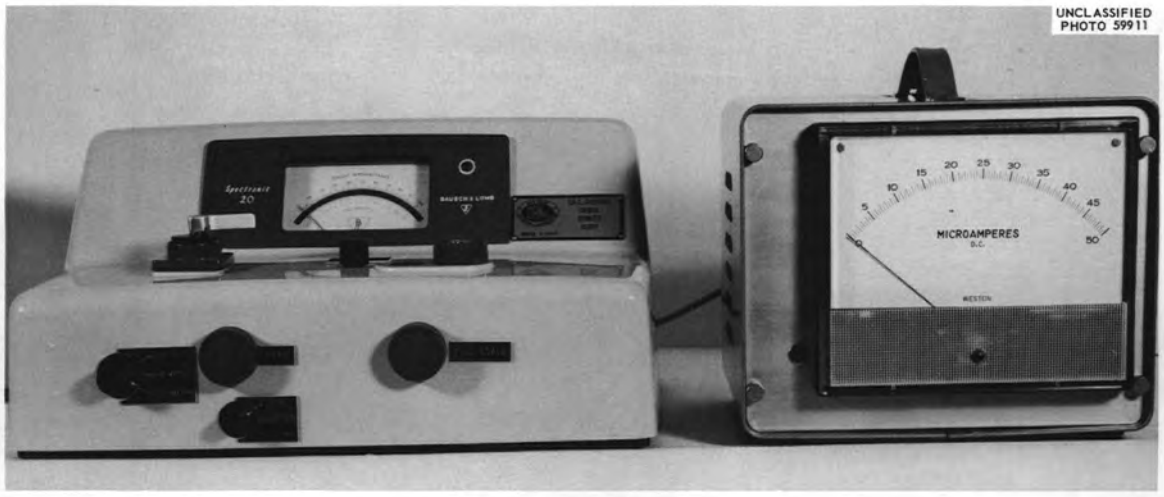

Fig. 7.16.1. Spectrophotometer and Meter.

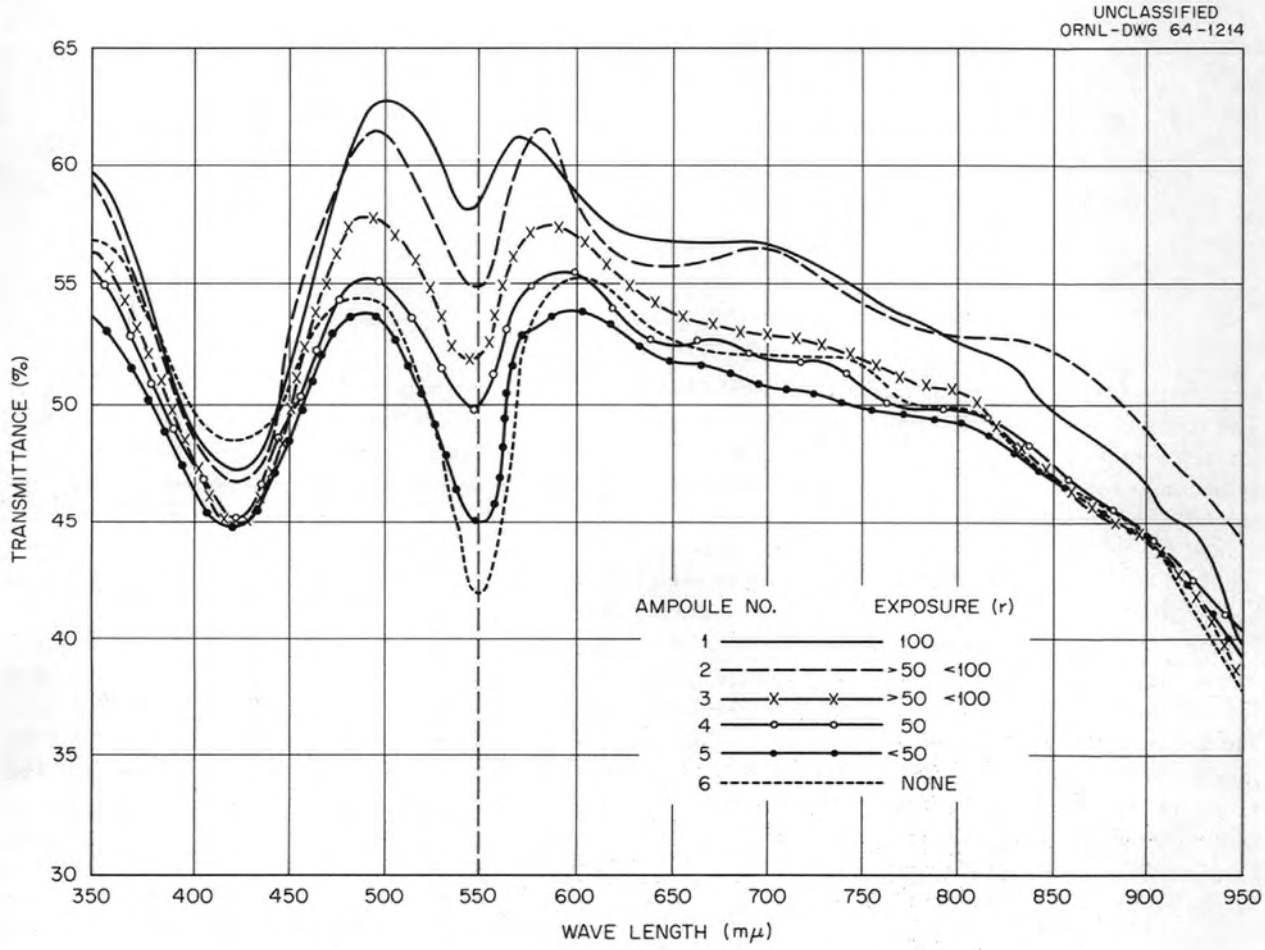

Fig. 7.16.2. Transmittance Measurements for Film-Badge Ampoules.

Fig. 7.16.3. Quick-Change Holder for Ampoules.

sensitivity for reading small transmittance changes. The external meter circuit employed a Zener diode for zero suppression and provided a zero–to–full-scale meter reading for the range of ampoules normally measured. Mechanical modifications included the addition of a manual shutter operator for rapid zero checking and a special quick-change holder (Fig. 7.16.3) for the ampoules to be tested. A holder was designed which simplified the checking of ampoules. With this holder, ampoules are fed by gravity to the holder, are quickly checked, and are released from the holder to fall completely through the machine to a tray beneath. This release is accomplished by a spring-loaded guillotine, which is tripped by a handle on top of the holder. The holder was equipped with a very narrow slit to minimize diffraction and scattering of the light beam by the glass walls of the ampoule.

Optical stability and reproducibility were excellent, despite continued and rapid ampoule changing. The original Bausch and Lomb power-supply–amplifier circuit was relatively stable and employed a separate reference phototube with a four-transistor feedback amplifier for regulation of the optical source. Long-term stability of the vacuum-tube readout circuit was improved by careful selection of the No. 5751 dual triodes for optimum balance. After a 30-min warmup period, the readout drift proved to be less than 5% for any 1-hr period. The effects of normal line-voltage fluctuations, ambient temperature, and room light variations were negligible.

7.17 INSTRUMENT FOR MEASURING SMALL WEIGHT CHANGES

C. D. Martin

An instrument was developed for measuring weight changes of solid samples being analyzed by thermogravimetric methods. Although such instruments are commercially available, the cost of this locally produced instrument was about half the cost of a comparable commercial model.

In order to obtain the desired resolution of 10 mg, the millivolt output of a Statham strain-gage, bridge-type force transducer, with a range of −3 to +3 oz, is suppressed by a stable millivolt referency supply.[1] The difference voltage (i.e., the output of the transducer minus the output of the reference supply) is amplified by a Philbrick P-2 operational amplifier and fed into a strip-chart recorder. One of the two feedback resistors in the amplifier is selected, by means of a switch, to change the gain; a recorder span of either 100 mg or 250 mg is selected in this manner.

The absolute accuracy of the transducer is about ±80 mg (1% of full scale).

[1]C. D. Martin, *Instrumentation and Controls Div. Ann. Progr. Rept. Sept. 1, 1962*, ORNL-3378, pp. 53–54.

7.18 ADJUSTABLE APPORTIONIZER

E. W. Hagen

An adjustable apportionizer was designed and developed as a manually operated device that would simultaneously inoculate up to ten sterile compartments, one row of a 10 × 10 array in a containment tray, each with an individually selected and metered quantity of fluid. Portions are adjustable from 0.05 to 0.7 cc.

The inoculating syringes are individually held in sockets in a stationary mounting block, and the compartmented tray is clamped to a mobile platform. The tray can be positioned so that each compartment can receive the inoculation in any corner. The tray is first raised onto the needles before the fluid is dispensed. A single stroke of the actuator bar completes the inoculation. A frame, designed to surround the rear half of the apportionizer, can support up to ten Erlenmeyer flasks ranging in size from 125 to 1000 ml.

7.19 EGCR ANALYTICAL INSTRUMENTATION CONSULTING

T. M. Gayle

Consultation with the Engineering Division, Oak Ridge Operations, Atomic Energy Commission, was held on a number of analytical instrument problems associated with the Experimental Gas-Cooled Reactor Project. A review of specific contractor's proposals and discussions of general analytical techniques and sample handling were carried out as part of the ORNL EGCR program for the Atomic Energy Commission. Designs proposed by contractors for the double-loop moisture detection and safety system were reviewed. An analysis of sample handling and graphite particulate elimination was offered. Suggestions were made regarding the moisture detection system, the total-hydrocarbons analyzer, the process gas chromatograph, hydrogen analyzers, and other miscellaneous analytical instruments.

8. Reactor Instrumentation and Controls Systems Engineering

8.1 STATUS OF INSTRUMENTATION AND CONTROLS FOR THE HEALTH PHYSICS RESEARCH REACTOR

L. C. Oakes C. F. Holloway

Since the previous report[1] of the instrumentation and control system for the Health Physics Research Reactor (formerly named the Fast Burst Reactor), the reactor was checked at the ORNL Critical Facility, operated at the Nevada Test Site, and installed and operated in its permanent location at ORNL.

To make use of commercial manpower and facilities for construction of the reactor, the equipment was supplied and installed through commercial sources, based on design criteria specified by ORNL. This cooperative effort was successful in that ORNL engineering manpower was conserved; however, during the first critical experiments at the Critical Facility, the performance of several items of equipment was wholly inadequate. The performance of counting-rate instrumentation, although not the only example, was particularly poor. Even though a great effort was expended to make the apparatus perform to the minimum acceptable performance level, it ultimately became necessary to replace a large percentage of the channel with ORNL components.

After the checkout was completed, the reactor was shipped to Nevada for the BREN experiments (Bare Reactor Experiment – Nevada).[2] During these experiments the reactor was operated successfully; the instrumentation and control system performed acceptably. The reactor was operated at steady power levels up to 1 kw and also was made to produce pulses with yields up to $\sim 5 \times 10^{16}$ neutrons.

The reactor is presently being operated at ORNL, where one change has been made in the safety system. To exploit the intermittent high-power capability of the reactor, the fast nuclear safeties are set at 15 kw. Because the maximum allowable core temperature (600°F) will be exceeded on sustained operation above 1 kw, unless the operator or instruments limit the total integrated reactor power, power-integrating trips monitor reactor power over the range of 1 to 15 kw. To apply this constraint, the two temperature channels that produce scrams when the core temperature exceeds 600°F were modified and improved to safety-system quality consistent with operation at high power transients. The response time of these channels is approximately 0.1 sec. Upscale burnout (a fail-safe feature) is incorporated in the equipment, and the channel operativity can be tested at will by the operator. The test is performed from the console by applying current to a heater surrounding an iron-constantan thermocouple placed in series with the core thermocouple. The channel response is observed on a recorder.

[1] L. C. Oakes and C. F. Holloway, *Instrumentation and Controls Div. Ann. Progr. Rept. July 1, 1961*, ORNL-3191, p. 78.

[2] J. A. Auxier *et al.*, *General Correlative Studies – Operation BREN*, CEX 62.03 (in press).

8.2 STATUS OF INSTRUMENTATION FOR THE MOLTEN-SALT EXPERIMENT[1]

R. L. Moore
J. R. Brown
G. H. Burger
P. G. Herndon
D. G. Davis
J. R. Tallackson
J. L. Redford
S. J. Ball
S. J. Ditto

Since the previous report,[2] basic criteria for MSRE instrumentation control and safety were established. Detailed design of the instrumentation system, purchase of commercially available instrument components, and development of special instrument components were continued.

The performance and installation requirements for control, safety, and containment were critically reviewed during this period by Project and Instrumentation and Controls Division personnel. Only minor revisions in the instrument system design were recommended by the reviewers. Additional revisions were required because of changes in the reactor system design. Although the number of revisions is not small, all can be made without compromise of safety, control, or operational requirements. To satisfy requirements for redundancy in safety circuitry, additional commercially available process instruments will be purchased, the cost of which will be less than 5% of the total cost of instrumentation.

Design Status

Design of 40 of the 53 panel board sections was completed, and 7 of the remaining 13 either were partly completed or were held for revision. Some preliminary design studies were made for the remaining six panels. Completion of the panel design was delayed pending establishment of criteria for the nuclear instrumentation and reactor safety systems. Since sufficient criteria have been made available, panel design will be resumed.

Design of interconnection tubing for pneumatic instrumentation and of interconnection wiring for electrical transmitting instruments (Foxboro ECI) was completed. Except for additional annunciators required for the nuclear control and safety system, annunciator wiring interconnections were completed.

Design of thermocouple installation and interconnection became more difficult than was originally expected. Because of the requirements for remote maintenance and the compactness of the in-cell reactor system, the location of disconnects and routing, as well as the point of attachment of each in-cell thermocouple, had to be carefully selected. The layout of this system was extremely sensitive to changes in the reactor design and to additional requirements for in-cell thermocouples, and numerous changes were required before the many conflicting requirements were satisfied. Layout of the in-cell thermocouple installations is now considered to be firm. Detail design of the thermocouple system, including interconnections, is approximately 80% complete. Scheduled for installation in the MSRE system are 920 thermocouples, of which approximately half (540) will be installed inside the reactor containment shell.

Requirements for process radiation monitors (which were strongly influenced by the requirements of the reactor safety and containment systems) were determined, and design of this system, including design of panels and field installation and shielding, was completed.

Requirements for Health Physics instrumentation were reviewed and approved, and installation design for this equipment is nearing completion.

Procurement

With the exception of some additional instrumentation required by recent revisions and the chemical processing system, preparation of specifications and initiation of procurement of process instrument components were completed. Most of these components are now on hand, and delivery of the remainder is expected within the next three months.

---

[1]See also, "Design of MSRE Automatic Rod Controller," Sect. 9.9.

[2]R. L. Moore *et al.*, *Instrumentation and Controls Div. Ann. Progr. Rept. Sept. 1, 1962*, ORNL-3378, p. 74.

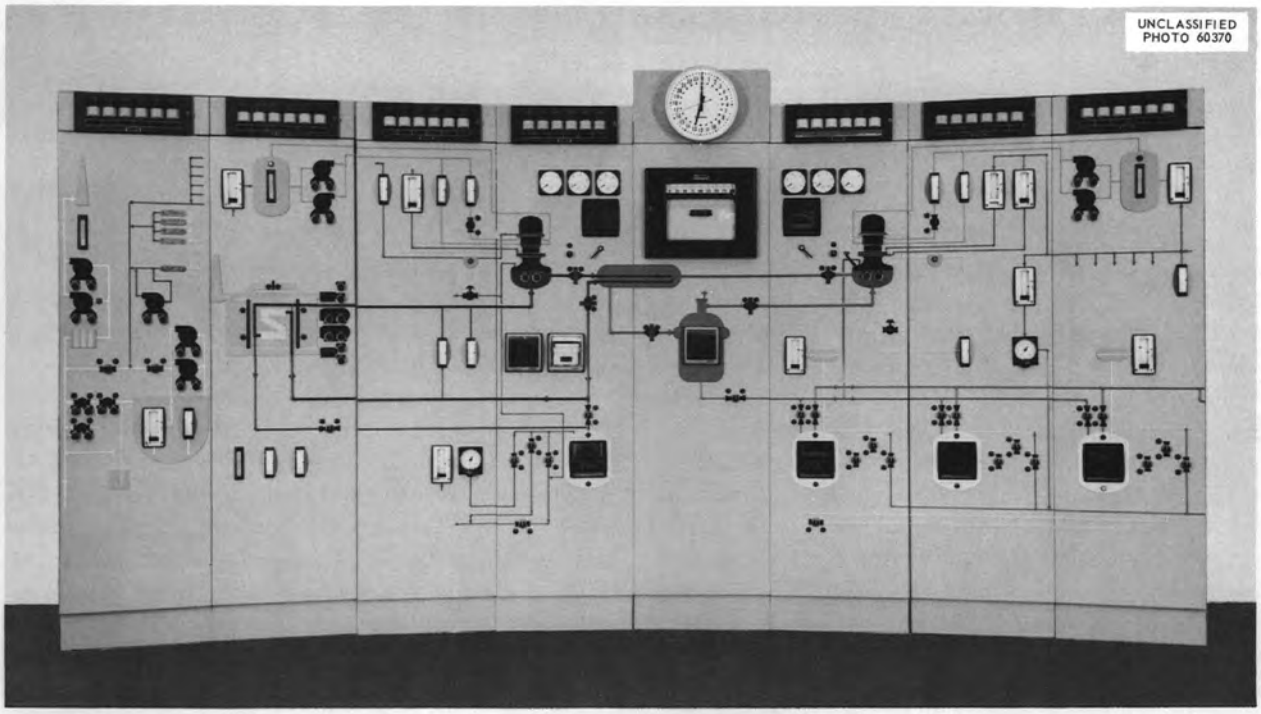

Fig. 8.2.1. Front View of Main Control Panel Board for the Molten-Salt Reactor Experiment.

AEC approval for purchase of a computer data-logging system was obtained, and proposals received from four vendors are being evaluated.

Most of the equipment required for the process radiation monitor system is on hand and the remainder is on order.

Health Physics instrumentation components are on order.

Procurement of nuclear instrument components is under way.

Fabrication and Installation

Figure 8.2.1 shows some completed sections of the main control panel.

Installation of 149 thermocouples in the MSRE radiator assembly has been completed, and preparations are being made for installation of thermocouples on other shop-fabricated components. The radiator installations were particularly difficult to make because of the special nature of the mechanical attachment to the thin-wall radiator tubes and the compactness of the radiator assembly.

Installation of equipment at the reactor site was started in June and is continuing at a rapidly accelerating pace.

8.3 PROCESS INSTRUMENTATION AND CONTROLS FOR ORR-GCR LOOP NO. 2

C. M. Burton

E. H. Bell G. H. Burger J. W. Cunningham
S. W. Fiveash[1] G. W. Greene C. C. Hall[2]
A. K. Stansberry[1]

In July 1963, the ORR-GCR Loop No. 2, an in-pile experimental facility, was placed in nuclear operation by the ORNL Reactor Division to test ceramic fuels.[3] The design, procurement, installation, and checkout of instrumentation and controls, which will provide sufficient protection and safety while permitting the experiment to operate under various conditions, required more than 3.5 yr for completion. The total cost for instrumentation is approximately $500,000.

Electronic instrumentation which develops 10- to 50-ma dc signals was used almost exclusively for process measurement and control throughout the facility for the following reasons:

1. to avoid the backup of radioactive gases and solutions, which could occur had air-signal lines and pneumatic instruments been used;
2. to be compatible with modern data-handling systems;
3. to minimize delay times in signal transmission over long distance.

A total of 48 such electronic channels was installed: 7 for pressure, 14 for flow or differential pressure, 23 for temperature, and 4 for radiation. Only four channels of pneumatic instrumentation were used in addition to flow, level, and pressure switches. To monitor fission products actually released from the test fuel, eleven G-M tubes, eight ion chambers, one constant air monitor, and two NaI scintillation detectors were placed at selected locations throughout the loop facility.

---

[1]ORGDP design assistance.

[2]Under contract from Lockheed.

[3]J. Zasler *et al.*, *In-Pile Gas-Cooled Fuel Element Test Facility*, ORNL-TM-250 (July 10, 1962).

9. Reactor Instrumentation and Controls Development

NUCLEAR INSTRUMENTATION

9.1 MODULAR ELECTRONIC INSTRUMENTS FOR REACTOR CONTROL AND SAFETY

J. L. Anderson C. C. Courtney J. T. DeLorenzo
E. N. Fray S. H. Hanauer Ronald Nutt

As part of the continuing program in the development of second-generation ORNL reactor control instruments,[1] a system of electronic instrument modules has been devised for reactor control and safety systems. Each module is a functional unit of one or more solid-state electronic or electromechanical instruments. The modules plug into the fronts of roll-out chassis drawers, which are replaceable after the coaxial- and AN-type plugs are disconnected. The height and depth of each module are the same, 4.7 in. high by 11.6 in. deep, but the width is variable in increments of 1.28 in. The overall drawer depth is about 16 in.; this allows space behind the modules for interconnecting wiring and components. The drawers fit standard 19-in. racks and are $5\frac{1}{4}$ in. high. The mechanical design of the modules is based on and is compatible with a scheme developed at CERN.[2] A typical module and drawer arrangement is shown in Fig. 9.1.1, and four modules are shown in Fig. 9.1.2. To date, 18 different modules have been designed and prototypes built, and several others are being developed. All of these instruments are designed to operate from 32-v station batteries in conjunction with various voltage regulators, inverters, and converters. To achieve better channel independence in safety and control systems, separate battery systems are provided for each channel. These batteries provide continuity of operation during temporary commercial power outages.

The first application of these modules and drawers will be for the safety, servo, and counting systems for the HFIR and MSRE. Some 210 modules in 39 drawers will make up the HFIR systems, and 71 modules in 19 drawers will make up the MSRE systems.

The present designs include the following units, each identified by an ORNL model number. (Some of the more significant units are described in more detail in other sections of this report.)

Q-2601, Chamber Voltage Monitor and Test Unit

Eddie Madden J. L. Anderson

This unit provides a variety of test signals for checking reactor safety instruments, either during reactor operation or during shutdown periods. An undervoltage detector, which monitors both the safety chamber polarizing voltage and the proper connection of cables to the ionization chamber, is included.

[1] S. H. Hanauer *et al.*, *Instrumentation and Controls Div. Ann. Progr. Rept. Sept. 1, 1962*, ORNL-3378, pp. 63–67.

[2] B. Sagnell, *CERN 19 in. Chassis Systems*, CERN 62-29, Proton Synchrotron Machine Division, European Organization for Nuclear Research, Geneva, Switzerland (Oct. 8, 1962).

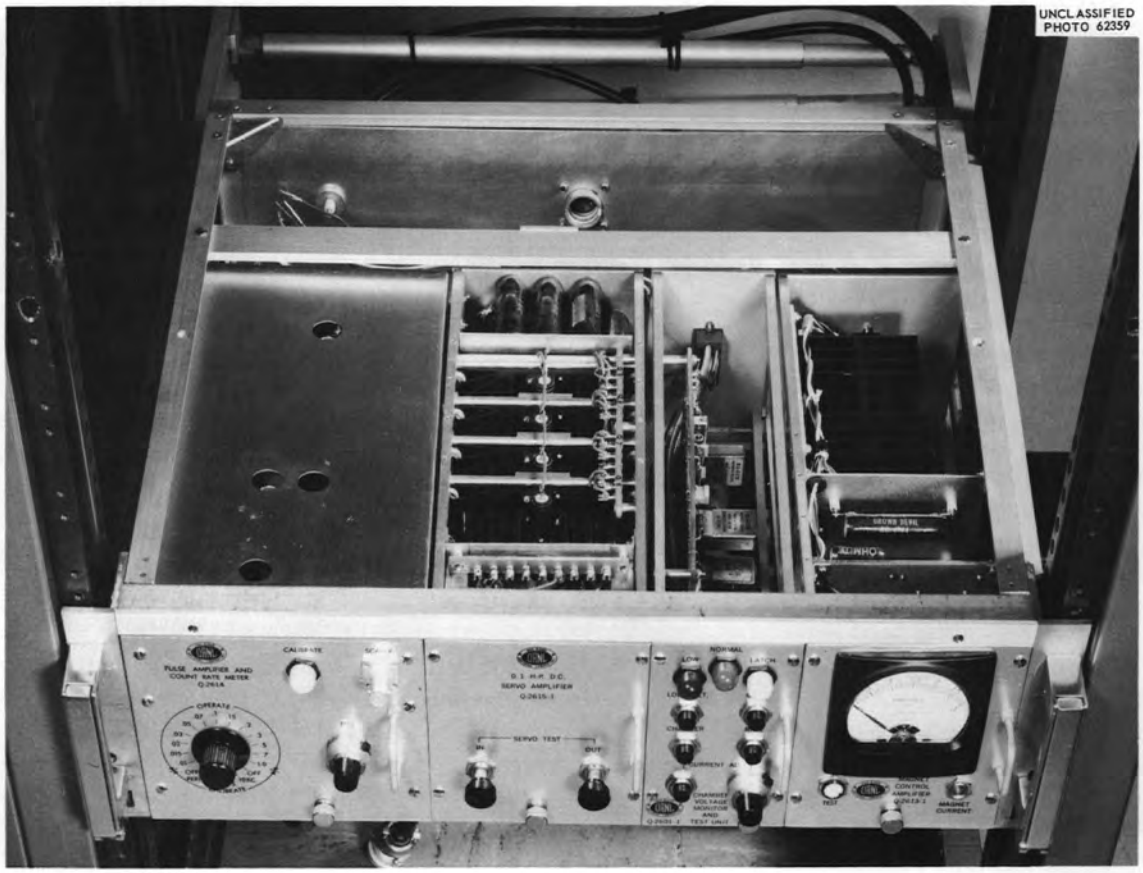

Fig. 9.1.1. Typical Module and Drawer Arrangement.

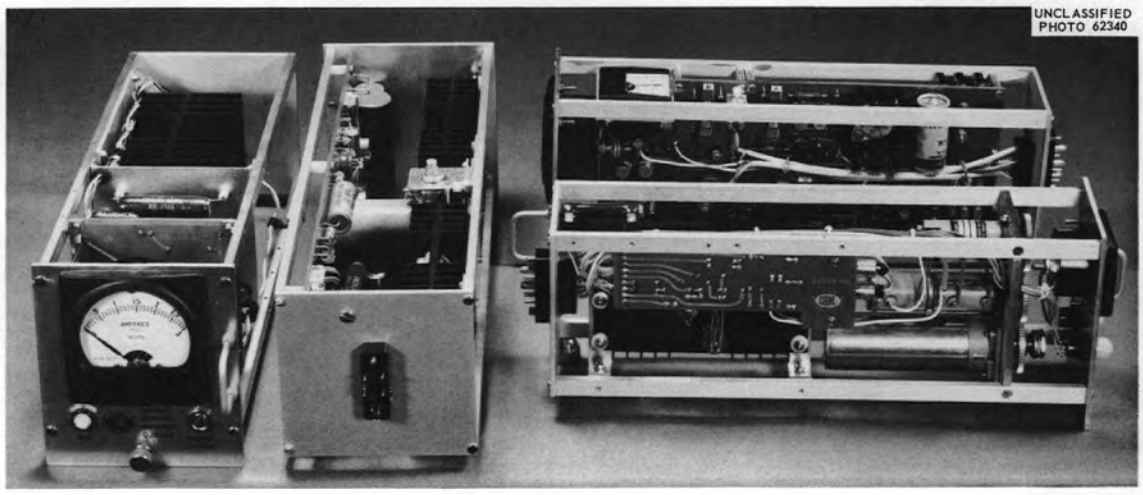

Fig. 9.1.2. Typical Modules.

Q-2602, Chamber High-Voltage Supply and Flux Amplifier

Eddie Madden Ronald Nutt

This unit combines an all-transistor, low-current amplifier (Sect. 9.2) with a dc-to-dc converter which supplies high voltage for an ion chamber.

Q-2603, Flux Reset Mechanism

Ronald Nutt C. C. Courtney

This unit contains a small instrument servo that drives a potentiometer which adjusts the gain of the flux amplifier to force the neutron-flux signal to agree with a computed heat power signal in steady state. The adjusting or resetting speed is intentionally slow so as not to interfere with transients.[3]

Q-2605, Dual Operational Amplifier

Electronic Associates, Inc.

This is a chopper-stabilized high-gain transistor operational amplifier, electrically identical to those used in general-purpose analog computers. It is used for amplification, differentiation, and integration in reactor instrumentation assemblies.

Q-2606, Dual Signal Converter

Rochester Instrument Systems, Inc.

This is an amplifier which enables signals to be fed into and out of reactor instruments. It can convert signals of any of several standard ranges to any other standard range, permitting communication between instruments having different signal spaces.

Q-2607, Servo Demand Drive Unit

J. L. Anderson C. C. Courtney

This unit consists of a motor-driven servo demand potentiometer with provisions for electrically limiting the output demand signal in accordance with a process signal such as coolant flow.

[3]S. H. Hanauer *et al.*, *Instrumentation and Controls Div. Ann. Progr. Rept. July 1, 1961*, ORNL-3191, p. 70.

Q-2608, Analog Multiplier

Systron-Donner Corp.

The output of this device is a voltage proportional to $xy/10$, where x and y are the two input voltages. The multiplier uses the quarter-square principle and is used with feedback to compute ratios.

Q-2609, Fast-Trip Comparator

J. F. Pierce[4] D. C. Shattuck[5]

This is a voltage-level comparator with fast response and exceptional accuracy and stability (Sect. 9.3).

Q-2612, OR Gate

Ronald Nutt

This is a unit used in safety systems to provide a single-action signal output when any one or more of its inputs is in an abnormal state.

Q-2613, Magnet Control Amplifier[1]

J. L. Anderson

This is a feedback amplifier for regulating and switching scram-latch magnet current for reactor safety.

Q-2614, Pulse Amplifier and Count-Rate Meter

J. T. DeLorenzo

This unit comprises a transistor pulse amplifier, pulse-height discriminator, and logarithmic count-rate meter of the Cooke-Yarborough type.

Q-2615, 0.1-hp DC Servo Amplifier

J. T. DeLorenzo

This is a servo amplifier for the fission-chamber positioning system of the wide-range counting channel.[6]

[4]Consultant.

[5]Graduate student in electrical engineering at the University of Tennessee.

[6]R. E. Wintenberg and J. L. Anderson, *Trans. Am. Nucl. Soc.* 3(2), 454 (1960).

Q-2617-5, Fission Chamber and Preamplifier DC Power Supply

Ronald Nutt

This unit supplies all necessary power to a counting-channel fission chamber and remote, vacuum-tube pulse preamplifier.[7]

Q-2619, Q-2620, and Q-2621, Voltage Regulators

W. E. Lingar

These units supply regulated dc supply voltages to the other instrument modules. The regulators operate directly from batteries; no inverter is used to isolate the source from the load or to transform the battery voltage to near the desired output potential. The line and load regulation of these devices is 0.05%, no load to full load at 28 to 36 v input. Their temperature coefficient is 0.01%/°C from 10 to 55°C, and their long-term stability is 0.05% in 8 hr at constant temperature.

Q-2622, Linear Count-Rate Meter

J. T. DeLorenzo

This unit contains the circuit to provide a voltage proportional to the counting rate of the preceding instrument channel. It is used to attain higher precision than is possible from a logarithmic counting-rate meter.

Q-2625, Inverter, 32 v DC to 115/6.3 v AC, 60 Cycle

Ronald Nutt

This unit converts the 32-v dc battery mains to 60-cycle power to drive signal converters, mechanical choppers, and other devices requiring ac power.

[7] D. P. Roux *et al.*, *Trans. Am. Nucl. Soc.* 5(1), 185 (1962).

9.2 LOW-CURRENT TRANSISTOR AMPLIFIER

Ronald Nutt

A current-sensitive amplifier (ORNL model No. Q-2602) has been developed specifically for use with the modular reactor instrumentation (Sect. 9.1). The amplifier (Fig. 9.2.1) has a unique combination of characteristics that makes it readily applicable where medium sensitivity, good stability, and a high degree of reliability are required.

The amplifier is used to amplify the current from an ionization chamber in the range of 10^{-8} to 10^{-5} amp. This range is such that the use of a field-effect transistor as the input stage of the amplifier introduces a negligible error in the measurement due to leakage current of the input stage. The Siliconix 2N2607 transistor, which is used as the input transistor, has a typical leakage current of 5×10^{-11} amp.

The bias-point instability of the input stage due to ambient temperature changes had to be minimized. The fact that certain types of field-effect transistors, when properly biased, exhibit zero temperature coefficient over a large ambient temperature range was used to establish the bias point of the 2N2607 transistor. The bias point was selected so that the 2N2607 transistor would exhibit a slightly negative temperature coefficient to cancel a net positive temperature coefficient due to the remaining semiconductor devices in the amplifier. Changes in dc characteristics of the 2N2607 transistor from one unit to another limit the effectiveness of the compensation, but for ten different transistors, the total amplifier drift was no greater than 0.3 mv/°C.

UNCLASSIFIED
ORNL-DWG 64-1215

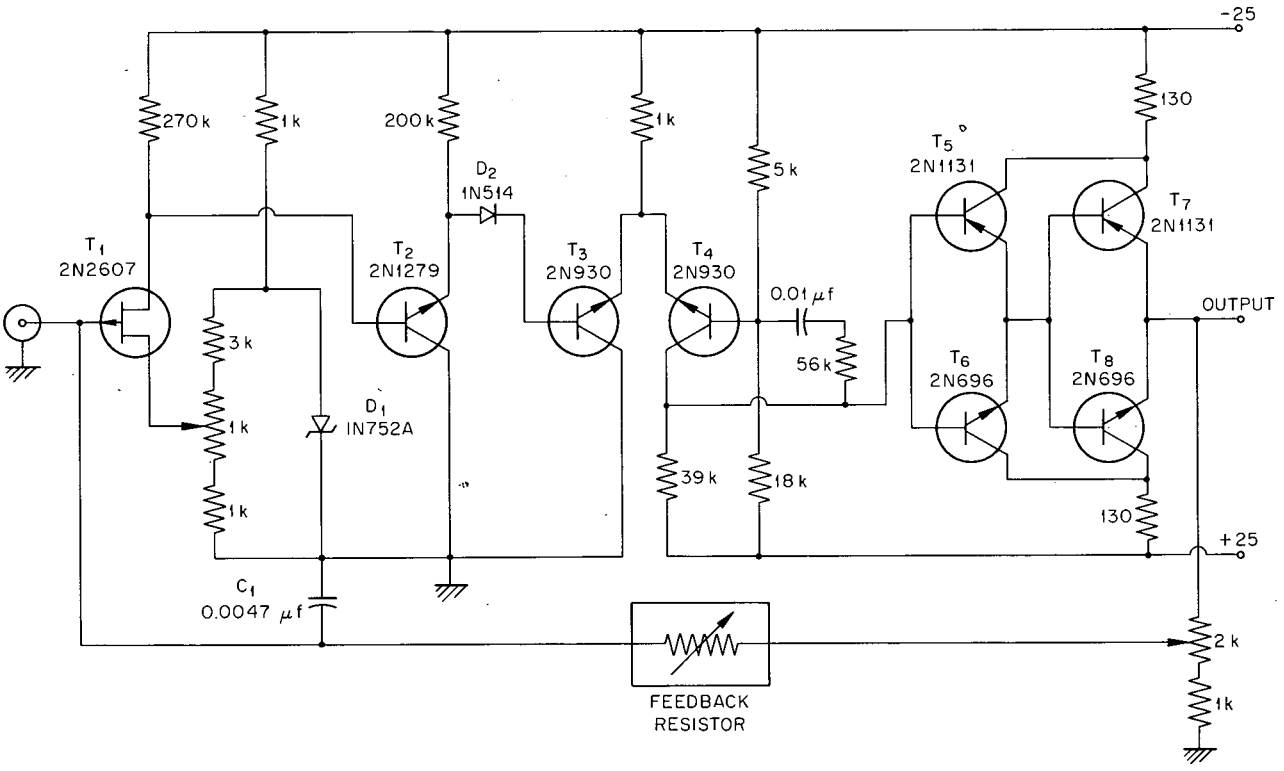

Fig. 9.2.1. Flux Amplifier Circuit.

The open-loop voltage gain of the amplifier is approximately 10^4; this consists of a gain of 20 in the field-effect transistor and a gain of approximately 500 in the differential stage (*T*3 and *T*4 in Fig. 9.2.1). Transistor *T*2 is an emitter-follower which drives the differential stage. The signal is taken from the collector of *T*4 and is fed into two power stages, *T*5 and *T*6 and *T*7 and *T*8. The output stage will deliver approximately 100 ma into a 300-ohm load with no appreciable degradation of the amplifier characteristics.

The frequency response of the amplifier is determined by the ac feedback network from the bases of *T*5 and *T*6 to the base of *T*4. Capacitor C1 is added to minimize the effect of long capacitive cables on the frequency response of the amplifier. The response of the amplifier to a unit step of current is approximately 50 μsec to rise from 0 to 10 v. This response is not altered appreciably with the addition of 0.005 μf of capacitance on the input with a 200-kilohm resistor in the feedback network.

The overall characteristics of the amplifier are given in Table 9.2.1.

Table 9.2.1. Characteristics of Low-Current Transistor Amplifier

Sensitivity	10^9 v/amp, maximum 10^4 v/amp, minimum
Temperature instability	0.3 mv/°C, maximum
Output voltage	±12 v, maximum
Long-term drift	1 mv/day, maximum
Rise time	50 μsec ($C_{in} = 0$, $R_f = 200$ kilohms)
Input leakage current	5×10^{-11} amp, typical
Allowable load	300 ohms, minimum
Drift due to supply voltage	0.01 output v/supply v

9.3 FAST-TRIP COMPARATOR CIRCUIT

J. F. Pierce[1] D. C. Shattuck[2]

Many operations in reactor control and safety systems are initiated by the output signal from a voltage comparator circuit on a *go, no-go* basis. Such a circuit compares the magnitude of two input dc signals having opposite polarities, and produces an output voltage having either of two possible values depending upon which input voltage is larger. Usually, a trip circuit contains both the comparator and the switching circuits necessary to drive external logic and control systems.

A study was initiated to establish what criteria underlie fast comparators and to develop a versatile, fast-trip transistor comparator with an accuracy of ±25 mv over a range of 1 to 10 v and a temperature range of 10 to 55°C.

The diagram of a prototype model is shown in Fig. 9.3.1. The voltage comparator section includes transistors *Q*1 through *Q*4 and their associated circuits. The input stage (*Q*1 and *Q*2) is a compound differential amplifier having good temperature stability and a high input impedance. This stage drives a simple differential amplifier *Q*3, which drives a Schmitt trigger circuit *Q*4. All transistors, after the Schmitt trigger, operate

[1]Consultant.

[2]Graduate student in electrical engineering at the University of Tennessee.

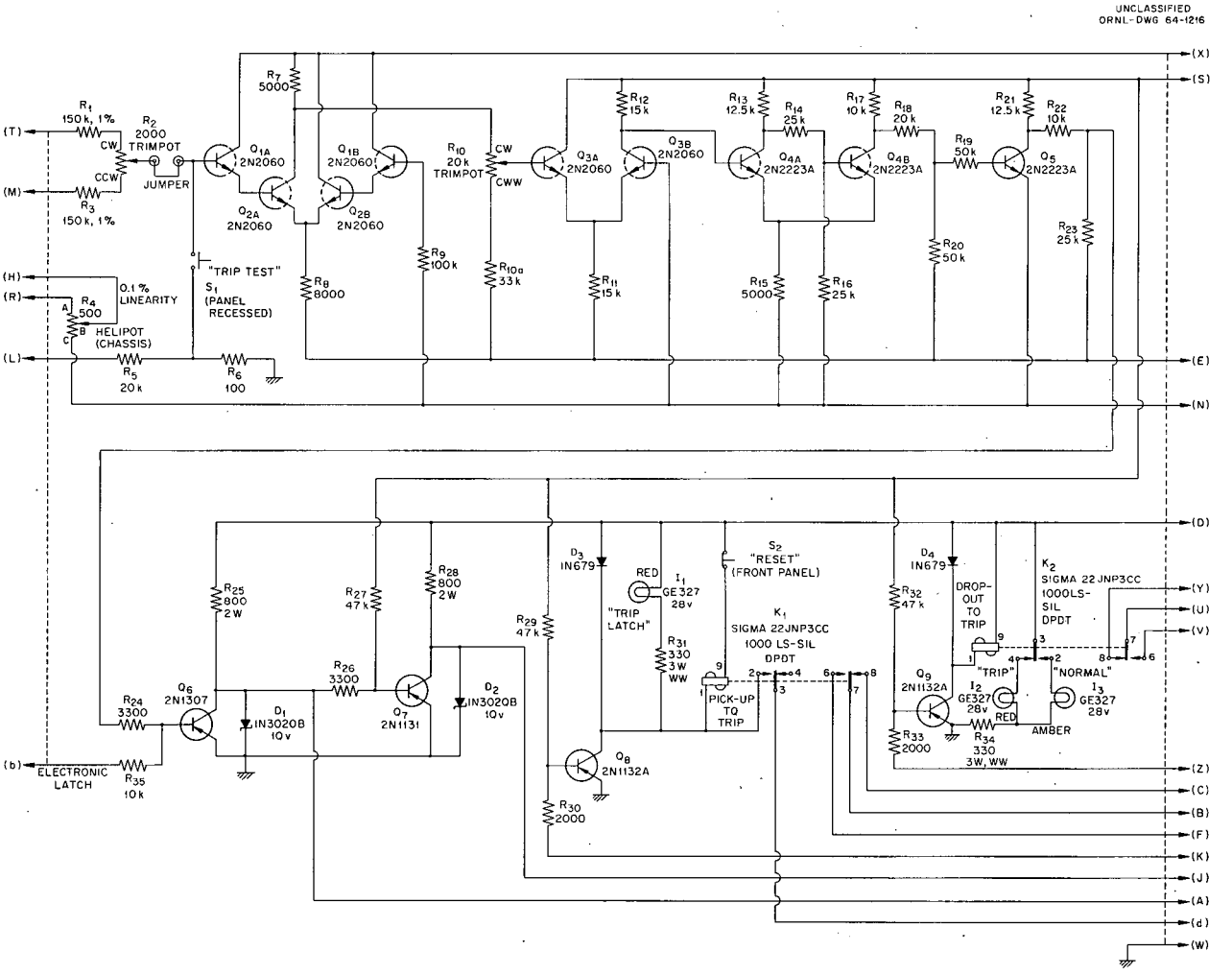

Fig. 9.3.1. Fast-Trip Comparator Circuit.

in the switching mode and are either saturated or nonconducting.

Two electronic outputs are provided to drive logic circuits external to this unit and two relay-drivers located within the comparator. Two voltages are available on each output, -0.2 v (0 nominal) and -10 ± 0.5 v. When one output voltage is zero, the other output voltage is -10 v. The change in voltage from one level to the other is completed in less than 50 μsec after the trip signal occurs. This delay can be reduced to less than 12 μsec by adding a capacitor to the circuit of $Q2$.

For flexibility, either relay driver may be excited from either electronic output. The relays can change states in approximately 10 msec. Each relay has one set of contacts available for external connections, and one set to perform an indicating function on the front panel. Relay $K1$ holds a fault indication after the fault has been corrected, and $K2$ indicates the immediate state of the circuit.

When two external signals are compared to each other, the circuit trips when the difference between the magnitudes of the two signals is 10 mv or less over a temperature range of 0 to 60°C. With only one signal available, the comparative signal may be obtained from a reference Helipot $R4$. In this mode, nonlinearities in the potentiometer and circuit loading degrade the accuracy. With the Helipot dial setting used as a reference, error performance data for one model are shown in Fig. 9.3.2 for two different temperatures. The errors in this unit were less than ±20 mv over a voltage range of 0 to 10 v and a temperature range of 0 to 60°C. The hysteresis varied from 2 to 4 mv over this same temperature range. Results from three other units were comparable.

The prototype model contains a trip test circuit that may be used to check the comparator while in use. An electronic lockout (optional) is also included to hold the circuit in the trip condition if the fault persists more than 10 msec.

Several external connections can be made which allow the circuit to trip for a variety of input conditions. For the case of two external signals, A and B, tripping action can take place when the magnitude of A is greater than or less than that of B, provided A and B have opposite polarities. The polarity may be positive or negative. Since tripping action occurs when the magnitude of the signal is equal to the magnitude of the reference voltage, the circuit can be tripped as the signal increases in magnitude through the trip point, or as the signal decreases in magnitude through the trip point.

The results from two breadboard models and two prototype units have been consistent. The accuracy and flexibility of this comparator should make it useful in a large number of applications.

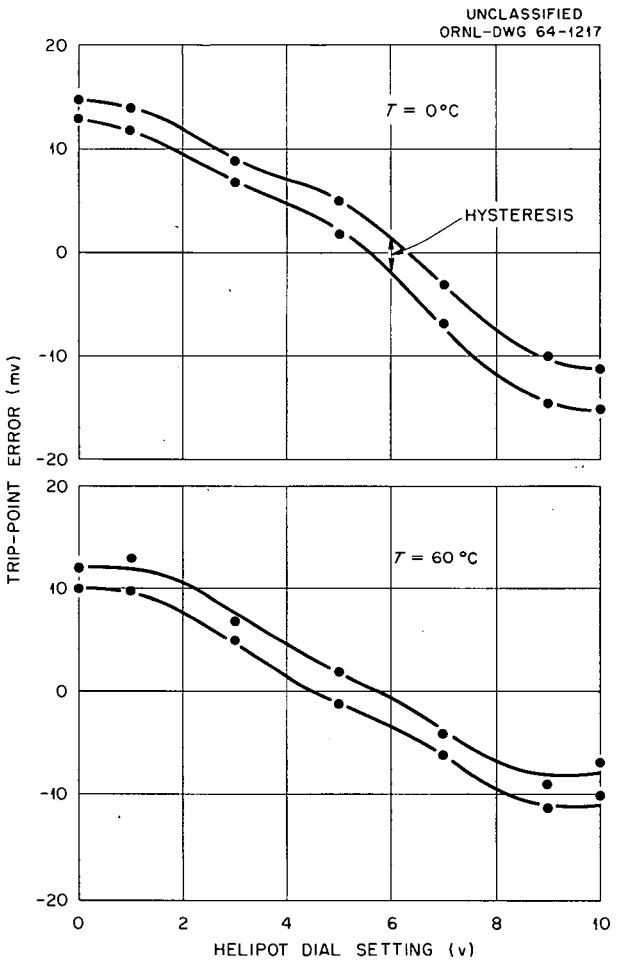

Fig. 9.3.2. Error as a Function of Helipot Dial Settings for Two Different Temperatures.

9.4 PROGRESS IN DEVELOPING A WIDE-RANGE COUNTING INSTRUMENT FOR REACTOR CONTROL

E. N. Fray J. T. DeLorenzo

A complete wide-range counting channel,[1] utilizing newly developed components, was installed in the ORR to establish the compatibility of channel components and to determine the channel performance (Fig. 9.4.1).

A component of particular interest is the function generator. Because neutron attenuation in the shielding medium about a reactor is a nonexponential function of position, the function generator is required to produce a signal at its output which is directly related to the position of the fission chamber and the neutron flux at that position. Fulfilling this requirement makes the output of the log count-rate meter and of the function generator at the input to the summing amplifier comparable; thus, the output of the summing amplifier is a direct measure of reactor power.

A three-part program was undertaken to evaluate the complete counting system. First, data were obtained from the ORR to program the function generator. Second, time constants for the log count-rate meter and the period amplifier were established to yield an optimum response time relative to a 20-sec reactor period against a tolerable level of statistical fluctuation. Finally, the values of the parameters governing the servo responses were established; namely, gain of the servo-amplifier and time constant of the linear count-rate meter. To determine the value of these two parameters, an analysis was made, based on the root-locus method.

A new set of modular components is being fabricated, and present plans call for the installation of a complete wide-range counting system

[1]R. E. Wintenberg and J. L. Anderson, *Trans. Am. Nucl. Soc.* 3(2), 454 (1960).

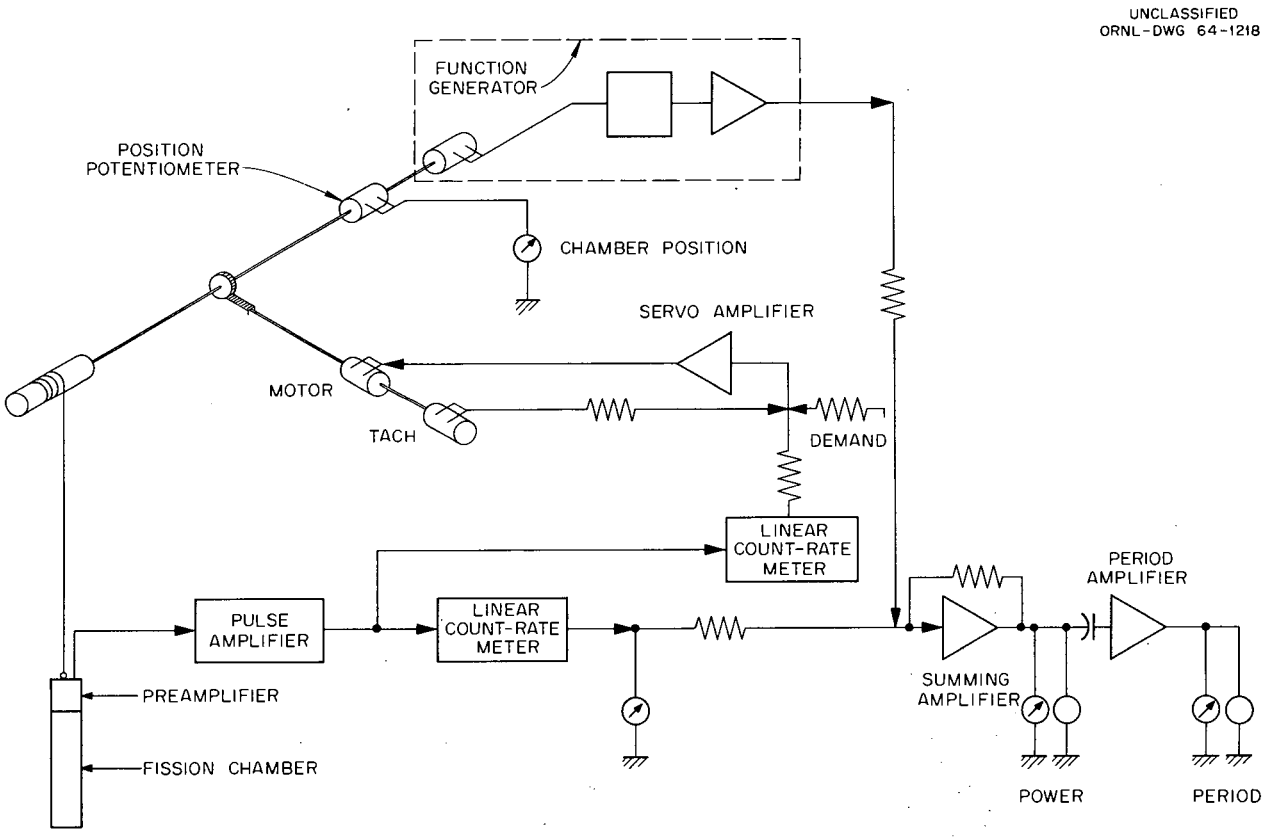

Fig. 9.4.1. Servo Fission Chamber.

in the Bulk Shielding Facility, using drive mechanisms designed for use in the MSRE and the HFIR.

Further experimental work is required to determine whether time constants of the log count-rate meter will give satisfactory transient performance while the instrument is behaving as a conventional (nonservo) log count-rate meter channel.

Reactor power and period were measured during several reactor startups, including a cold startup which required the instrument to work over a range of eight decades. In all cases, the instrument was capable of following normal reactor periods. At counting rates in excess of 10^3 counts/sec, it can follow a reactor period as short as 4 sec.

9.5 USE OF REACTOR GAMMA RADIATION AS A REACTOR CONTROL AND SAFETY PARAMETER[1,2]

D. P. Roux S. H. Hanauer

Although neutron flux is used universally as a parameter for reactor control and safety, the use of gamma radiation from the core can be advantageous. This is especially true when the region between the detector and the core attentuates neutrons much more strongly than gamma rays; the most common material having this characteristic is light water. This case could occur unexpectedly under accident conditions – for example, if water should leak into the interstices of a porous shield.

We report in this summary the results of several experiments with gamma-sensitive ionization chambers[3] in light-water reactor shields. Our object was to evaluate the advantages and limitations of using gamma-sensitive detectors for reactor control and safety.

The principal advantage to be gained by using gamma radiation is that the effects of changes in core and shield configurations are greatly reduced. This is because the high neutron attenuation of water restricts the effective volume through which a neutron detector "sees" the core to a relatively narrow region around the path of shortest length. A gamma-sensitive detector is not so restricted and, in general, has approximately equal effective sensitivity to gamma rays emitted anywhere in a rather large volume. We have observed in several configurations that this is indeed the case.

On the other hand, the use of gamma radiation for reactor control has two well-known potential limitations:

1. Approximately 25 to 30% of the gamma radiation from the core at full power originates in the radioactive decay of fission products; this gives rise to a signal that is not proportional to reactor power.

2. The gamma radiation at the detector has a component that originates in (n,γ) reactions. Those capture gamma rays formed away from the core are subject to perturbations of the neutron flux. To the extent that the detector response is due to such capture gamma rays, even a gamma detector will show effects of perturbations in neutron shielding.

A series of experiments was performed in the Bulk Shielding Reactor (BSR) pool to evaluate the two limitations. The fission product component of the chamber current was measured by scramming the reactor and observing the current decay. The chamber was located at distances between 30 and 100 cm from the core surface. In each case, after a small correction was made for aluminum activation in the chamber $(20 \pm 1)\%$ of the total current at steady reactor power was

---

[1]Abstract of published paper: *Trans. Am. Nucl. Soc.* **6**, 74 (1963).

[2]It is a pleasure to acknowledge the authors' indebtedness to J. C. Gundlach, whose early work with gamma-sensitive chambers preceded this investigation. We also wish to thank J. R. Tallackson and co-workers for permission to use their unpublished data, and C. B. Stokes and O. C. Cole for technical assistance.

[3]C. J. Borkowski *et al.*, *Instrumentation and Controls Div. Ann. Progr. Rept. Sept. 1, 1962*, ORNL-3378, pp. 68–70.

attributed to the fission product gamma rays; the decay curves agreed with the integrated data of Peelle *et al.*[4] and the data of Perkins and King[5] for gamma rays of approximately 2 to 4 Mev. Very little can be done with the shield energy-dependent attenuation to reduce further the component of ionization-chamber current due to the fission products, because in this energy range the spectra of prompt fission gamma rays and short-lived (<700 sec) fission products are so nearly the same.[6] In our configuration, this short-lived component comprised 80 to 90% of the total fission-product signal. The prompt fission gamma component was inferred from the short-lived fission-product component, using the ratio 7.2/5.5 (ref. 6). The reactor capture-gamma component was calculated using the compilation of Goldstein[7] and the composition[8] of the BSR core and reflector.

The effect of the neutron-to-gamma ratio was evaluated by inserting various thicknesses of lead between the core and the detector. These experiments in the BSR and an experiment in the Oak Ridge Research Reactor (ORR) indicate that if the thermal-neutron-to-gamma flux ratio exceeds 0.2 *nv* per photon/cm^2-sec anywhere along the path between the core and the detector, a significant component of the gamma radiation at the detector will originate in capture gamma rays produced far from the core. The most likely place for this large ratio to occur is in the water, just behind a heavy gamma shield.

Experiments with gamma-sensitive chambers during test reactor excursions at SPERT[9] were carried out with periods as short as 3 msec. As expected, the signal from the gamma chambers agreed with the reactor power as measured by neutron-sensitive instruments during these excursions. This demonstrates that gamma radiation is an adequate reactor safety parameter for the control of the short-period accidents.

The results of these experiments and several years' operating experience in the ORR lead to the conclusion that the use of gamma-sensitive detectors for reactor control and safety is feasible, and sometimes advantageous.

[4]R. W. Peelle *et al.*, "The Spectra of Gamma Rays Associated with Thermal Neutron Fission of U-235," pp. 273–97 in *Proc. Symp. Pile Neutron Research in Phys., Oct. 17–21, 1960, Vienna*, IAEA, Vienna, 1962.

[5]J. F. Perkins and R. W. King, *Nucl. Sci. Eng.* 3, 726–46 (1958).

[6]H. Goldstein, "Sources of Neutrons and Gamma Rays," pp. 27–32, *Reactor Handbook*, III, Part B (ed. by E. P. Blizard), Interscience, New York, 1962.

[7]*Ibid.*, pp. 44–62.

[8]R. G. Cochran *et al.*, "Reactivity Measurements with the Bulk Shielding Reactor," ORNL-1682 (1954).

[9]J. R. Tallackson *et al.*, unpublished data taken at SPERT.

9.6 A NEW CONFIGURATION FOR AN ELECTRICALLY ADJUSTABLE GAMMA-COMPENSATED IONIZATION CHAMBER

D. P. Roux

J. C. Gundlach[1] S. H. Hanauer C. B. Stokes

Suppression of the gamma-ray sensitivity of neutron-sensitive ionization chambers is often important in nuclear reactor instrumentation, because the gamma radiation is not always proportional to reactor power.

A gamma-compensated ionization chamber can be simply constructed by arranging the electrical connections so that alternate volumes as shown in Fig. 9.6.1 have positive and negative polarizing fields. By boron-coating only those surfaces in one (usually positive) set of these volumes, the output of the chamber is, in principle, proportional only to neutron flux, since the gamma currents from the alternate sections, assumed to be identical, cancel. Practically, this cancellation (compensation) is not exact, and either a certain error must be tolerated or a

[1]Present address: Reactor Controls Co., Oak Ridge, Tenn.

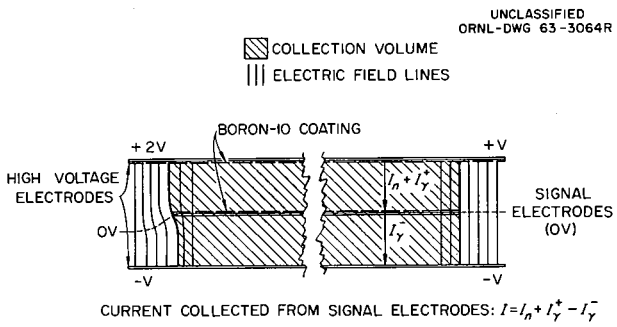

Fig. 9.6.1. Diagram of Adjustable Electrical Gamma Compensation.

means of adjustment of compensation must be provided. We report in this paper a parallel-plate configuration for which the adjustment of compensation can be accomplished electrically to avoid the disadvantages of fixed compensation.

The configuration for the chamber is shown schematically in Fig. 9.6.1. The signal electrodes are smaller than the high-voltage electrodes. For equal positive and negative polarizing potentials, the zero-equipotential surface (as shown on the right side of Fig. 9.6.1) is an extension of the signal electrode, and the electrical field lines are straight. For unequal polarizing potentials (as shown on the left side of Fig. 9.6.1), the field lines are distorted and the effective collection volumes, which are determined by the field lines drawn heavily in the figure, are changed accordingly. The saturation characteristics of the two situations are essentially the same; thus, adjustment of compensation by this method does not affect the saturation. In the present configuration, the compensation does not vary with flux intensity up to 100 μa gamma current, if the polarizing voltages are at least as large as 100 v.

The test chambers were designed and fabricated according to the foregoing concept, and employed a configuration previously reported.[2]

[2]S. H. Hanauer *et al.*, *Instrumentation and Controls Div. Ann. Progr. Rept. July 1, 1961*, ORNL-3191, p. 70.

The electrodes are made of nickel plates, 0.012 cm thick, spaced 0.1 cm apart. The chambers are filled with N_2 at 800 torrs. Their active sections contain 16 signal plates, 9 positive high-voltage plates, and 8 negative high-voltage plates. Without gamma compensation, the chamber sensitivities are 4.0×10^{-15} amp/*nv* and 1.3×10^{-12} amp-hr/r.

Manufacturing tolerances are such that initially the gamma currents cancel within 3%. Mechanical adjustment (slight bending of the signal electrodes) after assembly permits adjustment of compensation to better than ±1%. Figure 9.6.2 is a curve of gamma compensation as a function of electrode voltages. The slope of the curve corresponds to 1–3% compensation change per 100 v change in negative polarizing voltage, with the positive voltage equal to +300 v.

Experimental results show the insensitivity of the gamma compensation to wide variations in intensity, energy, and geometry of the gamma source (Table 9.6.1).

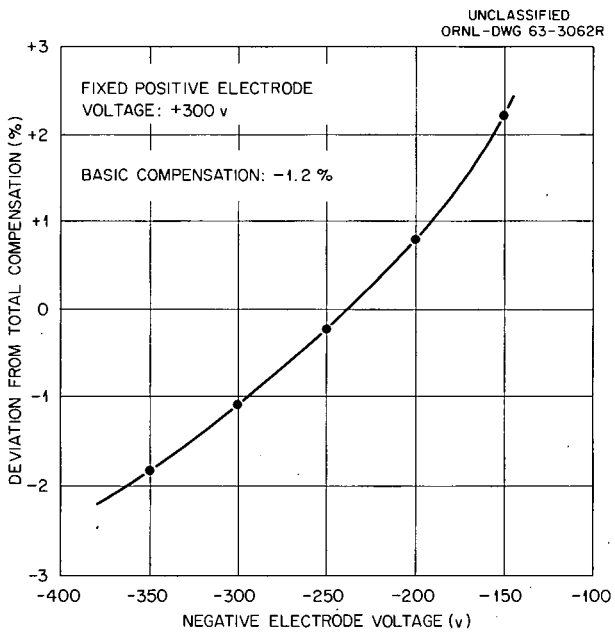

Fig. 9.6.2. Gamma Compensation as a Function of Electrode Voltages. Measurements made in a hot cell with a Co^{60} source.

Table 9.6.1. Gamma Compensation Obtained for Various Gamma Sources with Fixed Electrode Voltages (+300 v, −200 v)

Gamma Source Facility	Source Condition	Shield and Geometry	Deviation from Total Compensation[a] (%)
Hot cell, Co^{60}	2000 curies	10 cm air, source at front of chamber	+0.8
Hot cell, Co^{60}	2000 curies	10 cm air, source at side of chamber	+1.3
BSR,[b] fission products	10 min after reactor scram	20 cm of water	+0.9
BSR,[b] fission products	90 min after reactor scram	20 cm of water	+0.9
BSR,[b] fission products	1 week after reactor scram	20 cm of water	+0.6
BSR,[b] fission products	1 week after reactor scram	40 cm of water	+0.5

[a]The sign + means undercompensation; that is, $I_\gamma^+ > I_\gamma^-$ (see Fig. 9.6.2).
[b]Bulk Shielding Reactor.

9.7 A METHOD FOR MEASUREMENT OF NEGATIVE REACTIVITY BY ANALYSIS OF NEUTRON FLUCTUATION SPECTRAL DENSITY[1,2]

C. W. Ricker A. L. Colomb E. R. Mann

This describes a method that will, in principle, continuously measure the negative reactivity of a shutdown reactor. Instruments for this measurement have been built, and preliminary experimental investigations have been conducted with the Bulk Shielding Reactor (BSR) at ORNL.

The method makes use of the fact that negative reactivity can be determined by measuring the spectral density of the natural statistical fluctuations of the neutron population in a fixed-fuel subcritical reactor.[3–5] This can be done by measuring the ratio of the spectral densities in two fixed frequency intervals: $\Delta\omega_1$ about ω_1, and $\Delta\omega_2$ about ω_2.

If a point reactor model is assumed, the ratio R of two spectral densities as a function of reactivity ρ is (where all quantities are defined in ref. 6)

$$R = \frac{\left[\frac{\rho}{(1-\beta_e\rho)} + \frac{1}{(1-\beta_e\rho)}\sum_i \frac{\beta_i\omega_2^2/\beta}{(\omega_2^2+\lambda_1^2)}\right]^2 + \omega_2^2\left[\frac{\Lambda}{\beta_e} + \frac{1}{(1-\beta_e\rho)}\sum_i \frac{\beta_i\lambda_i/\beta}{(\omega_2^2+\lambda_1^2)}\right]^2}{\left[\frac{\rho}{(1-\beta_e\rho)} + \frac{1}{(1-\beta_e\rho)}\sum_i \frac{\beta_i\omega_1^2/\beta}{(\omega_1^2+\lambda_1^2)}\right]^2 + \omega_1^2\left[\frac{\Lambda}{\beta_e} + \frac{1}{(1-\beta_e\rho)}\sum_i \frac{\beta_i\lambda_i/\beta}{(\omega_1^2+\lambda_1^2)}\right]^2}, \quad (1)$$

[1]Abstract of published paper: *Trans. Am. Nucl. Soc.* **6**, 75–76 (1963).

[2]The authors gratefully acknowledge the assistance and cooperation of K. M. Henry and J. D. Kington for the calibration and operation of the BSR.

[3]P. R. Pluta, *An Analysis of Nuclear Reactor Fluctuations by Methods of Stochastic Processes, Ph.D.* thesis, University of Michigan, 1961.

[4]R. E. Uhrig, *Trans. Am. Nucl. Soc.* **4**, 85 (1961).

[5]R. W. Badgley, *Power Spectral Density of the University of Florida Training Reactor Operating in the Subcritical Region*, Master's thesis, University of Florida, 1962.

[6]A. F. Henry, *Nucl. Sci. Eng.* **3**, 52–70 (1958).

A better insight as to the relationship of R and ρ can be acquired by considering an example where the frequencies are greater than 1 cps and $\beta_e \rho << 1$. The reactivity can be expressed as a function of the spectral-density ratio by the approximate relation

$$\rho \cong 1 - \frac{\Lambda}{\beta_e} \sqrt{\frac{(\omega_2^2 - R\omega_1^2)}{(R-1)}} \, . \qquad (2)$$

Since the effective fraction of delayed neutrons β_e does not change appreciably with ρ, and since the neutron generation time Λ, to a good approximation, is constant for a subcritical system,[6] a suitable choice of ω_1 and ω_2 will yield a spectral-density ratio which is a sensitive measure of ρ. Optimum sensitivity can be obtained by selecting ω_1 as near as possible to the low-frequency cutoff of the instrumentation and ω_2 as close as possible to the high-frequency limit imposed by detector and amplifier noise.

This measurement of spectral-density ratio is made without perturbing the reactor and, therefore, offers a means for continuously monitoring shutdown margins. A monitor would include two fixed-frequency filters and a device for calculating the ratio of the spectral densities in the selected frequency intervals.

To determine the feasibility of measuring negative reactivity by this method, a preliminary experiment was performed with the BSR loaded with cold, clean fuel. Spectral densities were determined by filtering, squaring, and time averaging the amplified signal from a neutron-sensitive ionization chamber placed near the core. Operational amplifiers with twin-T networks in their feedback loops were used as filters. Reactivities were determined by comparing the measured values of R with those calculated using Eq. (1).

The experimental results agreed well with independent measurements[7] of negative reactivity performed with distributed poison (Table 9.7.1). The values for the spectral-density method are the averages of nine frequency ratios measured with different values of ω_1 and ω_2 in the range 6 to 100 cps.

Even though the instrumentation was not specifically designed for this type of measurement, 80% of the data points were within ±30% of the measurements made by the distributed-poison method. Because of the limitations resulting from instrument noise, the largest value of negative reactivity measured was approximately 1 dollar.

Simple theory indicates that the spectral density in the 100-cps channel at -5β will be about one-eighth of the spectral density at -1β. It therefore appears that increasing the detection efficiency and decreasing the noise contribution from the detector and amplifiers will permit measurement of -5β. This is not inconsistent with present technology. Now under development is specialized instrumentation that should extend the range of measurable reactivity to at least -5β without sacrificing the simplicity of either the instrumentation or the measuring technique.

Economical and safe operation of power reactors may require continuous knowledge of negative reactivity, particularly for reactors having small shutdown margins. There is considerable motivation to develop a shutdown monitor for these reactors, and the method discussed here is believed to hold considerable promise.

Table 9.7.1. Experimental Results of Measurement of Negative Reactivity (BSR)

Measurement Method	Reactivity (dollars)		
Spectral-density analysis	−0.27	−0.66	−1.1
Distributed poison	−0.28	−0.66	−0.99

[7] K. M. Henry and J. D. Kington, private communication.

9.8 LOW-NOISE SOLID-STATE DIFFERENTIAL AMPLIFIER

F. M. Glass[1]

A low-noise solid-state differential amplifier (ORNL model Q-2591) was developed to achieve long-term gain stability, a gain of 10,000, and a flat response within 1 db from 0.1 to 1000 cps. Such an instrument was needed to preamplify signals from an ion chamber and drive a multichannel spectrum analyzer for study of reactor noise (Sect. 9.7).

The amplifier has field-effect silicon planar transistors in the first two stages, an output-level meter, an overload indicator, and a built-in picoammeter for measuring the dc ion current.

Performance tests of the amplifier show a maximum gain of 10,000, with 3.5 decades of continuous control. The broad-band frequency response is flat within 0.5 db from 0.1 to 1000 cps. High- and low-pass filters, 12 db/octave, provide 6-db roll-off frequencies (all given in cycles per second) of 0.013, 0.13, 1.3, and 13 (high-pass filter), and 35, 350, and 3500 (low-pass filter). The gain is stable within ±0.1% for 60 hr. With the input shorted the equivalent noise referred to the input from 6 cps and greater is 33,000 ohms. The flicker noise in a bandwidth of 0.013 to 12 cps is 1.8 μv (rms), referred to the input. Common-mode rejection is 50 db. Input impedances of 2, 20, and 200 kilohms are provided by a 1-megohm resistor with current shunts.

The output impedance is 10 ohms. The turn-on ringing time is 3 min. Sixteen ranges of the picoammeter cover the current range of 1×10^{-12} to 3×10^{-7} amp. Circuit linearity of the picoammeter is 0.5%, and the zero drift is less than 1% per 24 hr after 10 min of warmup time.

[1]The excellent work of W. H. Williams in laying out and constructing this instrument is gratefully acknowledged.

9.9 DESIGN OF MSRE AUTOMATIC ROD CONTROLLER

E. N. Fray

S. J. Ditto D. N. Fry

The startup and low-power operation of the MSRE is based solely on neutron flux considerations; however, at power levels about 1 Mw and greater, heat generation and its removal from the reactor become prime considerations. In order to permit orderly operation of the reactor in both these ranges, while reducing the number of operator manipulations required to a tractable few, an automatic rod controller has been developed, based on two separate modes of operation. The first, called the flux mode, utilizes a conventional wide-range flux controller and is used to control neutron level in startup and low-power operation up to about 1 Mw. In this mode of operation the load must be adjusted by the operator to obtain steady-state temperature conditions, although a slight mismatch between the reactor power and load setting results in only a slow change in system temperature. The second, called the temperature mode, is used for automatically controlling the reactor power level as required to maintain the fuel outlet temperature at a set point selected by the operator over a range from 1 to 10 Mw. The rod controller complex, by sensing the temperature of the fuel salt entering the core and the fuel-salt outlet temperature set point, adjusts the reactor power automatically. Thus, the reactor power is slave to an externally applied load, while the fuel outlet temperature is maintained at the desired set point.

Because the novel features of the automatic rod controller are associated with the temperature

mode, only this aspect of the controller is described. The MSRE reactor system possesses a large heat capacity as well as large thermal time lags associated with the temperature measurements. Consequently, the direct use of temperature signals to control rod motion can create a stability problem in reactor control. For this reason, the automatic rod controller is designed to respond to the difference in neutron flux as measured by an ion chamber and a flux set point determined from temperature information. The control scheme, in the temperature mode, is based on the one-to-one correspondence between reactor power generation and fuel-salt core differential temperature in steady state at the fixed fuel-salt flow. To compute the flux necessary to operate at the selected outlet temperature, the reactor inlet temperature is measured and compared with the outlet temperature set point. The computed flux becomes the set point for the controller. Possible calibration errors between flux instruments and temperature instruments, long-term drifts, and possible long-term flow changes, make it necessary to provide a reset mechanism so that the steady-state outlet temperature will, in fact, become equal to the set point. This reset is accomplished by continuously comparing measured fuel-salt differential temperature with measured flux and slowly resetting the inlet temperature until the corrected differential temperature agrees with the measured flux. This corrected inlet temperature is used in the generation of the flux set point described above.

The ORNL analog computer facility was used to simulate the MSRE to establish the feasibility of the proposed scheme. A real-time simulation of the reactor was used so that the controller, using actual system components where possible, could be used in the study. Response characteristics of the rod-drive system and associated switchgear were estimated.

Results of the simulation indicate that the outlet temperature can be controlled within ±1°F at a normal operating temperature of 1225°F during normal load changes, with only a few degrees variation for severe load transients, such as scramming radiator doors. Thermal capacity of the fuel and an upper flux limit built into the controller limit the rate at which the outlet temperature can be increased at full load to about 5°F/min. However, the rate of the set-point increase will be limited to about 3°F/min, at which rate the controller can maintain the outlet temperature at the set point under all load conditions from 1 to 10 Mw.

9.10 MECHANICAL DRIVE FOR POSITIONING A FISSION CHAMBER IN THE MSRE

G. W. Allin H. J. Stripling, Jr.

A mechanical fission-chamber drive (Fig. 9.10.1) was developed for the Molten-Salt Reactor Experiment to provide continuous indication of neutron flux and pile period from source level to full power with a single detector.[1] In previous reactor startup procedures, the fission chamber is manually repositioned when the upper counting limit of the log count-rate meter is reached. The flux-level channel and the period channel are disabled while the chamber is being moved and for some time afterward, because the count-rate meter has a long recovery time constant. With the mechanical drive, movement of the fission chamber will be continuous and automatic.

One drive was operated at full speed and full stroke for 5400 cycles under simulated operating conditions (except for neutron flux). The drive was also operated for approximately 1300 hr in a continuously reversing mode; a random signal from a noise generator was used to simulate the statistical variation in the output of the linear count-rate meter under the same environmental

[1] J. L. Anderson and R. E. Wintenberg, *Instrumentation and Controls Div. Ann. Progr. Rept. July 1, 1959*, ORNL-2787, p. 145.

conditions. The results of these tests were within design specifications. The mechanical drive and fission chamber will be tested in a neutron flux, and the actual signal from the fission chamber will be used as the input to the linear count-rate meter.

Except for the motor-drive assembly and the position-sensing components, all parts will operate in an instrument penetration tube which is inclined approximately 45° from horizontal and is filled with water containing 2000 ppm of sodium nitrite corrosion inhibitor. The drive is servo-operated and can move the fission chamber at a rate of up to 72 in./min. A stroke of 90 in. will provide approximately ten decades of power-level indication.

A ball-bearing lead screw, turning at speeds up to 288 rpm, provides the rotational-to-linear motion conversion with an efficiency of approxi-

UNCLASSIFIED
ORNL-DWG 64-1219

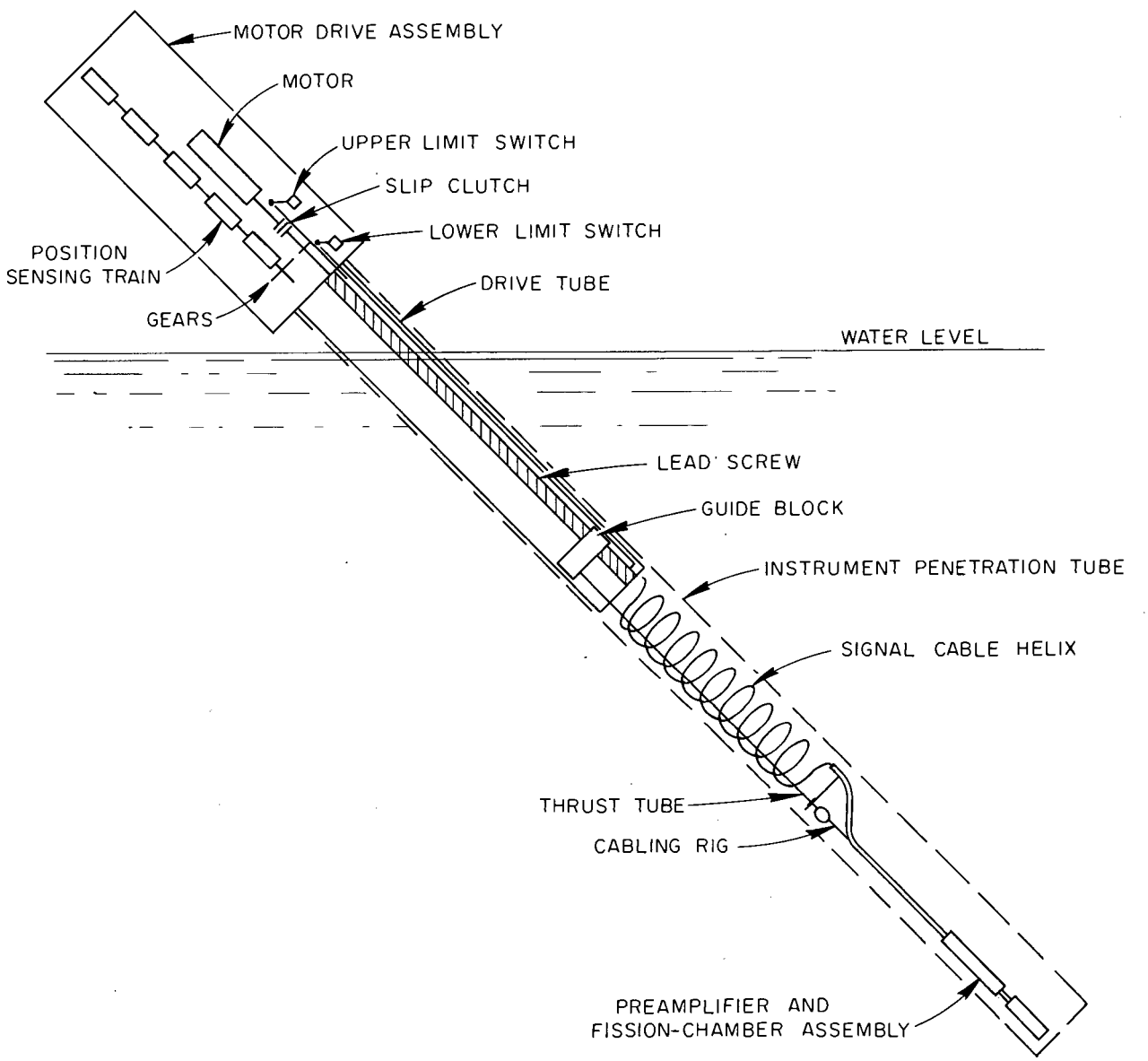

Fig. 9.10.1. Mechanical Drive for Positioning a Fission Chamber.

mately 90%. A calcium-complex-base grease is used as lubricant for the lead screw, because it is water resistant and compatible with the corrosion inhibitor being used. The lead-screw nut is attached to a guide block which rides on nylon runners between two aluminum guide rails. These rails are mounted within a $3\frac{3}{4}$-in.-OD stainless steel drive tube.

A thrust tube connects the guide block to the cabling rig, which is attached to the preamplifier and fission-chamber assembly. The fission-chamber signal cable, which is protected from the water by a sheath of Tygon tubing, and music wire are coiled together to form a helix and are held together by nylon spiral wrapping to form a spring-loaded coiled cord. This helix provides cable take-up and is coiled loosely around the thrust tube between the cabling rig and the lower end of the drive tube. The cabling rig rides on nylon rollers inside the 4-in.-ID instrument penetration tube. (The penetration tube is not a part of the positioner assembly.)

The direct-current drive motor with an integral gear reducer and a tachometer is protected from torque overloads by a disk-type slip clutch. The position-sensing components are connected directly to the lead-screw shaft ahead of the slip clutch by a pair of precision gears.

The position-sensing train contains a ten-turn position-sensing potentiometer driven through a 48:1 gear reducer. This reducer drives a 10:1 gear reducer which is connected to a one-turn logger input potentiometer. On the same shaft is a synchro transmitter for driving a position indicator on the console.

Upper and lower limit switches are tripped by rods that are actuated by the guide block at each end of its travel. These rods are spring loaded and are held captive in grooves between the guide rails and the drive tube. This configuration accommodates mounting the limit switches in the motor drive assembly, where they are readily accessible.

PROCESS INSTRUMENTATION

9.11 MSRE PROCESS INSTRUMENT DEVELOPMENT

R. L. Moore

G. H. Burger D. G. Davis J. W. Krewson

Special instrument components and systems reported previously were tested and redesigned as necessary.

Pump-Bowl Level Indicator

Testing of the ball-float-type molten-salt level transmitter[1] was continued. Two prototype transmitters were tested for more than 18 months above 1200°F without failure or degradation of the performance characteristics. A third transmitter of a similar design but with an INOR-8 metallic ball float instead of a graphite float was fabricated and installed in the molten-salt pump-test facility. The transmitter will be tested under dynamic conditions which are anticipated in the MSRE reactor system. Although the ball-float transmitter was accepted for use on the MSRE coolant pump, it will not be installed on the fuel pump unless serious difficulties are experienced with the bubbler level system during precritical operation of the reactor.

[1] J. W. Krewson and R. L. Moore, *Instrumentation and Controls Div. Ann. Progr. Rept. Sept. 1, 1962*, ORNL-3378, p. 59.

Single-Point Molten-Salt Level Indicator

A prototype two-level conductivity-type molten-salt level probe,[2] which will be used to detect molten-salt level in the MSRE drain tanks, was operated successfully for approximately 1 yr. Usable signals were obtained with excitation currents as high as 20 amp at 1 kc and as low as 0.1 amp at 1 kc. (Higher excitation currents are feasible if excitation lead resistance is low and sufficient power is available.) The signal amplitude generated when the salt contacted the probe was approximately 50 mv with an excitation current of 20 amp and varied directly with the excitation current strength. The signal-to-noise ratio was greater than 3 to 1. Attempts to improve this ratio were unsuccessful; however, the 3-to-1 ratio will probably be adequate for dependable operation. Although the signal level has drifted over a period of time, the drift is not objectionable because the output is basically "on-off."

Final testing of the level indicator will be done in the reactor system during precritical operation, because the probe signal is inherently a function of the configuration of the vessel in which it is installed.

Temperature Scanner

The temperature scanner system described previously[3] was tested on a molten-salt test loop to determine the performance and the long-term reliability of the system at operating conditions. Testing was started in August 1962, and during approximately 3000 hr of continuous operation, performance was satisfactory. After 3000 hr, the system developed excessive noise pulses. Examination of the commutator in the mercury switch revealed mercury oxidation and a bad bearing in the lower deck of the switch. The upper deck was in good condition. After the switch was cleaned, repaired, and modified to obtain better nitrogen purge of the lower deck, testing was resumed. Shortly after the start of the second test the top bearing became noisy, and the test was interrupted to permit replacement of the bearing. Testing was again resumed, and an additional two months of satisfactory operation was accumulated before testing was terminated.

The scanner system with five 99-point scanner channels was accepted for use on the MSRE, and design of the MSRE installation was completed. To meet operations requirements during various phases of reactor operations, the design will permit thermocouple signals to be removed from service or moved, either individually or in groups of 25, to other scanner channels. To minimize downtime, all major components, including the mercury switch commutators, utilize plug-in construction and are easily replaceable.

Closed-Circuit Television

The feasibility of viewing remote maintenance operations at the MSRE with a closed-circuit television system was investigated. The methods investigated included single-channel and two-channel stereo (three-dimensional) viewing and multichannel (one-dimensional) viewing which uses two or more cameras to view the subject from different angles.

For testing, both types of stereo systems were installed in a remote maintenance test facility, and operation of a multichannel one-dimensional system was observed at the Santo Susano site of Atomics International. Evaluation is continuing. Final choice of the system to be used at the MSRE will be based on results of these tests and on the requirements of remote maintenance operations.

---

[2] J. W. Krewson and R. L. Moore, *Instrumentation and Controls Div. Ann. Progr. Rept. Sept. 1, 1962*, ORNL-3378, p. 54.

[3] G. H. Burger *et al.*, *Instrumentation and Controls Div. Ann. Progr. Rept. Sept. 1, 1962*, ORNL-3378, p. 57.

9.12 PBRE BALL COUNTER

H. D. Wills

Because safe operation of the Pebble-Bed Reactor Experiment (PBRE) required that the location of the uranium-graphite balls within the reactor system be known, a device was developed to detect and count the flow of the balls as they passed through a stainless steel pipe. Since the detector did not penetrate the pipe, it did not obstruct the flow of the balls. Also, it had no moving parts. Although the counter operated successfully, if the PBRE program is reactivated, further development work will be required to make the counter a reactor-grade instrument.

The instrumentation system (Fig. 9.12.1) consisted of a differential transformer wound on the outside of the pipe, an oscillator, a demodulator, an amplifier, and an electronic counter. The differential transformer consisted of two 150-turn secondary windings wound on the pipe and connected differentially, and a 300-turn primary wound over the secondary. The primary was excited with an 8-kc sine wave. As a graphite ball passed through the detector, a wave was produced at the output of the demodulator because of the change in the effective permeability of the differential transformer. The period of this wave was equal to the time required for the ball to pass through the detector. The amplifier and the counter were adjusted to count the positive half of this wave.

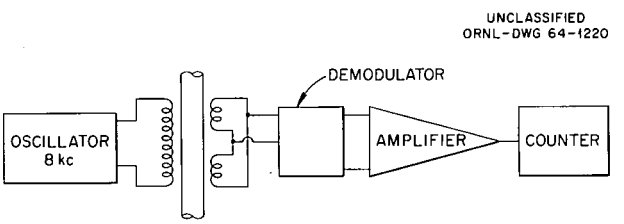

Fig. 9.12.1. Instrumentation for Counting Uranium-Graphite Balls in the Pebble-Bed Reactor Experiment.

9.13 WATER FLOWMETER

J. H. Todd E. E. Waugh

A flowmeter (ORNL model Q-2587) was designed to measure water flow rates through the seat switches and clutch assemblies and the total flow rate of water through the Tower Shielding Reactor II (TSR-II). Each module visually displays the flow rate and has pointers for setting the high and low flow-rate limits. When either the high or low flow-rate set point is reached, alarm relays are actuated. The contacts of these relays are incorporated into the reactor control interlock system and into the "scram" system.

The flowmeter consists of four main components (Fig. 9.13.1). A transducer, consisting of a small turbine rotating in close proximity to a magnetic pickup, produces output pulses which are proportional to the flow rate. Two different transducers are used. One transducer, at a maximum flow rate of 0.53 gpm, produces an output frequency of 500 cps. A similar transducer, at a maximum flow rate of 9 gpm, produces an output frequency of 290 cps.

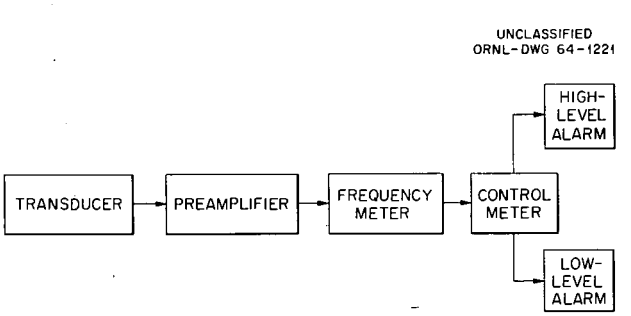

Fig. 9.13.1. Diagram of Water Flowmeter.

The output signal from each transducer is preamplified before transmission over several hundred feet of cable. The preamplifier increases the amplitude of the transducer output signal from a few millivolts to a level where the effect of noise is negligible.

The amplified signal is converted by a digital-to-analog converter, a duty-cycle frequency meter which is adjustable over the range of the transducers used, and is visually displayed by a control meter.

COMPONENTS AND MATERIALS

9.14 TESTS OF STRAIN-GAGE PRESSURE TRANSDUCERS ON IN-PILE EXPERIMENTS

T. L. McLean

Measurement of pressure developed in in-pile experiments has not been successfully accomplished, because the materials and components of pressure-sensitive devices previously employed in this service have not withstood damage from the intense radiation. To determine whether strain-gage pressure transducers will offer a practical means of making such measurements, several transducers were installed in three in-pile experiments for tests under operating conditions.

Two transducers, fabricated by Consolidated Electrodynamics Corporation, were installed at the ORR Poolside Facility[1] to measure the gaseous fission-product pressure buildup inside fuel cans located in a neutron-gamma field of approximately 1×10^9 *nvt*. Each transducer was neutron shielded with a $\frac{1}{4}$-in.-thick enclosure of cadmium. After two weeks of reliable operation, the transducers began to show erratic behavior. Examination of the assemblies in a hot cell revealed that the capillary tubing connecting the transducers to the fuel cans had cracked in two places.

In installations of this type the transducer must be carefully calibrated with its associated "L2 circuit" Brown recorder before it is attached to the capsule, because once installed, it is impossible to check either the zero or the span.

Standard off-the-shelf transducers were tested in two other experiments where the radiation level was between 200 and 300 r/hr. Four transducers, all of one brand, were installed at the MTR molten-salt experiment,[2] and two of another brand were installed at the GC-ORR loop No. 1.[3] Before being installed, each unit was calibrated in the laboratory with the required length of lead wire and under the same physical stress the unit was to receive at the experiment. At the MTR experiment, both the zero and the span could be checked in place, but at GC-ORR loop No. 1, only the zero could be checked. All six transducers maintained a precision of ±0.1 psi in the range of 0 to 15 psi after several months' exposure.

---

[1] D. B. Trauger and O. Sisman, *Gas Cooled Reactor Program Semiann. Progr. Rept. Sept. 30, 1962*, ORNL-3372, pp. 95–108.

[2] *Molten-Salt Reactor Program Semiann. Progr. Rept. Jan. 31, 1963*, ORNL-3149, pp. 94–107.

[3] D. B. Trauger and O. Sisman, *Gas Cooled Reactor Program Semiann. Rept. Sept. 30, 1963* (to be published).

9.15 DEVELOPMENT AND TESTING OF THERMOCOUPLE MATERIALS

N. H. Briggs

G. W. Greene E. G. Meyer R. R. Sellers[1]

The measurement of temperature is required in almost all experiments conducted at this Laboratory; and particularly in irradiation experiments, the temperatures to be measured are becoming increasingly higher – almost to the melting point of refractory metals. To provide a wide range of thermocouples that will meet the requirements of the many experimental programs at the Laboratory, the properties of many combinations of thermocouple wires, insulation, and sheathing at high temperatures and in varied atmospheres, both with irradiation and nonirradiation, are being investigated.

Several specifications were written and issued for the purchase of thermocouples for ORNL Stores and for in-pile experiments. These specifications covered bare wires, glass-fiber-insulated wires, and metallic-sheathed thermocouples. The common types of thermocouples were specified: platinum–10% rhodium vs platinum, Chromel-P–Alumel, iron-constantan, and copper-constantan. After having been purchased, these materials are tested to determine their conformance to the specifications (Sect. 7.10).

To determine the stability of thermocouples and other temperature sensors under various conditions of temperature (up to 4700°F) and atmosphere (argon, helium, and vacuum), two high-temperature furnaces are being installed and tested. In one furnace, a tungsten tube is the resistance heating element. The other furnace is an induction-heated furnace. The tungsten-tube furnace was tested up to 4700°F. Because the heating element tends to burn out, this furnace is limited to several hundred hours of continuous operation.

Chromel-P–Alumel thermocouples in a metallic, 0.031-in.-OD sheath were tested at a constant temperature of 1950°F in a helium atmosphere to determine their calibration drift over a long time at these conditions. Preliminary results after 1000 hr of heating show that thermocouples which had been heated at 1000°F for 24 hr prior to the extended test at the higher temperature produce less drift and much less scatter of the data points than thermocouples which had not been heat treated. The total drift for all thermocouples ranged from –100 to –150°F.

In power reactors, such as the EGCR, materials and components are selected to have a useful life for as much as 20 yr. One way to achieve temperature measurement under this condition with thermocouples is to design for replacement of the thermocouples when necessary. This will require installing tubing with a thermocouple well attached at the point of measurement. Whenever a thermocouple fails it can be withdrawn from the tubing and a new thermocouple inserted and pushed through the tubing to the point of measurement. This technique was tested on mockups to determine the force required to push the thermocouple through a 65-ft length of tubing with bends of various radii. The tubing was $\frac{1}{4}$-in. OD (0.152 in. ID) with a 0.049-in.-thick wall. The thermocouple was stainless steel sheathed, 0.063 in. OD. The tests were made at room temperature, and the tubing and sheath were cleaned prior to the tests.

In the first test, in which the tubing was bent in a configuration similar to permanently installed thermocouples in the EGCR, and with bends of $2\frac{1}{2}$-in. radii, the thermocouple could not be pushed through the tubing by a mechanical pushing device, which automatically measured the force being applied to the thermocouple. The test failed. The force required was in excess of the maximum force, 50 lb, available from the pusher. The second test, in which all radii of bends were 4 to 6 in., also failed. In a third test, in which all bends were 12 in. except for two bends of 4 in. and $4\frac{1}{2}$ in., the thermocouple was inserted successfully, with 20 to 30 lb of force required for the last few feet. (This force is considered to be excessive for the application.) It was concluded that this technique of thermocouple replacement could be applied to reactor design; however, the tubing runs require careful layout with very gentle bends throughout the entire length of tubing.

The performance of thermocouples under nuclear irradiation will be studied during the next year. A capsule, designed for insertion in the ORR, will

[1]Formerly with ORNL Reactor Division.

allow irradiation of up to 26 individual thermocouple wires at a constant temperature of 570°F. The capsule contains a 1-kw molybdenum-wound heater and a reentry tube for a standard thermocouple, which will be used to calibrate the test thermocouples at periodic intervals. All calibrations will be done with the capsule removed from the reactor. The planned total thermal neutron dose is 1.8×10^{21} *nvt*. A mockup of the capsule was built to test the heater concept. Satisfactory performance to 1500°F was obtained, and further testing is planned to 2500°F.

9.16 POTTED HERMETIC SEAL FOR SHEATHED THERMOCOUPLES

T. L. McLean

When a sheathed thermocouple is installed in reactor fuel cladding, a hermetic seal must be provided at the junction of the thermocouple and the extension wires to prevent fission products from diffusing out of the end of the thermocouple assembly. Previously, such seals were made with a special Conax fitting, which compressed a rubber plug between the sheath and wires. These units were difficult to assemble, expensive, and not as reliable as desired. A potted connector was developed which is smaller, less expensive, easier to assemble, and more reliable. The connector is $\frac{3}{4}$ in. long by $\frac{1}{4}$ in. in diameter. The wire-to-wire resistance of connectors made in this manner has always measured greater than 500 megohms. The connectors also form a helium-tight seal with the sheath.

Assembly of a connector is begun by clamping the sheathed thermocouple and two extension wires in place for welding. The fiber-glass-insulated extension wires are welded to the 0.01-in.-diam thermocouple lead wires with a resistance welder. A small ceramic insulator is placed at the end of the sheath to keep the wires separated. Clear epoxy is poured over the connection into a removable mold made from plastic tubing and two rubber washers.

10. Support for the High-Voltage Accelerator Program

10.1 SECOND-STAGE PULSE COUNTDOWN SYSTEM FOR THE ORNL 3-Mv VAN DE GRAAFF

R. F. King

The terminal beam pulser for the ORNL 3-Mv Van de Graaff delivers short-duration bursts of ions to the accelerator tube at a repetition rate of 10^6 pulses/sec.[1] The optimum repetition rate varies widely from one experiment to another. In general, it is difficult to produce beam pulsing equipment which can supply a wide range of repetition rates in the Van de Graaff terminal; for example, consider the beam-pulse diverter or countdown system external to the accelerator described in a previous report.[2] With that system, the accelerated beam pulses, or bursts of ions, were directed between a pair of deflector plates. A sine wave of 3500 v peak amplitude and an rf frequency of either 500, 250, or 125 kc was applied to one plate of the pair. This plate was biased with a dc voltage just equal to the peak value of the rf voltage. The other plate operated at rf ground with a small adjustable dc bias.

To establish the frequency of this beam deflection voltage as an exact submultiple of the nominal 1-Mc frequency of the master oscillator in the Van de Graaff terminal (and, therefore, of the repetition rate of the ion-beam bursts emerging from the accelerator), a signal from the master oscillator was picked up with a tuned ferrite-core antenna at ground potential mounted inside the Van de Graaff tank. After amplifying this signal and passing it through either one, two, or three frequency-divider stages and an adjustable 0–360° phase shifter, the 500-, 250-, or 125-kc frequencies were obtained. By manipulating the phase control, the peak of the rf deflecting voltage could be made to occur in time coincidence with the passage of a beam pulse through the deflector plates. The particular pulse in the deflector plates at time coincidence was passed through undeflected. All subsequent pulses in the train were deflected off target until the deflection voltage completed one full cycle. The process was then repeated. Sine-wave deflection voltages were chosen for this system, because the magnitude and the rate of change of voltage required, coupled with the approximately 40-$\mu\mu$f capacity of the deflector plates, precluded using rectangularly shaped gating voltages. With sine-wave voltages, a limiting factor of about 8 between the repetition rate of the beam pulses and the repetition rate of the deflection voltage could be used without requiring excessively large deflection voltages.

Because beam-pulse repetition rates lower than 125 kc are necessary for some experiments, a second stage of beam pulse countdown was built to work in conjunction with the first stage and to share the same deflector plates (Fig. 10.1.1). Since this second stage had only to discriminate between beam pulses already separated by 8 μsec, it became possible to use rectangularly shaped gating voltages effectively.

The second-stage pulse countdown system takes a signal from the 125-kc frequency already generated and divides it further by a factor of 4 to 31.25 kc. A pulse shaper and power amplifier produces a rectangular output voltage pulse, having approximately a 2-μsec rise time, a 3-μsec duration, a 2-μsec fall time, and a 1600-v amplitude. This voltage pulse is applied to the beam deflector plate that originally carried dc bias voltage only. The bias is so arranged that the

[1] J. W. Johnson *et al.*, *Instrumentation and Controls Div. Ann. Progr. Rept. July 1, 1961*, ORNL-3191, p. 91.

[2] R. F. King and W. H. duPreez, *Instrumentation and Controls Div. Ann. Progr. Rept. Sept. 1, 1962*, ORNL-3378, p. 85.

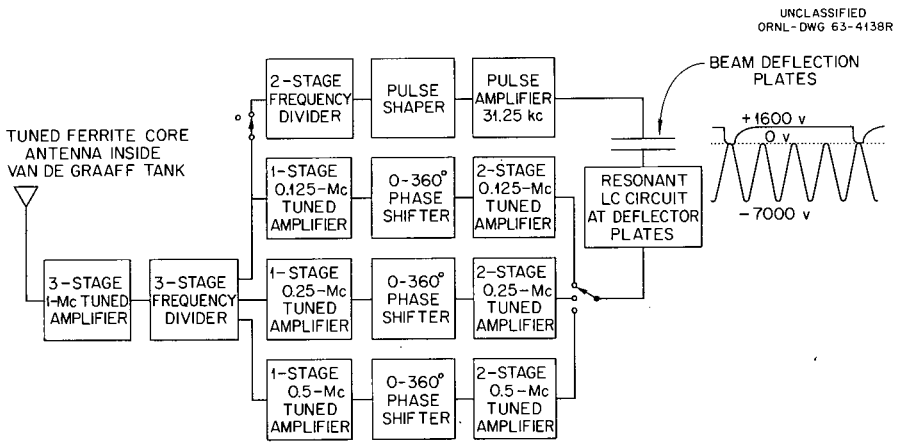

Fig. 10.1.1. Pulse Countdown System for Pulsed Van de Graaff.

3-μsec duration part of the voltage pulse coincides with zero voltage to ground. When both systems are operating, the result is that one beam pulse emerging from the accelerator is passed undeflected to the target and the following 31 pulses are diverted. If further reduction of repetition rate is required, only the number of frequency-divider stages in the second countdown system need be changed. No lower limit of repetition rate is imposed.

10.2 IMPROVED KLYSTRON BUNCHER FOR THE ORNL 3-Mv VAN DE GRAAFF

J. P. Judish R. F. King

The power amplifier for the preacceleration klystron ion-beam buncher for the 3-Mv Van de Graaff[1] was redesigned and increased in power. It is now capable of injecting the optimum bunching energy into the beam pulse at machine energies up to 2.1 Mv. The new amplifier operates at the same frequency (27 Mc) as the previous amplifier, but with a power input up to about 325 w. Most of this power is dissipated via loss mechanisms in the critically coupled LC circuit which contains the buncher electrode. Sine-wave voltages up to approximately 12 kv rms can be applied to the buncher electrode.

Klystron bunching decreases pulse duration, but increases beam-energy spread. Measurements of the width of the $C^{13}(p,\gamma)N^{14}$ resonance, which occurs at 1.747 Mv, showed an energy spread of about 0.5 kv in the 1-Mc pulsed, unbunched beam. After imposing optimum bunching, the energy spread increased to about 2.7 kv. With the buncher, the burst duration is reduced from 10×10^{-9} to 1.3×10^{-9} sec or less. At present, the measuring system is incapable of measuring beam pulse durations of less than about 1.3×10^{-9} sec.

[1]R. F. King *et al.*, *Instrumentation and Controls Div. Ann. Progr. Rept. Sept. 1, 1962*, ORNL-3378, p. 84.

10.3 TANDEM VAN DE GRAAFF MODIFICATIONS

G. F. Wells C. D. Moak[1]

A new accelerator tube was installed in the low-energy section of the Tandem accelerator because of interplanar insulation failure of the original tube. This failure, caused by planar arc-over within the tube section, was attributed to operations with O^- beam injection. Two beams of O^- at slightly different energies are produced by the duoplasmatron source. When one beam was properly injected into the accelerator, the other impinged on various planes in the low-energy section, causing local outgassing and secondary electron emission – two good conditions for inducing interplanar tube sparking. In the installation of the new tube, adjustable defining slits were placed at the entrance to the accelerator to exclude unwanted beams.

The design of the new accelerator tube incorporates the alternating inclined-field-gradient principle. When alternate groups of planes are inclined at a slight angle to the beam trajectory, a small force is generated perpendicular to the beam path. The direction of the force changes with alternate groups of planes and causes secondary electrons to be collected on the planes before the electrons are appreciably accelerated; the effect of this plane inclination in deflecting the ion beam is negligible. The resulting improvement in overall machine performance is due to a reduction in the x-ray background produced by stopping high-energy electrons at the accelerator terminal.

When the tube was replaced, two product-52 analyzing magnets were also installed: a main analyzer magnet immediately following the accelerator, and a 90° deflecting magnet in the experimental area below the accelerator. Power for these magnets is provided by new 7-kw solid-state power supplies with current regulation of 0.01%. These magnets have extended the useful range of energies obtainable in analyzed beams from the accelerator.

Allowable maximum terminal voltages were increased by using SF_6 gas (10 vol %) mixed with the normal N_2-CO_2 tank gas and by maintaining the moisture content of the gas mixture at 10 ppm or less.

For experimental use, 15-Mev protons, 52-Mev oxygen ions, and 118-Mev iodine ions were produced.

[1]Physics Division.

10.4 NEGATIVE-ION SOURCE DEVELOPMENT

W. H. duPreez[1] J. W. Johnson R. F. King

The negative-ion beam which is presently being injected into the Tandem Van de Graaff accelerator has certain undesirable qualities which limit the target current and make the beam unsuitable for pulsing and bunching. To obtain a better quality beam, two methods of producing a negative-hydrogen-ion beam were investigated: charge exchange of a positive-ion beam in a gas target and direct extraction of a negative-ion beam from the plasma in a duoplasmatron source. Charge exchange is the method now being used on the Tandem accelerator, and the investigation of this method showed that no meaningful improvement in the results was possible.

Direct extraction was then investigated, and the negative-ion output was found to depend strongly on the configuration and position of the duoplasmatron intermediate electrode, and on the duoplasmatron arc-discharge conditions of gas pressure, magnetic field, and arc current.

An ion-source configuration and an arc-discharge condition were found which stably and reliably

[1]Visitor from the South Africa Atomic Energy Board, Pretoria, South Africa.

yielded 30 μa of negative hydrogen ions through a 0.0085-in.-diam source aperture. At these optimum conditions, the ratio of electrons extracted from the ion-source plasma to the negative ions extracted was a minimum; a value of 500 was typical. Some arc conditions were found that yielded negative beam currents as high as 100 μa, but for unknown reasons, this intensity could not be maintained for more than 1 to 2 min before it drifted down to a value no greater than 30 μa.

The ion-optical qualities of the direct-extracted negative-ion beam are quite good compared to those of a beam produced by charge exchange because of the low, approximately 100 ev, energy spread of the duoplasmatron beam and the small object size from which the beam originates.

From these facts, it is concluded that direct extraction of a negative-hydrogen-ion beam is very promising; however, additional work will be required to improve its reliability at high outputs.

10.5 THERMAL LEAK-VALVE DEVELOPMENT

J. W. Johnson C. D. Moak[1]

Except for the isotopes of hydrogen, which may be leaked through a palladium barrier at elevated temperatures, the feeding of gas to an accelerator ion source, maximum flow rate of 3 to 5 cc/hr, is plagued with difficulties. Needle valves must be closed until the needle deforms the valve seat before these low gas-flow rates can be obtained and controlled. The deformation of the valve seat produces hysteresis and other uncertainties in control of the flow rate and may also gall the valve seat. Because a needle valve requires a mechanical drive for its control, and because the palladium-barrier leak valve requires electrical control of the voltage to the heater by means of a variable transformer (Variac), the conversion of an accelerator from hydrogen to other feed gases involves many hardware changes or completely separate control systems. An electrically controlled thermomechanical valve was adapted from a Harwell design[2] (Fig. 10.5.1) to be integrally mounted in the gas supply bottle in a manner similar to the present arrangement for the palladium-barrier leak valve for H_2. Since the palladium-barrier heater is used to control the sealing force on the $\frac{1}{8}$-in.-diam stainless steel ball (shown in Fig. 10.5.1) by thermal expansion of the tension

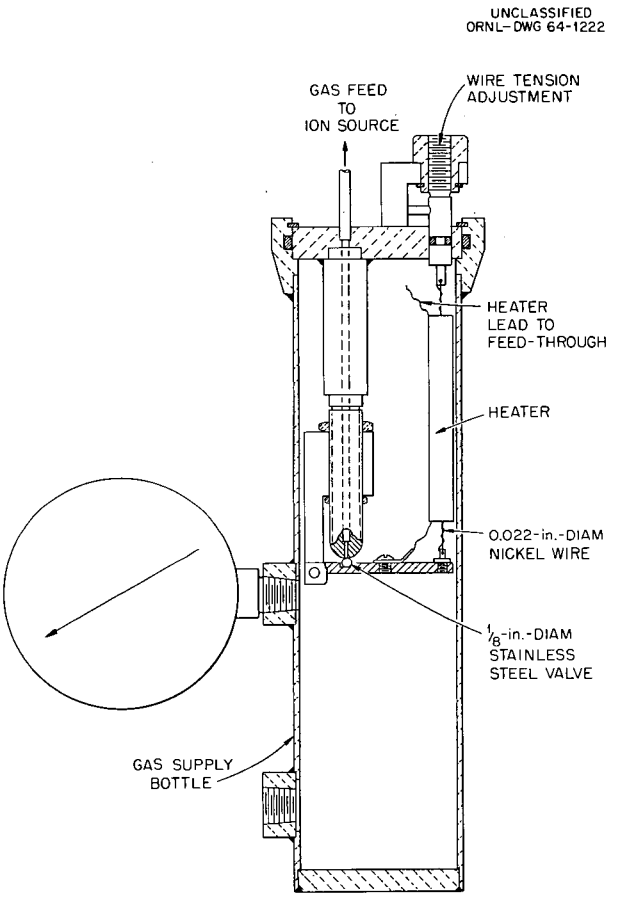

Fig. 10.5.1. Electrically Controlled Thermomechanical Valve.

[1]Physics Division.

[2]Private communication from F. D. Pilling, AERE, Harwell, England, to C. D. Moak.

wire, the valve assembly can be directly interchanged with the palladium-barrier leak-valve assembly without changing the control system.

This type of valve has been used to feed He in the 5.5-Mv Van de Graaff and He, O_2, Br_2, I_2, and H_2 in the Tandem Van de Graaff. Operation was stable, reliable, and reproducible. The flow-rate response to a change in control setting was smooth and quite like that obtained from a palladium-barrier leak valve. To reduce the poisoning of the discharge in the ion source for He^{2+} operation on the 5.5-Mv Van de Graaff, special care was taken to remove most of the hydrogenous materials from the gas bottle and valve. The results were excellent; 0.1 μa of He^{2+} beam current was obtained.

11. Miscellaneous

11.1 COSTS AND MANPOWER SUPPORT OF LABORATORY PROGRAMS

Joseph Guarneri

To fulfill its responsibility to the Laboratory research programs, the Instrumentation and Controls Division employs over 300 technical and other personnel of various skills and disciplines to carry out diverse functions ranging from research in basic instrumentation to routine maintenance and servicing of on-line instrumentation. Studies and investigations are pursued not only to keep abreast of the state of the art, but also to contribute to it. As new instruments and components become available on the market, they are tested and evaluated to determine their characteristics, performance, and reliability for future incorporation in new instrument design and development at ORNL. Development work is carried out to upgrade the performance and reliability of instrumentation in use at the Laboratory. On-line instrumentation and controls systems for processing plants, research reactors, and experiments are studied to formulate more advanced maintenance techniques or, if required, specialized training programs for maintenance and supervisory personnel.

The cost of Division labor required to carry out these activities in fiscal year 1963 was approximately $3 million, or 4% of the total expenditure of the Laboratory. Purchases of capitalized instrumentation and electronic components amounted to almost $4 million (Table 11.1.1). The actual value of these purchases, $4 million, was much larger than shown in Table 11.1.1, however, because this total does not include a large amount of experimental instrumentation which had not been capitalized or which had been purchased directly by or for other Laboratory Divisions. The asset accounts of the Laboratory contain approximately $16 million (Table 11.1.1) of capitalized instrumentation; moreover, this figure does not reflect the value of experimental instrumentation, which is not capitalized.

In the past ten years the annual budget for the Division increased from $0.5 million in 1953 to $1.3 million in 1963, with an attendant increase in manpower from 155 to 304 respectively (Table 11.1.2).

The distribution of Division manpower used in assisting other Laboratory divisions during fiscal year 1963 is shown in Fig. 11.1.1. Figure 11.1.1*b* excludes the Reactor Controls and Basic Instrumentation Departments. Neither chart includes manpower expended for research and development programs of the Instrumentation and Controls Division.

Table 11.1.1. Schedule of ORNL Instrumentation Costs, Fiscal Year 1963

Capitalized instrumentation acquired	~$3 million
Electronic components purchased	~$1 million
Electronic components issued from ORNL Stores	$880,000
Number of instruments, components, and electronic supplies stocked in ORNL Stores	>4200
Value of electronic inventory in ORNL Stores as of June 30, 1963	$509,853
Instrumentation in asset accounts as of June 30, 1963	$16 million

Table 11.1.2. Comparison of Cost and Manpower Expenditures in 1953 with 1963

	Cost		Manpower	
Function	1953	1963	1953	1963
Research	$250,000	$427,000	15	51
Support	254,000	905,000	140	253
	$504,000	$1,332,000	155	304

UNCLASSIFIED
ORNL-DWG 64-1223

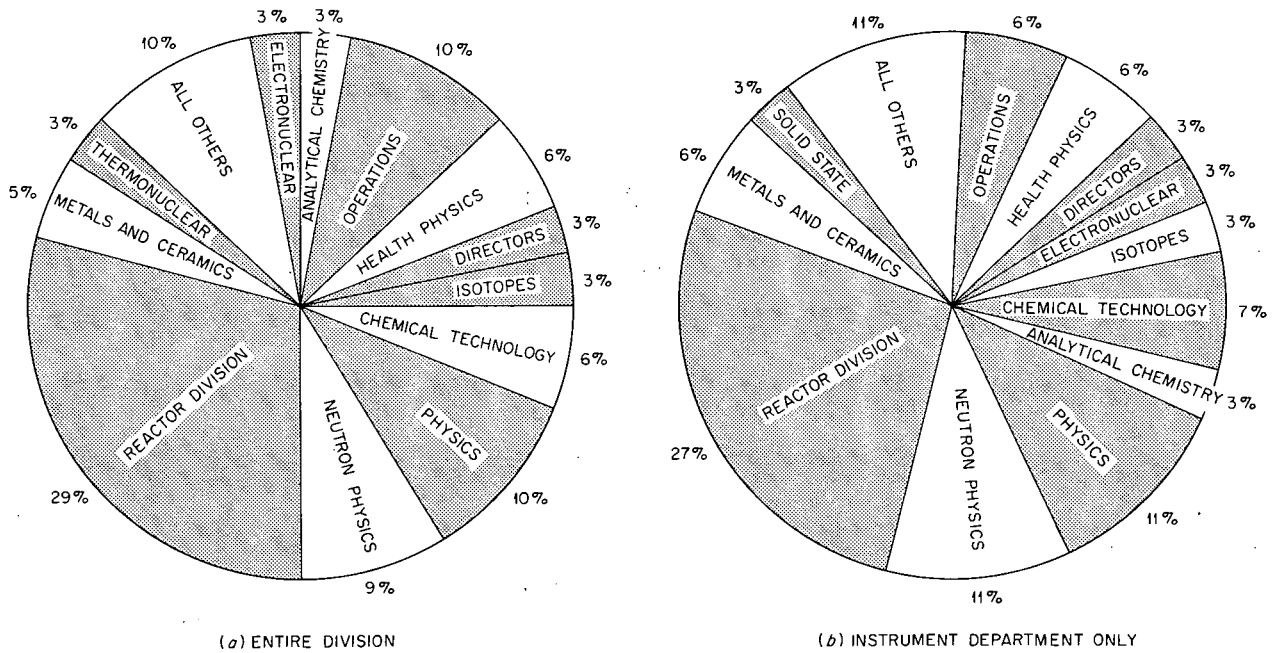

(*a*) ENTIRE DIVISION

(*b*) INSTRUMENT DEPARTMENT ONLY

Fig. 11.1.1. Distribution of Instrumentation and Controls Division Manpower in Fiscal Year 1963.

Publications

Anderson, J. L., "Role of Log-*N* Period Meter in Reactor Protection," *Nucl. Safety* 4(3), 48–50,54 (1963).

Ball, S. J., "Simulation Techniques for Plug-Flow Systems," *Instr. Control Systems* **36**, 133 (1963).

Ball, S. J., "Approximate Models for Distributed-Parameter Heat-Transfer Systems," pp. 131–39 in *Proc. 4th. Joint Automatic Control Conf., Minneapolis, Minn., June 1963,* Am. Inst. Chem. Engrs., New York, 1963.

Bates, A. E. G., "Control-Rod Drives," *Nucl. Safety* 4(4), 76–80 (1963).

Burke, O. W., "Reactor Behavior Analysis Using Analog Computers," *Nucl. Safety* 4(3), 50–52,54 (1963).

Chester, R. O., R. W. Peelle, and F. C. Maienschein, "Nonlinear Least-Squares Fitting Applied to Gamma-Ray Scintillation Detector Response Functions," pp. 201–12 in *Applications of Computers to Nuclear and Radiochemistry, Proc. Symp., Gatlinburg, Tenn., October 1962* (ed. by G. D. O'Kelley), NAS-NS-3107, 1963.

Epler, E. P., "Reliability of Reactor Systems," *Nucl. Safety* 4(4), 72–76, 83 (1963).

Hanauer, S. H., "Role of Neutron Source in Reactor Safety," *Nucl. Safety* 4(3), 52–55 (1963).

Mossman, C. A., "In-Core Temperature Measurement," *Nucl. Safety* 4(4), 81–84 (1963).

Mruk, W. F., *Analytical Details Concerning "Machine Time" in Time-Amplitude Conversion,* ORNL-TM-606 (June 20, 1963).

Mruk, W. F., *The Principles and Measurement of Fission Fragment Times of Flight,* ORNL-3486 (1963).

Ricker, C. W., A. L. Colomb, and E. R. Mann, "A Method for Measurement of Negative Reactivity by Analysis of Neutron Fluctuation Spectral Density," *Trans. Am. Nucl. Soc.* **6**, 75–76 (1963).

Roux, D. P., and S. H. Hanauer, "Use of Reactor Gamma Radiation as a Reactor Control and Safety Parameter," *Trans. Am. Nucl. Soc.* **6**, 74 (1963).

Walker, C. S., *Analog Computer Calculations for the Loss-of-Power Incident in the EGCR,* ORNL-TM-476 (Nov. 27, 1961).

West, K. W., "Relative Functions of Loop Containment and Instrumentation," *Nucl. Safety* 4(4), 80–81 (1963).

The following reports were written under subcontract (No. 2160) with the Engineering Experiment Station, Department of Electrical Engineering, University of Tennessee.

J. F. Pierce, *Progress Report on Subcontract No. 2160, Dec. 16, 1961, to Dec. 1, 1962.*

T. V. Blalock, *A Survey and Evaluation of the Semiconductor Noise Literature,* Scientific Report No. 1 (May 28, 1962).

E. J. Kennedy and J. F. Pierce, *A Survey and Evaluation of Bias Stabilization Techniques in Transistor Circuits,* Scientific Report No. 2 (June 29, 1962).

R. Nutt, T. V. Blalock, and J. F. Pierce, *A Transistor Hybrid-Pi Noise Model,* Scientific Report No. 3 (Oct. 1, 1962).

J. F. Pierce, *Progress Report on Subcontract No. 2160, Dec. 1, 1962, to Dec. 1, 1963.*

D. W. Coffman, E. J. Kennedy, and J. F. Pierce, *Trigger Point Stability of Emitter-Coupled Monostable Multivibrators,* Scientific Report No. 4 (Jan. 30, 1963).

A. S. Sabin, T. V. Blalock, and J. F. Pierce, *An Experimental Study of Noise in Silicon Planar Transistors,* Scientific Report No. 6 (Mar. 20, 1963).

T. V. Blalock and J. F. Pierce, *Application of Field Effect Transistors in Low Noise Wideband Voltage and Charge Sensitive Preamplifiers,* Scientific Report No. 5 (Mar. 15, 1963).

E. J. Kennedy and J. F. Pierce, *Stabilized Low-Power Operation of the Personnel Radiation Monitor,* Scientific Report No. 7 (Mar. 22, 1963).

S. J. Gourse, *A D-C to D-C Converter Utilizing a Ceramic Piezoelectric Transformer,* Scientific Report No. 8 (June 10, 1963).

J. C. Brooks, E. J. Kennedy, and J. F. Pierce, *A Temperature-Compensated, Low-Power Asymmetric Astable Multivibrator,* Scientific Report No. 9 (Aug. 20, 1963).

U. E. Hilger, T. V. Blalock, and J. F. Pierce, *An Evaluation of Two Proposed Noise Models for the Field-Effect Transistor,* Scientific Report No. 10 (Aug. 21, 1963).

R. E. Wintenburg and J. F. Pierce, *A Charge-Sensitive Pulse Preamplifier with a Field-Effect Transistor Input Stage,* Scientific Report No. 11 (Oct. 15, 1963).

G. R. Alspaugh and J. F. Pierce, *A Study of Transistor High-Speed Schmitt-Trigger Circuits,* Scientific Report No. 12 (Nov. 1, 1963).

Papers Presented at Professional Meetings

Conference on Instruments and Techniques in Nuclear Pulse Analysis (Sponsored by NAS-NRC), Monterey, California, April 29–May 3, 1963

Williams, C. W., and M. V. Harlow, "Pulse Shape Discrimination."

9th Annual Meeting of the American Nuclear Society, Salt Lake City, Utah, June 17–19, 1963

Ricker, C. W., A. L. Colomb, and E. R. Mann, "A Method for the Measurement of Negative Reactivity by Analysis of Neutron Fluctuation Spectral Density."

Roux, D. P., and S. H. Hanauer, "Use of Reactor Gamma Radiation as a Reactor Control and Safety Parameter."

Joint Automatic Control Conference (Sponsored by AIChE, IEEE, and ISA), Minneapolis, Minnesota, June 19–21, 1963

Ball, S. J., "Approximate Models for Distributed-Parameter Heat-Transfer Systems."

International Federation of Automatic Control Conference, Basel, Switzerland, August 27–September 4, 1963

Ball, S. J., "Discussion of Paper: Experimental Study of the Dynamic Behavior of a Heat Exchanger and of a Mixing Process, by L. Delvaux."

Walker, C. S., *et al.*, "Review of Technical Paper: Principles and Application of Automated Fuel Handling in a Nuclear Power Plant."

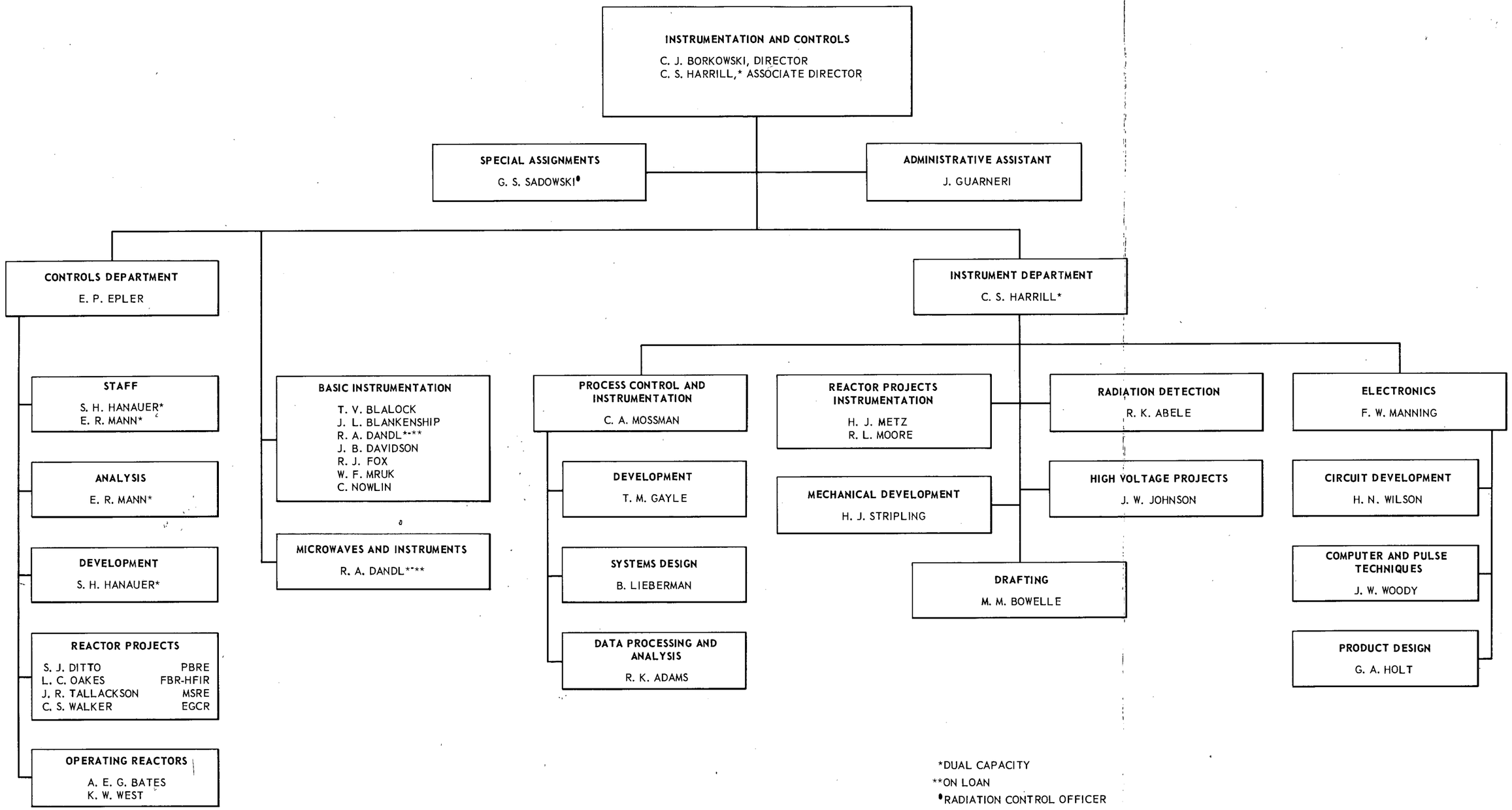

*DUAL CAPACITY
**ON LOAN
•RADIATION CONTROL OFFICER

ORNL-3578
UC-37 – Instruments
TID-4500 (29th ed.)

INTERNAL DISTRIBUTION

1. Biology Library
2-4. Central Research Library
5. Laboratory Shift Supervisor
6. Reactor Division Library
7-8. ORNL – Y-12 Technical Library Document Reference Section
9-168. Laboratory Records Department
169. Laboratory Records, ORNL R.C.
170. J. A. Auxier
171. P. R. Bell
172. T. V. Blosser
173. C. J. Borkowski
174. F. L. Culler
175. E. P. Epler
176. D. J. Fisher
177. J. L. Gabbard
178. C. S. Harrill
179. A. Hollaender
180. A. S. Householder
181. G. S. Hurst
182. W. H. Jordan
183. M. T. Kelley
184. C. E. Larson
185. T. A. Lincoln
186. S. C. Lind
187. R. S. Livingston
188. J. R. McNally, Jr.
189. K. Z. Morgan
190. M. L. Nelson
191. E. L. Olson
192-193. R. B. Parker
194. H. E. Seagren
195. E. D. Shipley
196. M. J. Skinner
197. A. H. Snell
198. E. G. Struxness
199. C. D. Susano
200. J. A. Swartout
201. E. H. Taylor
202. A. M. Weinberg
203. G. C. Williams

EXTERNAL DISTRIBUTION

204. N. F. Barr, Chief, Radiological Physics and Instrument Branch, Division of Biology and Medicine, AEC, Washington
205. R. W. McNamee, Union Carbide Corporation, New York
206. A. S. Lough, Division of Biology and Medicine, AEC, Washington
207. S. G. Nordlinger, Reactor Development Division, AEC, Washington
208. F. C. Legler, Reactor Development Division, AEC, Washington
209. J. Hitch, Office of Isotope Development, AEC, Washington
210-211. Ohio State University (Professor of Naval Science)
212. R. Hofstadter, Stanford University
213. J. C. Nance, Consolidated-Vultee Aircraft Corporation
214. E. A. Rollor, ANP Project Office, Fort Worth
215. R. N. Keller, University of Colorado
216. L. J. Rogers, Special Instruments Division, Union Carbide Olefins Co., P. O. Box 8361, South Charleston, W. Va.
217. R. P. Sullivan, Ohio State University
218. D. A. Bromley, Yale University
219. V. B. Bhanot, Physics Department, Panjab University, Chandigarh-3, India
220. Research and Development Division, AEC, ORO
221-851. Given distribution as shown in TID-4500 (29th ed.) under Instruments category (100 copies – OTS)